Molecular mechanisms involved in renal injury-repair and ADPKD progression

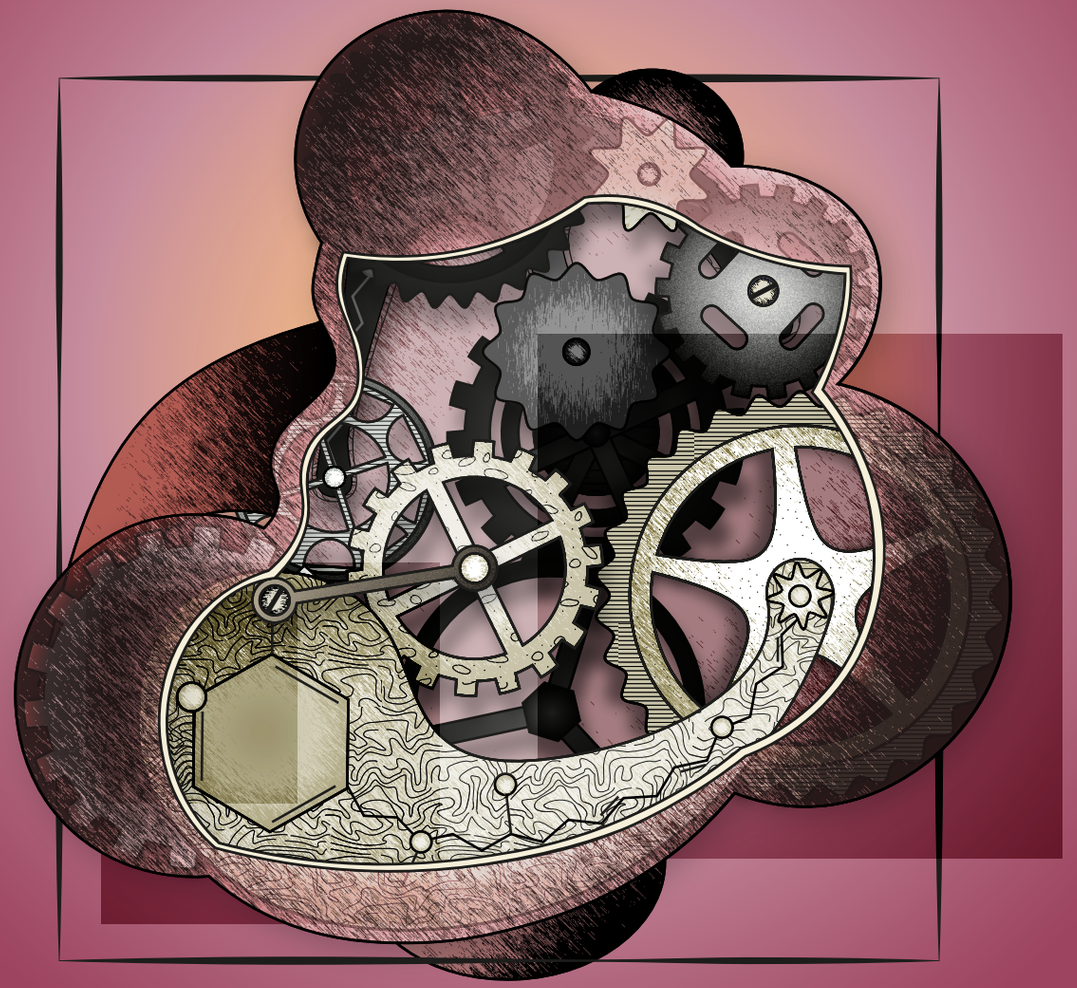

Chiara Formica

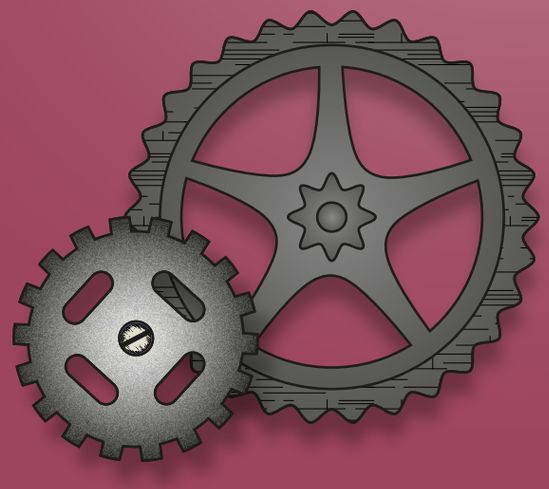

Molecular mechanisms involved in renal injury-repair and ADPKD progression Chiara Formica

MOLECULAR MECHANISMS INVOLVED IN RENAL INJURY-REPAIR AND ADPKD PROGRESSION

Chiara Formica

Molecular mechanisms involved in renal injury-repair and ADPKD progression

Chiara Formica
Leiden University Medical Center, The Netherlands

ISBN: 978-94-6380-882-8

Layout & cover design: Chiara Formica
Printing: ProefschriftMaken www.proefschriftmaken.nl

MOLECULAR MECHANISMS INVOLVED IN RENAL INJURY-REPAIR AND ADPKD PROGRESSION

PROEFSCHRIFT

ter verkrijging van
de graad van Doctor aan de Universiteit Leiden,
op gezag van Rector Magnificus prof.mr. C.J.J.M. Stolker,
volgens besluit van het College voor Promoties
te verdedigen op donderdag 10 september 2020
klokke 10:00 uur

door

Chiara Formica

geboren te Cisternino (BR), Italië
in 1987

Promotor:
Prof. Dr. D.J.M. Peters

Co-promotor:
Prof. Dr. P.A.C. ‘t Hoen

Promotiecommissie:
Prof. Dr. A. Aartsma-Rus
Prof. Dr. S. Florquin[1]
Prof. Dr. R. Goldschmeding[2]

[1]Department of Pathology, Academic Medical Center, University of Amsterdam, The Netherlands.
[2]Department of Pathology, University Medical Center Utrecht, The Netherlands.

The studies described in this thesis have been performed at the department of Human Genetics, Leiden University Medical Center, The Netherlands.

Table of contents

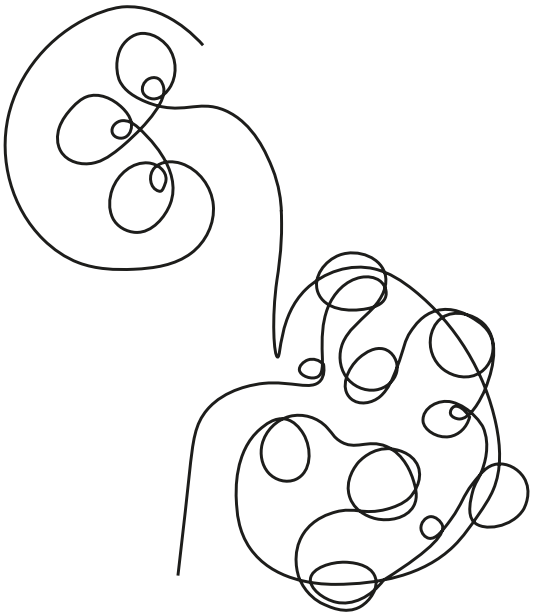

CHAPTER 1

General Introduction

Adapted from:

Molecular pathways involved in injury-repair and ADPKD progression

Chiara Formica[1] and Dorien J.M. Peters[1]

[1]Department of Human Genetics, Leiden University Medical Center, The Netherlands

Cell Signal. 2020;72:109648

1. Autosomal Dominant Polycystic Kidney Disease

Autosomal Dominant Polycystic Kidney Disease (ADPKD) is a heritable genetic disorder with a prevalence of <5/10.000 in the European Union[1]. The major hallmark of ADPKD is the formation of many fluid-filled cysts in the kidneys, which ultimately impairs the normal renal structure and function, leading to end-stage renal disease (ESRD)[2,3]. Additionally, extrarenal manifestations such as liver and pancreas cysts and cardiovascular abnormalities are also present[2].

In the majority of the cases, ADPKD is caused by a mutation in either of two genes: *PKD1* in 85% of the case; *PKD2* in 15% of the cases. *PKD1/2* genes encode for Polycystin 1 (PC1) and Polycystin 2 (PC2), respectively[2]. PC1 is a very large membrane protein of 4303 amino acids, with a long extracellular N-terminal, eleven transmembrane domains, and a small intracellular C-terminal[4]. PC2 is a much smaller transmembrane protein of 968 amino acids, with six transmembrane domains, and intracellular N- and C-terminal[5]. The polycystins are localised at various location in a renal epithelial cell. Particularly, PC1 expression has been observed at the apical and basal side of the epithelial cells, the primary cilium, and several lateral junctions. PC2, instead, have been observed mainly at the primary cilium, basolateral membrane and endoplasmic reticulum[6]. The exact functions of these two proteins are still not completely understood. PC1 may function as a receptor able to respond to both mechanical and chemical signals and transducing them to downstream signalling. Indeed, the intracellular portion of the protein can be cleaved and translocate to the nucleus where it interacts with several transcription factors like β-catenin and STATs[7-10]. PC2 seems to be a non-selective cation channel and might be regulating the intracellular Ca^{2+} concentration, influencing several signalling pathways[4,6]. However, the molecular mechanisms that lead to cyst initiation and progression after the loss of functional levels of PC1/2 are still not understood.

Conversely, the pathophysiology of the disease progression is mainly known (Figure 1). In most cases, ADPKD patients carry a germline mutation in one allele of *PKD1/2* genes. Throughout life, due to somatic mutations in the unaffected allele (second hit mutations) or to stochastic fluctuations in the gene dosage of *PKD1/2* (haploinsufficiency), the level of expression of PC1/2 drops below a critical threshold[11]. As a consequence, renal epithelial cells are more prone to cyst formation. Interestingly, the time between the critical reduction of PC1/2 and cyst initiation can be influenced by the biological context. As evidenced by several studies, differences in timing and location of gene inactivation, the metabolic status, the genetic context and introduction of renal injury can influence cyst formation and progression[12]. Once cysts have been formed, proliferation and fluid secretion contribute to the cyst size increase, which eventually cause stress on the surrounding tissue resulting

in local injury and fibrosis[13]. In the advanced stages of the disease, cystic kidneys are characterised by local injury, production of growth factors and cytokines, infiltrating cells and progressive fibrosis, which ultimately lead to loss of renal function[11].

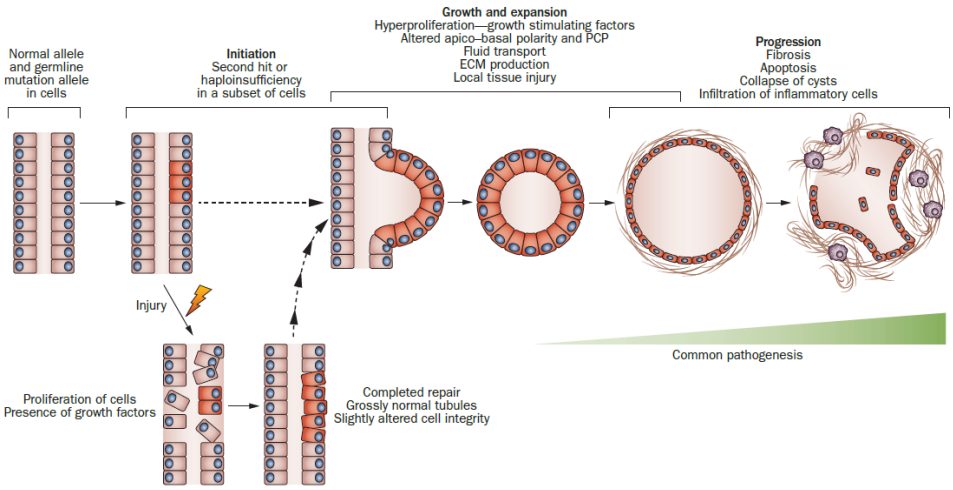

Figure 1. Disease progression in ADPKD

A single *PKD1* or *PKD2* allelic mutation is inherited in patients affected with ADPKD. Later in life, due to a second hit mutation in the unaffected allele or to stochastic variation in gene expression, the level of PC1/2 expression drops under a critical threshold. As a result, epithelial cells are more prone to initiate cyst formation. The time between the critical reduction of PC1/2 levels and the initiation of the cysts is variable and can be influenced by other events, for example, renal injury. After injury, the tissue repair occurs in the absence of sufficient levels of PC1/2 resulting in an abnormal tubular epithelium. The structurally altered epithelial cells are more prone to cyst formation, accelerating disease progression. After cysts are formed, increased proliferation and altered fluid secretion help the cyst to grow and expand, compressing the surrounding tissue. Mechanical stress, as well as secretion of cytokines and growth factors, generate additional injury locally, which contributes to cyst formation and fibrosis deposition. In the more advanced stages of the disease, the tissue is increasingly fibrotic, with visible cellular infiltrates and loss of normal parenchyma. Image from Happé *et al.* [11]

2. Renal injury and repair mechanisms

Following a renal insult, the kidneys are able to repair the injury themselves by inducing proliferation of surviving tubular epithelial cells[14]. During this regeneration phase, tubular epithelial cells are lost or show an aberrant morphology (e.g., loss of brush border and flattening of proximal tubular epithelial cells). Also, infiltration of inflammatory cells is observed[15]. All these events ensure a proper repair of kidney structures and function. However, in some cases the damage is too extensive, or the injury insult persists leading to tissue remodelling, progressive fibrosis and loss of renal function. This fibrotic phase is characterised by chronic inflammation, expansion of alpha-smooth muscle actin (αSMA) positive cells, capillary rarefaction and hypoxia, which fuel the deposition of extracellular

matrix (ECM) and, at the same time, perpetuate local injury leading eventually to chronic kidney injury (CKD) and ESRD[16] (Figure 2a).

3. Renal injury and progression of ADPKD

The link between cyst progression and injury has been already suggested by Weimbs, who postulated that a possible role for PC1 is to sense renal injury via changes in luminal fluid flow. As a result, PC1 activates molecular pathway transducers, such as mTOR and STAT6, leading to increased proliferation and repair of the injured kidney tissue. In ADPKD, reduced levels of PC1 might trigger the activation of proliferation even in the absence of injury, resulting in cyst growth and expansion[17]. However, especially in adult kidneys, deletion of *Pkd1* alone does not immediately translate in cyst formation, which occurs only after a lag period. Another event, such as renal injury, must occur to start cyst formation[17]. In line with this idea, several research groups employing different kinds of renal injury (e.g., nephrotoxic compound, ischemia-reperfusion or unilateral nephrectomy) demonstrated how acute kidney injury (AKI) was able to speed-up cyst progression in mice[18-22]. Additionally, cyst expansion causes mechanical stress to the surrounding tissue and vessels together with the secretion of cytokines and growth factors, activating pathways involved in cyst progression and resulting in a snowball effect that supports more cyst formation[13]. Interestingly, various mechanisms normally active during the injury-repair phase such as proliferation, inflammation, cell differentiation, cytokines and growth factors secretion, are also activated during PKD progression, and largely overlap with the mechanisms at play during renal development[17,22-24]. In fact, renal epithelial cells in ADPKD kidneys often appear "dedifferentiated" with reduced expression of the epithelial marker E-cadherin, which is compensated by increased expression of the mesenchymal marker N-cadherin. The switch in cadherins seems to be a direct effect of the missing interaction of PC1/2 with the E-cadherins at the adherens junctions. As a consequence, the cells lose the proper polarisation resulting in a less differentiated phenotype and alterations in cellular functions[25,26]. Moreover, ADPKD cells re-express genes normally expressed during developmental stages and silenced in adult tissues, in line with the partial dedifferentiated phenotype observed[27]. Altogether, these events can ultimately contribute to disease progression. In a normal situation, reactivation of the aforementioned pathways following renal injury allows remodelling of the tissue and a proper organ repair. Instead, in a context of PKD-related gene mutations, aberrant or chronic activation of these developmental pathways and repair/remodelling mechanisms results in exacerbation of the disease (Figure 2b).

In the following paragraphs, I will discuss some of the main pathways involved in injury-repair and ADPKD.

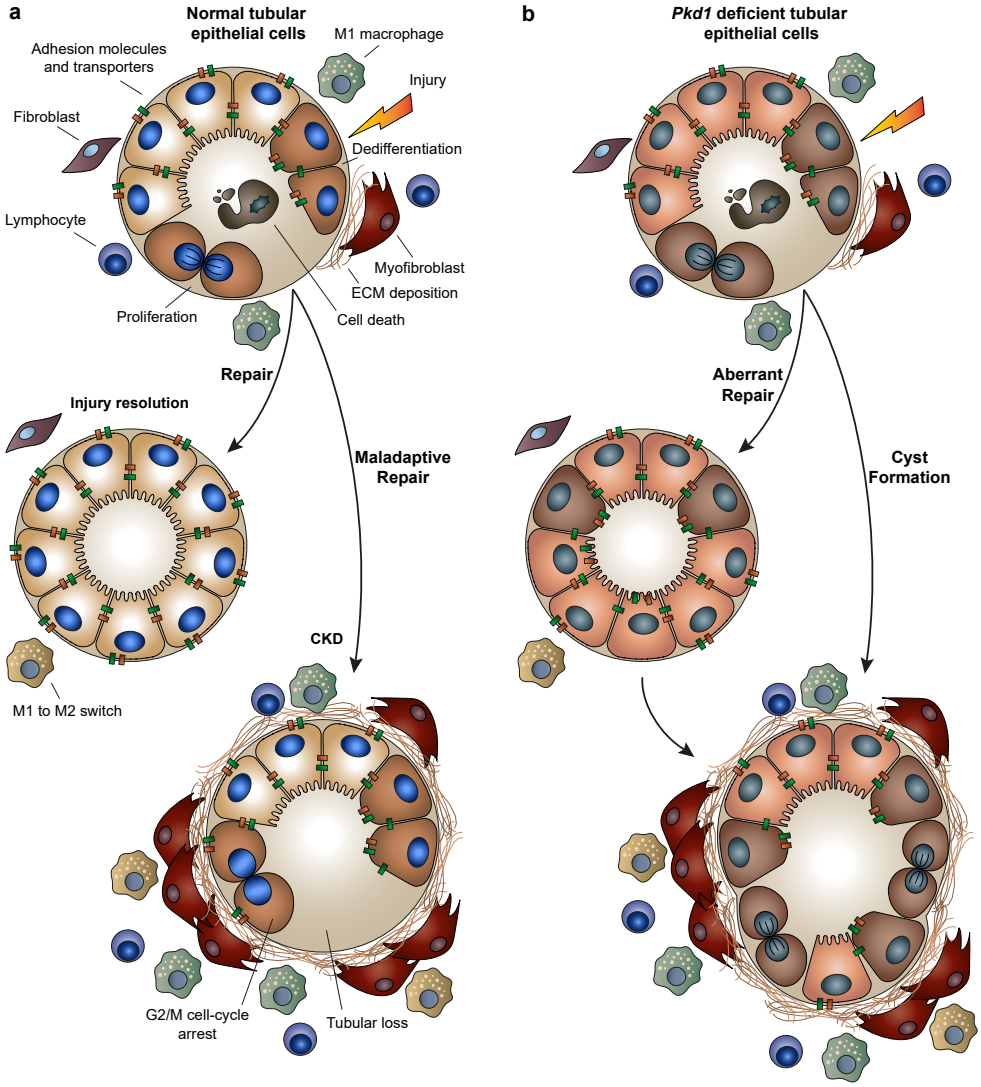

Figure 2. The evolution of injury in normal and *Pkd1* deficient kidneys

a) After injury, the renal epithelium can regenerate the damaged and lost tissue. This phase is characterised by the dedifferentiation and proliferation of epithelial cells, as well as the recruitment of leucocytes and the activation of fibroblasts in myofibroblasts. When all these processes work harmoniously, the tissue is restored and the injury resolved. The infiltrating macrophages undergo an M1-like to M2-like switch and help in the resolution of the inflammatory response and renal growth. However, in case of severe damage or chronic activation of the inflammatory signalling, it is possible to have maladaptive repair. Proliferating cells may arrest in G2/M phase and start to produce pro-inflammatory and pro-fibrotic molecules that fuel a chronic inflammation with progressive collagen deposition and loss of the normal parenchymal structure, leading to chronic kidney disease (CKD). **b)** After injury, *Pkd1* deficient kidneys can repair the tissue damage or can develop cysts, depending on how intense the injury insult was, and/or the genetic makeup of the organism. However, even in case of tissue repair, *Pkd1* deficient kidneys show aberrant repair with altered cell polarity and cell differentiation, providing a potential explanation for the increased speed of cyst formation observed after injury.

3.1 Injury-repair and fibrosis

3.1.1 Renal injury

Repair after renal injury relies on the surviving epithelial cells, which can dedifferentiate to be able to spread and migrate to cover exposed tubular tracts and to proliferate in order to restore the integrity of the tissue. Indeed, injured kidneys are strongly positive for proliferation markers such as Ki67 and proliferative cell nuclear antigen (PCNA)[28,29]. Once the integrity of the tubules is restored, cells need to differentiate back into fully mature epithelial cells to re-establish the proper function of the organ. It has been proposed that laminin-integrin interactions might drive re-differentiation of the epithelium. In particular, laminin-5 and $\alpha_3\beta_1$-integrin expression are increased after ischemic kidney injury[30]. Interestingly, laminin-5 expression is also increased in the ECM of ADPKD kidneys. Stimulation with purified laminin-5 can activate the extracellular-signal-regulated kinase (ERK) in traditional cell cultures and can stimulate proliferation and cyst formation in three-dimensional cultures[31]. Moreover, a hypomorphic mutation in laminin-5 in mice causes cyst formation, both in the cortex and medulla, showing that defects in ECM components are sufficient to cause PKD[32].

After renal injury, expression levels and activity of transforming growth factor-beta (TGF-β) are increased and play a role in maintaining the injured tubule in a dedifferentiated state. This is necessary for cell proliferation and repair of the tubule[33]. The TGF-β superfamily of proteins comprises a group of highly conserved secreted morphogens, which regulate a variety of developmental and homeostatic processes. Upon binding of the TGF-β family members to their receptors, a series of phosphorylation events are triggered. The signalling cascade ends up with the phosphorylation and subsequent activation of the SMAD transcription factors, which translocate to the nucleus where they can drive gene expression[34]. Thus, TGF-β can suppress the expression of epithelial markers and increase the expression of mesenchymal markers, such as αSMA and vimentin, leading to partial dedifferentiation, i.e. epithelial-to-mesenchymal transition (EMT). Although EMT is a physiological event during renal development and useful adaptive response to injury, sustained EMT can result in increased matrix deposition and cytokine production that lead to CKD. Moreover, TGF-β can stimulate ECM deposition by acting directly on the transcription of fibronectin, proteoglycans, collagens and integrins. At the same time, TGF-β antagonises matrix degradation by stimulating proteases inhibitors production[35]. In line with these findings, several *in vivo* and *in vitro* experiments have shown that TGF-β might be the mediator of AKI-to-CKD progression[36].

3.1.2 PKD

EMT and excessive ECM deposition are also characteristic features of ADPKD.

Immunohistochemical analyses of human kidneys in advanced stages of ADPKD showed increased αSMA^{+} myofibroblast and interstitial fibrosis, loss of epithelial markers in favour of mesenchymal ones in tubules, and increased TGF-β-SMAD signalling[37]. All these events suggest that local injury and TGF-β regulated EMT might play a role in ADPKD progression. Increased TGF-β and nuclear phospho-SMAD2 staining are often observed in cyst-lining epithelium and interstitial cells surrounding cysts, both in mice and humans[38]. Shear stress, induced by fluid flow, on wildtype and *Pkd1*$^{-/-}$ tubular epithelial cell cultures activates the TGF-β downstream targets SMAD2/3, which is prevented by administration of TGF-β-neutralizing antibodies and by inhibitors of the TGF-β-binding type-I-receptor ALK5 (activin receptor-like kinase 5). This indicates that autocrine TGF-β signalling is activated upon shear stress in renal epithelial cells[39-41]. This response was higher in *Pkd1*$^{-/-}$ cells because of more TGF-β-production. In addition, it has been shown that TGF-β can restrict cystogenesis in a three-dimensional culture of both murine and human cells[42,43]. However, in mice, conditional ablation of *Alk5* together with *Pkd1* in renal epithelium did not result in amelioration of PKD progression, while sequestering of activin A and B, other members of the TGF-β family, via administration of the soluble activin receptor IIB, lead to amelioration of PKD progression in three different mouse models[44]. Paracrine effects on interstitial cells, rather than autocrine effects might be critical in PKD, and it seems that there is context-dependent effect of TGF-β family members. Indeed, it is known that TGF-β can both inhibit and promote cell growth, drive differentiation but also dedifferentiation of cells, and can be helpful in injury but can also be the major driver of fibrosis. Although the signalling process is essentially the same, the context, cell types and the cofactors involved shape the outcome of the signalling[34]. Hence, further studies to investigate the role and the possible use of TGF-β as a therapeutic target in ADPKD are needed.

The cells mostly responsible for ECM deposition, are myofibroblasts. Myofibroblasts can originate from different precursor cells, but the most important seem to be renal fibroblasts, resident macrophages and other cells of hematopoietic origin that migrate into the kidney[45]. These cellular transitions, together with direct injury-induced damage to the vasculature, can contribute to the loss of capillaries surrounding the renal tubules resulting in local hypoxia, a known driver of fibrotic response in CKD[46]. In ADPKD, cyst formation and expansion is associated with altered vascular architecture. In particular, peritubular microvasculature shows signs of regression of larger capillaries together with flattened arterioles and atresic venules. At the same time, cysts are surrounded by a dense but disorganised capillary network, which forms a sort of "vascular capsule"[47]. The observed vascular alteration can be the result of expanding cysts, exerting mechanical compression of intrarenal vasculature and impairing its function. This could also be directly related to reduced expression of the polycystins in the vasculature where they have crucial roles in mechanosensation, fluid-shear stress sensing, signalling and maintaining structural integrity[48-52]. Regardless of

the primary mechanism, a final common outcome is the development of local hypoxia, which in turn induces expression of hypoxia-inducible factor-1 alpha (HIF-1α) in the cystic epithelium, and HIF-2α in interstitial cells[53] (Figure 3). Particularly, HIF-1α seems to have a central role in cyst growth *in vivo*, because deletion of *Hif1a* in a conditional kidney-specific *Pkd1* mutant mouse model was able to reduce fibrosis and improve PKD progression[54]. Additionally, gene expression studies of renal cells from cystic human and murine kidneys found a consistent hypoxia gene expression profile suggesting that hypoxia has an important role in ADPKD progression[23,55]. In fact, on one hand, hypoxia in ADPKD contributes to the

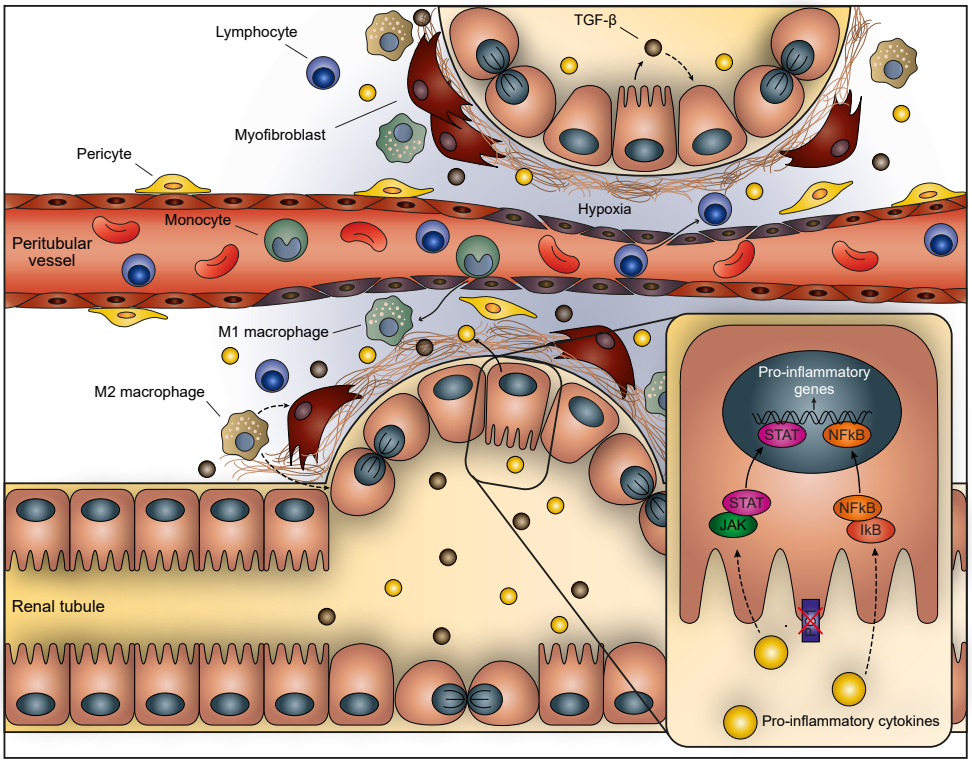

Figure 3. Effect of cyst expansion on the surrounding tissues

Cyst expansion causes mechanical stress to the surrounding tissue and vessels. As a result, injury-related mechanisms are activated, and cytokines and growth factors are secreted in the renal tubules and the surrounding interstitium. TGF-β secretion drives tubular cell dedifferentiation, recruitment of infiltrating cells to the cyst site, and activation of αSMA$^+$ myofibroblasts with increased extracellular matrix deposition. M2-like macrophages accumulate around the cysts where they secrete anti-inflammatory and pro-fibrotic molecules that stimulate tubular cells proliferation and myofibroblasts activation. Pro-inflammatory stimuli and accumulation of fibrosis lead to pericyte dissociation resulting in microvasculature rarefaction and local hypoxia, which exacerbates the fibrotic response. Inflammatory cytokines, such as TNF-α, IL-1β and INF-γ, as well as the deletion of PC1, activate two major inflammatory pathways in renal epithelial cells: NF-κB and JAK-STAT. As a result, pro-inflammatory molecules are produced and released, attracting and activating even more infiltrating cells, which aggravate the local injury and ultimately contribute to cyst progression.

hypervascularisation of cysts, increasing the cysts' nutrient intake, which is necessary to sustain their growth. On the other hand, it contributes to interstitial fibrosis by driving pro-fibrotic responses, ultimately leading to organ failure and contributing to ADPKD progression.

3.2 Inflammation

3.2.1 Renal injury

Following renal injury, both innate and adaptive immune responses intervene to respond to the tissue damage. Injured tubular epithelial cells release pro-inflammatory cytokines and chemokines, growth factors and adhesion molecules, such as interleukin-1 (IL-1), tumour necrosis factor-alpha (TNF-α), monocyte chemoattractant protein-1 (MCP-1) and TGF-β, which help with the recruitment and activation of immune cells[15]. This early pro-inflammatory response is crucial to clear the tissue from dead cells and cellular debris. At the same time, immune cells also secrete chemoattractant cytokines and growth factors in a self-perpetuating feedback loop that recruits and activates surrounding cells, stimulates angiogenesis and contributes further to the injury response. Two important pathways activated by this response are the nuclear factor-κB (NF-κB) pathway and the Janus kinase (JAK)-signal transducer and activator of transcription (STAT) pathway. The NF-κB pathway is activated by the pro-inflammatory cytokines secreted after injury (e.g., TNF-α, MCP-1), which bind to their specific ligands on the tubular cells resulting in the phosphorylation of the NF-κB inhibitor, IκB, and subsequent nuclear translocation of NF-κB complex[56]. Also JAK-STAT pathway is activated by pro-inflammatory cytokines (e.g., IL-6 and interferon-gamma/ INF-γ), which activate JAK that in turn, activates STAT proteins leading to their translocation into the nucleus[57]. The final effect of the activation of these two pathways is the transient transcription of pro-inflammatory genes that encodes for cytokines and growth factors, which sustain the recruitment of leucocytes to the site of injury. To counterbalance this first inflammatory phase, infiltrating leucocytes can also secrete anti-inflammatory and pro-fibrotic factors that lead to activation of myofibroblasts and ECM deposition. When these processes occur harmoniously together, and in collaboration with tubular epithelial cells, the injury can be successfully healed. Conversely, in case of persistent or extensive injury, chronic activation of this pro-inflammatory response together with the chronic production of anti-inflammatory and pro-fibrotic factors can result in a maladaptive repair and progressive fibrotic renal disease[58].

3.2.2 PKD

ADPKD cannot be defined as an inflammatory disorder. However, renal histology analysis of patients with ADPKD showed apparent interstitial inflammation and fibrosis in both minimally and severely cystic kidneys[59,60]. Also, pro-inflammatory molecules, such as TNF-α,

MCP-1, osteopontin and IL-1β can be found in the urine and cyst fluid of human patients[61-63]. Moreover, several studies described the accumulation of infiltrating inflammatory cells, such as macrophages and T cells, in the renal interstitium and urine of ADPKD patients[59,64,65] (Figure 3). Particularly, macrophages seem to have a key role in cyst progression. Transcriptome analysis in the congenital polycystic kidney (*cpk*) mutant mice (non-orthologous mice with a mutation in the *Cys1* gene), which are a model of cystic renal disease, showed that the most upregulated genes in the more progressive stages of disease were associated with the innate immune system, and particularly with the alternative macrophage activation pathway (M2-like macrophages)[66]. Furthermore, accumulation of M2-like macrophages around cyst was observed in several orthologous animal models for ADPKD[67,68]. Interestingly, accumulation of macrophages could already be observed at early stages and specifically around PC1 and PC2 deficient tubules[13,68]. Depletion of macrophages leads to the reduction of cyst-lining cell proliferation, lower cystic-index (percent of kidney occupied by cysts) and improved renal function in different mouse models[67,68]. Additionally, deletion of macrophage migration inhibitory factor (*Mif*) or pharmacological inhibition of MIF, which is upregulated in cyst-lining cells and is responsible for macrophage recruitment, resulted in reduced MCP-1-dependent macrophage accumulation in the cystic kidneys and subsequent delay of cyst growth in several PKD mouse models[69]. Since comparable results were observed in both orthologous (with a *Pkd1/2* mutant gene) and non-orthologous models (with mutations in genes other than *Pkd1/2*), it is plausible that M2-like macrophages have a common role in cyst development regardless of the genetic mutation that is causing it. Indeed, M2-like macrophages are able to stimulate tubular cells proliferation after injury, promoting tissue repair[70]. However, *in vitro* M2-like macrophages stimulated formation and proliferation of microcysts, and *in vivo* they might have increased the tubular proliferation observed after injury in a model of adult-induced cyst formation[68,71]. These results imply that M2-like macrophages in PKD have a detrimental role more than a protective one; thus, therapies that can target specifically this population in ADPKD patients might be beneficial.

3.2.2.1 Inflammatory cytokines

Among all the different inflammatory cytokines, TNF-α seems to have a particularly relevant role in cyst formation. High levels of TNF-α are found in cysts' fluids of ADPKD patients, and gene expression is increased in murine cystic kidneys, where it positively correlates with age and cyst size[61,72,73]. *In vitro*, stimulation of inner medullary collecting duct cells with TNF-α was accompanied with the altered subcellular localisation of PC2 and disruption of PC1-PC2 interaction. Moreover, both wild-type and *Pkd2*$^{+/-}$ embryonic kidney explants treated with TNF-α developed several cyst-like structures. *In vivo*, intraperitoneal injections of TNF-α increased the incidence of cyst formation in *Pkd2*$^{+/-}$ mice of 8.5 weeks of age. Additionally, also TNF-α receptor -I and -II, and TNF-α converting enzyme (TACE) are enriched in human ADPKD cyst fluids, where they contribute to accumulation and stabilisation of bioactive

TNF-α[74,75]. In fact, inhibition of TACE in *bpk* mice (non-orthologous model with mutation in the *Bicc1* gene) resulted in amelioration of PKD[76].

Another important inflammatory chemokine in ADPKD progression is MCP-1. MCP-1 is a pro-inflammatory cytokine that attracts monocytes at the site of injury[77]. Expression and urinary excretion of MCP-1 is increased already at early stages of the disease in rodent PKD models and human ADPKD patients[62,69,78]. Particularly, analysis of the urinary MCP-1 (uMCP-1) in patients from the TEMPO 3:4 trial, showed that uMCP-1 correlated with renal function and that tolvaptan treatment was able to reduce uMCP-1 levels[79]. Recently, *Cassini et al*. demonstrated that *Mcp-1* expression is increased after *Pkd1/2* deletion already in pre-cystic kidneys and prior to macrophage infiltration[80]. Increased MCP-1 levels led to the recruitment of pro-inflammatory macrophages (M1-like macrophages), which caused direct damage to tubules. Subsequently, these macrophages differentiated to M2-like macrophages, which stimulate tubules proliferation and cyst growth[80]. Genetic deletion of *Mcp-1* together with *Pkd1*, as well as administration of an MCP-1 receptor inhibitor, reduced macrophage infiltration, cyst growth and improved renal function and survival[80]. Therefore, targeting macrophage recruitment and activation might be a promising therapeutic approach in ADPKD. However, administration of an inhibitor of MCP-1 synthesis in a non-orthologous model of PKD in rats was able to reduce interstitial inflammation but did not affect cyst formation, questioning the importance of the MCP-1-recruited inflammatory infiltrates in cysts initiation[81].

3.2.2.2 Inflammatory cytokine related signalling pathways

The major inflammatory pathways activated in PKD are NF-κB and JAK-STAT. NF-κB complex proteins are regulators of transcription of several genes among which inflammatory genes like TNF-α, IL-1β and MCP-1[82]. Increased NF-κB activity has been described in several rodent models for PKD and human ADPKD[83-85]. Particularly, the expression of NF-κB proteins was described specifically in cyst-lining cells from early stages until more progressive ones both in human and rodent PKD model[85]. Interestingly, *in vitro* activation of NF-κB was observed following overexpression or depletion of *Pkd1* or *Pkhd1*, suggesting that upregulation of the NF-κB pathway might be an early feature of ADPKD[83,86,87]. Comparison of transcription profiles of AKI with those of rapidly progressive cystic kidneys revealed an extensive overlap of genes between injury and cyst progression, with the most enriched being NF-κB targets[23,88]. In agreement with these findings, NF-κB pathway inhibition using anti-inflammatory compounds successfully ameliorated PKD progression in animal models, indicating that NF-κB is a viable target for therapy[60,89-91]. However, more studies are needed to characterise the role of this pathway in inflammation in the context of ADPKD. Another link between inflammation and ADPKD is the JAK-STAT pathway. After an injury in normal cells, changes in fluid flow lead to proteolytic cleavage of the C-terminal tail of PC1, which is released

from the membrane and can translocate to the nucleus[7]. Here, PC1 tail can interact with JAK-activated STATs and other transcriptional coactivators (e.g., EBNA2 coactivator P100 and STAT6), participating in gene regulation and transient activation of pro-inflammatory cytokines and chemokines, which in turn recruit leucocyte to the injured tubules[9,10,92]. These findings suggest that PC1 regulation of STATs plays an important role in the transduction of mechanical stimuli from the cilia to the nucleus. Thus, in ADPKD local injury or defective ciliary signalling related to PC1/2 mutations interfere with the normal cilia-to-nucleus transduction and leads to persistent activation of JAK-STAT signalling. As a consequence, the production of pro-inflammatory and pro-fibrotic mediators is increased, ultimately contributing to driving cyst progression. Indeed, STAT3 and STAT6 have been described by several groups to be activated in cyst-lining cells in different PKD mouse models, and inhibition of STAT3 or STAT6 was able to ameliorate the cystic phenotype[93-96]. Consistent with these results, gene expression profiling in human and mouse cystic kidneys found JAK-STAT pathway and NF-κB pathway among the highest upregulated signalling pathways[23,55]. Thus, inhibition of the inflammatory response via modulation of NF-κB and/or JAK-STAT pathways seems to be a promising therapeutic strategy in PKD.

3.3 Growth factors

3.3.1 Renal injury

Recovery from renal injury requires that the damaged tubular cells are replaced with new ones ensuring that the structure and function of the nephrons are restored. For this purpose, the cells that participate in the repair process produce growth factors (GFs), which modulate metabolism, proliferation and differentiation, and allow the tissue to adapt to the injury and finally resolve it. Indeed, there are several lines of evidence showing that administration of epidermal growth factor (EGF), insulin-like growth factor (IGF) and hepatocyte growth factor (HGF) ameliorate the outcome of acute kidney injury, although for some of the GFs the evidence are still controversial[97-101]. Nevertheless, once the injury is repaired, these stimuli should stop. In the case of maladaptive repair, persistent and/or aberrant expression of GFs can lead to the development of fibrosis. Several other GFs have been implicated in fibrosis and CKD progression, i.e. TGF-β1, TGF-α, connective tissue growth factor (CTGF), vascular endothelial growth factor (VEGF), platelet-derived growth factor (PDGF) and fibroblast growth factor (FGF)[35,102-105].

3.3.2 PKD

Several of these GFs are also upregulated in ADPKD. Probably the best described are TGF-β1, which we already covered in a previous paragraph, and EGF (Figure 4). EGF and EGF family ligands (e.g., TGF-α and heparin-binding EGF/HB-EGF) play an important role in renal cyst expansion. This is based on the fact that cystic epithelial cells have higher expression of

EGF, TGF-α and HB-EGF[106,107]. Transgenic overexpression of *Tgf-α* in mice resulted in cyst formation and accelerated PKD progression in *pcy* mice (non-orthologous model with mutation in the *Nphp3* gene)[108,109]. Moreover, these ligands are found abundantly in cyst fluid of ADPKD patients, and stimulation of cultured epithelial cells with cysts fluid promotes cyst formation and expansion *in vitro*[110]. Interestingly, cystic epithelial cells isolated from ADPKD patients are more responsive to the proliferative stimulus of EGF[111]. Additionally, the EGF family ligands receptors (EGFR) are expressed at the basal side of normal adult tubular epithelial cells, while in ADPKD kidneys, they are also localised on the apical side[112,113]. As a consequence, the cystic epithelium establishes an autocrine loop where EGF is synthesised, released into the cyst lumen and utilised by the same cyst-lining epithelial cells, thereby driving their proliferation and cyst expansion. Further evidence is provided by *in vivo* experiments. *Orpk* mice (non-orthologous model with a mutation in *Tg737* gene) with an EGFR mutation that results in reduced EGFR tyrosine kinase activity showed a significant reduction of collecting tubular cysts compared to mice without this mutation. These findings paved the road to therapies that target the tyrosine kinase activity of the EGFR to ameliorate PKD progression[114]. Indeed, treatment with an inhibitor of EGFR tyrosine activity in *Han:SPRD-Cy/+* rats (a non-orthologous model with a mutation in *Anks6* gene), or combination treatment of an EGFR inhibitor together with the reduction of TGF-α in a mouse model of ARPKD (Autosomal Recessive PKD), were successful in reducing cyst formation and increasing survival[115,116]. However, these molecules affect not only the cystic epithelium but all the proliferating epithelia with broad adverse effects, which are not compatible with the life-long treatment necessary in ADPKD where tolerability is a major concern.

Also, other GFs, including IGF1, HGF, VEGF, PDGF, FGF and CTGF have been described to be involved in ADPKD. Increased gene expression of IGF1 and other IGF family members is observed in murine and human renal cysts and is associated with hyperproliferation of *Pkd1* mutant cystic cells[55,117]. HGF and its receptor, the tyrosine kinase receptor c-Met, are overexpressed in cyst-lining epithelial cells in human ADPKD, and levels of HGF are increased in proximal cysts fluid[118]. *In vitro*, *Pkd1*$^{-/-}$ cells showed defective ubiquitination of c-Met after HGF stimulation with a subsequent c-Met-dependent increase of the PI3K/Akt/mTOR signalling pathway[119]. This suggests that, as for IGF-1, also HGF and its receptor may contribute to epithelial cystic cells growth in an autocrine manner.

For other GFs, the effect is a bit broader and also extends to the interstitial cells. VEGF is an angiogenic cytokine that plays pivotal roles in the maintenance of the vascular networks. In rodent and human kidneys, VEGF is lowly expressed in the epithelium of the glomerulus and in collecting ducts[120,121]. On the contrary, in ADPKD VEGF and VEGF receptor-1 are expressed in some of the cysts and dilated tubules epithelial cells, which are also able to secrete VEGF when grown *in vitro*[121,122]. Consistently, increased levels of VEGF are detected in serum and

cystic fluids of *Cy/+* rats[121]. Overexpression of VEGF in mice using a transgenic mouse model (Pax8-rtTA/(tetO)$_7$VEGF) resulted in dose-dependent cyst formation and activation and proliferation of interstitial fibroblasts[102]. However, epithelial cells-secreted VEGF acts also in an autocrine fashion on cell proliferation. In fact, administration of ribozymes targeting mRNA of VEGF receptor 1 and 2 reduced the expression of the receptors in tubular cells with subsequent inhibition of proliferation of cystic epithelial cells[121]. Additionally, administration of VEGFC, a member of VEGF family normally downregulated in PKD, to *Pkd1*$^{nl/nl}$ mice led to the normalisation of the pericystic vascular vessels, reduction of M2-like macrophages infiltration and, in *Cys1*$^{cpk/cpk}$ mice, increase in life span[101]. Altogether, these results suggest that tubular cells in ADPKD aberrantly express VEGF, which in turn stimulates tubular cells,

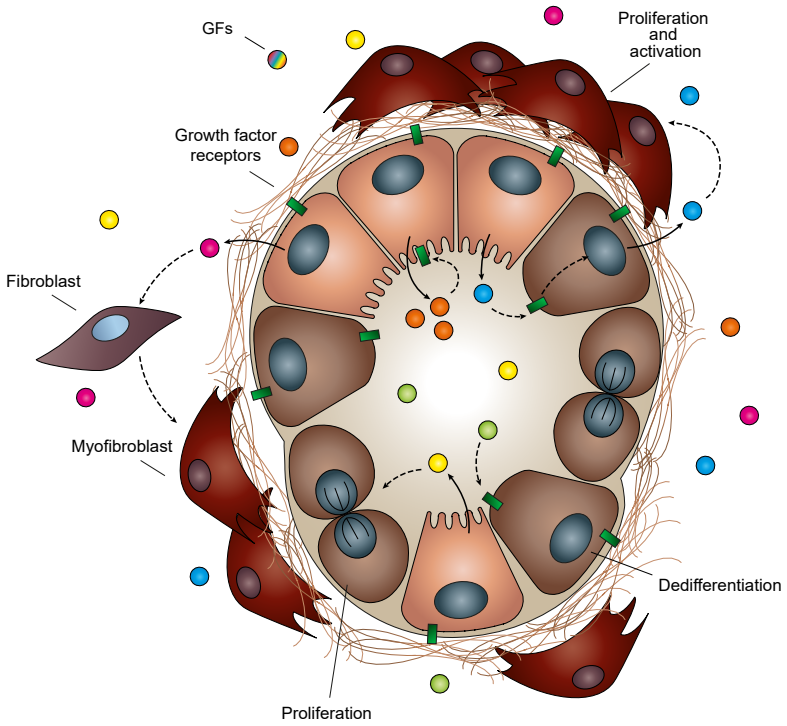

Figure 4. Growth factors (GFs) affecting cyst progression

After injury, secretion of GFs helps to replace the damaged tubular cells. In ADPKD, GFs are produced and secreted in the lumen of the tubules. For example, EGF and other EGF family ligands are overexpressed in cystic epithelial cells and accumulate in the cystic fluids. At the same time, EGF receptors are mislocalised at the apical side of cells in the cystic epithelium. As a result, EGF secreted in the lumen of the cysts can interact with its receptor establishing an autocrine and paracrine loop that drives proliferation and cyst expansion. Another well-known GF in PKD is TGF-β. Cystic epithelial cells often show increased TGFβ expression and nuclear phopspho-SMAD2 staining. TGFβ promotes dedifferentiation of epithelial cells into a more mesenchymal type, as well as ECM deposition and activation of myofibroblasts, contributing to the cystic phenotype. Some GFs like CTGF, but also PDGF and FGF, can be secreted in the interstitial space surrounding the cysts. Here, they can stimulate resident fibroblasts to differentiate into active myofibroblasts, but also sustain myofibroblasts proliferation and activation, with a subsequent extracellular matrix deposition, further contributing to cysts growth.

interstitial fibroblasts and endothelial cells, contributing to disease progression. Thus, targeting VEGF signalling cascade in PKD seems to be a viable therapeutic option. However, treatment of *Cy/+* rats with an anti-VEGF-A antibody led to exacerbation of the cystic disease and severe kidney injury, highlighting the need for more studies to better characterise the role of the different VEGF molecules and their receptors in kidney injury and cyst growth[123].

Other GFs involved in ADPKD, such as PDGF, FGF and CTGF, showed an effect mainly on interstitial cells (Figure 4). PDGF expression, especially PDGF-B, was found in cyst-lining epithelial cells using immunohistochemistry in a human ADPKD kidney[124]. However, PDGF did not show a mitogenic effect on epithelial cells *in vitro* but was able to stimulate the proliferation of ADPKD-derived fibroblasts *in vitro* more effectively than with healthy-derived fibroblasts[125]. A similar effect was observed upon FGF stimulation, which caused ADPKD-derived fibroblasts to proliferate more, produce and release more FGF and elicit a more consistent and lasting tyrosine phosphorylation signalling cascade compared to normal renal fibroblasts[126]. CTGF is most known for its role as a driver of interstitial fibrosis mediating, at least in part, the TGF-β pro-fibrotic program[127]. In normal kidneys, it is expressed mainly in the glomerulus, but in injured tubules and cystic kidneys, its expression is increased particularly at more advanced stages of the disease, in areas of focal fibrosis and in interstitial cells surrounding the cystic epithelium[128-130]. In addition to its role in renal fibrosis, CTGF can also participate in the recruitment of inflammatory cells by activating the NF-κB pathway[131]. Thus, CTGF is a common factor in renal fibrosis, both in injury and ADPKD, and might contribute to the progression of the cystic disease towards the end-stage. Anti-CTGF therapies using a human monoclonal antibody that targets CTGF have successfully improved fibrosis in several animal models and have been tested in clinical trials for pulmonary fibrosis, pancreatic cancer and diabetic kidney disease without notable adverse effects[127]. No data is available about a possible effect on PKD progression, but based on its positive effect on fibrosis and good tolerability, it is plausible to think that anti-CTGF drugs might be a useful adjuvant therapy in ADPKD.

Overall, GFs secreted by cystic tubular epithelial cells trigger surrounding epithelial and interstitial cells to produce proliferative and profibrotic factors, which regulate cyst growth and interstitial fibrosis observed in ADPKD progression.

3.4 Reactivation of developmental pathways

Gene expression analysis of human and rodent kidneys after injury and during CKD compared to healthy control kidneys unveiled aberrant expression of genes that belong to the Notch, wingless-related integration site (Wnt), hedgehog (Hh) and Hippo pathways[132-134]. Although these evolutionarily conserved pathways are regulated and signal through different

routes, they have in common a role in renal development, and illustrate the reactivation of developmental pathways in the injury-repair response[24,135]. However, prolonged activation of these developmental pathways due to chronic or repetitive injury may lead to a maladaptive response and CKD[136,137]. Also in ADPKD, gene expression analysis found signs of cell dedifferentiation and upregulation of developmental and mitogenic signalling pathways[55]. As observed after injury, genes belonging to Notch, Wnt, Hh and Hippo pathways are upregulated in ADPKD, in line with the idea that injury-repair and ADPKD progression share common molecular mechanisms[55].

3.4.1 Notch signalling pathway

3.4.1.1 Renal injury

Notch pathway controls cell proliferation, differentiation and cell fate[138]. During renal development, Notch2 downregulates Six2, a transcription factor expressed in nephron progenitor cells, by suppressing its upstream regulator, Pax2. This leads to the reduction of the progenitor pools in favour of the differentiation of proximal tubular cells[139,140]. Persistent activation of Notch signalling is associated with kidney fibrosis, which is ameliorated with the administration of Notch inhibitors[141]. Interestingly, a well-characterized Notch signalling partner is TGF-β, a known driver of fibrosis. Indeed, TGF-β can directly regulate downstream targets of Notch, and the targets *Hes* and *Hey*, and can induce the expression of Notch ligand *Jag1*. At the same time, the increased level of Notch can stimulate TGF-β expression, creating a positive-feedback loop that sustains renal fibrosis[133,142,143].

3.4.1.2 PKD

Notch signalling genes are enriched in ADPKD, in line with the dedifferentiation and increased proliferation of tubular epithelial cells[144-146]. Protein expression analysis of Notch signalling components in mouse and human ADPKD kidneys revealed increased expression in cysts lining epithelium. Particularly, Notch3 activation was increased, and *in vitro* inhibition of Notch resulted in reduced proliferation and cyst formation in 3D culture of primary human ADPKD cells[82]. Thus, modulation of Notch signalling may be an interesting therapeutic approach to prevent fibrosis and cyst growth. However, there is evidence showing that reduction of Notch signalling during nephrogenesis leads to proximal tubular cysts due to loss of oriented cell division, suggesting that the effect of this pathway on cyst progression might be more complex[145].

3.4.2 Wnt signalling

3.4.2.1 Renal injury

Wnt signalling pathways regulate a range of cellular processes including proliferation,

migration and polarity, thereby contributing to organ homeostasis. They are normally classified in canonical, which involves activation and nuclear translocation of β-catenin, and noncanonical, which is β-catenin-independent and includes the Wnt/planar cell polarity (PCP) route. In kidney morphogenesis, Wnt orchestrates the mesenchyme-to-epithelial transition necessary for nephrogenesis[147]. The involvement of aberrantly activated canonical Wnt pathway with renal fibrosis has been extensively shown in different injury animal model, as reviewed elsewhere[148].

3.4.2.2 PKD

In the context of ADPKD, transgenic mice with increased β-catenin activation present with renal cyst development[149-151]. Moreover, PC1 interacts with β-catenin at the plasma membrane, at cell-cell contacts and in the nucleus, suggesting that PC1 may have an important regulatory role on Wnt signalling[8,26,152]. Once this regulation is lost, for example due to *Pkd1* mutation, the resulting aberrant Wnt pathway activation might contribute to cyst formation. Indeed, one of the major downstream targets of the Wnt signalling, c-MYC, is upregulated in ADPKD, especially in the cystic tubular epithelium[153]. Specific overexpression of *c-Myc* in renal epithelial cells mimicked human ADPKD, and both direct and indirect inhibition of c-Myc *in vivo* resulted in amelioration of the cystic phenotype, placing this protein in a central position in PKD progression[153]. Interestingly, renal injury caused by ischemia-reperfusion (IRI) was associated with activation of Wnt signalling and increase in *c-Myc* expression both in transgenic *Pkd1* mice and non-transgenic control mice, in line with the idea that injury activates pathways involved in PKD progression[22].

Also noncanonical Wnt signalling has been implicated in cyst formation, in particular, the PCP route. PCP orchestrate cell polarity within the plane of epithelial cells and is essential to establish proper cell function and organ architecture[154]. Alteration of oriented cell division (OCD) has been associated with cyst formation[18,155]. However, a recent publication demonstrated that, although altered OCD is a feature of expanding cysts, it is not sufficient nor necessary for cyst initiation after *Pkd1/2* mutation, thus challenging the role of PCP in cyst formation[156]. In chapter 2, we investigate the role of Four-jointed box-1, a component of the PCP route.

3.4.3 Hh signalling pathway

3.4.3.1 Renal injury

The Hh signalling pathway controls embryonic development and tissue homeostasis. Deregulation of this pathway during kidney morphogenesis is associated with severe malformations, indicating that Hh signalling plays a critical role in this process[157]. In mammals, there are three Hh homologous. One of them, sonic hedgehog (Shh) is induced

early after renal injury in tubular epithelial cells and has been implicated in the pathogenesis of fibrosis and CKD by acting on interstitial fibroblasts leading to their activation and ECM deposition. Moreover, Hh signalling pathway can interact and cooperate with other key pathways known to be drivers of fibrosis, such as TGF-β, canonical Wnt and Notch[136,158].

3.4.3.2 PKD

The connection between Hh signalling and ADPKD is complex and mainly via cilia-dependent signalling. Mutations in ciliary genes lead to cystic renal disease, but also aberrant Hh signalling[159-161]. Also, the loss of a functional component of the Hh pathway, Glis2, resulted in the development of nephronophthisis in human and mice[162]. In the context of PKD, downregulation of Hh signalling is accompanied by reduced proliferation and cyst formation in *Pkd1* mutant mice and human primary ADPKD cell cultures[163,164]. However, a recent study using a conditional mouse model lacking *Pkd1* in combination with three Hh signalling members (*Smo*, *Gli2* and *Gli3*) demonstrated that Hh pathway is not required for cyst formation in mouse models of developmental or adult-onset of ADPKD[165]. Thus, it seems that the Hh pathway does not have a causative role for the disease *in vivo*, but it might contribute to disease progression due to its effect on renal fibrosis.

3.4.4 Hippo signalling pathway

3.4.4.1 Renal injury

The Hippo pathway regulates tissue growth and development. Unlike the pathways mentioned above, which are activated by the binding of specific ligands, a diversity of upstream Hippo pathway regulators have been identified. Identified upstream signals include cell polarity, cell junctions, cytoskeleton, mechanical forces, GPCR ligands and stress signals[166]. The core components of the Hippo pathway are a group of kinases (mammalian Ste20 like kinases 1/2 or MST1/2 and large tumour suppressor 1/2 or LTS1/2), which are responsible for the phosphorylation of the final effectors Yes-associated protein (YAP) and transcriptional coactivator with PDZ-binding motif (TAZ). When the Hippo pathway is activated, YAP and TAZ are phosphorylated and restrained into the cytoplasm; when the Hippo pathway is inactive, YAP and TAZ are unphosphorylated and can translocate to the nucleus where they can bind with a series of transcription factors, such as TEAD 1-4 but also SMADs and β-catenin, and regulate the transcription of a wide range of genes involved in cell proliferation, apoptosis and migration[167,168]. In renal development, mutations of the core kinases or the final effector YAP, lead to disruption of nephrogenesis[169,170]. Interestingly, deletion of the orthologous protein TAZ in a developmental mouse model does not impair nephrogenesis but results in renal cyst formation. This indicates that these two proteins, although having largely redundant functions, also have distinct roles[171]. In kidney injury, nuclear accumulation of YAP and TAZ is observed in both in epithelial and interstitial cells in

several models of injury. In particular, Yap expression is observed in dedifferentiated tubular cells in AKI-to-CKD transition, confirming that the Hippo pathway has a role in injury-repair mechanism[137]. Moreover, after injury, ECM production causes the tissue stiffness to increase, providing the driving cue for fibroblast TGF-β activation. The mechanosensitive response to TGF-β-induced activation of renal fibroblasts is mediated by YAP/TAZ, which interact with SMAD2/3, translocate to the nucleus and drive transcription of profibrotic genes[172].

3.4.4.2 PKD

Increased nuclear localisation of YAP and TAZ has been described in several diseases, among which ADPKD and nephronophthisis[129,173]. Moreover, zebrafish mutant for *Pkd2* and *Scrib*, a member of the SCRIB complex involved in the establishment and maintenance of cell polarity, showed increased nuclear YAP. Interestingly, expression of cytoplasmic but not nuclear YAP could rescue the phenotype, suggesting that cytoplasmic YAP has a role in the suppression of cyst formation[174]. Knock-out of *Yap* in a *Pkd1* mutant mouse model was able to reduce PKD progression mildly, and the effect was even increased by concomitant knock-out of *Taz*. In particular, YAP target, c-MYC, was found to critically contribute to kidney cystogenesis, implicating the Hippo pathway in the pathogenesis of PKD[175]. Interestingly, expression of *Ctgf*, a known YAP/TAZ target[176], which is also induced by TGF-β[127], was increased in *Pkd1* mutant mice but only in those presenting clear signs of fibrosis, suggesting that a certain level of signal crosstalk between TGF-β and Hippo pathways is occurring in the PKD context as well[129]. For its role in modulating cell proliferation and cell migration and fibrosis, Hippo pathway regulation has been proposed as a possible strategy to ameliorate ADPKD progression by acting on two major aspects of the disease. However, administration of YAP-specific antisense oligonucleotides (ASOs) in adult *Pkd1* mutant mouse model did not result in a reduction of cyst growth (data presented in chapter 3). Such results, together with the cystic effect of TAZ deletion in a developmental mouse model, suggest that the role of these proteins and the effect of targeting them in PKD is complex and need further characterisation[171].

3.5 Transcription factors (TFs) and epigenetics in renal injury and PKD

Injury-repair is a complex mechanism that involves several cell types and requires the modulation of a plethora of signalling pathways. Thus, a perfect time- and space-regulated transcription program is paramount for the good outcome of the tissue injury response. For this reason, a series of transcription factors (TFs) and epigenetic changes intervene to orchestrate all the different steps we discussed above, which ultimately lead to organ repair[177]. Altered TFs expression or epigenetic regulation can interfere with injury-repair and lead to CKD[178] and orchestrate and modulate signalling in PKD.

Gene expression analysis in ADPKD revealed dysregulation of TFs, many of which are involved in key processes of kidney development. Interestingly, from a meta-analysis study that identified a set of 1515 genes dysregulated in PKD emerged that 92 of them are TFs, and that about 35% of the identified TFs are known to be involved in injury-repair mechanisms (further shown in chapter 5). Mutations in *Pkd1* are also associated with other epigenetic changes, such as increased expression of DNA methyltransferases (DNMTs), histone deacetylases (HDACs) and bromodomain proteins[179]. For example, SET and MYND domain 2 (SMYD2) protein is a lysine methyltransferase upregulated in PKD. Inhibition of SMYD2 was able to delay cysts growth via interfering with SMYD2-dependent activation of STAT3 and the p65 subunit of NF-κB[180]. Treatment with HDACs inhibitors has also been proven effective in delaying cyst growth and preserving renal function in several *Pkd1/2* mutant mouse models, pointing to epigenetic modifiers drugs as promising candidates for PKD treatment[181-186]. Moreover, epigenetic changes such as hypomethylation of the *Pkd1* gene-body have been described in cystic tissues from ADPKD patients[187,188]. These modifications can interfere with the normal expression of *Pkd1* and might be responsible for disease progression.

4. Conclusions

Altogether, the current knowledge suggests that injury-repair mechanisms are part of ADPKD progression. The two events are so intertwined that it is difficult to dissect them. Indeed, injury can cause or accelerate cyst formation, but at the same time, cyst enlargement is a source of local injury, establishing an injury-like cyst milieu that exacerbates renal function decline. Further investigations are required to be able to separate a direct effect of the polycystins on the cyst initiating dysfunctional molecular mechanisms, from the secondary effects of disease progression and cyst expansion.

5. Aim and outline of the thesis

There is a consistent body of literature that describes the strong connections between the injury-repair mechanisms and ADPKD progression. The scope of this thesis is to identify and investigate molecular pathways involved in injury-repair and ADPKD progression to better characterise the steps in disease progression, and provide new cues for future studies and therapeutic approaches.

In **chapter 2,** we investigate the role of Four-jointed box protein 1 (FJX1) in injury and ADPKD progression. FJX1 is a Golgi kinase implicated in the regulation of two important dysregulated pathways in ADPKD: planar cell polarity (PCP) and Hippo signalling. In a previous study performed in our group, FJX1 was found aberrantly expressed during both the injury-repair

phase and PKD progression in mice, suggesting a possible role for FJX1 in cyst formation and progression. Specifically, we investigated if genetic deletion of FJX1 might influence PCP or Hippo pathway regulation, and result in a modification of the normal PKD progression. We did not find any evidence for differential regulation of PCP or Hippo pathway. However, we observed an effect of FJX1 on fibrosis and cellular infiltrates.

In **chapter 3,** we investigate further the role of the Hippo pathway in PKD progression. Hippo pathway is a highly conserved signalling pathway that regulates organ size. Several of the molecular mechanism modulated by Hippo pathways are also central to cyst growth. Indeed, in a previous study, we observed increased expression of one of the downstream effectors of the Hippo pathway, YAP, in the nucleus of the cystic epithelium. Therefore, in chapter 3 we hypothesise that reducing YAP level in *Pkd1* KO mice might ameliorate the cystic phenotype. We decided to take an approach based on antisense oligonucleotides (ASO) that target specifically YAP transcripts leading to a significant reduction of expression in the kidneys. We found no effect on cyst progression. We also investigated the effect of *Yap* or *Taz* knock-out on cyst formation *in vitro* using a 3D cyst assay.

In **chapter 4,** we use a combined approach based on RNAseq analysis of in house generated *Pkd1*-mutant mouse model and a meta-analysis of publicly available PKD expression profile to identify a list of genes normally dysregulated in PKD. Moreover, we investigated the link between PKD progression and injury-repair mechanisms. Finally, we employed different *Pkd1*-mutant mice, with or without toxic renal injury, to validate the findings.

In **chapter 5,** we elaborate on the work presented in chapter 4 using computational analysis. We primarily focus on the transcription factors (TFs) altered during both PKD progression and injury-repair. We validated our computational analysis with wet-lab experiments, including qPCR, immunohistochemistry, and chromatin immunoprecipitation.

Lastly, a general overview of the results described in the previous chapters and suggestions for future research are discussed in **chapter 6**.

References

1 Willey, C. J. *et al.* Prevalence of autosomal dominant polycystic kidney disease in the European Union. *Nephrol Dial Transplant* **32**, 1356-1363, doi:10.1093/ndt/gfw240 (2017).

2 Igarashi, P. Genetics and Pathogenesis of Polycystic Kidney Disease. *Journal of the American Society of Nephrology* **13**, 2384-2398, doi:10.1097/01.asn.0000028643.17901.42 (2002).

3 Takiar, V. & Caplan, M. J. Polycystic kidney disease: pathogenesis and potential therapies. *Biochim Biophys Acta* **1812**, 1337-1343, doi:10.1016/j.bbadis.2010.11.014 (2011).

4 Fedeles, S. V., Gallagher, A. R. & Somlo, S. Polycystin-1: a master regulator of intersecting cystic pathways. *Trends Mol Med* **20**, 251-260, doi:10.1016/j.molmed.2014.01.004 (2014).

5 Sutters, M. & Germino, G. G. Autosomal dominant polycystic kidney disease: molecular genetics and pathophysiology. *J Lab Clin Med* **141**, 91-101, doi:10.1067/mlc.2003.13 (2003).

6 Ong, A. C. & Harris, P. C. Molecular pathogenesis of ADPKD: the polycystin complex gets complex. *Kidney Int* **67**, 1234-1247, doi:10.1111/j.1523-1755.2005.00201.x (2005).

7 Chauvet, V. *et al.* Mechanical stimuli induce cleavage and nuclear translocation of the polycystin-1 C terminus. *J Clin Invest* **114**, 1433-1443, doi:10.1172/JCI21753 (2004).

8 Lal, M. *et al.* Polycystin-1 C-terminal tail associates with beta-catenin and inhibits canonical Wnt signaling. *Hum Mol Genet* **17**, 3105-3117, doi:10.1093/hmg/ddn208 (2008).

9 Low, S. H. *et al.* Polycystin-1, STAT6, and pathway that transduces P100 function in a ciliary mechanosensation and is activated in polycystic kidney disease. *Dev Cell* **10**, 57-69, doi:10.1016/j.devcel.2005.12.005 (2006).

10 Talbot, J. J. *et al.* Polycystin-1 regulates STAT activity by a dual mechanism. *Proc Natl Acad Sci U S A* **108**, 7985-7990, doi:10.1073/pnas.1103816108 (2011).

11 Happe, H. & Peters, D. J. Translational research in ADPKD: lessons from animal models. *Nat Rev Nephrol* **10**, 587-601, doi:10.1038/nrneph.2014.137 (2014).

12 Leonhard, W. N., Happe, H. & Peters, D. J. Variable Cyst Development in Autosomal Dominant Polycystic Kidney Disease: The Biologic Context. *J Am Soc Nephrol* **27**, 3530-3538, doi:10.1681/ASN.2016040425 (2016).

13 Leonhard, W. N. *et al.* Scattered Deletion of PKD1 in Kidneys Causes a Cystic Snowball Effect and Recapitulates Polycystic Kidney Disease. *Journal of the American Society of Nephrology* **26**, 1322-1333, doi:10.1681/Asn.2013080864 (2015).

14 Humphreys, B. D. *et al.* Intrinsic epithelial cells repair the kidney after injury. *Cell Stem Cell* **2**, 284-291, doi:10.1016/j.stem.2008.01.014 (2008).

15 Bonventre, J. V. & Yang, L. Cellular pathophysiology of ischemic acute kidney injury. *J Clin Invest* **121**, 4210-4221, doi:10.1172/JCI45161 (2011).

16 Chawla, L. S., Eggers, P. W., Star, R. A. & Kimmel, P. L. Acute Kidney Injury and Chronic Kidney Disease as Interconnected Syndromes. *New Engl J Med* **371**, 58-66, doi:10.1056/NEJMra1214243 (2014).

17 Weimbs, T. Polycystic kidney disease and renal injury repair: common pathways, fluid flow, and the function of polycystin-1. *Am J Physiol Renal Physiol* **293**, F1423-1432, doi:10.1152/ajprenal.00275.2007 (2007).

18 Patel, V. *et al.* Acute kidney injury and aberrant planar cell polarity induce cyst formation in mice lacking renal cilia. *Hum Mol Genet* **17**, 1578-1590, doi:10.1093/hmg/ddn045 (2008).

19 Takakura, A. *et al.* Renal injury is a third hit promoting rapid development of adult polycystic kidney disease. *Hum Mol Genet* **18**, 2523-2531, doi:10.1093/hmg/ddp147 (2009).

20 Happe, H. *et al.* Toxic tubular injury in kidneys from Pkd1-deletion mice accelerates cystogenesis accompanied by dysregulated planar cell polarity and canonical Wnt signaling pathways. *Hum Mol Genet* **18**, 2532-2542, doi:10.1093/hmg/ddp190 (2009).

21 Bastos, A. P. *et al.* Pkd1 haploinsufficiency increases renal damage and induces microcyst formation following ischemia/reperfusion. *J Am Soc Nephrol* **20**, 2389-2402, doi:10.1681/ASN.2008040435 (2009).

22 Kurbegovic, A. & Trudel, M. Acute kidney injury induces hallmarks of polycystic kidney disease. *Am J Physiol Renal Physiol* **311**, F740-F751, doi:10.1152/ajprenal.00167.2016 (2016).

23 Malas, T. B. *et al.* Meta-analysis of polycystic kidney disease expression profiles defines strong involvement of injury repair processes. *American Journal of Physiology - Renal Physiology* **312**, F806-F817 (2017).

24 Little, M. H. & Kairath, P. Does Renal Repair Recapitulate Kidney Development? *Journal of the American Society of Nephrology* **28**, 34-46, doi:10.1681/asn.2016070748 (2017).

25 Charron, A. J., Nakamura, S., Bacallao, R. & Wandinger-Ness, A. Compromised cytoarchitecture and polarized trafficking in autosomal dominant polycystic kidney disease cells. *J Cell Biol* **149**, 111-124, doi:10.1083/jcb.149.1.111 (2000).

26 Roitbak, T. *et al.* A polycystin-1 multiprotein complex is disrupted in polycystic kidney disease cells. *Mol Biol Cell* **15**, 1334-1346, doi:10.1091/mbc.E03-05-0296 (2004).

27 Drummond, I. A. Polycystins, focal adhesions and extracellular matrix interactions. *Biochim Biophys Acta* **1812**, 1322-1326, doi:10.1016/j.bbadis.2011.03.003 (2011).

28 Witzgall, R., Brown, D., Schwarz, C. & Bonventre, J. V. Localization of proliferating cell nuclear antigen, vimentin, c-Fos, and clusterin in the postischemic kidney. Evidence for a heterogenous genetic response among nephron segments, and a large pool of mitotically active and dedifferentiated cells. *J Clin Invest* **93**, 2175-2188, doi:10.1172/JCI117214 (1994).

29 Nadasdy, T., Laszik, Z., Blick, K. E., Johnson, L. D. & Silva, F. G. Proliferative activity of intrinsic cell populations in the normal human kidney. *J Am Soc Nephrol* **4**, 2032-2039 (1994).

30 Zuk, A. & Matlin, K. S. Induction of a laminin isoform and alpha(3)beta(1)-integrin in renal ischemic injury and repair in vivo. *Am J Physiol Renal Physiol* **283**, F971-984, doi:10.1152/ajprenal.00176.2002 (2002).

31 Joly, D. *et al.* Laminin 5 regulates polycystic kidney cell proliferation and cyst formation. *J Biol Chem* **281**, 29181-29189, doi:10.1074/jbc.M606151200 (2006).

32 Shannon, M. B., Patton, B. L., Harvey, S. J. & Miner, J. H. A hypomorphic mutation in the mouse laminin alpha5 gene causes polycystic kidney disease. *J Am Soc Nephrol* **17**, 1913-1922, doi:10.1681/ASN.2005121298 (2006).

33 Basile, D. P., Rovak, J. M., Martin, D. R. & Hammerman, M. R. Increased transforming growth factor-beta 1 expression in regenerating rat renal tubules following ischemic injury. *Am J Physiol* **270**, F500-509, doi:10.1152/ajprenal.1996.270.3.F500 (1996).

34 Massague, J. TGFbeta signalling in context. *Nat Rev Mol Cell Biol* **13**, 616-630, doi:10.1038/nrm3434

(2012).

35 Border, W. A. & Noble, N. A. TGF-beta in kidney fibrosis: a target for gene therapy. *Kidney Int* **51**, 1388-1396, doi:10.1038/ki.1997.190 (1997).

36 Gewin, L. S. Transforming Growth Factor-beta in the Acute Kidney Injury to Chronic Kidney Disease Transition. *Nephron*, 1-4, doi:10.1159/000500093 (2019).

37 Chea, S. W. & Lee, K.-B. TGF-β Mediated Epithelial-Mesenchymal Transition in Autosomal Dominant Polycystic Kidney Disease. *Yonsei Medical Journal* **50**, doi:10.3349/ymj.2009.50.1.105 (2009).

38 Hassane, S. *et al.* Elevated TGFβ-Smad signalling in experimental Pkd1 models and human patients with polycystic kidney disease. *The Journal of Pathology*, n/a-n/a, doi:10.1002/path.2734 (2010).

39 Egorova, A. D. *et al.* Tgfbeta/Alk5 signaling is required for shear stress induced klf2 expression in embryonic endothelial cells. *Dev Dyn* **240**, 1670-1680, doi:10.1002/dvdy.22660 (2011).

40 Grabias, B. M. & Konstantopoulos, K. Notch4-dependent antagonism of canonical TGF-beta1 signaling defines unique temporal fluctuations of SMAD3 activity in sheared proximal tubular epithelial cells. *Am J Physiol Renal Physiol* **305**, F123-133, doi:10.1152/ajprenal.00594.2012 (2013).

41 Kunnen, S. J. *et al.* Fluid shear stress-induced TGF-beta/ALK5 signaling in renal epithelial cells is modulated by MEK1/2. *Cell Mol Life Sci* **74**, 2283-2298, doi:10.1007/s00018-017-2460-x (2017).

42 Altieri, P. *et al.* Transforming growth factor beta blocks cystogenesis by MDCK epithelium in vitro by enhancing the paracellular flux: implication of collagen V. *J Cell Physiol* **177**, 214-223, doi:10.1002/(SICI)1097-4652(199811)177:2<214::AID-JCP3>3.0.CO;2-Q (1998).

43 Elberg, D., Jayaraman, S., Turman, M. A. & Elberg, G. Transforming growth factor-beta inhibits cystogenesis in human autosomal dominant polycystic kidney epithelial cells. *Exp Cell Res* **318**, 1508-1516, doi:10.1016/j.yexcr.2012.03.021 (2012).

44 Leonhard, W. N. *et al.* Inhibition of Activin Signaling Slows Progression of Polycystic Kidney Disease. *J Am Soc Nephrol* **27**, 3589-3599, doi:10.1681/ASN.2015030287 (2016).

45 Mack, M. & Yanagita, M. Origin of myofibroblasts and cellular events triggering fibrosis. *Kidney Int* **87**, 297-307, doi:10.1038/ki.2014.287 (2015).

46 Ow, C. P. C., Ngo, J. P., Ullah, M. M., Hilliard, L. M. & Evans, R. G. Renal hypoxia in kidney disease: Cause or consequence? *Acta Physiol (Oxf)* **222**, e12999, doi:10.1111/apha.12999 (2018).

47 Wei, W., Popov, V., Walocha, J. A., Wen, J. & Bello-Reuss, E. Evidence of angiogenesis and microvascular regression in autosomal-dominant polycystic kidney disease kidneys: a corrosion cast study. *Kidney Int* **70**, 1261-1268, doi:10.1038/sj.ki.5001725 (2006).

48 Kim, K., Drummond, I., Ibraghimov-Beskrovnaya, O., Klinger, K. & Arnaout, M. A. Polycystin 1 is required for the structural integrity of blood vessels. *P Natl Acad Sci USA* **97**, 1731-1736, doi:DOI 10.1073/pnas.040550097 (2000).

49 Liu, D. *et al.* A Pkd1-Fbn1 genetic interaction implicates TGF-beta signaling in the pathogenesis of vascular complications in autosomal dominant polycystic kidney disease. *J Am Soc Nephrol* **25**, 81-91, doi:10.1681/ASN.2012050486 (2014).

50 Sharif-Naeini, R. *et al.* Polycystin-1 and -2 dosage regulates pressure sensing. *Cell* **139**, 587-596, doi:10.1016/j.cell.2009.08.045 (2009).

51 Lorthioir, A. *et al.* Polycystin deficiency induces dopamine-reversible alterations in flow-mediated

dilatation and vascular nitric oxide release in humans. *Kidney Int* **87**, 465-472, doi:10.1038/ki.2014.241 (2015).

52 Brookes, Z. L. *et al.* Pkd2 mesenteric vessels exhibit a primary defect in endothelium-dependent vasodilatation restored by rosiglitazone. *Am J Physiol Heart Circ Physiol* **304**, H33-41, doi:10.1152/ajpheart.01102.2011 (2013).

53 Bernhardt, W. M. *et al.* Involvement of hypoxia-inducible transcription factors in polycystic kidney disease. *Am J Pathol* **170**, 830-842, doi:10.2353/ajpath.2007.060455 (2007).

54 Booij, T. H. *et al.* In Vitro 3d Phenotypic Drug Screen Identifies Celastrol as an Effective in Vivo Inhibitor of Polycystic Kidney Disease. *J Mol Cell Biol*, doi:10.1093/jmcb/mjz029 (2019).

55 Song, X. *et al.* Systems biology of autosomal dominant polycystic kidney disease (ADPKD): computational identification of gene expression pathways and integrated regulatory networks. *Hum Mol Genet* **18**, 2328-2343, doi:10.1093/hmg/ddp165 (2009).

56 Hayden, M. S. & Ghosh, S. NF-kappaB, the first quarter-century: remarkable progress and outstanding questions. *Genes Dev* **26**, 203-234, doi:10.1101/gad.183434.111 (2012).

57 O'Shea, J. J. *et al.* The JAK-STAT pathway: impact on human disease and therapeutic intervention. *Annu Rev Med* **66**, 311-328, doi:10.1146/annurev-med-051113-024537 (2015).

58 Black, L. M., Lever, J. M. & Agarwal, A. Renal Inflammation and Fibrosis: A Double-edged Sword. *J Histochem Cytochem* **67**, 663-681, doi:10.1369/0022155419852932 (2019).

59 Ibrahim, S. Increased apoptosis and proliferative capacity are early events in cyst formation in autosomal-dominant, polycystic kidney disease. *ScientificWorldJournal* **7**, 1757-1767, doi:10.1100/tsw.2007.274 (2007).

60 Ta, M. H., Harris, D. C. & Rangan, G. K. Role of interstitial inflammation in the pathogenesis of polycystic kidney disease. *Nephrology (Carlton)* **18**, 317-330, doi:10.1111/nep.12045 (2013).

61 Gardner, K. D., Jr., Burnside, J. S., Elzinga, L. W. & Locksley, R. M. Cytokines in fluids from polycystic kidneys. *Kidney Int* **39**, 718-724, doi:10.1038/ki.1991.87 (1991).

62 Zheng, D. *et al.* Urinary excretion of monocyte chemoattractant protein-1 in autosomal dominant polycystic kidney disease. *J Am Soc Nephrol* **14**, 2588-2595, doi:10.1097/01.asn.0000088720.61783.19 (2003).

63 Kenter, A. T. *et al.* Identifying cystogenic paracrine signaling molecules in cyst fluid of patients with polycystic kidney disease. *Am J Physiol Renal Physiol* **316**, F204-F213, doi:10.1152/ajprenal.00470.2018 (2019).

64 Zeier, M. *et al.* Renal histology in polycystic kidney disease with incipient and advanced renal failure. *Kidney Int* **42**, 1259-1265, doi:10.1038/ki.1992.413 (1992).

65 Zimmerman, K. A. *et al.* Urinary T cells correlate with rate of renal function loss in autosomal dominant polycystic kidney disease. *Physiol Rep* **7**, e13951, doi:10.14814/phy2.13951 (2019).

66 Mrug, M. *et al.* Overexpression of innate immune response genes in a model of recessive polycystic kidney disease. *Kidney Int* **73**, 63-76, doi:10.1038/sj.ki.5002627 (2008).

67 Karihaloo, A. *et al.* Macrophages promote cyst growth in polycystic kidney disease. *J Am Soc Nephrol* **22**, 1809-1814, doi:10.1681/ASN.2011010084 (2011).

68 Swenson-Fields, K. I. *et al.* Macrophages promote polycystic kidney disease progression. *Kidney Int* **83**,

855-864, doi:10.1038/ki.2012.446 (2013).

69 Chen, L. *et al.* Macrophage migration inhibitory factor promotes cyst growth in polycystic kidney disease. *J Clin Invest* **125**, 2399-2412, doi:10.1172/JCI80467 (2015).

70 Lee, S. *et al.* Distinct macrophage phenotypes contribute to kidney injury and repair. *J Am Soc Nephrol* **22**, 317-326, doi:10.1681/ASN.2009060615 (2011).

71 Zimmerman, K. A. *et al.* Tissue-Resident Macrophages Promote Renal Cystic Disease. *J Am Soc Nephrol* **30**, 1841-1856, doi:10.1681/ASN.2018080810 (2019).

72 Nakamura, T. *et al.* Increased endothelin and endothelin receptor mRNA expression in polycystic kidneys of cpk mice. *J Am Soc Nephrol* **4**, 1064-1072 (1993).

73 Li, X. *et al.* A tumor necrosis factor-alpha-mediated pathway promoting autosomal dominant polycystic kidney disease. *Nat Med* **14**, 863-868, doi:10.1038/nm1783 (2008).

74 Aderka, D., Engelmann, H., Maor, Y., Brakebusch, C. & Wallach, D. Stabilization of the bioactivity of tumor necrosis factor by its soluble receptors. *J Exp Med* **175**, 323-329, doi:10.1084/jem.175.2.323 (1992).

75 De Groote, D., Grau, G. E., Dehart, I. & Franchimont, P. Stabilisation of functional tumor necrosis factor-alpha by its soluble TNF receptors. *Eur Cytokine Netw* **4**, 359-362 (1993).

76 Dell, K. M. *et al.* A novel inhibitor of tumor necrosis factor-alpha converting enzyme ameliorates polycystic kidney disease. *Kidney Int* **60**, 1240-1248, doi:10.1046/j.1523-1755.2001.00963.x (2001).

77 Deshmane, S. L., Kremlev, S., Amini, S. & Sawaya, B. E. Monocyte chemoattractant protein-1 (MCP-1): an overview. *J Interferon Cytokine Res* **29**, 313-326, doi:10.1089/jir.2008.0027 (2009).

78 Cowley, B. D., Jr., Ricardo, S. D., Nagao, S. & Diamond, J. R. Increased renal expression of monocyte chemoattractant protein-1 and osteopontin in ADPKD in rats. *Kidney Int* **60**, 2087-2096, doi:10.1046/j.1523-1755.2001.00065.x (2001).

79 Grantham, J. J. *et al.* Tolvaptan suppresses monocyte chemotactic protein-1 excretion in autosomal-dominant polycystic kidney disease. *Nephrol Dial Transplant* **32**, 969-975, doi:10.1093/ndt/gfw060 (2017).

80 Cassini, M. F. *et al.* Mcp1 Promotes Macrophage-Dependent Cyst Expansion in Autosomal Dominant Polycystic Kidney Disease. *J Am Soc Nephrol* **29**, 2471-2481, doi:10.1681/ASN.2018050518 (2018).

81 Zoja, C. *et al.* Effects of MCP-1 inhibition by bindarit therapy in a rat model of polycystic kidney disease. *Nephron* **129**, 52-61, doi:10.1159/000369149 (2015).

82 Idowu, J. *et al.* Aberrant Regulation of Notch3 Signaling Pathway in Polycystic Kidney Disease. *Sci Rep* **8**, 3340, doi:10.1038/s41598-018-21132-3 (2018).

83 Qin, S., Taglienti, M., Cai, L., Zhou, J. & Kreidberg, J. A. c-Met and NF-kappaB-dependent overexpression of Wnt7a and -7b and Pax2 promotes cystogenesis in polycystic kidney disease. *J Am Soc Nephrol* **23**, 1309-1318, doi:10.1681/ASN.2011030277 (2012).

84 Park, E. Y., Seo, M. J. & Park, J. H. Effects of specific genes activating RAGE on polycystic kidney disease. *Am J Nephrol* **32**, 169-178, doi:10.1159/000315859 (2010).

85 Ta, M. H. *et al.* Constitutive renal Rel/nuclear factor-kappaB expression in Lewis polycystic kidney disease rats. *World J Nephrol* **5**, 339-357, doi:10.5527/wjn.v5.i4.339 (2016).

86 Mangolini, A. *et al.* NF-kappaB activation is required for apoptosis in fibrocystin/polyductin-depleted kidney epithelial cells. *Apoptosis* **15**, 94-104, doi:10.1007/s10495-009-0426-7 (2010).

87 Banzi, M. *et al.* Polycystin-1 promotes PKCalpha-mediated NF-kappaB activation in kidney cells. *Biochem Biophys Res Commun* **350**, 257-262, doi:10.1016/j.bbrc.2006.09.042 (2006).

88 Zhou, J. *et al.* Kidney injury accelerates cystogenesis via pathways modulated by heme oxygenase and complement. *J Am Soc Nephrol* **23**, 1161-1171, doi:10.1681/ASN.2011050442 (2012).

89 Gattone, V. H., 2nd *et al.* Methylprednisolone retards the progression of inherited polycystic kidney disease in rodents. *Am J Kidney Dis* **25**, 302-313, doi:10.1016/0272-6386(95)90013-6 (1995).

90 Leuenroth, S. J. *et al.* Triptolide is a traditional Chinese medicine-derived inhibitor of polycystic kidney disease. *P Natl Acad Sci USA* **104**, 4389-4394, doi:10.1073/pnas.0700499104 (2007).

91 Ogborn, M. R. *et al.* Dietary conjugated linoleic acid reduces PGE2 release and interstitial injury in rat polycystic kidney disease. *Kidney Int* **64**, 1214-1221, doi:10.1046/j.1523-1755.2003.00215.x (2003).

92 Weimbs, T., Olsan, E. E. & Talbot, J. J. Regulation of STATs by polycystin-1 and their role in polycystic kidney disease. *JAKSTAT* **2**, e23650, doi:10.4161/jkst.23650 (2013).

93 Olsan, E. E. *et al.* Signal transducer and activator of transcription-6 (STAT6) inhibition suppresses renal cyst growth in polycystic kidney disease. *P Natl Acad Sci USA* **108**, 18067-18072, doi:10.1073/pnas.1111966108 (2011).

94 Leonhard, W. N. *et al.* Curcumin inhibits cystogenesis by simultaneous interference of multiple signaling pathways: in vivo evidence from a Pkd1-deletion model. *Am J Physiol Renal Physiol* **300**, F1193-1202, doi:10.1152/ajprenal.00419.2010 (2011).

95 Takakura, A. *et al.* Pyrimethamine inhibits adult polycystic kidney disease by modulating STAT signaling pathways. *Hum Mol Genet* **20**, 4143-4154, doi:10.1093/hmg/ddr338 (2011).

96 Formica, C. *et al.* Characterisation of transcription factor profiles in polycystic kidney disease (PKD): identification and validation of STAT3 and RUNX1 in the injury/repair response and PKD progression. *J Mol Med (Berl)*, doi:10.1007/s00109-019-01852-3 (2019).

97 Norman, J., Tsau, Y. K., Bacay, A. & Fine, L. G. Epidermal growth factor accelerates functional recovery from ischaemic acute tubular necrosis in the rat: role of the epidermal growth factor receptor. *Clin Sci (Lond)* **78**, 445-450, doi:10.1042/cs0780445 (1990).

98 Miller, S. B., Martin, D. R., Kissane, J. & Hammerman, M. R. Insulin-like growth factor I accelerates recovery from ischemic acute tubular necrosis in the rat. *Proc Natl Acad Sci U S A* **89**, 11876-11880, doi:10.1073/pnas.89.24.11876 (1992).

99 Terzi, F. *et al.* Targeted expression of a dominant-negative EGF-R in the kidney reduces tubulo-interstitial lesions after renal injury. *J Clin Invest* **106**, 225-234, doi:10.1172/JCI8315 (2000).

100 Homsi, E., Janino, P., Amano, M. & Saraiva Camara, N. O. Endogenous hepatocyte growth factor attenuates inflammatory response in glycerol-induced acute kidney injury. *Am J Nephrol* **29**, 283-291, doi:10.1159/000159275 (2009).

101 Liu, P. *et al.* Enhanced renoprotective effect of IGF-1 modified human umbilical cord-derived mesenchymal stem cells on gentamicin-induced acute kidney injury. *Sci Rep* **6**, 20287, doi:10.1038/srep20287 (2016).

102 Hakroush, S. *et al.* Effects of increased renal tubular vascular endothelial growth factor (VEGF) on fibrosis, cyst formation, and glomerular disease. *Am J Pathol* **175**, 1883-1895, doi:10.2353/ajpath.2009.080792

(2009).

103 Phanish, M. K., Winn, S. K. & Dockrell, M. E. Connective tissue growth factor-(CTGF, CCN2)--a marker, mediator and therapeutic target for renal fibrosis. *Nephron Exp Nephrol* **114**, e83-92, doi:10.1159/000262316 (2010).

104 Laouari, D. *et al.* TGF-alpha mediates genetic susceptibility to chronic kidney disease. *J Am Soc Nephrol* **22**, 327-335, doi:10.1681/ASN.2010040356 (2011).

105 Ostendorf, T., Boor, P., van Roeyen, C. R. & Floege, J. Platelet-derived growth factors (PDGFs) in glomerular and tubulointerstitial fibrosis. *Kidney Int Suppl (2011)* **4**, 65-69, doi:10.1038/kisup.2014.12 (2014).

106 Sweeney, W. E. & Avner, E. D. Molecular and cellular pathophysiology of autosomal recessive polycystic kidney disease (ARPKD). *Cell Tissue Res* **326**, 671-685, doi:10.1007/s00441-006-0226-0 (2006).

107 Lee, D. C., Chan, K. W. & Chan, S. Y. Expression of transforming growth factor alpha and epidermal growth factor receptor in adult polycystic kidney disease. *J Urol* **159**, 291-296, doi:10.1016/s0022-5347(01)64084-9 (1998).

108 Sweeney, W. E., Jr. & Avner, E. D. Functional activity of epidermal growth factor receptors in autosomal recessive polycystic kidney disease. *Am J Physiol* **275**, F387-394, doi:10.1152/ajprenal.1998.275.3.F387 (1998).

109 Lowden, D. A. *et al.* Renal cysts in transgenic mice expressing transforming growth factor-alpha. *J Lab Clin Med* **124**, 386-394 (1994).

110 Ye, M. *et al.* Cyst fluid from human autosomal dominant polycystic kidneys promotes cyst formation and expansion by renal epithelial cells in vitro. *J Am Soc Nephrol* **3**, 984-994 (1992).

111 Wilson, P. D. Polycystic kidney disease. *N Engl J Med* **350**, 151-164, doi:10.1056/NEJMra022161 (2004).

112 Du, J. & Wilson, P. D. Abnormal polarization of EGF receptors and autocrine stimulation of cyst epithelial growth in human ADPKD. *Am J Physiol* **269**, C487-495, doi:10.1152/ajpcell.1995.269.2.C487 (1995).

113 Orellana, S. A., Sweeney, W. E., Neff, C. D. & Avner, E. D. Epidermal Growth-Factor Receptor Expression Is Abnormal in Murine Polycystic Kidney. *Kidney International* **47**, 490-499, doi:DOI 10.1038/ki.1995.62 (1995).

114 Richards, W. G. *et al.* Epidermal growth factor receptor activity mediates renal cyst formation in polycystic kidney disease. *J Clin Invest* **101**, 935-939, doi:10.1172/JCI2071 (1998).

115 Torres, V. E. *et al.* EGF receptor tyrosine kinase inhibition attenuates the development of PKD in Han:SPRD rats. *Kidney Int* **64**, 1573-1579, doi:10.1046/j.1523-1755.2003.00256.x (2003).

116 Sweeney, W. E., Jr. *et al.* Combination treatment of PKD utilizing dual inhibition of EGF-receptor activity and ligand bioavailability. *Kidney Int* **64**, 1310-1319, doi:10.1046/j.1523-1755.2003.00232.x (2003).

117 Nakamura, T. *et al.* Growth factor gene expression in kidney of murine polycystic kidney disease. *J Am Soc Nephrol* **3**, 1378-1386 (1993).

118 Horie, S. *et al.* Mediation of Renal Cyst Formation by Hepatocyte Growth-Factor. *Lancet* **344**, 789-791, doi:Doi 10.1016/S0140-6736(94)92344-2 (1994).

119 Qin, S. A. *et al.* Failure to ubiquitinate c-Met leads to hyperactivation of mTOR signaling in a mouse model of autosomal dominant polycystic kidney disease. *Journal of Clinical Investigation* **120**, 3617-3628, doi:10.1172/Jci41531 (2010).

120 Simon, M. *et al.* Expression of vascular endothelial growth factor and its receptors in human renal ontogenesis and in adult kidney. *Am J Physiol* **268**, F240-250, doi:10.1152/ajprenal.1995.268.2.F240 (1995).

121 Tao, Y. *et al.* VEGF receptor inhibition slows the progression of polycystic kidney disease. *Kidney Int* **72**, 1358-1366, doi:10.1038/sj.ki.5002550 (2007).

122 Bello-Reuss, E., Holubec, K. & Rajaraman, S. Angiogenesis in autosomal-dominant polycystic kidney disease. *Kidney Int* **60**, 37-45, doi:10.1046/j.1523-1755.2001.00768.x (2001).

123 Raina, S. *et al.* Anti-VEGF antibody treatment accelerates polycystic kidney disease. *Am J Physiol Renal Physiol* **301**, F773-783, doi:10.1152/ajprenal.00058.2011 (2011).

124 Herrera, G. A. C-erb B-2 amplification in cystic renal disease. *Kidney Int* **40**, 509-513, doi:10.1038/ki.1991.239 (1991).

125 Wilson, P. D., Du, J. & Norman, J. T. Autocrine, endocrine and paracrine regulation of growth abnormalities in autosomal dominant polycystic kidney disease. *Eur J Cell Biol* **61**, 131-138 (1993).

126 Kuo, N. T., Norman, J. T. & Wilson, P. D. Acidic FGF regulation of hyperproliferation of fibroblasts in human autosomal dominant polycystic kidney disease. *Biochem Mol Med* **61**, 178-191, doi:DOI 10.1006/bmme.1997.2583 (1997).

127 Toda, N., Mukoyama, M., Yanagita, M. & Yokoi, H. CTGF in kidney fibrosis and glomerulonephritis. *Inflamm Regen* **38**, doi:UNSP 1410.1186/s41232-018-0070-0 (2018).

128 Gauer, S. *et al.* CTGF Is Expressed During Cystic Remodeling in the PKD/Mhm (cy/+) Rat Model for Autosomal-Dominant Polycystic Kidney Disease (ADPKD). *J Histochem Cytochem* **65**, 743-755, doi:10.1369/0022155417735513 (2017).

129 Happe, H. *et al.* Altered Hippo signalling in polycystic kidney disease. *J Pathol* **224**, 133-142, doi:10.1002/path.2856 (2011).

130 Ito, Y. *et al.* Expression of connective tissue growth factor in human renal fibrosis. *Kidney Int* **53**, 853-861, doi:10.1111/j.1523-1755.1998.00820.x (1998).

131 Sanchez-Lopez, E. *et al.* CTGF promotes inflammatory cell infiltration of the renal interstitium by activating NF-kappaB. *J Am Soc Nephrol* **20**, 1513-1526, doi:10.1681/ASN.2008090999 (2009).

132 Woroniecka, K. I. *et al.* Transcriptome analysis of human diabetic kidney disease. *Diabetes* **60**, 2354-2369, doi:10.2337/db10-1181 (2011).

133 Bielesz, B. *et al.* Epithelial Notch signaling regulates interstitial fibrosis development in the kidneys of mice and humans. *J Clin Invest* **120**, 4040-4054, doi:10.1172/JCI43025 (2010).

134 Xu, J. *et al.* Involvement of the Hippo pathway in regeneration and fibrogenesis after ischaemic acute kidney injury: YAP is the key effector. *Clin Sci* **130**, 349-363, doi:10.1042/Cs20150385 (2016).

135 Villanueva, S., Cespedes, C. & Vio, C. P. Ischemic acute renal failure induces the expression of a wide range of nephrogenic proteins. *Am J Physiol Regul Integr Comp Physiol* **290**, R861-870, doi:10.1152/ajpregu.00384.2005 (2006).

136 Edeling, M., Ragi, G., Huang, S., Pavenstadt, H. & Susztak, K. Developmental signalling pathways in renal fibrosis: the roles of Notch, Wnt and Hedgehog. *Nat Rev Nephrol* **12**, 426-439, doi:10.1038/nrneph.2016.54 (2016).

137 Kim, C. L., Choi, S. H. & Mo, J. S. Role of the Hippo Pathway in Fibrosis and Cancer. *Cells* **8**, doi:10.3390/

cells8050468 (2019).

138 Kopan, R. Notch signaling. *Cold Spring Harb Perspect Biol* **4**, doi:10.1101/cshperspect.a011213 (2012).

139 Fujimura, S., Jiang, Q., Kobayashi, C. & Nishinakamura, R. Notch2 Activation in the Embryonic Kidney Depletes Nephron Progenitors. *Journal of the American Society of Nephrology* **21**, 803-810, doi:10.1681/Asn.2009040353 (2010).

140 Chung, E., Deacon, P., Marable, S., Shin, J. & Park, J. S. Notch signaling promotes nephrogenesis by downregulating Six2. *Development* **143**, 3907-3913, doi:10.1242/dev.143503 (2016).

141 Sweetwyne, M. T., Tao, J. & Susztak, K. Kick it up a notch: Notch signaling and kidney fibrosis. *Kidney Int Suppl (2011)* **4**, 91-96, doi:10.1038/kisup.2014.17 (2014).

142 Morrissey, J. *et al.* Transforming growth factor-beta induces renal epithelial jagged-1 expression in fibrotic disease. *J Am Soc Nephrol* **13**, 1499-1508, doi:10.1097/01.asn.0000017905.77985.4a (2002).

143 Niranjan, T. *et al.* The Notch pathway in podocytes plays a role in the development of glomerular disease. *Nat Med* **14**, 290-298, doi:10.1038/nm1731 (2008).

144 Chen, W. C., Tzeng, Y. S. & Li, H. Gene expression in early and progression phases of autosomal dominant polycystic kidney disease. *BMC Res Notes* **1**, 131, doi:10.1186/1756-0500-1-131 (2008).

145 Surendran, K., Selassie, M., Liapis, H., Krigman, H. & Kopan, R. Reduced Notch signaling leads to renal cysts and papillary microadenomas. *J Am Soc Nephrol* **21**, 819-832, doi:10.1681/ASN.2009090925 (2010).

146 Pandey, P., Qin, S., Ho, J., Zhou, J. & Kreidberg, J. A. Systems biology approach to identify transcriptome reprogramming and candidate microRNA targets during the progression of polycystic kidney disease. *BMC Syst Biol* **5**, 56, doi:10.1186/1752-0509-5-56 (2011).

147 Steinhart, Z. & Angers, S. Wnt signaling in development and tissue homeostasis. *Development* **145**, doi:10.1242/dev.146589 (2018).

148 Zhou, D., Tan, R. J., Fu, H. & Liu, Y. Wnt/β-catenin signaling in kidney injury and repair: a double-edged sword. *Laboratory Investigation* **96**, 156-167, doi:10.1038/labinvest.2015.153 (2015).

149 Qian, C. N. *et al.* Cystic renal neoplasia following conditional inactivation of apc in mouse renal tubular epithelium. *J Biol Chem* **280**, 3938-3945, doi:10.1074/jbc.M410697200 (2005).

150 Saadi-Kheddouci, S. *et al.* Early development of polycystic kidney disease in transgenic mice expressing an activated mutant of the beta-catenin gene. *Oncogene* **20**, 5972-5981, doi:10.1038/sj.onc.1204825 (2001).

151 Sorenson, C. M. Nuclear localization of beta-catenin and loss of apical brush border actin in cystic tubules of bcl-2 -/- mice. *Am J Physiol* **276**, F210-217, doi:10.1152/ajprenal.1999.276.2.F210 (1999).

152 Huan, Y. H. & van Adelsberg, J. Polycystin-1, the PKD1 gene product, is in a complex containing E-cadherin and the catenins. *Journal of Clinical Investigation* **104**, 1459-1468, doi:Doi 10.1172/Jci5111 (1999).

153 Trudel, M. in *Polycystic Kidney Disease* (ed X. Li) (Codon PublicationsCopyright: The Author., 2015).

154 McNeill, H. Planar Cell Polarity and the Kidney. *Journal of the American Society of Nephrology* **20**, 2104-2111, doi:10.1681/asn.2008111173 (2009).

155 Fischer, E. *et al.* Defective planar cell polarity in polycystic kidney disease. *Nat Genet* **38**, 21-23, doi:10.1038/ng1701 (2006).

156 Nishio, S. *et al.* Loss of oriented cell division does not initiate cyst formation. *J Am Soc Nephrol* **21**, 295-302, doi:10.1681/ASN.2009060603 (2010).

157 Cain, J. E. & Rosenblum, N. D. Control of mammalian kidney development by the Hedgehog signaling pathway. *Pediatr Nephrol* **26**, 1365-1371, doi:10.1007/s00467-010-1704-x (2011).

158 Zhou, D., Tan, R. J. & Liu, Y. Sonic hedgehog signaling in kidney fibrosis: a master communicator. *Sci China Life Sci* **59**, 920-929, doi:10.1007/s11427-016-0020-y (2016).

159 Avasthi, P., Maser, R. L. & Tran, P. V. Primary Cilia in Cystic Kidney Disease. *Results Probl Cell Differ* **60**, 281-321, doi:10.1007/978-3-319-51436-9_11 (2017).

160 Hildebrandt, F., Benzing, T. & Katsanis, N. Ciliopathies. *N Engl J Med* **364**, 1533-1543, doi:10.1056/NEJMra1010172 (2011).

161 Bangs, F. & Anderson, K. V. Primary Cilia and Mammalian Hedgehog Signaling. *Cold Spring Harb Perspect Biol* **9**, doi:10.1101/cshperspect.a028175 (2017).

162 Attanasio, M. *et al.* Loss of GLIS2 causes nephronophthisis in humans and mice by increased apoptosis and fibrosis. *Nat Genet* **39**, 1018-1024, doi:10.1038/ng2072 (2007).

163 Silva, L. M. *et al.* Inhibition of Hedgehog signaling suppresses proliferation and microcyst formation of human Autosomal Dominant Polycystic Kidney Disease cells. *Sci Rep* **8**, 4985, doi:10.1038/s41598-018-23341-2 (2018).

164 Tran, P. V. *et al.* Downregulating Hedgehog Signaling Reduces Renal Cystogenic Potential of Mouse Models. *Journal of the American Society of Nephrology* **25**, 2201-2212, doi:10.1681/Asn.2013070735 (2014).

165 Ma, M., Legue, E., Tian, X., Somlo, S. & Liem, K. F., Jr. Cell-Autonomous Hedgehog Signaling Is Not Required for Cyst Formation in Autosomal Dominant Polycystic Kidney Disease. *J Am Soc Nephrol* **30**, 2103-2111, doi:10.1681/ASN.2018121274 (2019).

166 Zheng, Y. & Pan, D. The Hippo Signaling Pathway in Development and Disease. *Dev Cell* **50**, 264-282, doi:10.1016/j.devcel.2019.06.003 (2019).

167 Meng, Z., Moroishi, T. & Guan, K. L. Mechanisms of Hippo pathway regulation. *Genes Dev* **30**, 1-17, doi:10.1101/gad.274027.115 (2016).

168 Attisano, L. & Wrana, J. L. Signal integration in TGF-beta, WNT, and Hippo pathways. *F1000Prime Rep* **5**, 17, doi:10.12703/P5-17 (2013).

169 McNeill, H. & Reginensi, A. Lats1/2 Regulate Yap/Taz to Control Nephron Progenitor Epithelialization and Inhibit Myofibroblast Formation. *Journal of the American Society of Nephrology* **28**, 852-861, doi:10.1681/Asn.2016060611 (2017).

170 Reginensi, A. *et al.* Yap- and Cdc42-dependent nephrogenesis and morphogenesis during mouse kidney development. *PLoS Genet* **9**, e1003380, doi:10.1371/journal.pgen.1003380 (2013).

171 Makita, R. *et al.* Multiple renal cysts, urinary concentration defects, and pulmonary emphysematous changes in mice lacking TAZ. *Am J Physiol Renal Physiol* **294**, F542-553, doi:10.1152/ajprenal.00201.2007 (2008).

172 Szeto, S. G. *et al.* YAP/TAZ Are Mechanoregulators of TGF-beta-Smad Signaling and Renal Fibrogenesis. *J Am Soc Nephrol* **27**, 3117-3128, doi:10.1681/ASN.2015050499 (2016).

173 Habbig, S. *et al.* The ciliopathy disease protein NPHP9 promotes nuclear delivery and activation of the

oncogenic transcriptional regulator TAZ. *Hum Mol Genet* **21**, 5528-5538, doi:10.1093/hmg/dds408 (2012).

174 Xu, D. *et al.* Scribble influences cyst formation in autosomal-dominant polycystic kidney disease by regulating Hippo signaling pathway. *FASEB J* **32**, 4394-4407, doi:10.1096/fj.201701376RR (2018).

175 Cai, J. *et al.* A RhoA-YAP-c-Myc signaling axis promotes the development of polycystic kidney disease. *Genes Dev* **32**, 781-793, doi:10.1101/gad.315127.118 (2018).

176 Zhao, B. *et al.* TEAD mediates YAP-dependent gene induction and growth control. *Genes Dev* **22**, 1962-1971, doi:10.1101/gad.1664408 (2008).

177 Sharifian, R. *et al.* Distinct patterns of transcriptional and epigenetic alterations characterize acute and chronic kidney injury. *Sci Rep* **8**, 17870, doi:10.1038/s41598-018-35943-x (2018).

178 Wanner, N. & Bechtel-Walz, W. Epigenetics of kidney disease. *Cell Tissue Res* **369**, 75-92, doi:10.1007/s00441-017-2588-x (2017).

179 Chang, M. Y. & A, C. M. O. Targeting new cellular disease pathways in autosomal dominant polycystic kidney disease. *Nephrol Dial Transplant* **33**, 1310-1316, doi:10.1093/ndt/gfx262 (2018).

180 Li, L. X. *et al.* Lysine methyltransferase SMYD2 promotes cyst growth in autosomal dominant polycystic kidney disease. *J Clin Invest* **127**, 2751-2764, doi:10.1172/JCI90921 (2017).

181 Zhou, X. *et al.* Sirtuin 1 inhibition delays cyst formation in autosomal-dominant polycystic kidney disease. *J Clin Invest* **123**, 3084-3098, doi:10.1172/JCI64401 (2013).

182 Fan, L. X., Li, X., Magenheimer, B., Calvet, J. P. & Li, X. Inhibition of histone deacetylases targets the transcription regulator Id2 to attenuate cystic epithelial cell proliferation. *Kidney Int* **81**, 76-85, doi:10.1038/ki.2011.296 (2012).

183 Liu, W. *et al.* HDAC6 regulates epidermal growth factor receptor (EGFR) endocytic trafficking and degradation in renal epithelial cells. *PLoS One* **7**, e49418, doi:10.1371/journal.pone.0049418 (2012).

184 Zhou, X. *et al.* Therapeutic targeting of BET bromodomain protein, Brd4, delays cyst growth in ADPKD. *Hum Mol Genet* **24**, 3982-3993, doi:10.1093/hmg/ddv136 (2015).

185 Zhou, X. *et al.* SIRT2 regulates ciliogenesis and contributes to abnormal centrosome amplification caused by loss of polycystin-1. *Hum Mol Genet* **23**, 1644-1655, doi:10.1093/hmg/ddt556 (2014).

186 Cao, Y. *et al.* Chemical modifier screen identifies HDAC inhibitors as suppressors of PKD models. *P Natl Acad Sci USA* **106**, 21819-21824, doi:10.1073/pnas.0911987106 (2009).

187 Woo, Y. M. *et al.* Genome-wide methylation profiling of ADPKD identified epigenetically regulated genes associated with renal cyst development. *Hum Genet* **133**, 281-297, doi:10.1007/s00439-013-1378-0 (2014).

188 Bowden, S. A. *et al.* Genome-Scale Single Nucleotide Resolution Analysis of DNA Methylation in Human Autosomal Dominant Polycystic Kidney Disease. *Am J Nephrol* **48**, 415-424, doi:10.1159/000494739 (2018).

1

CHAPTER 2

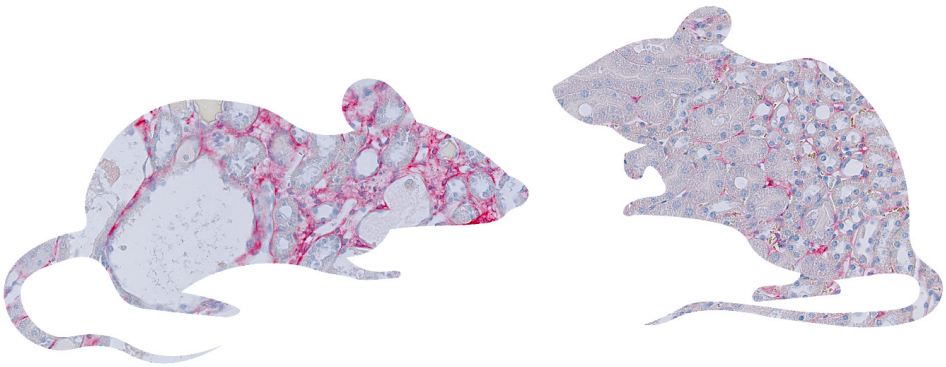

Four-Jointed knock-out delays renal failure in an ADPKD model with kidney injury

Chiara Formica[1], Hester Happé[1], Kimberley A.M. Veraar[2], Andrea Vortkamp[3], Marion Scharpfenecker[2], Helen McNeill[4], Dorien J.M. Peters[1]

[1]Department of Human Genetics, Leiden University Medical Center, The Netherlands

[2]Department of Pathology, Leiden University Medical Center, The Netherlands

[3]Department of Developmental Biology, Centre of Medical Biotechnology, Essen, Germany

[4]Department of Developmental Biology, Washington University School of Medicine, St. Louis, USA; Department of Molecular Genetics, University of Toronto, Canada; Lunenfeld-Tanenbaum Research Institute, Sinai Health System, Toronto, Canada

J Pathol. 2019 Sep;249(1):114-125

Abstract

Autosomal Dominant Polycystic Kidney Disease (ADPKD) is characterized by the development of fluid-filled cysts in the kidneys which lead to end-stage renal disease (ESRD). In the majority of cases, the disease is caused by a mutation in the *Pkd1* gene. In a previous study, we demonstrated that renal injury can accelerate cyst formation in *Pkd1* knock-out (KO) mice. In that study, we found that Four-jointed (FJX1), an upstream regulator of planar cell polarity and the Hippo pathway, was aberrantly expressed in *Pkd1* KO mice compared to wild-type after injury. Therefore we hypothesized a role for FJX1 in injury/repair and cyst formation. We generated single and double deletion mice for *Pkd1* and *Fjx1*, and we induced toxic renal injury using the nephrotoxic compound 1,2-dichlorovinyl-cysteine (DCVC). We confirmed that nephrotoxic injury can accelerate cyst formation in *Pkd1* mutant mice. This caused *Pkd1* KO mice to reach ESRD significantly faster; unexpectedly, double KO mice survived significantly longer. Indeed, cyst formation was comparable in both models, but we found significantly lower fibrosis and macrophage infiltrates in double KO mice. Taken together, these data suggest that *Fjx1* disruption protects the cystic kidneys against kidney failure by reducing inflammation and fibrosis. Moreover, we describe, for the first time, an interesting (yet unidentified) mechanism that partially discriminates cyst growth from fibrogenesis.

Introduction

Autosomal Dominant Polycystic Disease (ADPKD) is a genetic disease caused in the majority of the cases by a mutation in the *Pkd1* gene, which encodes Polycystin 1, and in the remaining cases by a mutation in the *Pkd2* gene, encoding Polycystin 2[1]. The hallmark of this disease is the formation of fluid-filled cysts in the kidneys, which slowly grow and progressively disrupt the renal parenchyma, ultimately leading to kidney failure[1,2]. The exact mechanisms behind cyst formation are still elusive, and effective therapies are still missing, although the Vasopressin V2R antagonist Tolvaptan has become recently available for selected patients[3-5].

Recently, our group showed that a substantial proportion of genes typically deregulated in ADPKD also plays a role in injury-repair mechanisms[6]. Indeed, less than a decade ago, injury has emerged as an important player in cyst formation and progression, and now it is considered a "modifier" of ADPKD[7]. Several other groups and we described that both nephrotoxic[8] and ischemic injury, as well as unilateral nephrectomy[9-12], were able to speed up cyst formation and progression, reinforcing the link between ADPKD progression and injury. In particular, we identified one gene, *Four-jointed box1* (*Fjx1*), as an interesting player in these processes. In our study, *Fjx1* showed aberrant expression during both the injury-repair phase and cyst progression in *Pkd1* KO mice compared with wild-type mice[8]. Moreover, *Fjx1* is implicated with two important pathways normally aberrant in ADPKD: planar cell polarity (PCP) and the Hippo pathway.

FJX1 is the mammalian homolog of the *Drosophila* protein Fj, discovered for its pivotal role in the correct development of leg joints, wings and eyes[9,10]. Fj regulates the interaction of Fat (Ft) with Dachsous (Ds), which controls PCP signalling, most likely in parallel with the Frizzled signals[10-12]. *Fj* mutant *Drosophila* models have a clear alteration of PCP, while *Fjx1* KO mice do not show any evident morphological defects in the kidneys or other organs[13,14]. However, deleting the target of FJX1, *Fat4*, leads to loss of PCP in the inner ear, cochlea and the neural tube, and mild cyst formation in mouse kidney. Loss of both, *Fat4* and *Fjx1,* slightly aggravates the phenotype suggesting that FJX1 may also act via Fat4-independent pathways. Yet, the effect of *Fjx1* in a *Pkd1* mutant context is to date unknown[14].

In *Drosophila,* Fj is also an upstream regulator of the Hippo pathway, through its downstream target Ft. The Hippo pathway regulates proliferation and tissue size through the activity of the final effector and transcriptional co-activator Yorki (Yki)[15-16]. In mammals, there are two *Yki* orthologs: *Yes-associated protein 1* (*Yap1*) and *transcriptional coactivator with PDZ-binding motif* (*Wwtr1* or *Taz*). When the Hippo pathway is active, YAP1 and TAZ are phosphorylated and retained in the cytoplasm, preventing their nuclear translocation and transcriptional activity. In ADPKD, YAP and TAZ activity is upregulated in the cyst-lining

epithelium as indicated by their nuclear localization, suggesting a role for this pathway in cyst progression[17]. In mammals, regulation of the Hippo pathway by FAT4 has recently been shown in the prenatal heart[18]; however, whether this regulatory mechanism also takes place in the kidneys is not clear[14,19].

This study aims to investigate the role of FJX1 during ADPKD progression, particularly after kidney injury and the involvement of the PCP and Hippo pathways. We show that mice that are double mutant for *Fjx1* and *Pkd1* display cyst formation comparable to that of single *Pkd1* KO mice but survive longer. This effect was probably not due to differences in PCP and the Hippo pathway, which were not affected by *Fjx1* deletion, but rather due to reduced fibrosis and macrophage infiltration in the double KO mice. We also show a reduction of fibrosis which is independent of cyst formation. Indeed, in our study, reduced fibrogenesis is directly caused by *Fjx1* deletion and not an indirect consequence of the improved cystic phenotype.

Materials and Methods

Animal Models

All the animal experiments were evaluated and approved by the local animal experimental committee of the Leiden University Medical Centre and the Commission Biotechnology in Animals of the Dutch Ministry of Agriculture. The kidney specific tamoxifen-inducible *Pkd1*-deletion mouse model (*Pkd1*-cKO) and the *Fjx1*$^{-/-}$ (*Fjx1* KO) has been described previously[13,20]. By cross-breeding *Pkd1*-cKO with the *Fjx1* KO mice, we generated the *Fjx1*$^{-/-}$/*Pkd1*-cKO double KO mouse model (double KO). Inactivation of the *Pkd1* gene was achieved by oral administration of tamoxifen in adult mice (13 to 14 weeks old). Renal injury was induced a week after gene disruption by a single intraperitoneal injection of S-(1,2-dichlorovinyl)-L-cysteine (DCVC) or vehicle. Injury was evaluated by measurement of blood urea nitrogen (BUN) level after 40 hours, as described before[8]. More detailed protocols in Supplementary materials.

Immunohistochemistry

Formalin-fixed paraffin-embedded kidneys were sectioned at 4 µm thickness. Sections were stained with Periodic acid-Schiff (PAS) to determine the cystic index (CI) and with Picro Sirius Red (PSR) to determine fibrotic index. Kidney slides were also stained for αSMA, F4/80, YAP, pSTAT3, GM130. More detailed protocols in Supplementary materials.

qPCR

Snap-frozen kidneys were homogenized using Magnalyser technology (Roche). Total RNA was isolated using Tri-Reagent (Sigma-Aldrich). cDNA synthesis was performed using the Transcriptor First Strand cDNA Synthesis Kit (Roche), and qPCR was done using 2× FastStart SYBR-Green Master (Roche) according to the manufacturer's protocol. Primer sequences are provided in Supplementary Table 1. Gene expression was normalized to *Hprt* and fold-change was used for representation in the graphs.

Statistical Analysis

Data were analysed using ANOVA in GraphPad Prism 8.00 for Windows and linear-mixed effects models in IBM SPSS Statistics for Windows, version 23.

Results

Mice double KO for *Pkd1* and *Fjx1* survive longer after toxic tubular damage compared with mice single KO for *Pkd1*.

Inactivation of the *Pkd1* gene was achieved by oral administration of tamoxifen in adult mice. This type of mouse model is characterized by a relatively slow cyst growth that allows having reasonable time windows for the study of the different steps of disease progression. We showed previously that upon nephrotoxic injury cyst initiation is faster in mice with *Pkd1* deletion compared with the non-injured group[8]. Using the same injury model, we administered the nephrotoxic compound DCVC to Wt, *Pkd1* KO, *Fjx1* KO and double KO mice (Figure 1A). We used PBS injection as a control (vehicle group). At 40 h upon DCVC injections, renal injury was confirmed by a substantial rise in the BUN level in all mice, which returned to baseline after 1 week, suggesting a full recovery of the kidney function with no differences among the genotypes (Figure 1B).

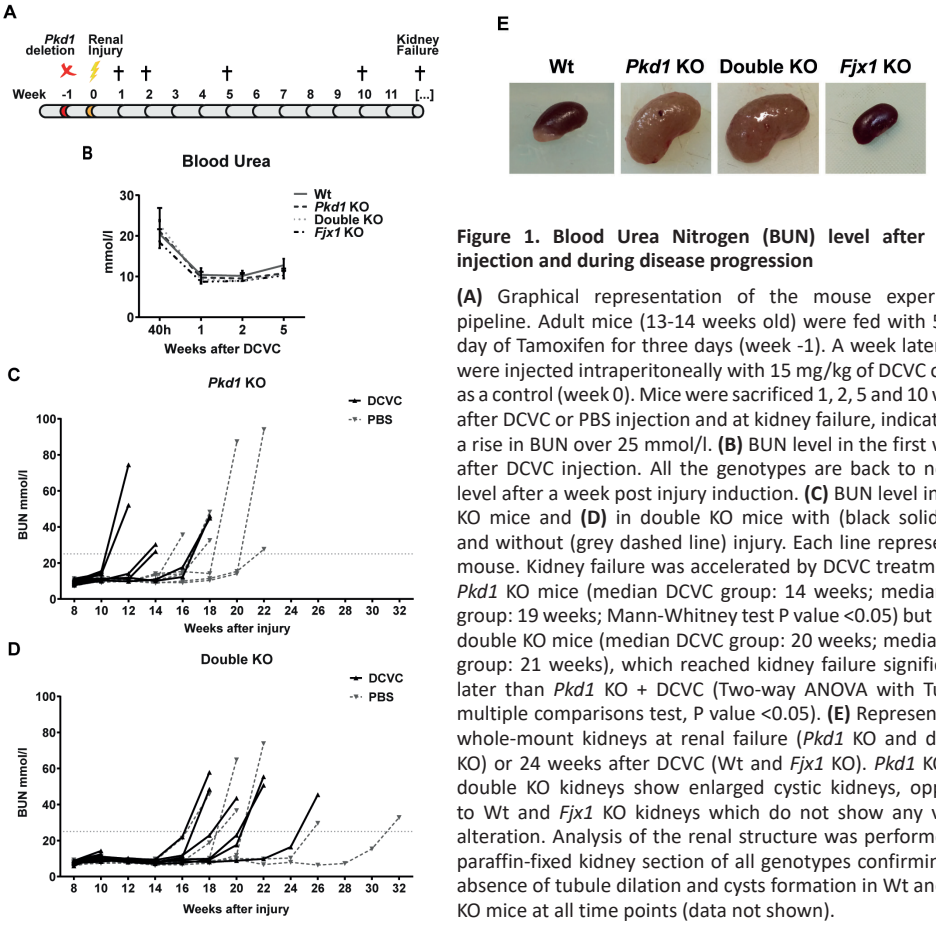

Figure 1. Blood Urea Nitrogen (BUN) level after DCVC injection and during disease progression

(A) Graphical representation of the mouse experiment pipeline. Adult mice (13-14 weeks old) were fed with 5 mg/day of Tamoxifen for three days (week -1). A week later they were injected intraperitoneally with 15 mg/kg of DCVC or PBS as a control (week 0). Mice were sacrificed 1, 2, 5 and 10 weeks after DCVC or PBS injection and at kidney failure, indicated by a rise in BUN over 25 mmol/l. **(B)** BUN level in the first weeks after DCVC injection. All the genotypes are back to normal level after a week post injury induction. **(C)** BUN level in *Pkd1* KO mice and **(D)** in double KO mice with (black solid line) and without (grey dashed line) injury. Each line represents a mouse. Kidney failure was accelerated by DCVC treatment in *Pkd1* KO mice (median DCVC group: 14 weeks; median PBS group: 19 weeks; Mann-Whitney test P value <0.05) but not in double KO mice (median DCVC group: 20 weeks; median PBS group: 21 weeks), which reached kidney failure significantly later than *Pkd1* KO + DCVC (Two-way ANOVA with Tukey's multiple comparisons test, P value <0.05). **(E)** Representative whole-mount kidneys at renal failure (*Pkd1* KO and double KO) or 24 weeks after DCVC (Wt and *Fjx1* KO). *Pkd1* KO and double KO kidneys show enlarged cystic kidneys, opposite to Wt and *Fjx1* KO kidneys which do not show any visible alteration. Analysis of the renal structure was performed on paraffin-fixed kidney section of all genotypes confirming the absence of tubule dilation and cysts formation in Wt and *Fjx1* KO mice at all time points (data not shown).

Pkd1 KO mice injected with DCVC reached end-stage renal disease (ESRD) around 14 weeks after injury. This was significantly earlier than in the vehicle group, which survived for about 19 weeks, in accordance with previously generated data (Figure 1C)[8]. Surprisingly, we observed that the double KO mice did not show a difference between DCVC and vehicle treatment with a median survival of 20 and 21 weeks, respectively (Figure 1D). When compared with *Pkd1* KO mice, double KO mice survived significantly longer after injury, indicating that the lack of *Fjx1* improved survival of double KO mice upon renal damage.
Both Wt and *Fjx1* KO mice subjected to renal injury did not develop cysts still 24 weeks after DCVC, the time point when mice were sacrificed (Figure 1E and data not shown).

Knocking-out *Fjx1* in *Pkd1* mutant mice does not affect cyst formation

Since renal injury accelerates cyst formation in *Pkd1* KO mice[8,21-24], we wondered whether prolonged survival observed in the double KO group treated with DCVC could be due to delayed cyst initiation. We measured the cystic index in kidneys from *Pkd1* KO and double KO mice at 10 weeks after DCVC injection when mice start to show a mild cystic phenotype. We compared *Pkd1* KO and double KO mice with and without DCVC, and did not find any difference in the cystic index, and two kidneys weight to body weight (2KW/BW) ratio's between the genotypes at this time point (Figure 2A-C). Thus, the initiation of cyst formation is not different in the two models, suggesting a role in cyst growth.

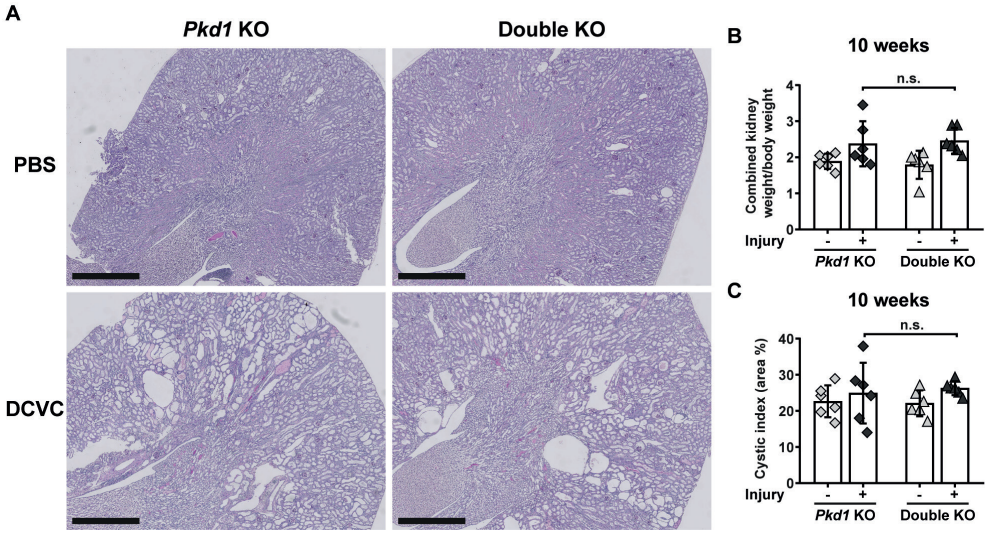

Figure 2. Cysts formation at 10 weeks after DCVC

(A) Representative Periodic Acid Schiff (PAS) staining of *Pkd1* KO and double KO mice at 10 weeks after DCVC, showing comparable cyst formation in the two genotypes. Scale bars, 1 mm. **(B)** Evaluation of kidney size at 10 weeks time-point in *Pkd1* KO and double KO mice with and without injury using two kidney weight/body weight ratio. **(C)** Cystic index at 10 weeks time-point in *Pkd1* KO and double KO mice with and without injury. Each symbol shows data from one mouse. Mean ± SD. Two-way ANOVA with Tukey's multiple comparisons test.

This is also evident when ESRD kidneys are compared. Indeed, *Pkd1* KO mice injected with DCVC, which reach ESRD faster, had a shorter phase of cyst growth and displayed mainly small cysts at kidney failure. Conversely, double KO mice, which have a slower progression to ESRD and therefore a longer phase of cyst growth, show frequently larger cysts (Figure 3A, B). Thus, our data suggest that FJX1 is not directly involved in cyst formation and that prolonged survival of the double KO mice cannot be explained by delayed cyst formation.

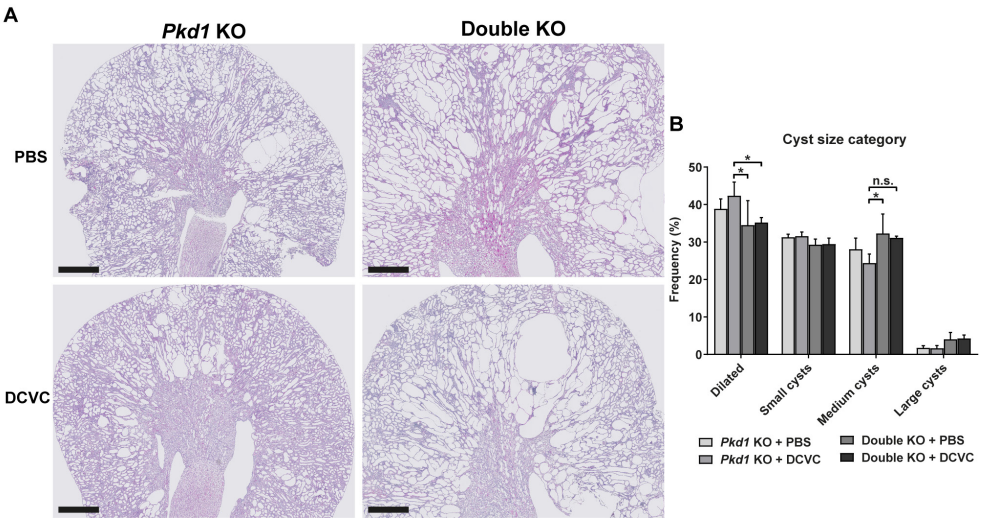

Figure 3. Cysts size at kidney failure

(A) Representative PAS staining of *Pkd1* KO and double KO mice at kidney failure. Scale bars, 1 mm. **(B)** Quantification of cysts size frequency in *Pkd1* KO and double KO mice with and without injury. Data represent the mean of 4 mice ± SD. Three-way ANOVA (P value <0.0001) with Tukey's multiple comparisons test. * P value <0.05.

Chronic injury caused by cyst formation leads to differences in injury markers expression, fibrosis and inflammatory responses in double KO compared with *Pkd1* KO mice

Cyst formation is accompanied by inflammation and fibrosis which ultimately leads to complete loss of renal function. As changes in these processes might affect survival, we analysed whether *Fjx1* deletion altered the expression of injury markers, fibrosis and inflammation.

The expression of the well-established kidney injury molecule *Kim1* (*Havcr1*)[25] was analysed using qPCR. We observed increased *Kim1* expression already at 10 weeks after DCVC injection in *Pkd1* KO and in double KO mice, a time-point when dilation of tubules and small cysts were evident. In contrast, Wt and *Fjx1* KO mice, which do not develop a renal phenotype after DCVC injection, did not show increased *Kim1* expression, reinforcing the idea of cyst-induced chronic injury (Figure 4A). Interestingly, at kidney failure, *Kim1* expression was significantly higher in *Pkd1* KO mice compared to double KO (Figure 4B).

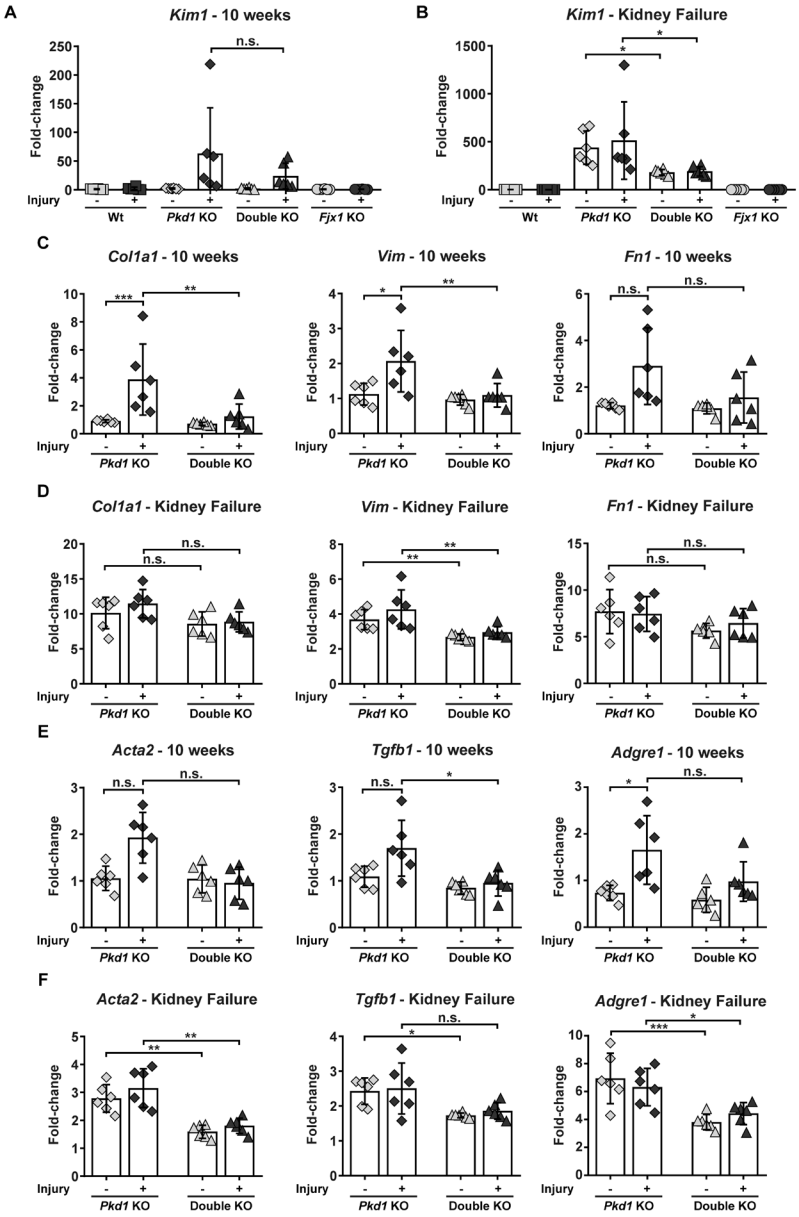

Figure 4. Expression of genes involved in injury-repair in *Pkd1* KO and double KO mice

(A) Gene expression of *Kim1* (*Havcr1*) at 10 weeks after DCVC injection. Both *Pkd1* KO and double KO have a significant increase of *Kim1* expression compared to the PBS groups and the Wt and *Fjx1* KO with and without injury (significance not shown on graph), but not compared to each other. **(B)** Gene expression of *Kim1* at kidney failure after DCVC injection (significance to Wt and *Fjx1* KO not shown on graph). **(C)** Gene expression of *Col1a1*, *Vim* and *Fn1* at 10 weeks after DCVC injection. **(D)** Gene expression of *Col1a1*, *Vim* and *Fn1* at kidney failure. **(E)** Gene expression of *Acta2*, *Tgfb1* and *Adgre1* (F4/80) at 10 weeks after DCVC injection. **(F)** Gene expression of *Acta2*, *Tgfb1* and *Adgre1* at kidney failure. Each symbol shows data from one mouse. Mean ± SD. Two-way ANOVA with Tukey's multiple comparisons test. * P value <0.05; ** P value <0.01; *** P value <0.001.

When we analysed fibrogenesis at 10 weeks after DCVC and kidney failure, expression of alpha-1 type I collagen (*Col1a1*) and Vimentin (*Vim*) was significantly reduced in the double KO compared to *Pkd1* KO at 10 weeks after DCVC, both at the mRNA (Figure 4C, D) and protein levels (Figure 5A, B); expression of Fibronectin (*Fn1*) showed a similar trend (Figure 4C, D). Interestingly, while in *Pkd1* KO mice the expression of these genes was significantly correlated with kidney size, this was not observed in the double KO mice, suggesting that in these mice cyst progression and fibrosis are two independent events (Supplementary Figure 1). Likewise, the expression of transforming growth factor beta-1 (*Tgfb1*), was significantly less in double KO compared to *Pkd1* KO mice at 10 weeks and at kidney failure. Also, double KO mice at 10 weeks had tendentially lower alpha-smooth muscle actin (*Acta2*) transcript and significantly less αSMA positive area (Figure 4E, F; Figure 5C, D).

To characterize the inflammatory response, we looked at the expression of the macrophage marker *Adgre1* (F4/80) and found it to be significantly less expressed in double KO compared to *Pkd1* KO mice at kidney failure (Figure 4E, F). At 10 weeks after DCVC *Adgre1* showed a trend but at the protein level F4/80 expression was significantly reduced in double KO mice (Figure 5E, F). We also checked the expression of *Jak2* and *Stat1*, involved in the transduction of a series of signals, like growth factors and cytokines in response to injury[26]. We found significantly lower expression in double KO compared to *Pkd1* KO mice (Figure 5G, H). On the other hand, Stat3 activation, known to be involved in cyst growth[27], was not significantly different between the two genotypes, supporting the idea that FJX1 role is related to the inflammatory/fibrotic response and not to cyst formation (Supplementary Figure 2). These results indicate that the lack of *Fjx1* leads to a reduced inflammatory/fibrotic response which translates into a longer survival after DCVC administration.

Investigation of pathways involved in renal fibrosis

We also studied the expression of key genes of several pathways known to be involved in renal fibrosis, such as Notch[28,29], Hedgehog[30,31], Wnt[32,33], hypoxia[34-38] and Egf[39-41]. However, we could not find any differences between the double KO and *Pkd1* KO mice, except for Pdgfb (Supplementary Figure 3) and Wnt target genes. Indeed, *Axin2*, *Cd44*, *Ccnd1* (Figure 6A, B) and to certain extent *Myc* (Supplementary Figure 4), showed significantly lower expression in double KO compared with *Pkd1* KO mice, both at 10 weeks after DCVC and at kidney failure, suggesting a reduced activation of the canonical Wnt signalling in the absence of *Fjx1*.

Mice double KO for *Pkd1* and *Fjx1* show less sensitivity to DCVC induced injury than mice single KO for *Pkd1*

To further investigate the role of FJX1 in injury, we performed a pilot experiment in which mice treated with DCVC were sacrificed after 24 h, 48 h and 72 h, i.e. during the

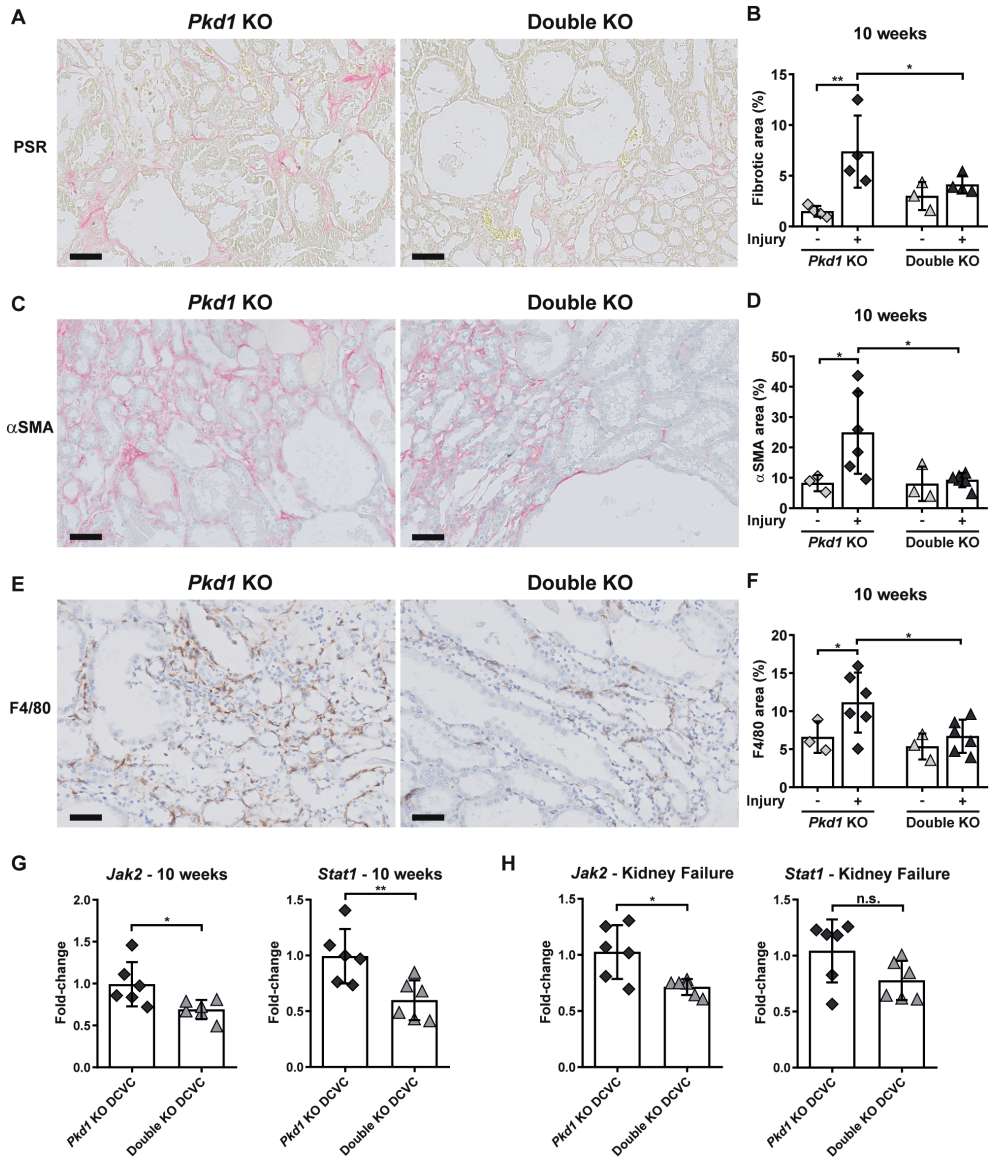

Figure 5. Fibrosis, fibroblast activation and macrophage infiltrates in *Pkd1* KO and double KO mice

(A) Representative Picro Sirius Red (PSR) staining of *Pkd1* KO and double KO mice at 10 weeks after DCVC. Scale bars, 50 µm. **(B)** Quantification of PSR staining in the cortico-medullary region. **(C)** Representative αSMA staining of *Pkd1* KO and double KO mice at 10 weeks after DCVC. Scale bars, 50 µm. **(D)** Quantification of αSMA staining in the cortico-medullary region. **(E)** Representative F4/80 staining of *Pkd1* KO and double KO mice at 10 weeks after DCVC. Scale bars, 50 µm. **(F)** Quantification of F4/80 staining in the cortico-medullary region. Each symbol is a mouse and data represent the mean ± SD. Two-way ANOVA with Tukey's multiple comparisons test. * P value <0.05; ** P value <0.01. **(G)** Gene expression of *Stat1* and *Jak2* at 10 weeks after DCVC in *Pkd1* KO and double KO mice. **(H)** Gene expression of *Stat1* and *Jak2* at kidney failure in *Pkd1* KO and double KO mice treated with DCVC. Each symbol shows data from one mouse. Mean ± SD. Unpaired t-test. * P value <0.05; ** P value <0.01.

nephrotoxin-induced acute injury phase. At all time-points, we found a trend consistent with that observed in the cyst-induced chronic injury, showing that the *Kim1* expression was less in double KO mice than in *Pkd1* KO. At 1 week after DCVC *Kim1* expression is strongly reduced in both genotypes suggesting that the DCVC-induced acute injury is largely repaired in the first week (Supplementary Figure 5). In line with the findings from the chronic injury experiments, the expression of genes involved in fibrogenesis, such as *Cola1a*, *Vim* and *Fn1,* was lower in double KO compared with *Pkd1* KO mice (Supplementary Figure 5).
Together with the results observed during the cyst-induced chronic injury, these data suggest that the lack of *Fjx1* leads to a reduced sensitivity to DCVC-induced injury.

PCP is altered in *Pkd1* mutant mice after injury but is not significantly affected by the lack of *Fjx1*

Tissue injury causes inversion or loss of PCP in epithelial cells, which recovers during the repair phase[42]. *Fj* has been described as an important PCP gene in *Drosophila* as is *Fjx1* in mammals, in particular in the regulation of the brain architecture[13] and inner ear polarity[14]. Therefore we decided to characterize renal PCP at 1 week after injury in *Pkd1* KO and double KO mice.
The levels of expression of *Fat4* and its ligand *Dchs1*[43] were unchanged by *Fjx1* KO (Figure 6C) suggesting that, at the expression level, the Fat/Ds PCP pathway was unaltered in kidneys of mutant mice. We also used the Golgi position to assess the degree of polarity perturbation in tubular cells (Figure 6D). Although Golgi position is not a direct read-out of PCP core proteins, it is found to be aberrant when PCP genes are knocked-out[44], and is also associated with loss of directed secretion, cell polarity and wound healing capacity[45].
We confirmed that altered polarity was associated with loss of *Pkd1* and kidney injury already at the pre-cystic stage, with a significantly higher aberrant Golgi position in *Pkd1* KO and double KO mice compared with Wt and *Fjx1* KO. However, we could not identify any difference between double KO and *Pkd1* KO or between Wt and *Fjx1* KO (Figure 6E), indicating that *Fjx1* did not contribute to an altered PCP.

The effect of *Fjx1* on injury response is not mediated by the Hippo pathway

FJX1 is thought to be an upstream regulator of the Hippo pathway through the activity of FAT4[46]. The Hippo pathway is pivotal in the regulation of organ growth, tissue renewal and regeneration[47] but is also deregulated in ADPKD[17]. Therefore, we investigated this pathway in *Pkd1* KO and double KO mice after DCVC treatment.
The Yap staining of kidney sections confirmed the pattern described before in our lab with increased nuclear localization of Yap in the cystic epithelium[17]. However, we could not detect any significant difference between double KO and *Pkd1* KO. Also, neither mRNA levels of *Yap1* and its paralog *Taz*, nor their transcriptional targets, *Amotl2*, *Cyr61*, *Wtip*, *Ctgf*, *Ajuba* (Supplementary Figure 6), showed any significant difference among genotypes.

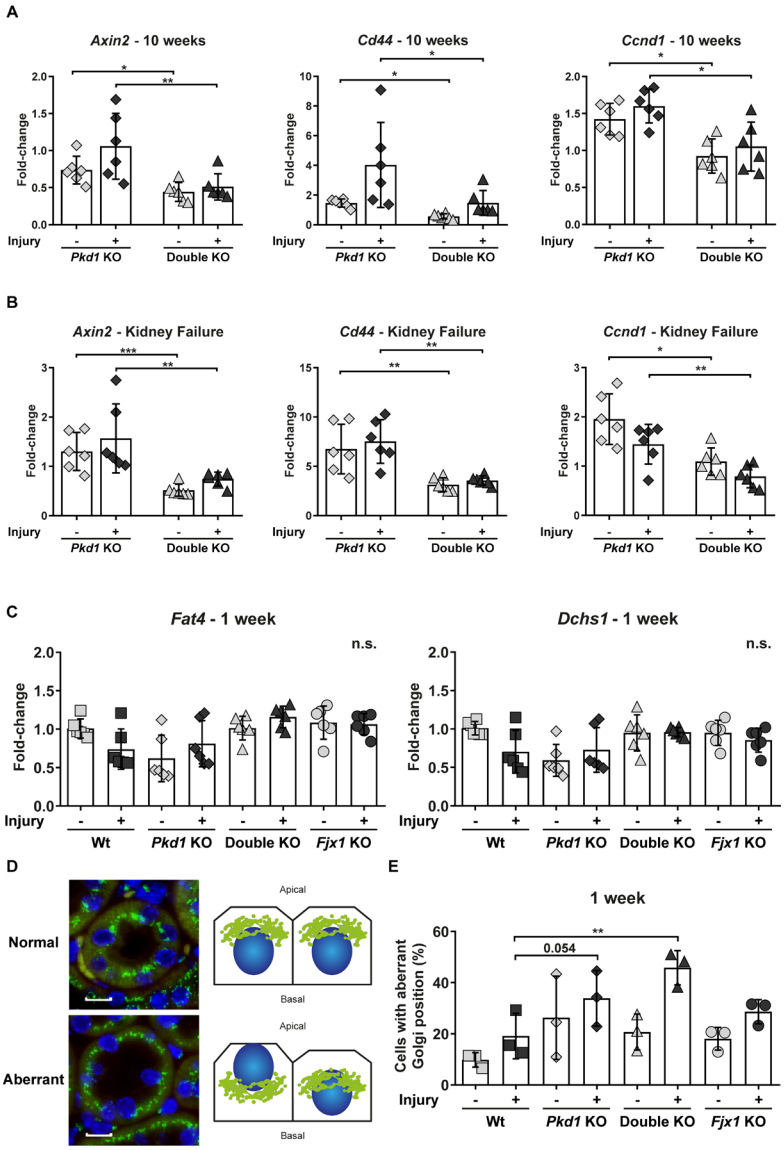

Figure 6. Expression of Wnt pathway target genes and expression level of Fjx1 targets and Golgi position in tubular cells

(A) *Axin2*, *Cd44* and *Ccnd1* mRNA levels at 10 weeks after DCVC injection. **(B)** Gene expression of *Axin2*, *Cd44* and *Ccnd1* at kidney failure. **(C)** Gene expression of *Fat4* and *Dchs1* at 1 week after DCVC injection. Each symbol shows data from one mouse. Mean ± SD. Two-way ANOVA with Tukey's multiple comparisons test. * P value <0.05; ** P value <0.01; *** P value <0.001. **(D)** Representative GM130 (green) staining on kidney tissue. Nuclei are stained in blue. In the normal situation the Golgi is positioned in a peri-centrosomal position at the top of the nucleus towards the lumen of the tubules, but after injury we often observed altered Golgi position. Scale bars, 10 µm. **(E)** Golgi position has been scored from 1 (normal position) to 3 (really abnormal position) in the round shaped tubules in the cortico-medullary region. Results are represented as the percentage of aberrant Golgi position (score ≥2.5) per tubules. Each symbol is the mean ± SD of about 90 tubules scored in a mouse. Two-way ANOVA with Fisher's LSD. ** P value <0.01.

This suggests that despite the clear nuclear localization of Yap in the cystic epithelium this pathway is not responsible for the difference in survival between *Pkd1* KO and double KO mice.

Taken together, these data indicate that knocking-out *Fjx1* does not affect PCP and the Hippo pathway in the kidneys. Therefore, the differences observed in response to injury in double KO mice cannot be explained by the effect of *Fjx1* on one of its canonical targets but suggests the existence of other, yet unknown, FJX1 targets.

Discussion

In this study we showed that nephrotoxic injury can accelerate disease progression in *Pkd1* KO mice but that this effect is abolished in the absence of *Fjx1* expression, allowing the *Pkd1*/*Fjx1* double KO mice to survive on average 5 weeks longer than the single *Pkd1* KO mice. Interestingly, the initiation of cyst formation and cyst growth were not different among the two models, as shown by 2KW/BW ratios and the cystic index. At 10 weeks after DCVC and kidney failure, however, we observed a reduction in injury marker expression together with reduced fibrosis and macrophage infiltration in *Pkd1* KO mice compared with double KO. Therefore, these data suggest that FJX1 does not play a critical role in cyst formation and expansion but seems to be involved in the fibrotic and inflammatory response to injury. As a result, the mice lacking both, *Fjx1* and *Pkd1*, have less fibrosis, which leads to a slower progression to ESRD and longer survival.

Fj is, together with the Ft-Ds cassette, part of a signalling complex, which is involved in the regulation of PCP in *Drosophila*[48-51]. Nevertheless, the absence of *Fjx1* did not alter PCP in the kidneys when compared with Wt mice, or in double KO compared to *Pkd1* KO mice. Although we observed significant deregulation of PCP in pre-cystic kidneys after injury in both single *Pkd1* mutant mice and double KO, the additional deletion of *Fjx1* did not further change the PCP phenotype in the *Pkd1* KO. These results are consistent with the published work of Probst *et al.*[13] showing that *Fjx1* KO mice do not have aberrant PCP in the kidneys but show only defects in neuronal branching. An effect on renal PCP was only seen after knocking-out *Fat4*, a target of FJX1, suggesting a more indirect effect of FJX1 on PCP in mammals[14,19]. We already showed in a previous study that PCP is impaired in *Pkd1* KO mice but not in Wt mice after injury, and that *Pkd1* KO mice injected with DCVC also develop cysts earlier when compared with the PBS group[8]. Whether pre-cystic alterations of PCP are critical for cyst formation is still controversial. Several studies are suggesting that PCP and cilium-associated control of oriented cell division (OCD) as well as convergent extension (CE) are necessary during renal tubular morphogenesis and also during proliferation phases in adult kidneys. Alterations of both OCD and CE are involved in PKD[23,52-54]. However, there are also studies showing that alterations in OCD and CE occur only after cyst formation, or that mutations of PCP-core proteins do not result in cyst formation[55,56]. This means that simple alteration of PCP is not sufficient to start cyst formation but disrupted PCP together with other events, such as injury, presumably increases the likelihood of cyst initiation.

Another pathway altered in ADPKD is the Hippo pathway, which is also regulated via the FJX1 target FAT4. In particular, the pathway's effectors Yap1 and Taz have been associated with cyst formation. We showed in the past that Yap1 accumulates in the nuclei of the cyst-lining epithelium[8,17], and other groups showed how deregulations of YAP1 activity

could induce cyst formation in Zebrafish models[57,58]. Moreover, knocking-out *Taz* in mice leads to glomerular and proximal tubular cyst formation[59-61]. Nevertheless, we did not see an effect of FJX1 on the Hippo pathway when comparing *Pkd1* KO and double KO mice. *Yap1* and *Taz* levels, as well as the levels of several of their target genes, were comparable in the two genotypes throughout disease progression. Also, *Fat4* levels were unchanged by *Fjx1* deletion (data not shown). Currently, clear proof that the FJX1-FAT4-DCHS cassette interaction controls PCP and Hippo pathway in kidneys is still missing[14,19,62].

Once cysts start to form and expand, they compress the surrounding tissue, compromise the normal tubular structure and also interfere with the extracellular compartment. This is accompanied by the expression of injury markers and activation of transcription factors like Stat3, Creb and ERK, known to be involved in ADPKD pathogenesis, and with an increased likelihood of more cyst formation[22,27,63,64]. All these cues are perceived by the organ like a constant injury insult and accompanied by a fibrotic and inflammatory response. Concomitantly, a severe cystic phenotype is associated with renal function decline due to the accumulation of fibrosis and inflammatory infiltrates, which interfere with normal organ function[65,66]. Nonetheless, it is unclear whether inflammation and fibrosis are responsible for or just a consequence of cyst formation. In our study, we observed separation between cyst formation and fibrotic response when *Fjx1* is inactivated. Indeed double KO mice had significantly reduced fibrosis and leukocytes infiltrates compared with *Pkd1* KO mice even though cyst formation was comparable. We could exclude the involvement of some fibrosis-related pathways, such as Notch, Hedgehog, hypoxia and Egfr signalling, while we found a significant reduction of expression of *Pdgfb*, *Tgfb1*, *Jak2* and *Stat1*, and Wnt pathway target genes in double KO compared to *Pkd1* KO mice. Considering the well described role of Tgfb and Wnt pathways in renal fibrosis[32,33,67,68], it is plausible to think that they might be responsible for the reduced fibrosis observed in double KO mice. Indeed, Tgfb can regulate the expression of *Pdgfb*[69], *Fn1* and type I collagen[70,71] all found downregulated in double KO mice. Similarly, Wnt targets *Axin2*[72], *Cd44*[73], *Ccnd1*[74,75] and *Myc*[76] were lower in double KO mice. Further studies are required to link FJX1 with the Tgfb and Wnt pathways mechanistically. An interesting connection between FJX1 and Jak/Stat pathways has been described in the literature, with Fj as the effector of the pleiotropic pathway Jak/Stat in *Drosophila*[10]. Although it is tempting to speculate that this might be the route through which FJX1 modulates the injury response, it is more likely that reduced *Jak2*/*Stat1* levels in the double KO mice mirror a reduced inflammatory response. Overall, these data suggest that FJX1 is involved in the fibrotic/inflammatory response after injury. We also showed that a different response to injury in the double KO mice could also play a role during the acute injury phase between 24 and 72 h after DCVC injection. This is not surprising, considering that *Fjx1* is mainly expressed in the developing kidneys while its expression is almost absent in adult kidneys[77]. Indeed, as for many other developmental genes, injury causes an increase

in expression of *Fjx1*[8]. Yet, the mechanism through which FJX1 is influencing these processes is still unclear.

As the function of FJX1 is still obscure, we cannot exclude that, besides the canonical targets Fat and Dachsous, additional direct targets of FJX1 exist. This is because FJX1 is a Golgi secretory pathway kinase and therefore likely involved in many biological processes, as already shown for its closely related homolog Fam20C[78,79]. Additionally, FJX1 protein undergoes partial proteolytic cleavage at the N-terminus, with the secretion of the resultant fragment that can function as signalling ligand, influencing surrounding cells. FJX1 fusion protein experiments have shown several FJX1 binding sites present in different organs, including kidneys[77]. Therefore, a better understanding of FJX1 functions in mammals might help to explain the effect we unveiled on fibrogenesis.

In conclusion, we show that cyst progression and fibrosis in *Pkd1*/*Fjx1* double KO mice are partially uncoupled and demonstrate a new, yet undefined, role of FJX1 in fibrosis, ultimately resulting in longer survival. Unveiling the underlying molecular mechanism might open the path for future therapies that can specifically target injury-induced fibrosis, and could not only help to slow down ADPKD, but also the progression of other chronic kidney diseases.

Acknowledgements

This work was supported by grants from the People Program (Marie Curie Actions) of the European Union's Seventh Framework Program FP7/2077-2013 under Research Executive Agency Grant Agreement 317246, and by the Dutch Kidney Foundation consortium grant (CP10.12 -DIPAK). The DIPAK Consortium is an inter-university collaboration in The Netherlands that is established to study Autosomal Dominant Polycystic Kidney Disease and to develop rational treatment strategies for this disease. Principal investigators are (in alphabetical order): J.P.H. Drenth (Dept. Gastroenterology and Hepatology, Radboud UMC Nijmegen), J.W. de Fijter (Dept. Nephrology, Leiden UMC), R.T. Gansevoort (Dept. Nephrology, UMC Groningen), D.J.M. Peters (Dept. Human Genetics, Leiden UMC), J. Wetzels (Dept. Nephrology, Radboud UMC Nijmegen) and R. Zietse (Dept. Internal Medicine, Erasmus MC Rotterdam).

Author contributions

C.F. (concept design, data acquisition, data interpretation, writing paper), H. H. (concept design), D.J.M.P. (concept design, data interpretation, writing paper), K.A.M.V. (histopathology), M.S. (data interpretation and manuscript reviewing), A.V. and H.M.N. (mice, data discussion, manuscript reviewing).

References

1 Igarashi, P. Genetics and Pathogenesis of Polycystic Kidney Disease. Journal of the American Society of Nephrology 13, 2384-2398, doi:10.1097/01.asn.0000028643.17901.42 (2002).

2 Takiar, V. & Caplan, M. J. Polycystic kidney disease: pathogenesis and potential therapies. Biochim Biophys Acta 1812, 1337-1343, doi:10.1016/j.bbadis.2010.11.014 (2011).

3 Torres, V. E. et al. Tolvaptan in patients with autosomal dominant polycystic kidney disease. N Engl J Med 367, 2407-2418, doi:10.1056/NEJMoa1205511 (2012).

4 Ong, A. C. M. Polycystic kidney disease: Tolvaptan slows disease progression in late-stage ADPKD. Nat Rev Nephrol, doi:10.1038/nrneph.2017.180 (2018).

5 Gansevoort, R. T. et al. Recommendations for the use of tolvaptan in autosomal dominant polycystic kidney disease: a position statement on behalf of the ERA-EDTA Working Groups on Inherited Kidney Disorders and European Renal Best Practice. Nephrol Dial Transpl 31, 337-348, doi:10.1093/ndt/gfv456 (2016).

6 Malas, T. B. et al. Meta-analysis of polycystic kidney disease expression profiles defines strong involvement of injury repair processes. American Journal of Physiology - Renal Physiology 312, F806-F817 (2017).

7 Leonhard, W. N., Happe, H. & Peters, D. J. Variable Cyst Development in Autosomal Dominant Polycystic Kidney Disease: The Biologic Context. J Am Soc Nephrol 27, 3530-3538, doi:10.1681/ASN.2016040425 (2016).

8 Happé, H. et al. Toxic tubular injury in kidneys from Pkd1-deletion mice accelerates cystogenesis accompanied by dysregulated planar cell polarity and canonical Wnt signaling pathways. Human Molecular Genetics 18, 2532-2542, doi:10.1093/hmg/ddp190 (2009).

9 Tokunaga, C. & Gerhart, J. C. The effect of growth and joint formation on bristle pattern in D. melanogaster. J Exp Zool 198, 79-95, doi:10.1002/jez.1401980110 (1976).

10 Zeidler, M. P., Perrimon, N. & Strutt, D. I. The four-jointed gene is required in the Drosophila eye for ommatidial polarity specification. Curr Biol 9, 1363-1372, doi:Doi 10.1016/S0960-9822(00)80081-0 (1999).

11 Rawls, A. S., Guinto, J. B. & Wolff, T. The cadherins fat and dachsous regulate dorsal/ventral signaling in the Drosophila eye. Curr Biol 12, 1021-1026 (2002).

12 Casal, J., Lawrence, P. A. & Struhl, G. Two separate molecular systems, Dachsous/Fat and Starry night/Frizzled, act independently to confer planar cell polarity. Development 133, 4561-4572, doi:10.1242/dev.02641 (2006).

13 Probst, B., Rock, R., Gessler, M., Vortkamp, A. & Puschel, A. W. The rodent Four-jointed ortholog Fjx1 regulates dendrite extension. Dev Biol 312, 461-470, doi:10.1016/j.ydbio.2007.09.054 (2007).

14 Saburi, S. et al. Loss of Fat4 disrupts PCP signaling and oriented cell division and leads to cystic kidney disease. Nat Genet 40, 1010-1015, doi:10.1038/ng.179 (2008).

15 Staley, B. K. & Irvine, K. D. Hippo signaling in Drosophila: recent advances and insights. Dev Dyn 241, 3-15, doi:10.1002/dvdy.22723 (2012).

16 Reddy, B. V. V. G. & Irvine, K. D. The Fat and Warts signaling pathways: new insights into their regulation, mechanism and conservation. Development 135, 2827-2838, doi:10.1242/dev.020974 (2008).

17 Happe, H. et al. Altered Hippo signalling in polycystic kidney disease. J Pathol 224, 133-142, doi:10.1002/path.2856 (2011).

18 Ragni, C. V. et al. Amotl1 mediates sequestration of the Hippo effector Yap1 downstream of Fat4 to restrict heart growth. Nat Commun 8, 14582, doi:10.1038/ncomms14582 (2017).

19 Mao, Y. et al. Characterization of a Dchs1 mutant mouse reveals requirements for Dchs1-Fat4 signaling during mammalian development. Development 138, 947-957, doi:10.1242/dev.057166 (2011).

20 Lantinga-van Leeuwen, I. S. et al. Kidney-specific inactivation of the Pkd1 gene induces rapid cyst formation in developing kidneys and a slow onset of disease in adult mice. Hum Mol Genet 16, 3188-3196, doi:10.1093/hmg/ddm299 (2007).

21 Takakura, A. et al. Renal injury is a third hit promoting rapid development of adult polycystic kidney disease. Hum Mol Genet 18, 2523-2531, doi:10.1093/hmg/ddp147 (2009).

22 Leonhard, W. N. et al. Scattered Deletion of PKD1 in Kidneys Causes a Cystic Snowball Effect and Recapitulates Polycystic Kidney Disease. J Am Soc Nephrol 26, 1322-1333, doi:10.1681/ASN.2013080864 (2015).

23 Patel, V. et al. Acute kidney injury and aberrant planar cell polarity induce cyst formation in mice lacking renal cilia. Hum Mol Genet 17, 1578-1590, doi:10.1093/hmg/ddn045 (2008).

24 Bell, P. D. et al. Loss of primary cilia upregulates renal hypertrophic signaling and promotes cystogenesis. J Am Soc Nephrol 22, 839-848, doi:10.1681/ASN.2010050526 (2011).

25 Han, W. K., Bailly, V., Abichandani, R., Thadhani, R. & Bonventre, J. V. Kidney Injury Molecule-1 (KIM-1): a novel biomarker for human renal proximal tubule injury. Kidney Int 62, 237-244, doi:10.1046/j.1523-1755.2002.00433.x (2002).

26 Yang, N. S. et al. Blockage of JAK/STAT signalling attenuates renal ischaemia-reperfusion injury in rat. Nephrol Dial Transpl 23, 91-100, doi:10.1093/ndt/gfm509 (2008).

27 Weimbs, T. & Talbot, J. J. STAT3 Signaling in Polycystic Kidney Disease. Drug Discov Today Dis Mech 10, e113-e118, doi:10.1016/j.ddmec.2013.03.001 (2013).

28 Dees, C. et al. Inhibition of Notch signaling prevents experimental fibrosis and induces regression of established fibrosis. Arthritis Rheum 63, 1396-1404, doi:10.1002/art.30254 (2011).

29 Hu, B. & Phan, S. H. Notch in fibrosis and as a target of anti-fibrotic therapy. Pharmacol Res 108, 57-64, doi:10.1016/j.phrs.2016.04.010 (2016).

30 Hu, L., Lin, X., Lu, H., Chen, B. & Bai, Y. An overview of hedgehog signaling in fibrosis. Mol Pharmacol 87, 174-182, doi:10.1124/mol.114.095141 (2015).

31 Kramann, R. Hedgehog Gli signalling in kidney fibrosis. Nephrol Dial Transplant 31, 1989-1995, doi:10.1093/ndt/gfw102 (2016).

32 Piersma, B., Bank, R. A. & Boersema, M. Signaling in Fibrosis: TGF-beta, WNT, and YAP/TAZ Converge. Front Med (Lausanne) 2, 59, doi:10.3389/fmed.2015.00059 (2015).

33 Tan, R. J., Zhou, D., Zhou, L. & Liu, Y. Wnt/beta-catenin signaling and kidney fibrosis. Kidney Int Suppl (2011) 4, 84-90, doi:10.1038/kisup.2014.16 (2014).

34 Parrish, A. R. The cytoskeleton as a novel target for treatment of renal fibrosis. Pharmacol Therapeut 166, 1-8, doi:10.1016/j.pharmthera.2016.06.006 (2016).

35 Kawakami, T., Mimura, I., Shoji, K., Tanaka, T. & Nangaku, M. Hypoxia and fibrosis in chronic kidney disease: crossing at pericytes. Kidney Int Suppl 4, 107-112, doi:10.1038/kisup.2014.20 (2014).

36 Edeling, M., Ragi, G., Huang, S., Pavenstadt, H. & Susztak, K. Developmental signalling pathways in renal fibrosis: the roles of Notch, Wnt and Hedgehog. Nat Rev Nephrol 12, 426-439, doi:10.1038/nrneph.2016.54 (2016).

37 Ruthenborg, R. J., Ban, J. J., Wazir, A., Takeda, N. & Kim, J. W. Regulation of wound healing and fibrosis by hypoxia and hypoxia-inducible factor-1. Mol Cells 37, 637-643, doi:10.14348/molcells.2014.0150 (2014).

38 Darby, I. A. & Hewitson, T. D. Hypoxia in tissue repair and fibrosis. Cell Tissue Res 365, 553-562, doi:10.1007/s00441-016-2461-3 (2016).

39 Zhuang, S. G. & Liu, N. EGFR signaling in renal fibrosis. Kidney Int Suppl 4, 70-74, doi:10.1038/kisup.2014.13 (2014).

40 Chen, J. et al. EGFR signaling promotes TGFbeta-dependent renal fibrosis. J Am Soc Nephrol 23, 215-224, doi:10.1681/ASN.2011070645 (2012).

41 Terzi, F. et al. Targeted expression of a dominant-negative EGF-R in the kidney reduces tubulo-interstitial lesions after renal injury. J Clin Invest 106, 225-234, doi:10.1172/JCI8315 (2000).

42 Siegel, N. J., Devarajan, P. & Van Why, S. Renal cell injury: metabolic and structural alterations. Pediatr Res 36, 129-136, doi:10.1203/00006450-199408000-00001 (1994).

43 Mao, Y. P., Francis-West, P. & Irvine, K. D. Fat4/Dchs1 signaling between stromal and cap mesenchyme cells influences nephrogenesis and ureteric bud branching. Development 142, 2574-U2569, doi:10.1242/dev.122630 (2015).

44 Caddy, J. et al. Epidermal wound repair is regulated by the planar cell polarity signaling pathway. Developmental cell 19, 138-147, doi:10.1016/j.devcel.2010.06.008 (2010).

45 Yadav, S., Puri, S. & Linstedt, A. D. A primary role for Golgi positioning in directed secretion, cell polarity, and wound healing. Mol Biol Cell 20, 1728-1736, doi:10.1091/mbc.E08-10-1077 (2009).

46 Das, A. et al. Stromal–epithelial crosstalk regulates kidney progenitor cell differentiation. Nature Cell Biology 15, 1035, doi:10.1038/ncb2828 (2013).

47 Piccolo, S., Dupont, S. & Cordenonsi, M. The biology of YAP/TAZ: hippo signaling and beyond. Physiol Rev 94, 1287-1312, doi:10.1152/physrev.00005.2014 (2014).

48 Casal, J., Struhl, G. & Lawrence, P. A. Developmental compartments and planar polarity in Drosophila. Curr Biol 12, 1189-1198 (2002).

49 Yang, C. H., Axelrod, J. D. & Simon, M. A. Regulation of Frizzled by fat-like cadherins during planar polarity signaling in the Drosophila compound eye. Cell 108, 675-688 (2002).

50 Matakatsu, H. & Blair, S. S. Interactions between Fat and Dachsous and the regulation of planar cell polarity in the Drosophila wing. Development 131, 3785-3794, doi:10.1242/dev.01254 (2004).

51 Cho, E. & Irvine, K. D. Action of fat, four-jointed, dachsous and dachs in distal-to-proximal wing signaling. Development 131, 4489-4500, doi:10.1242/dev.01315 (2004).

52 Fischer, E. et al. Defective planar cell polarity in polycystic kidney disease. Nat Genet 38, 21-23, doi:10.1038/ng1701 (2006).

53 Luyten, A. et al. Aberrant regulation of planar cell polarity in polycystic kidney disease. J Am Soc Nephrol 21, 1521-1532, doi:10.1681/ASN.2010010127 (2010).

54 Castelli, M. et al. Polycystin-1 binds Par3/aPKC and controls convergent extension during renal tubular morphogenesis. Nat Commun 4, 2658, doi:10.1038/ncomms3658 (2013).

55 Nishio, S. et al. Loss of oriented cell division does not initiate cyst formation. J Am Soc Nephrol 21, 295-302, doi:10.1681/ASN.2009060603 (2010).

56 Kunimoto, K. et al. Disruption of Core Planar Cell Polarity Signaling Regulates Renal Tubule Morphogenesis but Is Not Cystogenic. Curr Biol 27, 3120-3131 e3124, doi:10.1016/j.cub.2017.09.011 (2017).

57 Skouloudaki, K. et al. Scribble participates in Hippo signaling and is required for normal zebrafish pronephros development. P Natl Acad Sci USA 106, 8579-8584, doi:10.1073/pnas.0811691106 (2009).

58 He, L. L. et al. Yes-Associated Protein (Yap) Is Necessary for Ciliogenesis and Morphogenesis during Pronephros Development in Zebrafish (Danio Rerio). Int J Biol Sci 11, 935-947, doi:10.7150/ijbs.11346 (2015).

59 Hossain, Z. et al. Glomerulocystic kidney disease in mice with a targeted inactivation of Wwtr1. Proc Natl Acad Sci U S A 104, 1631-1636, doi:10.1073/pnas.0605266104 (2007).

60 Makita, R. et al. Multiple renal cysts, urinary concentration defects, and pulmonary emphysematous changes in mice lacking TAZ. Am J Physiol Renal Physiol 294, F542-553, doi:10.1152/ajprenal.00201.2007 (2008).

61 Reginensi, A. et al. Yap- and Cdc42-dependent nephrogenesis and morphogenesis during mouse kidney development. PLoS Genet 9, e1003380, doi:10.1371/journal.pgen.1003380 (2013).

62 Bagherie-Lachidan, M. et al. Stromal Fat4 acts non-autonomously with Dchs1/2 to restrict the nephron progenitor pool. Development 142, 2564-2573, doi:10.1242/dev.122648 (2015).

63 Aguiari, G. et al. Polycystin-1 regulates amphiregulin expression through CREB and AP1 signalling: implications in ADPKD cell proliferation. J Mol Med 90, 1267-1282, doi:10.1007/s00109-012-0902-3 (2012).

64 Yamaguchi, T. et al. Cyclic AMP activates B-Raf and ERK in cyst epithelial cells from autosomal-dominant polycystic kidneys. Kidney Int 63, 1983-1994, doi:10.1046/j.1523-1755.2003.00023.x (2003).

65 Norman, J. Fibrosis and progression of autosomal dominant polycystic kidney disease (ADPKD). Biochim Biophys Acta 1812, 1327-1336, doi:10.1016/j.bbadis.2011.06.012 (2011).

66 Song, C. J., Zimmerman, K. A., Henke, S. J. & Yoder, B. K. Inflammation and Fibrosis in Polycystic Kidney Disease. Results Probl Cell Differ 60, 323-344, doi:10.1007/978-3-319-51436-9_12 (2017).

67 Akhmetshina, A. et al. Activation of canonical Wnt signalling is required for TGF-beta-mediated fibrosis. Nat Commun 3, 735, doi:10.1038/ncomms1734 (2012).

68 Meng, X. M., Tang, P. M., Li, J. & Lan, H. Y. TGF-beta/Smad signaling in renal fibrosis. Front Physiol 6, 82, doi:10.3389/fphys.2015.00082 (2015).

69 Geng, H. et al. Lysophosphatidic acid increases proximal tubule cell secretion of profibrotic cytokines PDGF-B and CTGF through LPA2- and Galphaq-mediated Rho and alphavbeta6 integrin-dependent activation of TGF-beta. Am J Pathol 181, 1236-1249, doi:10.1016/j.ajpath.2012.06.035 (2012).

70 Ono, K., Ohtomo, T., Ninomiya-Tsuji, J. & Tsuchiya, M. A dominant negative TAK1 inhibits cellular fibrotic responses induced by TGF-beta. Biochem Biophys Res Commun 307, 332-337 (2003).

71 Kim, S. I. et al. TGF-beta-activated kinase 1 and TAK1-binding protein 1 cooperate to mediate TGF-beta1-induced MKK3-p38 MAPK activation and stimulation of type I collagen. Am J Physiol Renal Physiol 292, F1471-1478, doi:10.1152/ajprenal.00485.2006 (2007).

72 Jho, E.-h. et al. Wnt/beta-catenin/Tcf signaling induces the transcription of Axin2, a negative regulator of the signaling pathway. Molecular and cellular biology 22, 1172-1183, doi:10.1128/MCB.22.4.1172-1183.2002 (2002).

73 Wielenga, V. J. et al. Expression of CD44 in Apc and Tcf mutant mice implies regulation by the WNT pathway. Am J Pathol 154, 515-523, doi:10.1016/s0002-9440(10)65297-2 (1999).

74 Tetsu, O. & McCormick, F. Beta-catenin regulates expression of cyclin D1 in colon carcinoma cells. Nature 398, 422-426, doi:10.1038/18884 (1999).

75 Shtutman, M. et al. The cyclin D1 gene is a target of the beta-catenin/LEF-1 pathway. Proc Natl Acad Sci U S A 96, 5522-5527 (1999).

76 He, T. C. et al. Identification of c-MYC as a target of the APC pathway. Science 281, 1509-1512 (1998).

77 Rock, R., Heinrich, A. C., Schumacher, N. & Gessler, M. Fjx1: a notch-inducible secreted ligand with specific binding sites in developing mouse embryos and adult brain. Dev Dyn 234, 602-612, doi:10.1002/dvdy.20553 (2005).

78 Tagliabracci, V. S. et al. Secreted Kinase Phosphorylates Extracellular Proteins That Regulate Biomineralization. Science 336, 1150-1153, doi:10.1126/science.1217817 (2012).

79 Sreelatha, A., Kinch, L. N. & Tagliabracci, V. S. The secretory pathway kinases. Biochim Biophys Acta 1854, 1687-1693, doi:10.1016/j.bbapap.2015.03.015 (2015).

Supplementary Figures

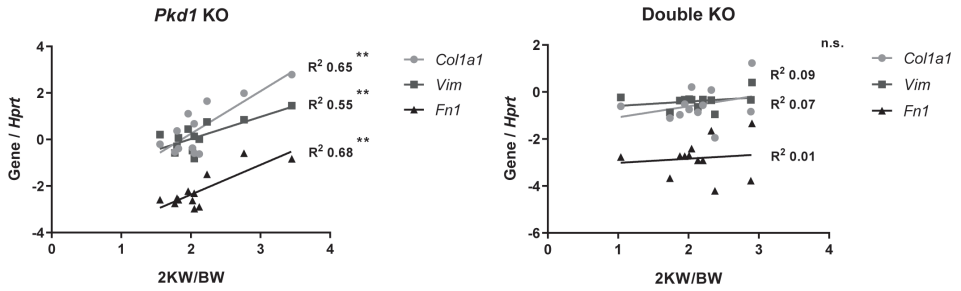

Supplementary Figure 1. Correlation of fibrosis and kidney size in *Pkd1* KO and *Pkd1/Fjx1* double KO mice

Linear regression of 2KW/BW ratio and gene expression normalized on *Hprt* of *Col1a1*, *Vim* and *Fn1* at 10 weeks time point. ** P value <0.01

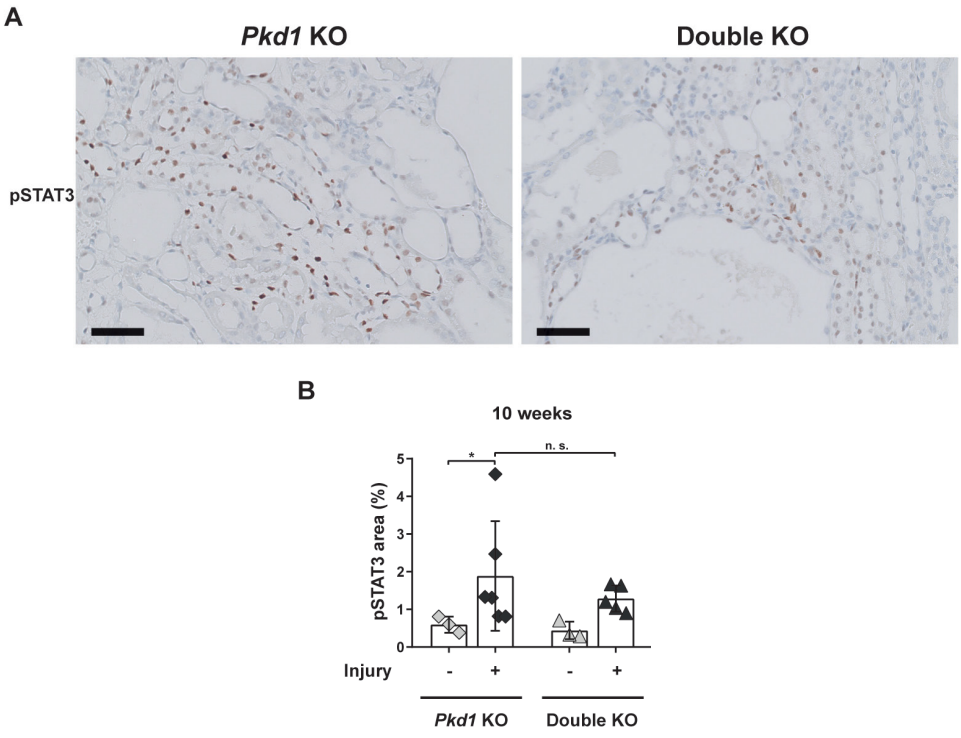

Supplementary Figure 2. Expression of pSTAT3 in *Pkd1* KO and double KO mice

(A) Representative immunostaining for pSTAT3 at 10 weeks after injection of the nephrotoxic compound S-(1,2-dichlorovinyl)-L-cysteine (DCVC) in *Pkd1* KO and *Pkd1/Fjx1* double KO mice kidneys, indicated as ± injury. Scale bars, 50 µm. **(B)** Quantification of pSTAT3 staining. Each symbol shows data from one mouse. Mean ± SD. Two-way ANOVA with Tukey's multiple comparisons test. * P value <0.05.

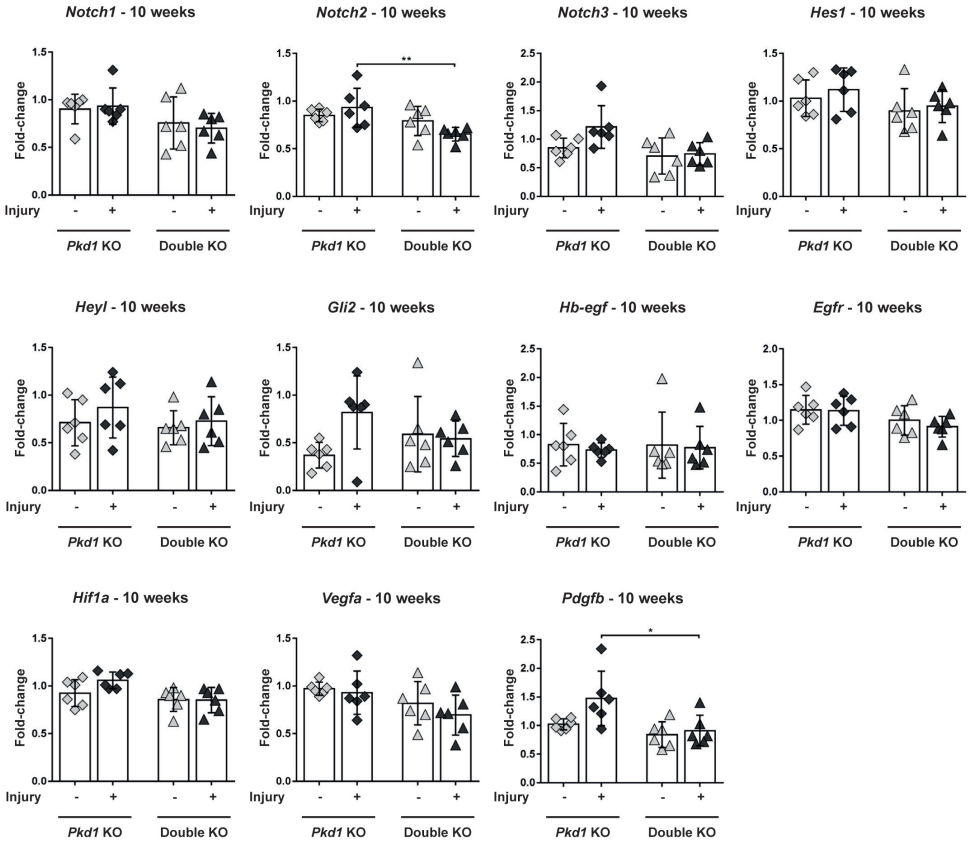

Supplementary Figure 3. Investigation of pathways involved in renal fibrosis at 10 weeks after injection of the nephrotoxic compound S-(1,2-dichlorovinyl)-L-cysteine (DCVC)

Gene expression in *Pkd1* KO mice and *Pkd1*/*Fjx1* double KO mice with or without renal injury induced via injection of DCVC, of Notch target genes (*Notch1*, *Notch2*, *Notch3*); Hedgehog target genes (*Hes1*, *Hey1*, *Gli2*); Egf pathway (*Hb-egf*, *Egfr*); hypoxia pathway (*Hif1a*, *Vegfa*, *Pdgfb*). Each symbol shows data from one mouse. Mean ± SD. Two-way ANOVA with Tukey's multiple comparisons test. * P value <0.05; ** P value <0.01.

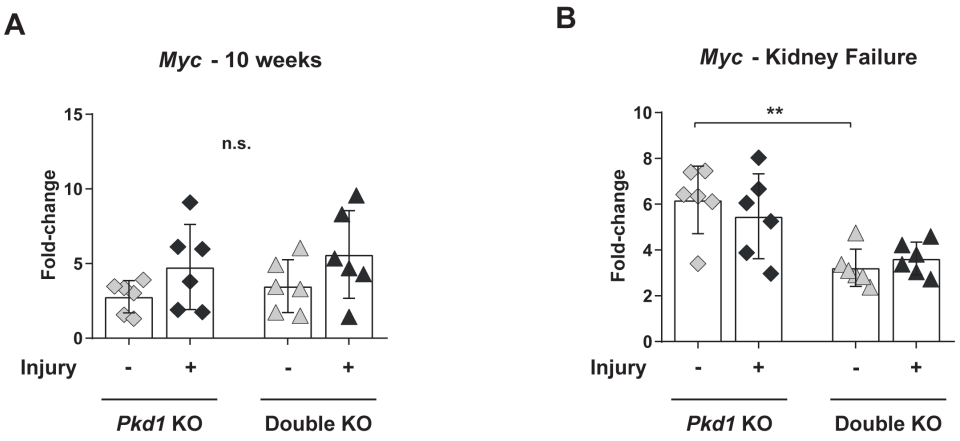

Supplementary Figure 4. Wnt pathway target Myc

(A) Gene expression of *Myc* 10 weeks after injection of the nephrotoxic compound S-(1,2-dichlorovinyl)-L-cysteine (DCVC) or PBS in *Pkd1* KO mice and *Pkd1*/*Fjx1* double KO mice. **(B)** Gene expression of *Myc* at kidney failure in *Pkd1* KO mice and *Pkd1*/*Fjx1* double KO mice. Each symbol shows data from one mouse. Mean ± SD. Two-way ANOVA with Tukey's multiple comparisons test. ** P value <0.01.

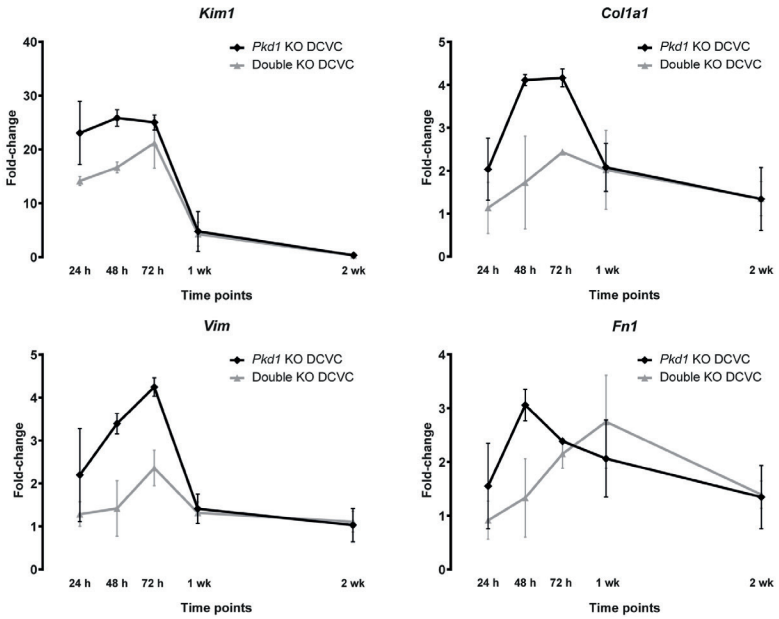

Supplementary Figure 5. Injury and fibrotic genes expression at early time points after injury

Gene expression of *Kim1*, *Col1a1*, *Vim* and *Fn1* at 24 h, 48 h, 72 h, 1 and 2 weeks after S-(1,2-dichlorovinyl)-L-cysteine (DCVC) injection. Each point is the mean of two mice (24 h, 48 h, 72 h) or six mice (1 and 2 weeks) ± SD.

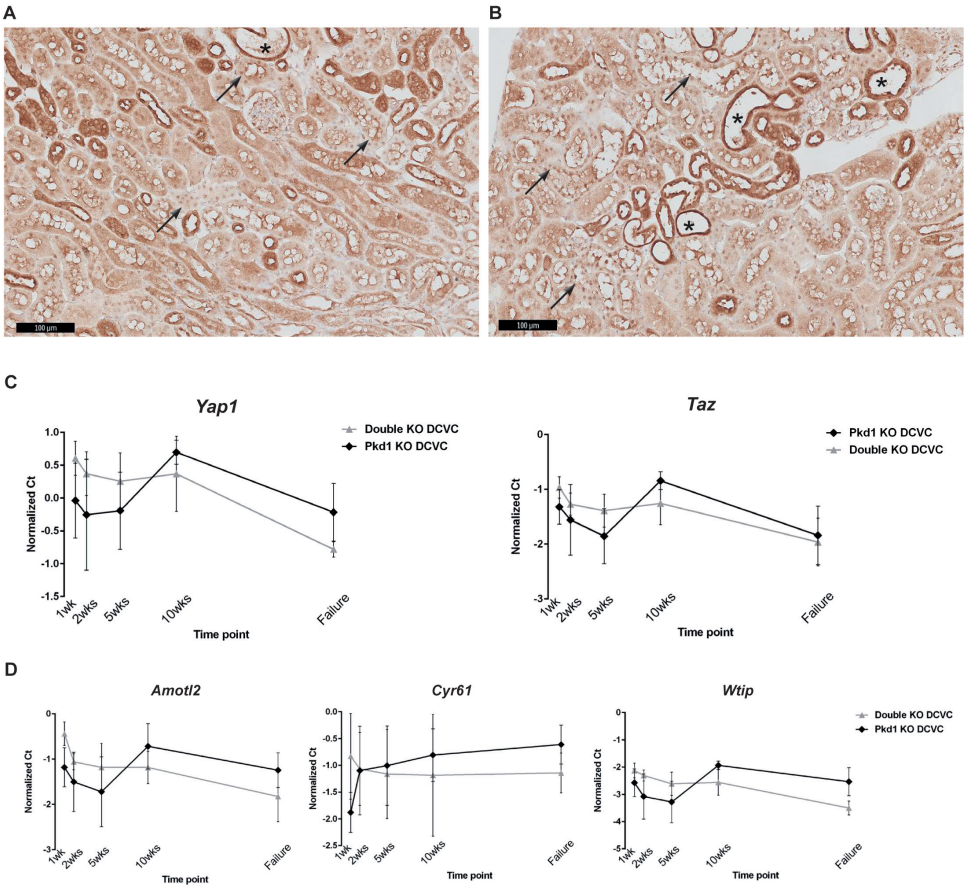

Supplementary Figure 6. Hippo Pathway activation in *Pkd1* KO and *Pkd1*/*Fjx1* double KO mice

(A) Representative immunostaining for Yap1 on kidney tissue in *Pkd1* KO mice after injection of the nephrotoxic compound S-(1,2-dichlorovinyl)-L-cysteine (DCVC) and **(B)** double KO mice after DCVC. In both genotypes, it is possible to observe some dilated tubules which intensely stain for Yap1 and diffuse nuclear localization. Scale bars, 100 µm. Arrows indicate tubules showing nuclear Yap1; asterisks indicate dilated tubules. **(C)** *Yap1* and *Taz* expression during disease progression. **(D)** Gene expression of representative Yap1/Taz targets. Each point is the mean expression of six mice ± SD.

Supplementary Methods

Animal Models

The kidney specific tamoxifen-inducible *Pkd1*-deletion mouse model (*Pkd1*-cKO) has been described previously[1]. The *Fjx1*$^{-/-}$ (*Fjx1* KO) were generated via insertion of the *LacZ* gene followed by a PGK-neo resistance cassette in the single exon of *Fjx1* gene, as described previously[2]. This results in a germline disruption of *Fjx1*. By cross-breeding the kidney specific tamoxifen-inducible *Pkd1*-deletion mice (*Pkd1* KO) with the *Fjx1* KO mice, we generated the *Fjx1*$^{-/-}$/*Pkd1*-cKO double KO mouse model (double KO). Control mice (Wt) carry the *Lox*P site that flanks *Pkd1* exons 2-11 but miss the tamoxifen-inducible Cre recombinase (*Pkd1*^{lox,lox}). Inactivation of the *Pkd1* gene was achieved by oral administration of tamoxifen (5 mg/day, 3 consecutive days) in adult mice that were between 13 to 14 weeks old. Only male mice were used for all the experimental groups. The *Fjx1* KO and the Wt mice also received tamoxifen. Renal injury was induced a week after gene disruption by a single intraperitoneal (i.p.) injection of S-(1,2-dichlorovinyl)-L-cysteine (DCVC) (15 mg/kg) or vehicle. Injury was evaluated by measurement of blood urea level after 40 hours, as described before[3].

Mice were sacrificed at 24, 48 and 72 hours after DCVC injection to study acute injury; at 1, 2, 5 and 10 weeks after DCVC injection to study injury/repair and disease progression and when reaching renal failure indicated by urea levels in the blood equal or over 25 mmol/l. Blood urea nitrogen (BUN) level assessment has been described previously[3]. At sacrifice, mice were weighed; then kidneys were collected and weighed to calculate the 2 kidneys weight to body weight ratios (2KW/BW).

IHC, Golgi position, Cystic and Fibrotic indices

Formalin-fixed paraffin-embedded kidneys were sectioned at 4µm thickness. Section stained with Periodic acid-Schiff (PAS) staining were used to determine cystic index (CI). CI is measured as the ratio of cystic area over the total parenchyma area using Image J software (open source software; National Institutes of Health, Bethesda, MD) and expressed as a percentage. Sections stained with Picro Sirius Red (PSR) staining were used to determine fibrotic index (FI). FI was calculated using a designed color palettes and Photoshop software (Adobe Systems, Inc., San Jose, CA). First a palette was used to remove the pixels of the renal outline area and of the cystic and tubular areas. Then a second palette was used to remove the pixels of the kidney parenchyma except those colored by the PSR staining. Big arteries were manually excluded. The ratio of PSR positive pixels over the total parenchyma pixels was expressed as a percentage and indicated as FI. The same analysis was used to calculate the area positive for alpha Smooth Muscle Actin (αSMA) and for the area positive for F4/80. These antibodies were used for the IHC: rabbit anti αSMA-AP (1:50; Sigma-Aldrich #A5691); rat anti-F4/80 (1:250; Serotec); rabbit anti-Yap (1:800; Cell Signaling Technology #14074), rabbit anti-pStat3 (1:75; Cell Signaling #9145); mouse anti-GM130 (1:500; BD Bioscience

#610822). Anti-rabbit envision HRP (Dako) or anti-rat Immpress HRP (Vector Laboratories) or Alexa 488 goat anti-mouse IgG1 (1:200; Invitrogen) were used as secondary antibodies.
The frequency of cyst size was calculated using Image J software. Pictures of whole kidneys stained with PAS staining were used. The area of the renal outline was removed and then the area of the tubules lumen was measured in pixels and divided in four groups: Normal tubule or mildly dilated tubules up to 1000 pixels; small cysts between 1000 and 2000 pixels; medium cysts between 2000 and 10000 pixels; big cysts more than 10000 pixels.
For the evaluation of the Golgi position as a read-out of the PCP we used a mouse anti-GM130 followed by a secondary Alexa 488 Goat Anti-mouse IgG1 and mounted with Vectashield with Dapi (Vector Laboratories) to visualize the nuclei. From each individual kidney we selected at least 90 tubules with a circularity ≥ 0.995, which was evaluated by Image J software. We scored the Golgi position in relation to the nucleus from 1 to 3, with 1 being the normal peri-centrosomal position at the top of the nucleus towards the lumen, and 3 being very aberrant at the bottom of the nucleus; a score ≥ 2,5 was considered aberrant and the total count was normalized on the number of cells per tubule and expressed as a percentage.

References

1 Lantinga-van Leeuwen, I. S. *et al.* Kidney-specific inactivation of the Pkd1 gene induces rapid cyst formation in developing kidneys and a slow onset of disease in adult mice. *Hum Mol Genet* **16**, 3188-3196, doi:10.1093/hmg/ddm299 (2007).

2 Probst, B., Rock, R., Gessler, M., Vortkamp, A. & Puschel, A. W. The rodent Four-jointed ortholog Fjx1 regulates dendrite extension. *Dev Biol* **312**, 461-470, doi:10.1016/j.ydbio.2007.09.054 (2007).

3 Happé, H. *et al.* Toxic tubular injury in kidneys from Pkd1-deletion mice accelerates cystogenesis accompanied by dysregulated planar cell polarity and canonical Wnt signaling pathways. *Human Molecular Genetics* **18**, 2532-2542, doi:10.1093/hmg/ddp190 (2009).

Supplementary Tables

Supplementary Table 1. List of primer sequences used for qPCR

	Forward	Reverse
Kim1	TCTCTAAGCGTGGTTGCCTT	TGTCTTCAGCTCGGGAATGC
Col1a1	TGACTGGAAGAGCGGAGAGT	AGACGGCTGAGTAGGGAACA
Vim	CCAACCTTTTCTTCCCTGAA	TGAGTGGGTGTCAACCAGAG
Fn1	AATCCAGTCCACAGCCATTCC	CCTGTCTTCTCTTTCGGGTTCA
Acta2	CATCATGCGTCTGGACTTG	ATCTCACGCTCGGCAGTAG
Tgfb	ACTATTGCTTCAGCTCCACAGA	AAGTTGGCATGGTAGCCCTT
Adgre1	GGCAGGGATCTTGGTTATGCT	GCTGCACTCTGTAAGGACACT
Fat4	ACCGATGCAGATGATGGTGTC	ACTCCGTGCTTATCCACTGC
Dchs1	GACAATCGTCCCACCATCCC	AGCCCAACAGTGCATCTTCT
Yap1	TTCCGATCCCTTTCTTAACAGT	GAGGGATGCTGTAGCTGCTC
Taz (Wwtr1)	ATGGACGAGATGGATACAGGTGA	AGACTCCAAAGTCCCGAGGT
Amotl2	ACCAGGAGATGGAGAGCAGATT	GAAGGACCTTGATCACCGCA
Cyr61	CACTGAAGAGGCTTCCTGTCT	CCAAGACGTGGTCTGAACGA
Wtip	TTCATCTGTGACTCCTGTGGGA	TGGCAGTACACTTTCTCACCC
Notch1	GGTGCTCTGATGGACGACAA	TACTGGCTCCTCAAACCGGA
Notch2	AGGCTAACCTGATTGGTTCTGG	AAGCCTCATCCTCAGCCTTG
Notch3	CTGGGAGTCAGTGTCAGAACC	GGTGGACAAATGCAGTAAGCC
Hes1	GGCCTCTGAGCACAGAAAGT	TTGGAATGCCGGGAGCTATC
Heyl	AAGAAGCGCAGAGGGATCATAG	GGGACCAATCGTCGCAATTC
Gli1	CAGCATGGGAACAGAAGGACT	ACCCTGGGACCCTGACATAA
Hb-egf	GAGGAGGACCTGAGCTATAGGAA	AACGTGTAACGAACCACTGTCT
Egfr	GAAGTACAGCTTTGGTGCCACCTG	CTTGCGGATGCCATCTTCTTCCAC
HIF1a	AGTCAGCAACGTGGAAGGTG	GCACGTCATGGGTGGTTTCT
Vegfa	CTCCACCATGCCAAGTGGTC	GTCCACCAGGGTCTCAATCG
Pdgfb	CAAGAGTGTGGGCAGGGTTAT	CCGAATCAGGCATCGAGACA
Axin2	GACAGCGAGTTATCCAGCGA	AGGAGGGACTCCATCTACGC
Jak2	ACCTTTGCTGTTGAGCGAGA	CTTAGTCCCGCTGAGGTTGT
Stat1	TTCCGACACCTGCAACTGAAG	TCTTCGGTGACAATGAGAGGC

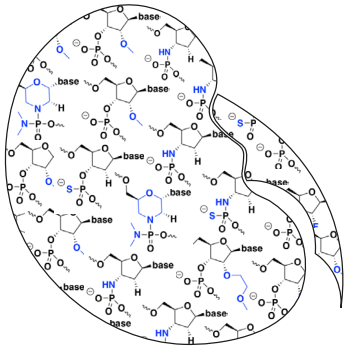

CHAPTER 3

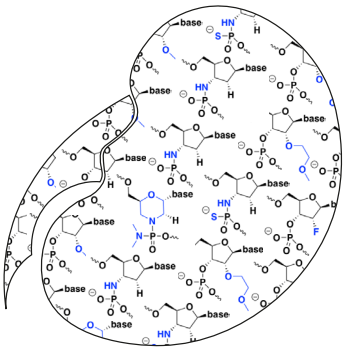

Adapted from:

Reducing YAP expression in *Pkd1* mutant mice does not improve the cystic phenotype

Chiara Formica[1], Sandra Kunnen[1], Johannes G. Dauwerse[1], Adam E. Mullick[2], Kyra L. Dijkstra[3], Marion Scharpfenecker[3], Dorien J.M. Peters[1]*; on behalf of the DIPAK Consortium

[1]Department of Human Genetics, Leiden University Medical Center, The Netherlands

[2]IONIS Pharmaceuticals, Carlsbad, California

[3]Department of Pathology, Leiden University Medical Center, The Netherlands

J Cell Mol Med. 2020;10.1111/jcmm.15512

Abstract

The Hippo pathway is a highly conserved signalling route involved in organ size regulation. The final effectors of this pathway are two transcriptional co-activators, Yes-associated protein (YAP) and Transcriptional co-activator with PDZ-binding motif (WWTR1 or TAZ). Previously, we showed aberrant activation of the Hippo pathway in Autosomal Dominant Polycystic Kidney Disease (ADPKD), suggesting that YAP/TAZ might play a role in disease progression. Using Antisense Oligonucleotides (ASOs) in a mouse model for ADPKD, we efficiently downregulated *Yap* levels in the kidneys. However, we did not see any effect on cyst formation or growth. Moreover, the expression of YAP/TAZ downstream targets was not changed, while WNT and TGF-β pathways downstream targets *Myc*, *Acta2* and *Vim*, were more expressed after *Yap* knock-down. Differences in YAP/TAZ expression pattern *in vivo*, as well as *in vitro* experiments using *Yap* or *Taz* mutant renal cells, suggest that YAP/TAZ might play cell-type-specific roles in kidneys. *In vitro* experiments revealed that knock-out of *Yap* is associated with cytoskeleton changes and aberrant expression of *Itga1* and *Itgav*. Although highly impaired, cyst formation and swelling were not prevented by *Yap* nor *Taz* knock-out *in vitro* indicating that YAP levels reduction is not a viable strategy to modulate PKD progression.

Introduction

The Hippo pathway is a highly conserved signalling route involved in the regulation of key cellular processes like proliferation, apoptosis and differentiation, which ultimately results in the regulation of organ size. The pathway is named after the core pathway component, the kinase Hippo, which has two homologues in mammals: mammalian sterile 20-like protein kinases 1 and 2 (MST1/2). MST1/2 together with large tumour suppressors 1 and 2 (LATS1/2) can phosphorylate the pathway effectors Yes-associated protein (YAP) and its paralogue Transcriptional co-activator with PDZ-binding motif (WWTR1 or TAZ), resulting in their retention into the cytoplasm. When the Hippo pathway is inactive, YAP and TAZ are unphosphorylated and can shuttle to the nucleus where they can work as transcriptional co-activators driving the transcription of genes involved in proliferation and apoptosis[1,2]. Indeed, elevated YAP/TAZ protein levels and nuclear localisation have been observed in multiple human cancers[1,3-6].

In a previous study, we showed altered Hippo signalling in Autosomal Dominant Polycystic Kidney Disease (ADPKD)[7]. ADPKD is characterised by progressive deterioration of kidney function as a consequence of the formation of thousands of epithelium-derived cysts, leading to renal failure beyond mid-life. In the majority of the cases, ADPKD is caused by a mutation in either the *PKD1* or *PKD2* gene, which encode for Polycystin 1 (PC1) and Polycystin 2 (PC2) respectively[8,9]. We observed strong nuclear accumulation of YAP in dilated tubules and cysts of several orthologous mouse models, which was accompanied by up-regulation of the YAP transcriptional targets *Birc-3*, *Ctgf*, *Inhba* and *Fjx1*. This was further observed also in human ADPKD cystic kidneys and cystic liver tissues[7]. Interestingly, YAP and TAZ have been described to interact with and regulate the activity of many other transcription factors implicated in APDKD, such as TEAD, GLIS3, SMAD, ERBB4, TP73 and RUNX2[10-17]. In addition, canonical WNT signalling, as well as, the stability of the PC1 and PC2 proteins can be modulated by Hippo signalling, placing YAP and TAZ in a central position in the regulation of PKD associated molecular pathways[18-21]. Therefore, we hypothesise that reducing nuclear localisation of YAP may slow down the renal cystic disease.

In this study, we used Antisense Oligonucleotides (ASOs) to specifically downregulate YAP level in iKsp*Pkd1*^{del} mice to modulate renal cyst growth. However, we did not see any effect of YAP downregulation on cyst formation or growth. This suggests that knockdown of *Yap* is not sufficient to slow disease progression in a mouse model for ADPKD.

Materials and Methods

Cell culture

Wild-type (Wt) mouse inner medulla collecting duct cells from ATCC (mIMCD3, CRL-2123™ ATCC®, City of Manassas, VA, USA) and Madin-Darby canine kidney (MDCK) cells (CCL-34™; ATCC) were commercially available. Briefly, cells were maintained at 37°C, and 5% CO_2 in DMEM/F-12 with GlutaMAX (#31331-093; Gibco, Life Technologies, Carlsbad, CA, USA) supplemented with 100 U/mL Penicillin-Streptomycin (#15140-122; Gibco, Life Technologies), 10% Fetal bovine serum (#S1860; Biowest, Nuaillé, France). Cell cultures were monthly tested for mycoplasma contamination using MycoAlert Mycoplasma Detection Kit. For 3D cyst assay, cells were grown in Matrigel as described previously[22]. Briefly, cells were mixed with Matrigel (#354230; Corning, NY, USA) supplemented with 10% rat tail collagen I (kindly provided by OcellO B.V., Leiden, ZH, The Netherlands) and seeded in 96-wells. Cells were cultured in normal condition for 72 h and subsequently stimulated with forskolin (#344270, Calbiochem, Millipore B.V., Amsterdam, NH, The Netherlands) or DMSO for 72 h. Cells were collected for immunohistochemistry (IHC) or RNA extraction.

Generation of knock-out cell lines

Generation of the *Pkd1* knock-out cell line mIMRFNPKD5E4 was described before[23] by making use of the FokI nucleases (RFN) method, described by *Tsai et al.*[24] in mIMCD3. A comparable method was used to generate the *Yap1* knock-out cell lines, using RFN guide RNAs for *Yap1* exon 2. Sequencing of the selected clones mIMRFNYap9 and mIMRFNYap14, revealed an 8bp out of frame deletion in one allele and a 22bp out of frame deletion in the other allele for clone mIMRFNYap9 and revealed 13bp and 26bp out of frame deletions for clone mIMRFNYap14.

Using a similar method we set out to make knock-out cell lines for *Wwtr1* (202: ENSMUST00000120977.1), by targeting exon 2 or exon 4. However, after screening 200 single clones, we noticed that mIMCD3 has three *Wwtr1* alleles, and we were unable to identify any clone with an out of frame deletion in all three alleles. Therefore, we switched strategy: using two guide RNAs to delete exon 3 to be sure that every Cas9 induced deletion leads to a *Wwtr1* mRNA with an out of frame deletion. CRISPR/Cas9 RNA-guides were designed targeting introns 2 and 3 with the online tool of the Zhang lab (https://zlab.bio/guide-design-resources) to obtain a genomic exon 3 deletion. In the end, single clones were isolated using G418 selection. In none of the 250 clones analysed exon 3 deletion was observed in three alleles. We applied the same exon deletion strategy to MDCK cells. We designed guide RNAs to delete exon 4 of the canine *Wwtr1* gene (201: ENSCAFT00000013268.4). In 4 out of 40 clones, deletion of exon 4 was found in both alleles, leading to a frameshift in the *Wwtr1* mRNA.

To generate *Yap1/Pkd1* double knock-outs, mIMCD3 cells guide RNAs were designed and

cloned into a vector containing a hygromycin selection gene, to facilitate the deletion of exon 3 *Yap1* gene in the *Pkd1* knock-out cell line mIMRFNPKD5E4. After co-transfection with eSpCasCsy and hygromycin selection (0.1 mg/ml), approximately 75 single colonies were analysed: 2 clones had deletions on both *Yap1* alleles and were verified using RT-PCR and sequencing. For detailed protocols, see Supplementary Methods.

Experimental animals and study design

All the animal experiments performed have been approved by the local animal experimental committee of the Leiden University Medical Center and the Commission Biotechnology in Animals of the Dutch Ministry of Agriculture.

Inducible kidney-specific *Pkd1* deletion mice (iKsp*Pkd1*^{del}) and tamoxifen administration have been described before[25]. *Pkd1* gene has been knocked-out at post-natal day 18 (PN18). 32 male mice have been divided into two experimental groups of 16 animals each: one received scrambled antisense oligonucleotide (ASO), the other received *Yap*-specific ASO. Both groups received an injection of 100 mg/kg of ASO via i.p. injection, starting two weeks after *Pkd1* inactivation (PN18 + 2 weeks), once a week, until sacrifice (PN18 + 8 weeks). ASOs were provided by IONIS Pharmaceuticals (Carlsbad, CA, USA). Both ASOs were 16mer S-constrained ethyl gapmers with a 3-10-3 chimeric design and a phosphorothioate backbone. *Yap* ASO sequence was: 5'-AACCAACTATTACTTC-3'; scrambled ASO sequence was: 5'- GGCCAATACGCCGTCA-3'. The *Yap* ASO was selected from leads identified following *in vitro* screens which were then evaluated *in vivo* for renal activity and tolerability. Scrambled ASO did not bind to any known target and was included as a control for non-specific effects. At sacrifice, both kidneys were collected and used for IHC or snap-frozen for RNA and protein extraction. Blood urea nitrogen level (BUN) was measured using the Reflotron Plus (Roche Basel, Switzerland). Three age-matched Wt mice were also included for IHC purposes.

Immunofluorescence, Immunohistochemistry and Western blotting

Cells were grown on coverslips and fixed in 4% paraformaldehyde for 15 min, at room temperature. Then, cells were permeabilised in 0.2% Triton-X100 in PBS for 10 min, at room temperature. Cells were blocked in 5% non-fat dried milk in PBS for 1 hour and then incubated with Phalloidin Atto 594 (1:1500) in 2% BSA in PBS. Immunofluorescence slides were mounted with Vectashield containing DAPI and pictures were taken on the Leica DM5500 B microscope.

For IHC, formalin-fixed paraffin-embedded kidneys or cysts in Matrigel were sectioned at 4µm thickness. Sections were stained with Haematoxylin-Eosin (H&E), Periodic acid-Schiff (PAS) or with these antibodies: rabbit anti-YAP (1:800 for kidneys and 1:1000 for 3D cysts; #14074; Cell Signaling Technology, Danvers, MA, USA); rabbit anti-TAZ (1:500 for kidneys and 1:1000 for 3D cysts; #4883; Cell Signaling Technology); rabbit anti-Ki-67 (1:3000, Novocastra, Leica Biosystems, Wetzlar, Germany).

For Western blot, snap-frozen kidneys were homogenised using the Magnalyser technology (Roche) in Ripa buffer supplemented with protease inhibitors cocktails (#05892970001; Roche). Antibodies used: rabbit anti-YAP (1:1000; #14074; Cell Signaling Technology), rabbit anti-TAZ (1:1000; #4883; Cell Signaling Technology), mouse anti-GAPDH (1:5000; #97166; Cell Signaling Technology). Secondary antibodies: goat-anti-rabbit IRDye 800CW (1:10000; #926-32211; LI-COR Biosciences; Lincoln, NE, USA) and goat-anti-mouse IRDye 680RD (1:10000; #926-32220; LI-COR Biosciences).

Quantification of Ki-67 positive cells

Formalin-fixed paraffin-embedded kidneys were sectioned at 4 µm thickness and stained overnight at room temperature with rabbit anti-Ki-67 antibody and counterstained with haematoxylin. Sections were acquired using Philips Ultra Fast Scanner at 20x magnification factor and pictures of 15 random areas of the kidney were taken. ImageJ software (public domain software, NIH, USA) was used to measure the Ki-67 positive area and the haematoxylin positive area. The relative Ki-67 area was calculated as a percentage of the ratio of Ki-67 positive area over haematoxylin positive area.

Gene expression analysis

Total RNA was isolated from cultured cells or snap-frozen kidneys using TRI Reagent (#T9424; Sigma-Aldrich; St. Louis, MO, USA) according to manufacturer's protocol, and gene expression analysis was performed by quantitative PCR (qPCR) as described previously[26]. Briefly, cDNA synthesis was done using Transcriptor First Strand cDNA Synthesis Kit (#04897030001; Roche) according to the manufacturer's protocol. qPCR was done in triplicate on the LightCycler 480 II (Roche) using 2x FastStart SYBR-Green Master (#04913914001; Roche) according to the manufacturer's protocol. Data were analysed with LightCycler 480 Software, Version 1.5 (Roche). Gene expression was normalised to the housekeeping gene *Hprt* or *GAPDH*. For primer sequences see Supplementary Table 1.

Quantification of cysts swelling

Cells were seeded in Matrigel in triplicate and cultured for four days. Subsequently, cells were stimulated with forskolin or DMSO as a control, for three days. At the end of the stimulation, the plates were imaged using a transmitted light microscope (Leica AXIO Observer.A1) at a magnification factor of 5x. One picture per well was taken, and the experiment was repeated four times. Using ImageJ, the circumference of the cysts was manually assessed. Around 90 cysts per well in triplicate have been evaluated, and the average cyst size was calculated for the four independent experiments. The average cyst size of the forskolin-treated cells was divided by the average cyst size of the DMSO treated cells (i.e. Wt cells + FSK / Wt cells - FSK) and compared between genotypes.

Statistical Analysis

Data were analysed using GraphPad Prism 7.00 for Windows (GraphPad Software, La Jolla California USA, www.graphpad.com)

Results

Effect of YAP knock-out on cyst formation *in vitro*

To study the effect of YAP on cyst growth, we generated mIMCD3 *Yap* knock-out (KO) cells and cultured them in Matrigel. Epithelial cells grown in this condition, spontaneously develop cystic structures with a visible lumen. After stimulation with forskolin, the cysts start to swell (Figure 1a). Interestingly, *Yap* KO cells (two different clones) showed impaired cyst formation, with only sporadic lumen formation. Most structures were very disorganised, resembling a tumour-like mass. Stimulation with forskolin did not result in swelling of the tumour-like agglomerates. Only the sporadic cysts that already had developed a lumen before forskolin treatment, increased in size. These data indicate that cyst growth per se is not impaired (Figure 1a), suggesting that *Yap* KO impairs cyst formation, but not growth, *in vitro*.

mIMCD3 cells double knock-out for *Yap* and *Pkd1* do not form cysts *in vitro*

We are interested in the role of YAP in the context of ADPKD. Therefore, we generated mIMCD3 cells knock-out for *Pkd1* as well as cells double KO for *Yap* and *Pkd1*. *Pkd1* KO cells, when grown in Matrigel, form cysts that respond to forskolin stimulation (Figure 1a)[23]. However, *Yap*/*Pkd1* double KO cells showed impaired cyst formation, as observed before for single *Yap* KO cells. Again, we saw sporadic forskolin-responsive cysts while the majority of cells grew in tumour-like agglomerates, suggesting that *Yap* KO, alone or together with *Pkd1* KO, causes impaired cyst formation in cell culture (Figure 1a).

Effect of TAZ knock-out on cyst formation *in vitro*

YAP has a paralogue protein, TAZ (or WWTR1). To study the role of TAZ in cyst formation *in vitro*, we tried to generate mIMCD3 cells knock-out for *Taz*. To our surprise, we could not obtain any viable knock-out clone for *Taz*. We screened hundreds of clones and, although we found evidence for CRISPR/Cas guide RNA activity, we were not able to produce *Taz* KO clones suggesting that full deletion of *Taz*, but not *Yap*, in mIMCD3 cells is lethal. Thus, YAP and TAZ might play specific roles in the different cells of the kidney. Indeed, differences in the expression of YAP and TAZ in the different renal segments are also observed *in vivo*. Staining of sequential sections of Wt kidneys showed a complementary pattern of expression for YAP and TAZ, with tubule segments strongly positive for one protein but not the other (Supplementary Figure 1).

Next, we tried to generate *TAZ* KO MDCK cells. MDCK cells, when grown in Matrigel, can form cystic structures that respond to forskolin stimulation, as observed in mIMCD3 cells (Figure 1b). We could successfully achieve homozygous deletion of *TAZ*, and when cultured in Matrigel, MDCK *TAZ* KO cells were able to form cysts. Interestingly, although cysts were formed, the size of cysts was reduced in *TAZ* KO compared to MDCK Wt cells (Figure 1b). Nevertheless, the relative increase in the size of *TAZ* KO cysts upon forskolin stimulation

was comparable to that observed in Wt (Figure 1c). Thus, *TAZ* KO does not prevent cyst formation and growth *in vitro,* and we found a cell-type difference in TAZ dependency.

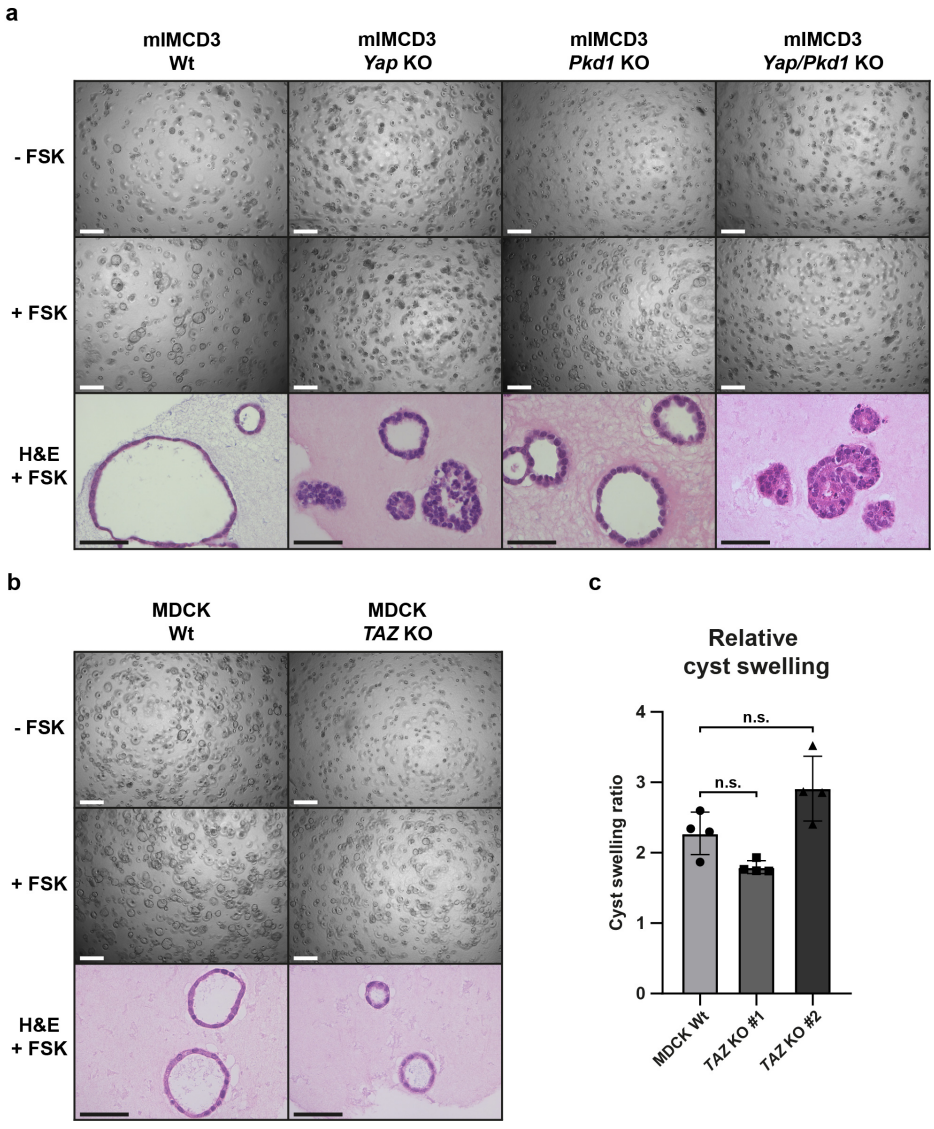

Figure 1. 3D cyst assay using Wt and mutant cells

(a) Light microscopy of mIMCD3 Wt and mutant cells before and after forskolin stimulation (respectively -FSK and +FSK). H&E staining of formalin-fixed, paraffin-embedded cysts grown in Matrigel after forskolin stimulation (bottom row). **(b)** Light microscopy of MDCK Wt and mutant cells before and after forskolin stimulation. H&E staining of formalin-fixed, paraffin-embedded cysts grown in Matrigel after forskolin stimulation (bottom row). White scale bar 200 µm; black scalebar 50 µm. **(c)** Bar graph representing the cyst swelling ratio calculated in MDCK Wt cells versus two different *TAZ* KO clones. Every symbol represents one independent experiment. Mean with ±SD. Mann-Whitney test. n.s. not significant.

The localisation of YAP and TAZ in 3D cysts assay

Since nuclear YAP accumulation was previously seen in cyst-lining epithelia[7], we investigated whether knocking out *Yap* or *Taz* has an influence on each other's subcellular localisation during cyst growth. Staining of Wt and mutant cells that were grown in Matrigel revealed that both YAP and TAZ are expressed in the cytoplasm and the nuclei of Wt cysts (mIMCD3 and MDCK). Particularly, mIMCD3 cells formed small cysts with a relatively thick wall but also larger stretched cysts. These cysts had a thin epithelial layer and showed more often nuclear YAP and TAZ staining (Figure 2a). In *Yap* KO cells, and *Yap*/*Pkd1* double KO cells, nuclear TAZ staining was observed, and it was not limited to stretched cysts but also visible in the tumour-like agglomerates. This was especially clear in the tumour-like agglomerates before forskolin treatment (Supplementary Figure 2), suggesting that lack of YAP increases TAZ shuttling (Figure 2a). In MDCK cells, 3D cysts assay lead to the formation of cysts with an overall flatter wall, and both nuclear and cytoplasmic YAP and TAZ localisation were visible within the same cyst. In *TAZ* KO cells, YAP expression does not clearly differ from the localisation observed in Wt cells (Figure 2b). Thus, *Yap* KO seems to affect TAZ localisation *in vitro*, but not vice versa.

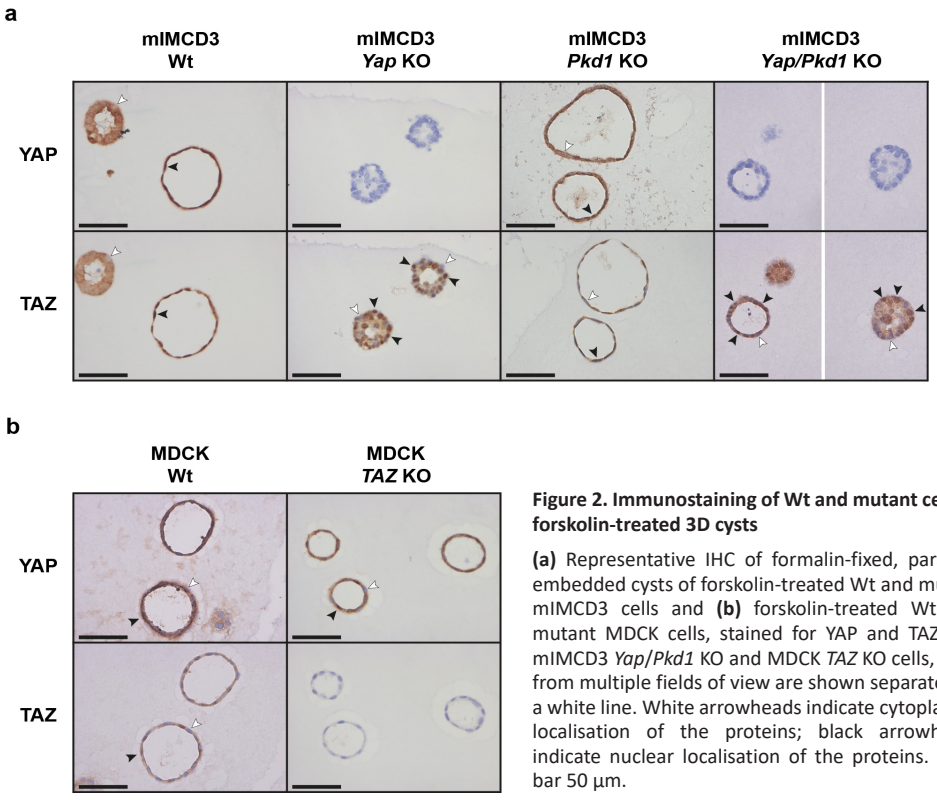

Figure 2. Immunostaining of Wt and mutant cells in forskolin-treated 3D cysts

(a) Representative IHC of formalin-fixed, paraffin-embedded cysts of forskolin-treated Wt and mutant mIMCD3 cells and **(b)** forskolin-treated Wt and mutant MDCK cells, stained for YAP and TAZ. For mIMCD3 *Yap*/*Pkd1* KO and MDCK *TAZ* KO cells, cysts from multiple fields of view are shown separated by a white line. White arrowheads indicate cytoplasmic localisation of the proteins; black arrowheads indicate nuclear localisation of the proteins. Scale bar 50 µm.

YAP knock-down using ASOs does not improve cystic phenotype *in vivo*

We showed in the past that cyst-lining epithelia have intense nuclear YAP localisation, both in *Pkd1*-mutant mouse models and in ADPKD patients[7]. Therefore, we hypothesised that YAP could actively contribute to cyst formation or cyst growth, through upregulation of target genes involved in cell proliferation and apoptosis.

To check the effect of YAP on the cystic phenotype *in vivo*, we knocked-down *Yap* using ASOs in young adult iKsp*Pkd1*^{del} mice. The *Pkd1* gene was inactivated in 18 day old mice (PN18), and 2 weeks after gene inactivation they were injected i.p., with *Yap* specific ASO (n=16) or scrambled ASO (n=16), every week until sacrifice. Mice were sacrificed 8 weeks after gene inactivation (PN18 + 8 weeks) (Figure 3a).

The *Yap* ASO treatment resulted in about 70% reduction of *Yap* gene expression levels without affecting *Taz* expression, confirming its efficacy and specificity *in vivo* (Figure 3b). YAP reduction was confirmed at the protein level, while TAZ protein expression was unchanged by the ASO treatment (Figure 3c-e).

Analysis of kidney size, by measuring two kidney weight/body weight ratios, and of renal function, using BUN levels, revealed comparable disease progression in the two experimental groups (Figure 4b, c). PAS staining revealed tubule dilation and cyst formation in different segments of the kidneys, both in *Yap* ASO and scrambled ASO treated mice, suggesting that *Yap* knock-down did not affect cyst formation *in vivo* (Figure 4a).

YAP and TAZ downstream targets expression are not changed by *Yap* knock-down *in vivo*

YAP and TAZ are transcriptional co-activators and can translocate into the nucleus where they can drive gene expression. To study the effect of *Yap* knock-down on the expression of its target genes, we quantified the expression of known YAP/TAZ targets, *Wtip*, Ajuba, *Cyr61* and *Amotl2*[27]. Despite the consistent *Yap* reduction at the mRNA level, the expression of target genes is not changed in *Yap* ASO treated compared to scrambled ASO treated mice (Figure 4d). Additionally, we evaluated the expression of Ki-67, a marker for cell proliferation, as YAP and TAZ can regulate transcriptional programs that control cell proliferation[27]. The Ki-67 positive areas in *Yap* ASO treated mice were not significantly different from those observed in scrambled ASO treated mice (Figure 4e, f). In conclusion, the knockdown of *Yap* does not affect the expression of the downstream targets we tested.

WNT and TGF-β pathways seem to be more active in *Yap* ASO mice

It is well known that both YAP and TAZ can interact with the final effectors of the WNT and TGF-β pathways[28]. For this reason, we checked the expression levels of several target genes regulated by β-catenin (*Axin2* and *Myc*) and Smads (*Acta2*, *Col1a1*, *Vim*, *Fn1*, *Pai1* and *Mmp2*). We observed increased *Myc* expression in *Yap* ASO treated mice compared to scrambled ASO, but only a trend for *Axin2* expression (Figure 5a). Moreover, we saw significantly increased expression of alpha-smooth muscle actin (*Acta2*) and vimentin (*Vim*)

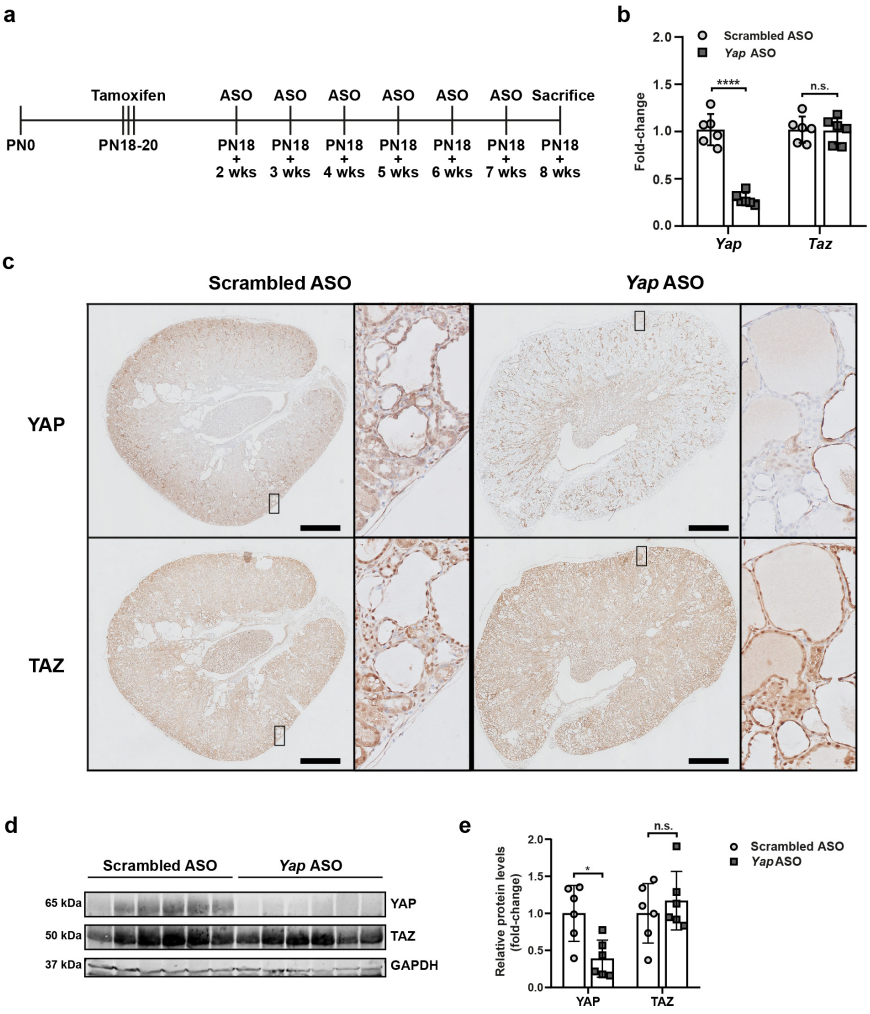

Figure 3. *In vivo* downregulation of *Yap* with ASOs

(a) Schematic representation of the *in vivo* experimental pipeline. *Pkd1* gene inactivation was achieved with three consecutive administrations of tamoxifen at post-natal day 18 (PN18). Two weeks after gene inactivation, mice were injected weekly intraperitoneally with *Yap* specific ASO or scrambled ASO as control. Mice were sacrificed at 8 weeks after gene inactivation. **(b)** Gene expression (fold-change) of *Yap* and *Taz* at the sacrifice in mice treated with *Yap* ASO and scrambled ASO. Each symbol represents a mouse. Mean with ± SD. **** $P < 0.0001$, *t*-test. **(c)** Representative IHC of renal tissue from mice treated with scrambled ASO and *Yap* ASO, showing YAP and TAZ. Scale bar 1 mm. **(d)** Total kidney protein lysates of mice treated with scrambled ASO and *Yap* ASO blotted for endogenous YAP, TAZ and GAPDH. **(e)** Quantification of YAP and TAZ protein level in total kidney normalised on GAPDH. Each symbol represents a mouse. Mean with ± SD. * $P < 0.05$, n.s. not significant, *t*-test.

and a consistent trend for collagen 1 alpha-1 (*Col1a1*), fibronectin (*Fn1*), plasminogen activator inhibitor-1 (*Pai1*) and matrix metallopeptidase 2 (*Mmp2*) (Figure 5b). Thus, although not conclusive, these results suggest that WNT and TGF-β pathways are more active upon *Yap* knock-down.

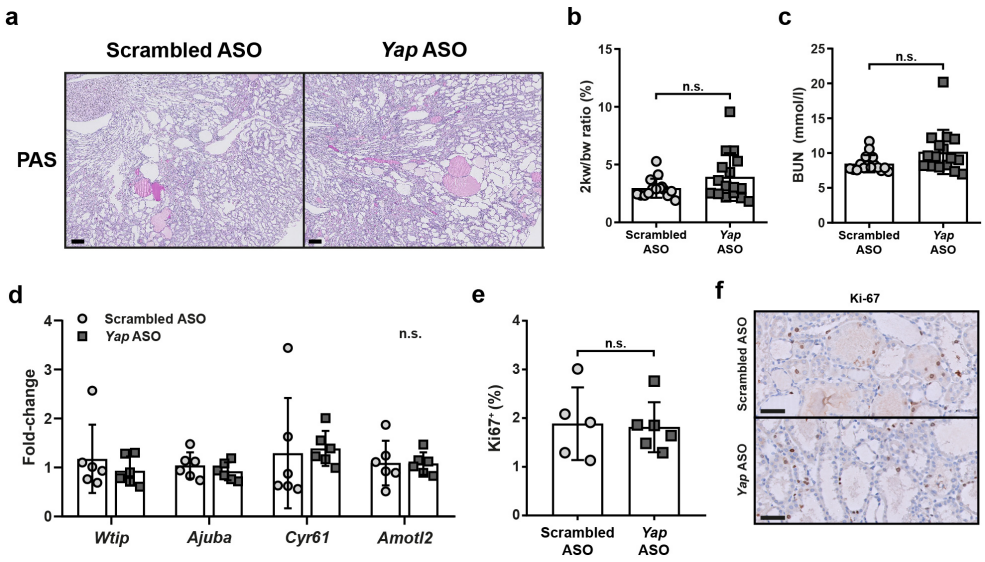

Figure 4. Effect on PKD progression of *in vivo* downregulation of *Yap* with ASOs

(a) Representative Periodic acid-Schiff (PAS) staining of renal tissue from mice treated with scrambled ASO and *Yap* ASO. Scale bar 200 µm. **(b)** Quantification of kidney size using two kidney weight/body weight ratio. n.s. not significant **(c)** Blood urea nitrogen (BUN) level at the sacrifice. n.s. not significant **(d)** Gene expression (fold-change) of YAP/TAZ targets at the sacrifice in mice treated with *Yap* ASO and scrambled ASO. Each symbol represents a mouse. Mean with ± SD. n.s. (not significant) refers to all the genes in the graph, *t*-test. **(e)** Quantification of Ki-67 positive area. Each symbol represents a mouse. Mean with ± SD. n.s. not significant, *t*-test. **(f)** Representative pictures of renal tissue stained for Ki-67. Scale bar 50 µm.

Yap KO affects cytoskeleton integrity and integrins expression *in vitro*

Following up on the aberrant phenotype observed in *Yap* KO cells grown in Matrigel, we decided to characterise these cells further. We stained the actin cytoskeleton using fluorescent dye-conjugated phalloidin, a well-known marker for filamentous actin. Wt mIMCD3 cells showed a normal cytoskeleton with clear cortical cytoskeletal and stress fibres present throughout the cell body. Also, *TAZ* KO cells showed a normal cytoskeleton, similar to Wt cells. Conversely, *Yap* KO cells showed aberrant cytoskeleton and rarely stress fibres, suggesting that the effect on the actin structure was a consequence of *Yap* gene disruption (Figure 5c).

Additionally, gene expression of integrin-alpha 1 (*Itgα1*) and -alpha v (*Itgαv*) was significantly reduced in *Yap* KO cells, before and after forskolin stimulation, compared to Wt cells. This was not observed in *TAZ* KO cells, in which the level of *Itgα1* was significantly increased compared to Wt cells (Figure 5d). These results might explain the loss of polarity observed in *Yap* KO cells leading to impaired cyst formation and development of tumour-like structures in 3D cultures.

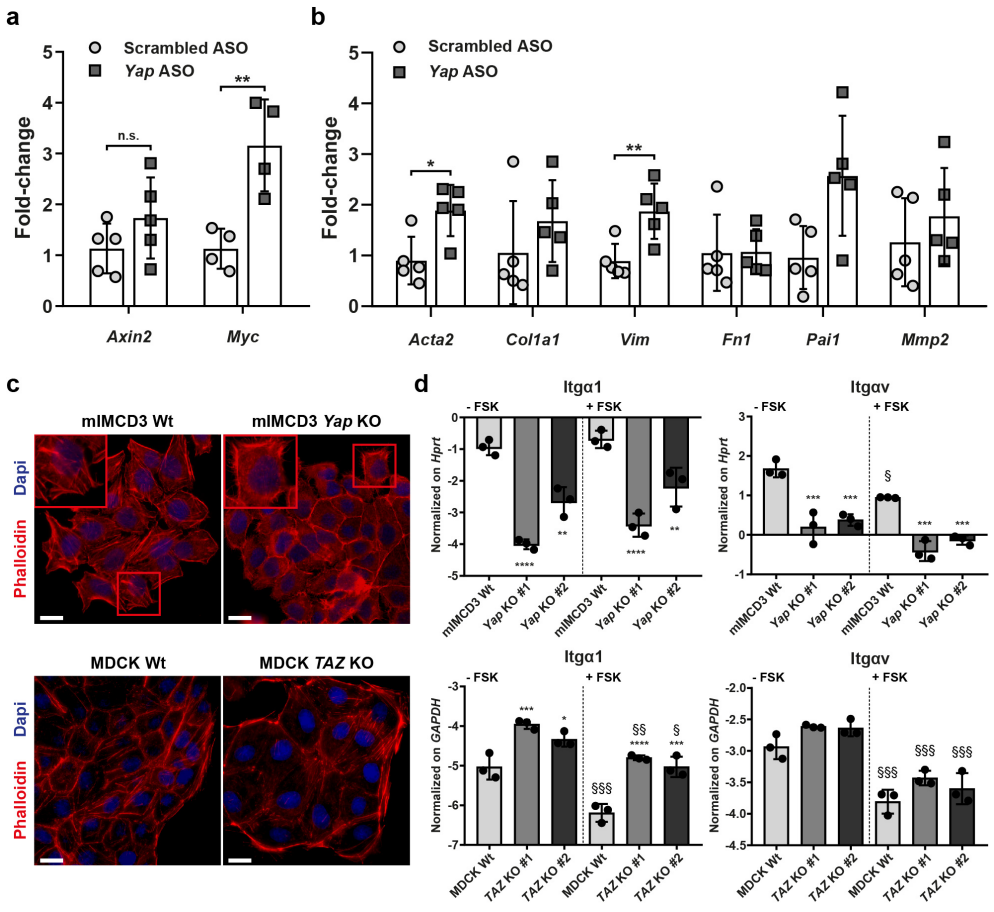

Figure 5. WNT and TGF-β pathway targets *in vivo*, and characterisation of mutant cell lines

(a) Gene expression (fold-change) of WNT pathway targets *Axin2* and *Myc* at the sacrifice in mice treated with *Yap* ASO and scrambled ASO. Each symbol represents a mouse. Mean with ± SD. ** $P < 0.01$, n.s. not significant, *t*-test. **(b)** Gene expression (fold-change) of TGF-β pathway targets, *Acta2*, *Col1a1*, *Vim*, *Fn1*, *Pai1* and *Mmp2*, at the sacrifice in mice treated with *Yap* ASO and scrambled ASO. Each symbol represents a mouse. Mean with ±SD. * $P < 0.05$, ** $P < 0.01$, *t*-test. If no significance is indicated, the comparison is not significant. **(c)** Representative immunofluorescence of Wt and mutant mIMCD3 cells and Wt and mutant MDCK cells. In red, the actin cytoskeleton is stained using phalloidin Atto 594. In blue, nuclei are stained using Vectashield containing DAPI. Scale bar 20µm. **(d)** Gene expression normalised on housekeeping genes (*Hprt* for mIMCD3 cell lines and *GAPDH* for MDCK cell lines) of Integrins alpha-1 and alpha-v. Cells are grown in Matrigel and allowed to form cysts. Subsequently, forskolin is added to the medium (+FSK) or DMSO as control (-FSK). Cells are then collected for RNA extraction, and gene expression of the integrins mentioned above is evaluated. For mutant cells, two different clones are included. Each symbol represents an independent experiment. Mean with ± SD. Asterisks indicates significance of the comparison of mutant cell lines versus the Wt in the same stimulation group (Wt-FSK vs. mutant-FSK and Wt+FSK vs. mutant+FSK) * $P < 0.05$, ** $P < 0.01$, *** $P < 0.001$, **** $P < 0.0001$. § indicates the significance of the comparison of the same cell line in the two stimulation group (Wt-FSK vs. Wt+FSK or mutant-FSK vs. mutant+FSK). ANOVA significance test with Tukey's multiple comparisons test.

Discussion

ADPKD is the fourth most common renal disease that requires renal replacement therapy[29]. Indeed, the majority of patients with ADPKD will develop the end-stage renal disease (ESRD), severely impacting patients' lives and representing a substantial economic burden to the healthcare system[30]. Thus, finding viable intervention strategies aimed to slow down the disease progression is of paramount importance.

In a previous study, we showed that the Hippo pathway's effector YAP was more active in the cyst-lining epithelia both in murine and human renal tissues with PKD[7]. When in the nucleus, YAP can modulate the transcription of genes involved in the regulation of proliferation and apoptosis[3,4,6]. Therefore, we hypothesised that reducing nuclear localisation of YAP might slow down the renal cystic disease. In this study, we used ASOs to selectively knock-down the expression of *Yap* in young adult iKsp*Pkd1*^{del} mice. We reached about 70% reduction in gene expression, indicating that ASOs can be a viable strategy to effectively and selectively downregulate a target in kidneys in models for PKD, as also shown for a few other targets[31,32]. Our data clearly indicate that *Yap* knock-down using ASOs in a mouse model for ADPKD does not improve the cystic phenotype. Indeed, also *in vitro*, *Yap* KO did not impair the growth of the sporadic cysts that were able to form, suggesting that proliferation is not affected.

Considering that TAZ (or WWTR1) levels are not changed by *Yap* ASO, we hypothesised that TAZ could be compensating for *Yap* knock-down. Indeed, expression levels of the target genes are not changed by *Yap* knock-down, and TAZ shows a clear nuclear localisation in most of the renal tubules, both cystic and dilated ones. This suggests that TAZ is compensating for the loss of YAP and might be contributing to cyst growth, hence targeting TAZ together with YAP might be a viable strategy to inhibit cyst progression. However, we also showed that *TAZ* KO did not result in impaired cyst formation nor cyst growth in a 3D cyst assay, arguing against it. This is further supported by *in vivo* results, since mice with a constitutive or conditional *Taz* KO, develop mild cysts even in the absence of a *Pkd1* mutation[18,33]. Moreover, *Merrick et al.* showed that TAZ physically interacts with the C-terminal tail of PC1 (PC1-CTT) in HEK293 cells. They also proved in zebrafish, that the bone phenotype and curly tail observed after injection of *Pkd1* morpholino were rescued by co-injection of PC1-CTT mRNA but not if also *Taz* was knocked out[21]. Altogether, these results suggest that PC1 and TAZ participate in common signalling routes, and reducing or depleting *Taz* levels might worsen PKD progression.

In contrast to our work, a recent paper showed that *Yap* KO, especially together with *Taz* KO, was able to reduce PKD progression mildly in *Pkd1* deficient mice. However, the mouse model used was based on leaky Cre recombinase activity, suggesting that gene inactivation already

occurred during development, rather than in adult mice[34]. Indeed, constitutive *Yap* KO can lead to impaired kidney development, which might affect subsequent cyst development[35]. Another difference with our study is that we did not use a genetic deletion of *Yap*, but we decided to use a strategy based on antisense oligonucleotides that could potentially be translated to the clinic. The use of ASOs allows to reduce YAP levels consistently, but not to altogether abolish the expression. Additionally, by treating young adult mice that develop cysts relatively slowly and in every renal segment, we mimic the disease observed in patients even more.

Although YAP and TAZ have some overlapping functions, they also partly interact with and are regulated by different partners, indicating that YAP and TAZ also have unique functions[36]. Interestingly, we could generate *Yap* KO but not *Taz* KO mIMCD3 cells, suggesting that TAZ plays a crucial role in mIMCD3 cells and potentially in specific segments of the kidney. Indeed, we observed differential expression patterns for YAP and TAZ in the various renal segments (Supplementary Figure 1), corroborating the idea that the two transcriptional co-activators also have distinct functions in the kidneys. However, if and how modulation of YAP levels affects the activity of TAZ in kidneys, and vice versa, is not clear and should be further investigated.

YAP and TAZ are transcriptional co-activators that can modulate a variety of biological processes. They have been associated with fibrogenesis and epithelial-to-mesenchymal transition *in vivo* and *in vitro* via interaction with both TGF-β and WNT signalling pathways. Particularly, when the Hippo pathway is active, YAP and TAZ are phosphorylated and restrained in the cytoplasm where they can interact with SMADs and β-catenin, preventing their nuclear translocation and transcriptional activity[28]. In our study, we observed increased expression of some of the downstream targets of WNT and TGF-β pathways in *Yap* ASO treated mice. This might suggest that reduced YAP levels cause an imbalance in the regulation of these interacting signalling pathways, either because YAP cannot physically interact with SMADs and β-catenin anymore, or due to increased activation of TAZ overcompensating for YAP loss. Indeed, YAP has been shown to inversely regulate TAZ protein levels in a process conserved from mouse to human, and we also observed increased nuclear TAZ in *Yap* KO cells grown in 3D[37]. Based on this, *Yap* knock-down might result in overactivation of TAZ, in turn causing increased activation of WNT or TGF-β pathways, which are well known for promoting cyst formation in ADPKD[38,39]. Such a process might explain why we did not see any amelioration of the phenotype with *Yap* knock-down *in vivo*, although further studies are necessary to unveil the exact molecular mechanisms.

YAP/TAZ were initially identified as downstream effectors of the Hippo pathway. Nevertheless, in the last years a variety of upstream regulators, dependent or independent of the Hippo

pathway, have been identified affecting YAP/TAZ sub-localization. These include mechanical signals via cell-cell contacts, polarity proteins and cadherin-β-catenin complexes, focal adhesions, extracellular matrix (ECM) elasticity and cytoskeletal tension[40], as well as several mitogens like epidermal growth factor (EGF), lysophosphatidic acid (LPA), sphingosine-1 phosphate, insulin and the protease thrombin, which can control YAP/TAZ localisation[41-45]. Indeed, we also showed that in *Yap* KO mIMCD3 cells, expression of *Itga1* and *Itgav* is impaired and that the architecture of the cytoskeleton is aberrant. In 3D cysts, this results in non-polarized growth of the cells that fail to form a lumen and grow as a tumour-like mass. *In vivo*, mice mutant for proteins involved in the formation of cell-cell junctions, focal adhesions and related to cytoskeletal assembly, develop renal cysts[46]. Thus, the aberration of any of the processes mentioned above can lead to cyst formation. For these reasons, the modulation of Hippo pathway effectors YAP and TAZ to intervene on cyst progression might not be a viable option.

In conclusion, although we cannot exclude that the Hippo pathway is involved in cyst growth, we believe that the strong nuclear YAP localisation observed in cyst-lining epithelia is more a consequence of cell stretching or stiffer ECM or mitogen-induced signalling rather than a driving force for cell proliferation. Indeed, downregulation of YAP using ASOs did not affect cell proliferation nor the cystic phenotype in our *Pkd1* KO mouse model. Moreover, due to its profound interconnection with other signalling pathways, such as WNT and TGF-β, a therapeutic intervention for PKD based on the modulation of YAP levels might not be feasible, at least with the current knowledge.

Funding

This work was supported by funding from the Dutch Kidney Foundation [NSN P12.18 to S.K.]; Dutch government [LSHM15018 to C.F.]; People Program (Marie Curie Actions) of the European Union's Seventh Framework Program FP7/2007-2013 under Research Executive Agency Grant Agreement [317246 to C.F.]; the DIPAK Consortium, which is an inter-university collaboration in the Netherlands established to study Autosomal Dominant Polycystic Kidney Disease and to develop treatment strategies for this disease, sponsored by the Dutch Kidney Foundation [CP10.12, CP15.01] and Dutch government [LSHM15018]; and IPSEN Farmaceutica BV, the Netherlands, which provided an unrestricted grant.

Acknowledgements

The authors would like to thank Janne Plugge and Hester Bange for technical assistance.

Authors contributions

C.F., S.K. and D.J.M.P. conceived and designed research; C.F., S.K., J.G.D. and K.L.D. performed experiments; C.F., S.K., M.S. and D.J.M.P interpreted results of experiments; A.E.M. designed and provided AONs; C.F. and D.J.M.P. drafted manuscript; C.F., S.K., J.G.D., A.E.M., K.L.D, M.S. and D.J.M.P. critically reviewed and approved final version of manuscript.

Conflict of interests

The authors declare no competing or financial interests.

Data Availability Statement

No additional data were generated beyond the data presented in the manuscripts and its supplements

References

1 Yu, F. X., Zhao, B. & Guan, K. L. Hippo Pathway in Organ Size Control, Tissue Homeostasis, and Cancer. *Cell* **163**, 811-828, doi:10.1016/j.cell.2015.10.044 (2015).

2 Udan, R. S., Kango-Singh, M., Nolo, R., Tao, C. Y. & Halder, G. Hippo promotes proliferation arrest and apoptosis in the Salvador/Warts pathway. *Nat Cell Biol* **5**, 914-920, doi:10.1038/ncb1050 (2003).

3 Camargo, F. D. *et al.* YAP1 increases organ size and expands undifferentiated progenitor cells. *Curr Biol* **17**, 2054-2060, doi:10.1016/j.cub.2007.10.039 (2007).

4 Dong, J. *et al.* Elucidation of a universal size-control mechanism in Drosophila and mammals. *Cell* **130**, 1120-1133, doi:10.1016/j.cell.2007.07.019 (2007).

5 Zhao, B., Li, L. & Guan, K. L. Hippo signaling at a glance. *J Cell Sci* **123**, 4001-4006, doi:10.1242/jcs.069070 (2010).

6 Zhao, B., Lei, Q. Y. & Guan, K. L. The Hippo-YAP pathway: new connections between regulation of organ size and cancer. *Curr Opin Cell Biol* **20**, 638-646, doi:10.1016/j.ceb.2008.10.001 (2008).

7 Happé, H. *et al.* Altered Hippo signalling in polycystic kidney disease. *The Journal of Pathology* **224**, 133-142, doi:10.1002/path.2856 (2011).

8 The European Polycystic Kidney, D. The polycystic kidney disease 1 gene encodes a 14 kb transcript and lies within a duplicated region on chromosome 16. *Cell* **77**, 881-894, doi:10.1016/0092-8674(94)90137-6 (1994).

9 Mochizuki, T. *et al.* PKD2, a gene for polycystic kidney disease that encodes an integral membrane protein. *Science* **272**, 1339-1342, doi:DOI 10.1126/science.272.5266.1339 (1996).

10 Strano, S. *et al.* Physical interaction with Yes-associated protein enhances p73 transcriptional activity. *J Biol Chem* **276**, 15164-15173, doi:10.1074/jbc.M010484200 (2001).

11 Vassilev, A., Kaneko, K. J., Shu, H., Zhao, Y. & DePamphilis, M. L. TEAD/TEF transcription factors utilize the activation domain of YAP65, a Src/Yes-associated protein localized in the cytoplasm. *Genes Dev* **15**, 1229-1241, doi:10.1101/gad.888601 (2001).

12 Komuro, A., Nagai, M., Navin, N. E. & Sudol, M. WW domain-containing protein YAP associates with ErbB-4 and acts as a co-transcriptional activator for the carboxyl-terminal fragment of ErbB-4 that translocates to the nucleus. *Journal of Biological Chemistry* **278**, 33334-33341, doi:10.1074/jbc.M305597200 (2003).

13 Hong, J. H. *et al.* TAZ, a transcriptional modulator of mesenchymal stem cell differentiation. *Science* **309**, 1074-1078, doi:10.1126/science.1110955 (2005).

14 Zaidi, S. K. *et al.* Tyrosine phosphorylation controls Runx2-mediated subnuclear targeting of YAP to repress transcription. *EMBO J* **23**, 790-799, doi:10.1038/sj.emboj.7600073 (2004).

15 Vitolo, M. I. *et al.* The RUNX2 transcription factor cooperates with the YES-associated protein, YAP65, to promote cell transformation. *Cancer Biol Ther* **6**, 856-863 (2007).

16 Varelas, X. *et al.* TAZ controls Smad nucleocytoplasmic shuttling and regulates human embryonic stem-cell self-renewal. *Nat Cell Biol* **10**, 837-848, doi:10.1038/ncb1748 (2008).

17 Kang, H. S., Beak, J. Y., Kim, Y. S., Herbert, R. & Jetten, A. M. Glis3 Is Associated with Primary Cilia and Wwtr1/TAZ and Implicated in Polycystic Kidney Disease. *Mol Cell Biol* **29**, 2556-2569, doi:10.1128/

Mcb.01620-08 (2009).

18 Tian, Y. *et al.* TAZ promotes PC2 degradation through a SCFbeta-Trcp E3 ligase complex. *Mol Cell Biol* **27**, 6383-6395, doi:10.1128/MCB.00254-07 (2007).

19 Varelas, X. *et al.* The Hippo pathway regulates Wnt/beta-catenin signaling. *Dev Cell* **18**, 579-591, doi:10.1016/j.devcel.2010.03.007 (2010).

20 Yim, H., Sung, C. K., You, J., Tian, Y. & Benjamin, T. Nek1 and TAZ interact to maintain normal levels of polycystin 2. *J Am Soc Nephrol* **22**, 832-837, doi:10.1681/ASN.2010090992 (2011).

21 Merrick, D. *et al.* Polycystin-1 regulates bone development through an interaction with the transcriptional coactivator TAZ. *Hum Mol Genet* **28**, 16-30, doi:10.1093/hmg/ddy322 (2019).

22 Booij, T. H. *et al.* In Vitro 3d Phenotypic Drug Screen Identifies Celastrol as an Effective in Vivo Inhibitor of Polycystic Kidney Disease. *J Mol Cell Biol*, doi:10.1093/jmcb/mjz029 (2019).

23 Booij, T. H. *et al.* High-Throughput Phenotypic Screening of Kinase Inhibitors to Identify Drug Targets for Polycystic Kidney Disease. *SLAS Discov* **22**, 974-984, doi:10.1177/2472555217716056 (2017).

24 Wyvekens, N., Topkar, V. V., Khayter, C., Joung, J. K. & Tsai, S. Q. Dimeric CRISPR RNA-Guided FokI-dCas9 Nucleases Directed by Truncated gRNAs for Highly Specific Genome Editing. *Hum Gene Ther* **26**, 425-431, doi:10.1089/hum.2015.084 (2015).

25 Lantinga-van Leeuwen, I. S. *et al.* Lowering of Pkd1 expression is sufficient to cause polycystic kidney disease. *Hum Mol Genet* **13**, 3069-3077, doi:10.1093/hmg/ddh336 (2004).

26 Formica, C. *et al.* Four-jointed knock-out delays renal failure in an ADPKD model with kidney injury. *J Pathol*, doi:10.1002/path.5286 (2019).

27 Zanconato, F. *et al.* Genome-wide association between YAP/TAZ/TEAD and AP-1 at enhancers drives oncogenic growth. *Nat Cell Biol* **17**, 1218-+, doi:10.1038/ncb3216 (2015).

28 Attisano, L. & Wrana, J. L. Signal integration in TGF-beta, WNT, and Hippo pathways. *F1000Prime Rep* **5**, 17, doi:10.12703/P5-17 (2013).

29 Spithoven, E. M. *et al.* Renal replacement therapy for autosomal dominant polycystic kidney disease (ADPKD) in Europe: prevalence and survival--an analysis of data from the ERA-EDTA Registry. *Nephrol Dial Transplant* **29 Suppl 4**, iv15-25, doi:10.1093/ndt/gfu017 (2014).

30 Barnawi, R. A., Attar, R. Z., Alfaer, S. S. & Safdar, O. Y. Is the light at the end of the tunnel nigh? A review of ADPKD focusing on the burden of disease and tolvaptan as a new treatment. *Int J Nephrol Renovasc Dis* **11**, 53-67, doi:10.2147/IJNRD.S136359 (2018).

31 Ravichandran, K. *et al.* An mTOR anti-sense oligonucleotide decreases polycystic kidney disease in mice with a targeted mutation in Pkd2. *Hum Mol Genet* **23**, 4919-4931, doi:10.1093/hmg/ddu208 (2014).

32 Ravichandran, K., Ozkok, A., Wang, Q., Mullick, A. E. & Edelstein, C. L. Antisense-mediated angiotensinogen inhibition slows polycystic kidney disease in mice with a targeted mutation in Pkd2. *Am J Physiol-Renal* **308**, F349-F357, doi:10.1152/ajprenal.00478.2014 (2015).

33 Hossain, Z. *et al.* Glomerulocystic kidney disease in mice with a targeted inactivation of Wwtr1. *P Natl Acad Sci USA* **104**, 1631-1636, doi:10.1073/pnas.0605266104 (2007).

34 Cai, J. *et al.* A RhoA-YAP-c-Myc signaling axis promotes the development of polycystic kidney disease. *Genes Dev* **32**, 781-793, doi:10.1101/gad.315127.118 (2018).

35 Reginensi, A. *et al.* Yap- and Cdc42-dependent nephrogenesis and morphogenesis during mouse kidney development. *PLoS Genet* **9**, e1003380, doi:10.1371/journal.pgen.1003380 (2013).

36 Varelas, X. The Hippo pathway effectors TAZ and YAP in development, homeostasis and disease. *Development* **141**, 1614-1626, doi:10.1242/dev.102376 (2014).

37 Finch-Edmondson, M. L. *et al.* TAZ Protein Accumulation Is Negatively Regulated by YAP Abundance in Mammalian Cells. *Journal of Biological Chemistry* **290**, 27928-27938, doi:10.1074/jbc.M115.692285 (2015).

38 Lancaster, M. A. & Gleeson, J. G. Cystic kidney disease: the role of Wnt signaling. *Trends Mol Med* **16**, 349-360, doi:10.1016/j.molmed.2010.05.004 (2010).

39 Hassane, S. *et al.* Elevated TGFbeta-Smad signalling in experimental Pkd1 models and human patients with polycystic kidney disease. *J Pathol* **222**, 21-31, doi:10.1002/path.2734 (2010).

40 Meng, Z., Moroishi, T. & Guan, K. L. Mechanisms of Hippo pathway regulation. *Genes Dev* **30**, 1-17, doi:10.1101/gad.274027.115 (2016).

41 Miller, E. *et al.* Identification of Serum-Derived Sphingosine-1-Phosphate as a Small Molecule Regulator of YAP. *Chem Biol* **19**, 955-962, doi:10.1016/j.chembiol.2012.07.005 (2012).

42 Strassburger, K., Tiebe, M., Pinna, F., Breuhahn, K. & Teleman, A. A. Insulin/IGF signaling drives cell proliferation in part via Yorkie/YAP. *Dev Biol* **367**, 187-196, doi:10.1016/j.ydbio.2012.05.008 (2012).

43 Mo, J. S., Yu, F. X., Gong, R., Brown, J. H. & Guan, K. L. Regulation of the Hippo-YAP pathway by protease-activated receptors (PARs). *Genes Dev* **26**, 2138-2143, doi:10.1101/gad.197582.112 (2012).

44 Fan, R., Kim, N. G. & Gumbiner, B. M. Regulation of Hippo pathway by mitogenic growth factors via phosphoinositide 3-kinase and phosphoinositide-dependent kinase-1. *P Natl Acad Sci USA* **110**, 2569-2574, doi:10.1073/pnas.1216462110 (2013).

45 Yu, F. X. *et al.* Regulation of the Hippo-YAP pathway by G-protein-coupled receptor signaling. *Cell* **150**, 780-791, doi:10.1016/j.cell.2012.06.037 (2012).

46 Wilson, P. D. Apico-basal polarity in polycystic kidney disease epithelia. *Biochim Biophys Acta* **1812**, 1239-1248, doi:10.1016/j.bbadis.2011.05.008 (2011).

Supplementary Figures

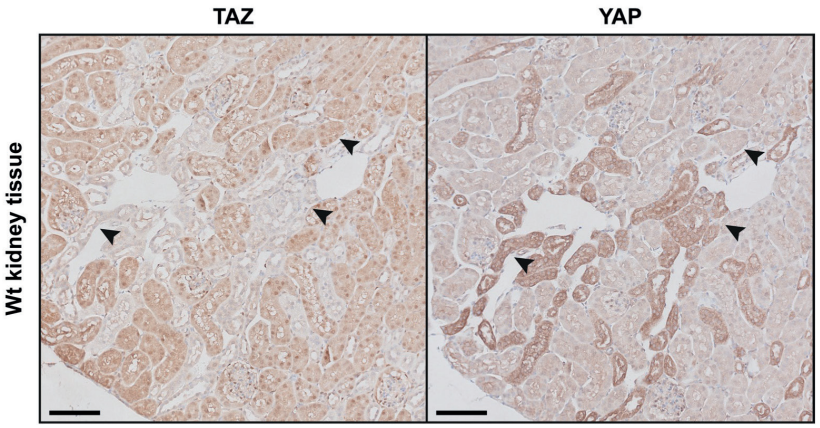

Supplementary Figure 1. YAP and TAZ expression in Wt kidneys

Representative IHC for YAP and TAZ on sequential slides of Wt mice kidneys at post-natal day 100. The staining shows a complementary expression pattern of YAP and TAZ in the various segments of the kidneys, with tubule segments strongly positive for one protein but not the other. Arrowheads show the same tubules stained for the two different proteins. Scale bar 200 µm.

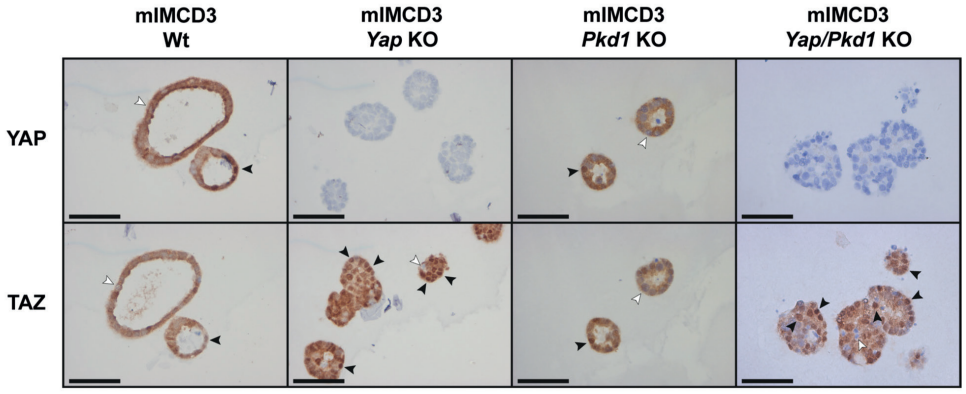

Supplementary Figure 2. YAP and TAZ staining of Wt and mutant mIMCD3 cells

Cells are grown in Matrigel and allowed to form cysts. In the pictures, Wt and mutant mIMCD3 cells are shown, which were not stimulated with forskolin. Representative IHC of formalin-fixed, paraffin-embedded cysts stained for YAP and TAZ shows intense nuclear TAZ staining in *Yap* single and double KO cells. White arrowheads indicate cytoplasmic localisation of the proteins; black arrowheads indicate nuclear localisation of the proteins. Scale bar 50 µm

Supplementary methods

Generation of knock-out cell lines

Generation of the *Pkd1* knock-out cell line mIMRFNPKD 5E4 was described before[1] by making use of the FokI nucleases (RFN) method, described by *Tsai et al.*[2] in mouse kidney, medulla/collecting duct cell line mIMCD3 (mIMCD3, ATCC® CRL-2123™). A comparable method was used to generate the *Yap1* knock-out cell lines. In short, the RFN guide RNAs for *Yap1* exon 2 were selected using ZiFiT (http://zifit.partners.org/ZiFiT/Disclaimer.aspx) and cloned into vector pSQT1313neo. This is a modified version of pSQT1313 (Addgene #53370), in which we replaced the ampicillin gene of pSQT1313 by the kanamycin/neomycin resistance cassette of pEGFP-N1 (Clontech). This was done to facilitate G418 selection of clones that have taken up pSQT1313neoRFN and enrich for clones that carry a *Yap1* exon 2 deletion. The RFN-guide RNA clone was co-transfected with pSQT1601 (Addgene #53369) a plasmid expressing the Csy4 and dCas9-FokI fusion proteins. mIMCD3 cells were grown to 80% confluency in a 9 cm petri dish and transfected with 2µg Yap1ex2RFN and 8µg pSQT1601 DNA using Lipofectamin 2000 (Invitrogen). G418 (0.5mg/ml) selection was applied after 48 hours. After 7 days, cells were re-plated at a density of ~50 cells per 9 cm plate. In total 60 single colonies were picked and analysed using PCR with primers flanking the RFN target sites. PCR products were digested with restriction-endonuclease BpmI, which cuts between the Yap1ex2 RFN target sites. From 7 clones that showed undigested PCR products, demonstrating a deletion of the BpmI, restriction site on both alleles, the PCR products were subcloned using the TOPO® cloning kit (Invitrogen). Fifteen subclones were analysed by Sanger sequencing. The sequences for clone mIMRFNYap9 revealed an 8bp out of frame deletion in one allele and a 22bp out of frame deletion in the other allele and clone mIMRFNYap14, revealed 13bp and 26bp out of frame deletions.

Using a similar method we set out to make knock-out cell lines for *Wwtr1* (202: ENSMUST00000120977.1), by targeting exon 2 or exon 4. However, after screening 200 single clones, we noticed that mIMCD3 has three *Wwtr1* alleles and we were unable to identify any clone with an out of frame deletion in all three alleles. We switched strategy: using two guide RNAs to delete exon 3 to be sure that every Cas9 induced deletion leads to a *Wwtr1* mRNA with an out of frame deletion. CRISPR/Cas9 RNA-guides were designed targeting introns 2 and 3 with the online tool of the Zhang lab (https://zlab.bio/guide-design-resources) to obtain a genomic exon 3 deletion. RNA guides were cloned into pSQT1313neo, both guide RNAs flanked and separated from each other by Csy4 recognition sites, and co-transfected with eSpCasCsy, a modified eSpCas9(1.1) (Addgene #71814) which expresses both the high specificity SpCas9 protein together with the Csy4 RNAse. Single clones were isolated using G418 selection. In none of the 250 clones analysed exon 3 deletion was observed in three alleles. Sequencing of many clones revealed, deletion of exon 3 in two alleles and indels were observed at the Cas9 cutting sides of the guide RNA recognition

sides in the third allele, but these events did not lead to a deletion of exon 3. From these results we conclude that knocking-out three alleles in mIMCD3 leads to cell death. We applied the same exon deletion strategy to MDCK cells (ATCC® CCL-34™). We designed guide RNAs to delete exon 4 of the canine *Wwtr1* gene (201: ENSCAFT00000013268.4), and cloned these into pSQT1313neo. After co-transfection with eSpCasCsy and G418 selection 40 single colonies were analysed using PCR. In 4 clones a deletion of exon 4 in both alleles was observed. RT-PCR and sequencing on RNA isolated of these clones, revealed deletion of exon 4 leading to a frameshift in the *Wwtr1* mRNA and knocking-out both alleles.
Finally, we generated a *Pkd1*/*Yap1* double knock-out in mIMCD3. Guide RNAs were designed and cloned into a vector containing a hygromycin selection gene, to facilitate the deletion of exon 3 *Yap1* gene in the *Pkd1* knock-out cell line mIMRFNPKD 5E4. After co-transfection with eSpCasCsy and hygromycin selection (0.1mg/ml), approximately 75 single colonies were analysed: 2 clones had deletions on both *Yap1* alleles, and were verified using RT-PCR and sequencing.

References

1 Booij, T. H. *et al.* High-Throughput Phenotypic Screening of Kinase Inhibitors to Identify Drug Targets for Polycystic Kidney Disease. *SLAS Discov* **22**, 974-984, doi:10.1177/2472555217716056 (2017).

2 Wyvekens, N., Topkar, V. V., Khayter, C., Joung, J. K. & Tsai, S. Q. Dimeric CRISPR RNA-Guided FokI-dCas9 Nucleases Directed by Truncated gRNAs for Highly Specific Genome Editing. *Hum Gene Ther* **26**, 425-431, doi:10.1089/hum.2015.084 (2015).

Supplementary Tables

Supplementary Table 1. List of primer sequences used for qPCR

Mouse	Forward	Reverse
Acta2	CATCATGCGTCTGGACTTG	ATCTCACGCTCGGCAGTAG
Ajuba	CCAGAGAAGATTACTTTGGCACC	ACAAAGCACTGGGTGTGGTA
AmotL2	ACCAGGAGATGGAGAGCAGATT	GAAGGACCTTGATCACCGCA
Axin2	GACAGCGAGTTATCCAGCGA	AGGAGGGACTCCATCTACGC
Col1a1	TGACTGGAAGAGCGGAGAGT	AGACGGCTGAGTAGGGAACA
Cyr61	CACTGAAGAGGCTTCCTGTCT	CCAAGACGTGGTCTGAACGA
Fn1	AATCCAGTCCACAGCCATTCC	CCTGTCTTCTCTTTCGGGTTCA
Hprt	GGCTATAAGTTCTTTGCTGACCTG	AACTTTTATGTCCCCCGTTGA
Itga1	ACCAGTACGTCGCTGGTTC	GCAGACGCCTAGGATAACGG
Itgav	GGTCGCCTATCTTCGGGATG	CGTTCTCTGGTCCAACCGAT
Mmp2	GACCGGTTTATTTGGCGGAC	TCATTCCCTGCGAAGAACACA
Myc	CCTTCTCTCCTTCCTCGGACT	CCTCATCTTCTTGCTCTTCTTCAG
Pai1	GCCAACAAGAGCCAATCAC	ACCCTTTCCCAGAGACCAG
Taz (Wwtr1)	ATGGACGAGATGGATACAGGTGA	AGACTCCAAAGTCCCGAGGT
Vim	CCAACCTTTTCTTCCCTGAA	TGAGTGGGTGTCAACCAGAG
Wtip	TTCATCTGTGACTCCTGTGGGA	TGGCAGTACACTTTCTCACCC
Yap1	TTCCGATCCCTTTCTTAACAGT	GAGGGATGCTGTAGCTGCTC

Dog	Forward	Reverse
Gapdh	GAGTCCACTGGGGTCTTCAC	TCAGCAGAAGGAGCAGAGATG
Itga1	GTGCTGCCCTCTTCTGGTC	TTTCCTTCCACACGGCAGTT
Itgav	CAAAGGAGCACTTCCCACGA	ACCTGGAGACCGGTTATGGA

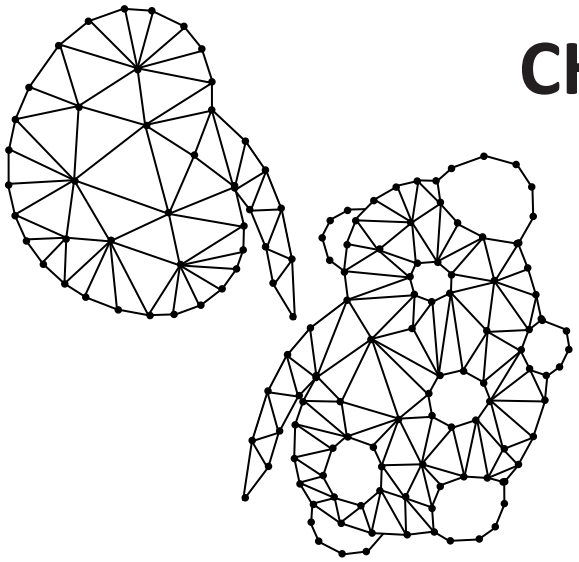

CHAPTER 4

Meta-analysis of polycystic kidney disease expression profiles defines strong involvement of injury repair processes

Tareq Malas[1]*, Chiara Formica[1]*, Wouter N. Leonhard[1], Pooja Rao[2], Zoraide Granchi[2], Marco Roos[1], Dorien J.M. Peters[1], Peter A.C. 't Hoen[1]

[1]Department of Human Genetics, Leiden University Medical Center, The Netherlands

[2]GenomeScan, Plesmanlaan 1 /d 2333 BZ, Leiden, The Netherlands

* Authors contributed equally

Am J Physiol Renal Physiol. 2017 Apr 1;312(4):F806-F817

Abstract

Polycystic kidney disease (PKD) is a major cause of end-stage renal disease. The disease mechanisms are not well understood and the pathogenesis toward renal failure remains elusive. In this study, we present the first RNASeq analysis of a *Pkd1*-mutant mouse model in a combined meta-analysis with other published PKD expression profiles. We introduce the PKD Signature, a set of 1,515 genes that are commonly dysregulated in PKD studies. We show that the signature genes include many known and novel PKD-related genes and functions. Moreover, genes with a role in injury repair, as evidenced by expression data and/or automated literature analysis, were significantly enriched in the PKD Signature, with 35% of the PKD Signature genes being directly implicated in injury repair. NF-kB signaling, epithelial-mesenchymal transition, inflammatory response, hypoxia, and metabolism were among the most prominent injury or repair related biological processes with a role in the PKD etiology. Novel PKD genes with a role in PKD and in injury were confirmed in another *Pkd1*-mutant mouse model as well as in animals treated with a nephrotoxic agent. We propose that compounds that can modulate the injury-repair response could be valuable drug candidates for PKD treatment.

Introduction

Polycystic Kidney Disease (PKD) is a genetic disease of the kidney characterized by the gradual replacement of normal kidney parenchyma by fluid-filled cysts and fibrotic tissue. Autosomal Dominant Polycystic Kidney Disease (ADPKD) is caused by mutations in the *PKD1* or *PKD2* gene and the less frequent autosomal recessive form, Autosomal Recessive Polycystic Kidney Disease (ARPKD), is caused by mutations in the *PKHD1* gene[4,40,67]. It is not entirely clear why the disruption of these genes lead to PKD and what functions their protein products might have in normal and diseased kidneys. Furthermore, it is expected that a vasopressin V2 receptor antagonist, recently approved in Europe, will probably not be sufficient for life-long treatment, warranting the search for additional therapies[65]. Therefore, a detailed knowledge of the molecular pathology and signaling pathways at different phases of the disease is needed. To answer these questions, several PKD-related expression profiling studies have been conducted in the last decade[10,20,30,39,43-45,51,54,56]. These studies, however, varied considerably by the type and number of the samples used, i.e., cystic and normal cell lines, patient-derived material, kidneys from different rat or mouse models at different stages of the disease, and the analysis platforms and methods, as reviewed by Menezes and Germino[37]. As a result, a variety of different pathways and processes were suggested to contribute to the disease, but with no strong evidence of which of these differences in the reported results are a consequence of experimental biases or disease complexity.

Several studies indicated a tissue injury-repair component in the pathology of PKD[16,24,70]. Indeed, there are numerous similarities between PKD and renal injury, since both phenotypes are accompanied by a combination of processes including proliferation, secretion of growth factors, as well as inflammation. Weimbs[70] proposed a model where Polycystin 1 (PC1), the protein encoded by *PKD1*, and primary cilia have a critical function in sensing renal injury by detecting changes in luminal fluid flow and triggering proliferation. Besides a proposed mechanistic overlap, several studies showed that renal injury could stimulate cyst progression. For example, nephrotoxic injury in an ADPKD adult mouse model resulted in accelerated cyst formation and a more progressive phenotype[16]. This is further supported by findings that ischemic reperfusion injury and also tubular cell hypertrophy following unilateral nephrectomy accelerated PKD[6,16,33,47,62]. Although the link between PKD and renal injury seems rather strong, until now a thorough comparison between the two conditions at the molecular level has not been made, and little is known about the key genes and pathways shared between the two.

In this work, we performed a meta-analysis of PKD expression profiles to come to a consistent expression signature of the disease that minimizes experimental and technology

biases. We also performed an in-depth comparison between PKD and injury-repair models to characterize genes and functions involved in injury-repair processes and PKD pathology. The novelty of our approach lies in its ability to overcome single study biases in describing the PKD and injury-repair expression signatures, and in the combined use of experimental data and prior knowledge, retrieved from databases and mined from the literature.

Materials and methods

Experimental animals and RNA Sequencing

Pkd1 Mutant and Wild-type mice

The inducible kidney-specific *Pkd1*-deletion mouse model (tam-KspCad-CreER^{T2};*Pkd1*$^{lox2\text{-}11;lox2\text{-}11}$, referred to as iKsp-*Pkd1*^{del}) and tamoxifen treatments were previously described[32,42]. RNA sequencing was done on five wild-type (Wt) mice and kidneys of four iKsp-*Pkd1*^{del} mice with gene disruption at the age of 38-40 days (mutant). Mutant mice, euthanized 84 days later, had moderate cystic disease. The local animal experimental committee of the Leiden University Medical Center and the Commission Biotechnology in Animals of the Dutch Ministry of Agriculture approved the experiments performed.

DCVC Injury Model

Wt mice were fed with tamoxifen (5 mg/day, 3 consecutive days) at adult age, i.e. between 13 to 14 weeks of age[42] as a control for the tamoxifen treatment used in the iKsp-*Pkd1*^{del} mice. Renal injury was induced one week after tamoxifen administration by a single intraperitoneal injection of S-(1,2-dichlorovinyl)-L-cysteine (DCVC) (15 mg/kg). Mice were euthanized at determined time points (1, 2, 5, 10 and 24 weeks after DCVC injection). RNA sequencing was performed on the DCVC-injected Wt mice euthanized at 1, 2 and 5 weeks after DCVC (4 mice per each time point).

RNA Sequencing Methodology.

RNA sequencing was performed on the Illumina® Hi Seq 2500. mRNA-Seq Sample Prep Kit was used to process the samples according to the manufacturer's protocol. Briefly, mRNA was isolated from total RNA using the oligo-dT magnetic beads. After fragmentation of the mRNA, a cDNA synthesis was performed. This was used for ligation with the sequencing adapters and PCR amplification of the resulting product. The quality and yield after sample preparation were measured with a DNA 1000 Lab-on-a-Chip. The expected broad peak between 300 and 500 bp was observed.

Clustering and DNA sequencing using the Illumina cBot and HiSeq 2500 was performed according to manufacturer's protocols. A concentration of 15.0 pM of DNA was used.

HiSeq control software HCS v2.2.38 was used. Image analysis, base calling, and quality check was performed with the Illumina data analysis pipeline RTA v1.18.64 and Bcl2fastq v1.8.4. All samples had a quality score Q30 for more than 93.6% of reads.

Resulting reads were aligned to the mouse reference genome version GRCm38[68] using Tophat2[25] followed by bowtie2[31] in the local highly sensitive mode (bowtie2-local-very-sensitive-local). After alignment, HTSeq-count[3] (Version 0.6.1) was used to estimate gene expression by counting reads that were mapped to each gene using default options.

Differential gene expression analysis was performed using *limma* package with default parameters after applying Voom transformation[52]. Differentially expressed genes were selected where false discovery rate (FDR) is < 0.05. Data were deposited in ArrayExpress[27] and given the following identifier E-MTAB-5319.

Experimental animals and Fluidigm Assay

***Pkd1* Mutant, Wt and DCVC-induced mice**

Wt mice and iKsp-*Pkd1*^{del} mice were feed with tamoxifen (5 mg/day, 3 consecutive days) in adult mice, i.e. between 13 to 14 weeks of age[42] to achieve *Pkd1* gene inactivation in the mutant. Renal injury was induced in Wt mice by a single intraperitoneal Injection of DCVC (15 mg/kg). All Mice were euthanized at determined time points (1, 2, 5, 10 and 24 weeks after DCVC injection for the DCVC induced Wts and respective time points for the non-DCVC treated mice).

Fluidigm quantitative PCR and data processing

The TaqMan Gene Expression Assays of the selected genes and three housekeeping genes were obtained from Applied Biosystems. Best coverage probes were used, according to the sample characteristics. Real-Time PCR analysis was performed at GenomeScan (GenomeScan B.V., Leiden, The Netherlands) using the 96.96 BioMark™ Dynamic Array for Real-Time PCR (Fluidigm Corporation, San Francisco, CA, U.S.A), according to the manufacturer's instructions. Before use on the BioMark array, the cDNA was first subjected to 14 cycles of Specific Target Amplification using a 0.2X mixture of all Taqman Gene Expression assays in combination with the TaqMan PreAmp Master Mix (Applied Biosystems), followed by fivefold dilution. Thermal cycling and real-time imaging of the BioMark array was done on the BioMark instrument, using the default Taqman PCR protocol with an annealing temperature of 60˚C and a total of 35 cycles of PCR. Ct values (cycle threshold values) were extracted using the BioMark Real-Time PCR analysis software (version 3.0.2) and the threshold default value of 0.65. The quality of the amplification curves was checked for each reaction, evaluating the curve shape and signal level. For each gene, Ct values were normalized based on the geometric mean of the housekeeping genes (*Rplp0*, *Hnrnpa2b1*, *Ywhaz*) and then compared across the samples for differential expression in PKD (PKD vs Wt) and injury (Wt injury induced by DCVC vs Wt) by using (ANOVA). A $P < 0.01$ cut-off was used to determine significantly dysregulated genes.

Data Acquisition and Meta-Analysis

Meta-Analysis PKD Signature.

In addition to our iKsp-*Pkd1*^{del}, public expression profiling experiments of PKD were

downloaded from ArrayExpress using ArrayExpress R Package[23] available on Bioconductor[15]. Published PKD expression profiling studies were included based on the following selection criteria: 1) expansion renal cystic tissues were obtained from animal models with disruption of a gene either involved in ADPKD or in ARPKD (PCK rat used as a model for PKD) or taken from ADPKD patients. For the large phenotypic and physiological differences between postnatal and embryonic PKD models, embryonic PKD models were excluded. Asymptotic models were excluded as well. 2) The study included at least three biological replicates for mutant and control tissues (Wts). 3) Normalized gene expression values were publicly available for all samples. Processed data were used for each dataset and log transformed if data were provided on a linear scale. Then, we calculated differentially expressed genes for each study using the *limma* package with default parameters[52]. Genes were considered significantly dysregulated if they had FDR < 0.05 and < 0.0005 for the validation study. When a study had different models or phenotypes of the disease, we processed the samples independently when calculating the differentially expressed genes, and only included in our analysis the models/samples that are useful to us (refer to the relevant table for sample description). When including more than one model from a single study, we took the resulting lists of differentially regulated genes of each model and combined them in a one gene-list per study. Conversion to human homologs was done by using the *db2db* tool part of BioDBnet[41].

Public Injury Models and other Kidney Diseases.
In addition to our DCVC treated Wts, we included six published studies of renal ischemia. Study inclusion criteria were based on the availability of treated and nontreated Wts and availability of data as described in the previous paragraph. Other kidney diseases were included as mentioned in Results. Differentially expressed genes for each study were calculated as described in the previous paragraph.

Literature-based Signatures

Literature-Based Signatures were obtained using Biosemantics Concept Profile technology[17a,21], calculating the literature association scores between all *Homo Sapiens* genes with concept profiles and the literature concept profiles of renal injury repair in PubMed until July 2012. The literature association (concept profile matching) score is based on the strength of explicit associations (the two concepts co-occurring in the same PubMed abstract) and implicit associations (the two concepts not co-occurring in the same abstract together, but each in abstracts with the same third concept). The literature mining technology handles and disambiguates gene names and symbols.

Functional enrichment analysis

Functional enrichment analysis was performed against Molecular Signature Database (MSigDB) collections[58,59] using standard hypergeometric distribution with correction for multiple hypotheses testing using the FDR. Annotation with DAVID v6.8[27,28] was performed with default parameters for confirmation purposes where mentioned in the text.
The significance of the overlaps between gene profiles and gene sets, were evaluated with a χ^2-test ($P < 0.05$) and the representation factor (RF) calculated as follows: x = # of genes in common between two groups, n = # of genes in group 1, D = # of genes in group 2, N = total genes available, the RF = x / expected # of genes, expected # of genes = (n X D) / N

Results

Identification of PKD Signature

To identify a comprehensive expression signature of PKD during disease progression, we generated new RNASeq-based expression profiles of inducible, kidney epithelium-specific *Pkd1*-deletion mice (iKsp-*Pkd1*^{del}) with moderate cystic disease and matched controls[32,42] (Figure 1A).

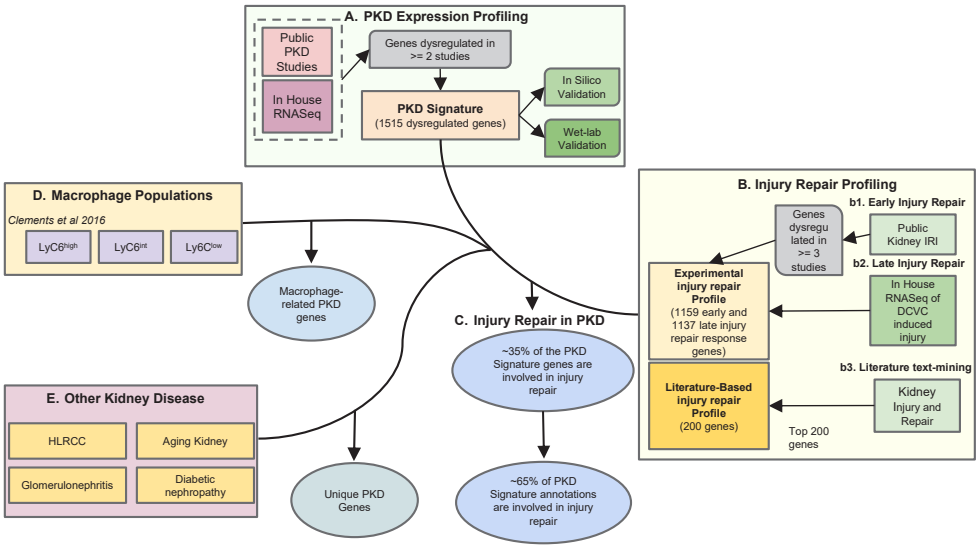

Figure 1. Overview of the approach used to identify the PKD Signature and comparison to renal injury and repair, macrophages and other kidney diseases

The approach consisted of five steps. **A:** the PKD Signature was defined by combining publicly available PKD expression profiling studies with our in-house RNAseq of iKsp-*Pkd1*^{del} in mice. **B:** the Injury Repair Profile was defined by experimental expression profiles of kidneys with ischemia-reperfusion injury (IRI) (**b1**), in-house RNAseq of kidneys from DCVC-treated animals (**b2**) and literature-based text-mining of genes associated with injury terms in PubMed abstracts (**b3**). **C:** comparing significantly dysregulated genes from PKD Signature and Injury Repair Profile we identified the Injury Repair Component of PKD, which consists of ~35% of the genes implicated in PKD. **D:** we used the data produced by Clements *et al.*[11] in 2016 of the different macrophage populations triggered after renal injury to identify macrophage-related genes in PKD. **E:** we acquired expression profiling experiments of different renal diseases and compared them to the PKD Signature to identify the overlapping genes and the unique PKD Signature genes. HLRCC, hereditary leiomyomatosis and renal cell cancer.

We identified 2,376 genes (FDR < 0.05) that clearly distinguished iKsp-*Pkd1*^{del} from Wt mice (Data Set 1, Figure 2A). Next, we compared our expression profile to other publicly available PKD expression studies (Figure 1A). We used stringent study inclusion criteria (See Methods) and identified three studies suitable for meta-analysis[39,43,56] (Table 1). By comparing the independent PKD expression studies (our dataset included), we assessed the level of similarity/dissimilarity between each study and defined a group of high confidence

genes that are consistently dysregulated in PKD. Every significantly dysregulated gene (PKD *vs.* Wt) obtained from the studies, was classified as a shared gene (if dysregulated in at least two independent studies) or a unique gene (if dysregulated in just a single study). Strikingly, only ~22% (N=1515) of all dysregulated genes from all PKD studies (N=6963), were shared, of which the vast majority (~86% of the 1515 genes) were dysregulated in just two studies (Figure 2B). Moreover, none of the PKD studies used in this analysis had more than 50% of its dysregulated genes shared with any of the other three studies (Figure 2C).
To arrive to a robust PKD signature, we selected PKD genes that were significantly dysregulated in at least two independent studies (50% of the studies). Thus, our PKD signature consists of 1515 genes (1641 mouse homologs), comprising 775 up- and 740 downregulated genes (Data Set 2a and 2b).

Table 1. Expression profiling studies used in the definition of the PKD Signature

Authors	Organism/Sex	Accession Number	Datasets Included	No of DEGs after HC	No. of DEGs in PKD Signature
Menezes *et al.*[39]	Mouse/M and F	GSE32586	*Pkd1cko.P12* vs WT.12	40	17
			Pkd1cko.P14 vs WT.14	1,200	594
O'Meara *et al.*[43]	Rat/M	GSE33056	PCK vs SD	1,586	561
Song *et al.*[56]	Human/NM	GSE7869	Non-cystic vs normal	280	68
			Small cysts vs normal	4,554	1,025
			Medium cysts vs normal	4,650	1,033
Malas *et al.* (this study)	Mouse/M	E-MTAB-5319	*Pkd1cko.P40* vs WT	2,376	924

PKD, polycystic kidney disease; DEGs, differentially expressed genes; HC, homolog conversion; SD, Sprague-Dawley; WT, wild type; M, males; F, females; NM, not mentioned in the Methods of the paper.

Validation of the PKD Signature in an independent dataset

We validated the PKD Signature in an independent dataset that was published during the writing of this manuscript[38]. This dataset includes 80 mouse samples with induced deletion of *Pkd1* at P40 (14 control females, 21 mutant females, 19 control males and 26 mutant males). We evaluated the overlap by calculating the representation factor (RF), defined as the number of overlapping genes divided by the expected number of overlapping genes drawn from two independent groups. We looked for the enrichment of the PKD Signature genes in the genes differentially expressed (FDR < 0.0005) in mild, moderate and advanced stages of the disease, in males and in females (Figure 2D). We repeated the enrichment test with equally sized gene sets from the genes that are dysregulated in only one PKD study and from randomly sampled genes. The results revealed that the PKD Signature is at least three times more enriched in the validation dataset in contrast to the random genes and genes dysregulated in only one study. This significance is observed in all stages of the PKD disease and in both genders.

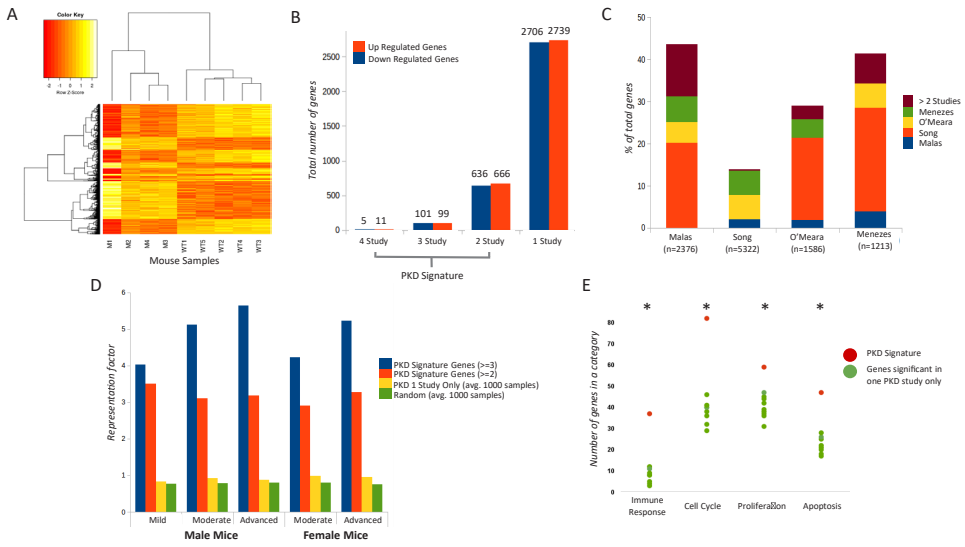

Figure 2. Identification of the PKD Signature

A: Heat map showing the expression values of all differentially expressed genes in iKsp-*Pkd1*^{del} (M) compared to wild-type mice (WT). Expression values were normalized using the Vroom function in *limma* R Package. Hierarchical clustering was applied on the samples and values were scaled by row. **B:** analysis of the number of overlapping genes from the four studies included in the meta-analysis. **C:** comparison of the significantly dysregulated genes in each of the four studies revealed that none of the studies shared more than 50% of its genes with other studies. **D:** bar chart plotting the enrichment (representation factor, y-axis) of the PKD Signature (blue and red bars), the genes dysregulated only in a single PKD study (yellow) and a random set of genes (green) in an independent dataset from *Pkd1cko* mice at mild, moderate and advanced stages of the disease, in males and females. **E:** a dot plot showing the number of genes from the PKD Signature (red) and from 10 equally sized gene-sets randomly sampled from the genes dysregulated in only one study (green) with functional annotations previously attributed to PKD. **P* < 0.05 (binomial test, where the fraction of genes in the PKD Signature was compared with the expected fraction of genes in a functional category (averaged gene counts from the 10 random sets). Functional categories were based on three annotation databases (GSEA_HALLMARKS, KEGG and Gene Ontology – *Biological Processes*).

Functional annotation of the PKD Signature

We annotated the up- and downregulated gene sets using the Molecular Signature Database Hallmarks (MSigDB)[34] and The Database for Annotation, Visualization and Integrated Discovery (DAVID) v6.8[18,19] (Data Set 3). Both resources revealed the strong downregulation of mitochondrial and peroxisome genes, specifically those involved in fatty acid metabolism, lipogenesis, and oxidation-reduction process. In addition, we see strong dysregulation of genes involved in ion transport (i.e. *CP, SLC4A1, SLC2A9, SLC12A1*).

On the other hand, several pathways and processes are upregulated in the PKD Signature listed in Data Set 3. We further grouped the genes shared between three or more studies into defined gene families (protein kinases, cytokines and growth factors, transcription factors and oncogenes) to facilitate their usage in translational research (Data Set3c and 3d).

To measure the relevance of the PKD Signature at the molecular-function level, we defined four categories that are known to be dysregulated in PKD: cell cycle[46], apoptosis[13],

proliferation[71] and inflammatory response[61]. We found that the PKD Signature had significantly more functional annotations related to these categories than equally-sized random sets of genes pooled from the genes significant in only one PKD study (binomial test, $P < 0.0005$) (Figure 2E).

Identification of Injury Repair genes in the PKD Signature

Experimental Injury Repair Profile

We acquired datasets from renal ischemia reperfusion (IRI) experiments in murine models and identified six studies (3 mouse and 3 rat), that met our inclusion criteria (Table 2) (Figure 1B)[9,12,28,35,57,73]. Differentially expressed genes from all of the six renal injury repair studies were enriched within the PKD Signature (RF > 1 and $P < 0.05$) (Figure 3B). The studies varied in the reperfusion time, from immediately harvesting the samples after reperfusion to waiting for up to 120 h. Using these samples, we defined a 1,193-gene signature of early injury repair response, by combining the six studies and looking for consistently dysregulated genes in at least 50% of the studies (Data Set 4a).

Table 2. Published expression profiling studies used in the definition of the experimental injury repair profile

Authors	Organism	Accession	Injury Model	Time after reperfusion
Chen *et al.*[9]	Mouse	GSE34351	ARI	4 h
Correa-Costa *et al.*[12]	Mouse	GSE39548	ARI	6 h
Liu *et al.*[35]	Mouse	GSE52004	ARI	24 h
Yuen *et al.*[73]	Rat	GSE3219	ARI	2, 8 h
Krishnamoorthy *et al.*[28]	Rat	GSE27274	ARI	6, 24, 120 h
Speir *et al.*[57]	Rat	GSE58438	ARI	Immediate

ARI, acute renal injury

Several renal IRI studies reported that the maximum peak of renal damage is reached at the 3rd day of injury induction and gradually drops as the kidney repairs itself, until about day 7 when the tissue looks mostly repaired. Since none of the IRI studies we could include publicly harvested samples within the late injury period (after 7 days), we generated novel data by inducing renal injury in Wt mice using the nephrotoxic DCVC. The samples were harvested at 1, 2 and 5 weeks after injury induction. Measurements of blood urea showed that mice have normal functional kidneys at 7 days after injury, confirming that most of the acute injury insult is repaired at that time point (Figure 3A). Renal histology sections at 1 week show slightly dilated tubules with protein casts, infiltrating cells and fibrosis at the cortico-medullary junction, the most damage-sensitive region of the kidney. At 2 weeks after DCVC treatment the tissue morphology is improved and at 5 weeks, the kidneys have almost completely been recovered from the injury (Figure 3A). Comparing the different injury repair time points from our injury-induced model against each other we identified

1,137 differentially expressed genes (Data Set 4b). Comparing the functional annotations of the early and late injury repair genes showed that they are distinct (Figure 3C). We combined the early and late injury repair response genes to establish a general Experimental Injury Repair Profile, consisting of 2137 genes.

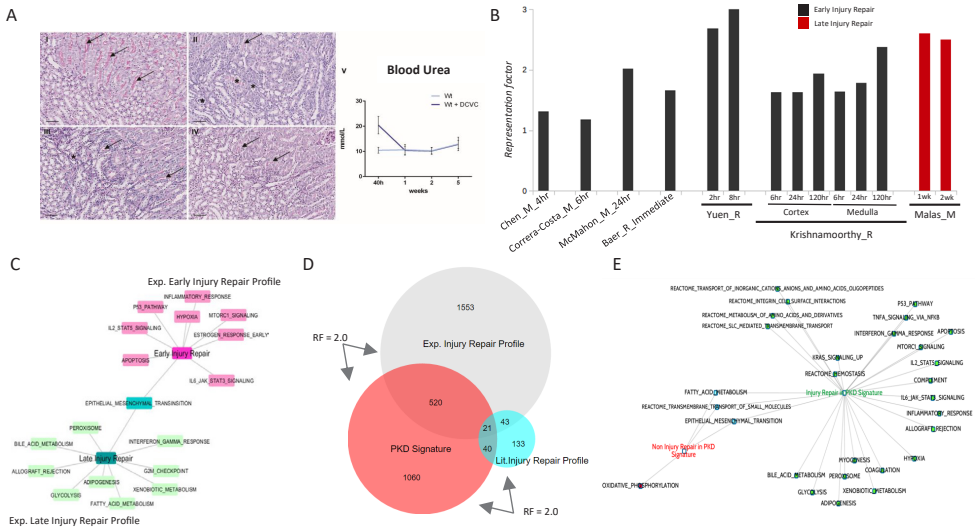

Figure 3. Identification of the Injury Repair Component of the PKD Signature

A: injury repair progression in Wt mice injected with DCVC. **I-IV:** periodic-acid Schiff (PAS) staining on formalin fixed, paraffin embedded kidney sections; scale bar = 50 µm. *Dilated tubules with luminal protein inclusions; →normal brush border. **I:** Wt without injury. Normal morphology with visible brush border. **II:** 1 week after DCVC injection damaged and slightly dilated tubules with luminal protein inclusions were observed. **III:** 2 weeks after DCVC the tissue is almost repaired with only sporadic protein inclusion observable but some infiltrating cells present. **IV:** 5 weeks after DCVC injection the tissue was almost completely repaired and less infiltrating cells were present. **V:** blood urea (BU) levels (mmol/l) at different time points after DCVC injection, peaking at 40 h and returning to baseline after 2 weeks, when the tissue is repaired. **B:** enrichment (representation factor, y-axis) of each injury dataset in the PKD Signature. Dataset from mice (M) or rats (R) with early injury response (IRI, black) and late injury repair response (DCVC treatment, red) were all enriched in the PKD Signature. **C:** the top ten enriched terms for the early injury repair (pink) and late injury repair (green) genes based on MSigDB Hallmark categories [false discovery rate (FDR) < 0.05]. On the one hand, the early injury repair genes had apoptosis, hypoxia and inflammatory response related pathways in the most enriched functions identified from MSigDB and, on the second hand, the late injury repair genes had functions related to peroxisome, glycolysis and fatty acid metabolism amongst the most enriched functions. **D:** comparison of the experimental (Exp.) and literature (Lit.) based injury repair profiles and their overlap with the PKD Signature. Approximately, 35% (581/1,641) of the PKD Signature genes are involved in injury repair related functions. Representation Factor (RF) denotes the level of enrichment of each injury repair profile in the PKD Signature (RF of Experimental Injury Repair = 2.0, RF of Literature Injury Repair = 2.0) where values greater than 1 denote strong enrichment. **E:** a clear distinction in the functional profiles of the injury (red) and non-injury (green) components of the PKD Signature, as represented in a network view of the more enriched terms from MSigDB (FDR < 1e-11) for each of the two components.

Literature Injury Repair Profile

The Literature Injury Repair Profile is based on published knowledge of genes involved in injury repair processes in PubMed. We set our text-mining algorithm to retrieve the top

200 genes that are most associated with renal injury in PubMed abstracts (Data Set 4c). In addition, as negative controls, we retrieved the top 200 genes most associated with other conditions that we believe to be unrelated to PKD, namely fertility and Parkinson's disease. The literature renal injury repair genes were significantly enriched in the PKD Signature (RF = 2), contrary to the two negative sets (Fertility RF = 0.9, Parkinson's disease RF = 1.1).

Injury Repair processes in PKD

To find injury repair involvement in PKD, we compared the PKD Signature with the Experimental Injury Repair Profile and the Literature Injury Repair Profile (Figure 1C). Our analysis revealed that both injury repair profiles were significantly enriched in the PKD Signature (Figure 3D), with *P* values of 1.3×10^{-29} and 2.8×10^{-7} for the Experimental and Literature Injury Repair profiles, respectively. Of the total PKD Signature genes, 35% (581 genes) are involved in injury repair processes (Data Set 5).

We extended the functional analysis that we performed on the PKD Signature to the injury repair and non-injury repair genes in PKD. For each set of genes, we identified the most enriched functional terms from MSigDB with stringent FDR cutoff (< 1e-11). Interestingly, 22 terms were found to be more enriched in the injury repair genes and only 1 term is more enriched in the non-injury repair genes when compared with each other (Figure 3E, Data Set6). This demonstrates the cohesiveness of the injury repair genes. Many of the injury repair functions are related to NF-kB signaling, epithelial-to-mesenchymal transition, inflammatory response, hypoxia, and metabolism. Although these functional terms are expected in a well-defined injury repair signature, they demonstrate that we zoomed in on a relevant group of genes (Table 3).

Table 3. Top 5 annotations for genes in the injury repair PKD Signature component

Term Name	Count	FDR	Genes (Gene Symbol)
TNFA_SIGNALING_VIA_NFKB	43	1.9E-38	*CD44, GADD45B, RHOB, PLAUR, JUN, CYR61, CXCL1, TNC, MAFF, F3, KLF6, CSF1, MYC, NFIL3, PHLDA1, GCH1, CDKN1A, BTG2, HBEGF, SPHK1, TLR2, ICAM1, CCL2, KYNU, ETS2, PPP1R15A, BTG1, FOSL2, BIRC3, MCL1, PLK2, IER5, SOCS3, CXCL3, BCL3, CEBPB, JUNB, CXCL2, TGIF1, CEBPD, EGR1, PANX1, LITAF*
EPITHELIAL_MESENCHYMAL_TRANSITION	37	1.44E-30	*CD44, GADD45B, RHOB, PLAUR, JUN, CYR61, CXCL1, TNC, TIMP1, SPARC, FN1, FBN1, THBS1, SPP1, ITGA5, DCN, TGFBI, TNFRSF12A, SDC1, COL4A2, COL3A1, COL1A1, ITGB1, ITGB5, TAGLN, TPM2, COL1A2, LAMC2, FSTL1, BASP1, DPYSL3, LOXL2, MGP, PCOLCE, SFRP4, TPM4, VIM*
COAGULATION	25	3.65E-20	*TIMP1, SPARC, FN1, FBN1, THBS1, MAFF, F3, MEP1A, KLF7, ANXA1, CFH, MMP9, DUSP6, CAPN5, PF4, C3, CSRP1, FGA, FGG, MSRB2, CFI, APOC3, P2RY1, PROC, CAPN2*
INFLAMMATORY_RESPONSE	28	8.01E-20	*TIMP1, F3, MEP1A, PLAUR, ITGA5, KLF6, CSF1, MYC, GCH1, CDKN1A, BTG2, HBEGF, SPHK1, TLR2, ICAM1, CCL2, RGS16, TNFRSF1B, IL4R, TPBG, CD14, OSMR, TAPBP, BST2, RHOG, SLC7A1, PDPN, AXL*
XENOBIOTIC_METABOLISM	28	8.01E-20	*GCH1, KYNU, ETS2, GABARAPL1, AHCY, RETSAT, CROT, HSD11B1, ALDH9A1, TNFRSF1A, CAT, ACOX1, POR, APOE, FMO1, BPHL, PDK4, SLC6A12, TMBIM6, ESR1, SLC46A3, GSS, ARG2, MAN1A1, NDRG2, SLC12A4, NFS1, ENTPD5*

Count represents the number of genes that belong to a functional annotation term and the tested PKD Signature component. FDR, false discovery rate, based on MSigDB.

Injury Repair in different PKD disease stages

We evaluated the enrichment of the genes in the signature at the different phases of disease progression. We used the data of Menezes *et al*[26] that included mouse samples from mild, moderate and advanced PKD disease stages. Injury repair and non-injury repair PKD genes are enriched in all stages of the disease (RF > 1) (Figure 4A). However, in the mild phase of the disease, the non-injury repair is twice as enriched in comparison to the injury repair genes. In the advanced stage of the disease, the opposite is observed. These results are in accordance with our understanding of the disease, as more injury repair processes are expected with disease progression. That said, injury repair genes are enriched in the early phases of PKD, and appear to be involved in cell cycle, extracellular matrix modulation and growth, epithelial-to-mesenchymal transition and metabolism (Data Set 7b). In addition, several cytokines that are associated with kidney injury are upregulated in the early phases of PKD, such as osteopontin (*OPN*) and growth differentiation factor 15 (*GDF15)*.

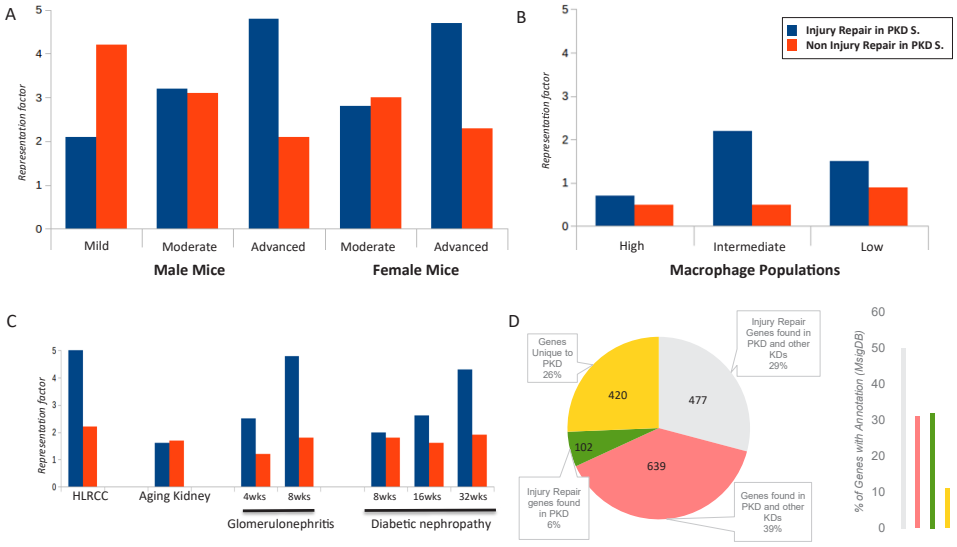

Figure 4. Validation of Injury Repair processes in PKD Signature

A: enrichment analysis (RF, y-axis) of the injury repair (blue) and non-injury repair (red) components of the PKD Signature (PKD S.) in the different phases of the severity of PKD disease in *Pkd1cko* mice[38]. **B:** bar chart showing the strong enrichment of different macrophage population ("CD11b+/Ly6C^{high}", "CD11b+/Ly6C^{intermediate}" and "CD11b+/Ly6C ^{low}", Clements *et al.*[11]) gene signatures activated upon injury induction in mouse models in the injury repair (blue) and non-injury repair (red) components of the PKD Signature. **C:** the enrichment of the injury repair (blue) and non-injury repair (red) components of the PKD Signature in expression profiles from other kidney diseases. **D:** characterization of the PKD Signature into groups based on the overlap with renal injury repair and other kidney diseases. On the left, a pie chart showing the total number of genes within each of the four groups and on the right a bar chart reflecting the percentage of genes that matched to at least one annotation term based on MsigDB Hallmarks and Reactome pathway database after running the enrichment comparison with the following settings (FDR < 0.05, top 20 terms).

Experimental validation of the injury component in independent samples

To validate our results, we generated an independent set of adult-onset slow-progressing inducible *Pkd1*-deletion mice as a PKD model not included in the generation of the PKD Signature. We harvested mice at five different time points (1, 2, 5, and 10 weeks after injury and at kidney failure) (Figure 5A).

These samples were analyzed by Fluidigm qPCR chip to quantify mRNA levels of selected genes; Inflammatory response (*Pcdh7* and *Stat3*), hypoxia (*Akap12 and Anxa2),* epithelial-to-mesenchymal transition *(Dpysl3* and *Tnfrsf12a),* TNF-α/NF-κB signaling (*Socs3),* coagulation (*Fgg*), transcription factor *(Glis2)* and transporters *(Cp).* Additionally, we have included an age-matched set of mouse samples, i.e. wild-type mice with and without treatment with the nephrotoxic compound DCVC to reflect the injury repair component. Normalized Ct values were tested for statistical significance between the groups (mutant vs. Wt, and Wt + DCVC vs. Wt). All genes from the PKD Signature were significantly dysregulated between mutant and Wts and all genes we classified as injury-repair related were significantly dysregulated between (Wt and Wt + DCVC) (Figure 5B).

Macrophages in Polycystic Kidney Disease

Macrophages have important roles in renal injury repair and PKD[3,50,60]. Having identified the injury repair genes of the PKD Signature, we proceeded to identify novel macrophage-related molecular pathways involved in PKD progression. Using data of Clements *et al.*[11], which contains unique expression profiles of different macrophage populations upon renal injury induction. They identified three distinct macrophage populations: the "CD11b+/Ly6C^{high}" population associated with the onset of renal injury and increase in proinflammatory cytokines, the "CD11b+/Ly6C^{intermediate}" population that peaked during kidney repair, and the "CD11b+/Ly6C^{low}" population that emerged with developing renal fibrosis. We looked for genes that are up-regulated in the PKD Signature and uniquely upregulated in each of the three macrophage populations by selecting, for each population, the genes that are upregulated to the other two (logFC ≥ 2, $P < 0.05$). The most enriched populations in PKD are the "CD11b+/Ly6C^{intermediate}" and "CD11b+/Ly6C^{low}" populations, both are two times more enriched in the injury repair genes when compared with the non-injury repair genes (Figure 4B). As these are macrophages activated upon injury induction, stronger enrichment in the injury repair component in contrast to the non-injury repair component is expected and observed.

Using these datasets, we identified several novel genes that are involved in macrophage-related wound healing and fibrosis processes in PKD (Data Set 8a). KEGG pathway annotations revealed that these genes are involved in pathways related to extracellular matrix-receptor interaction, focal adhesion, regulation of actin cytoskeleton and cytokine-cytokine receptor interaction (Data Set 8b).

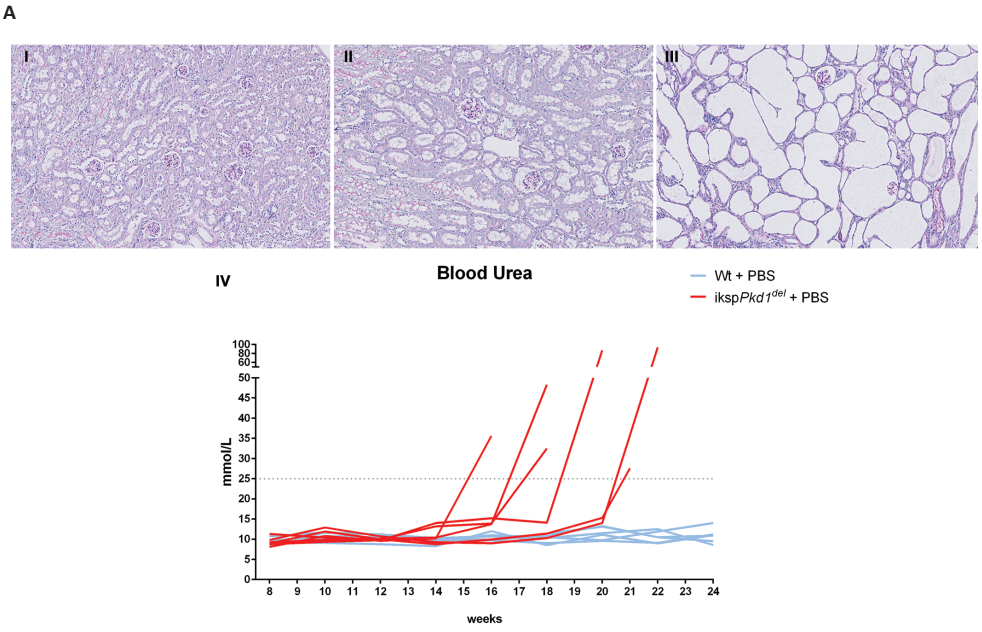

Figure 5. Validation of the PKD Signature in an adult onset iKsp-*Pkd1*^{del} model and in a nephrotoxic injury model

A: cyst progression in the adult iKsp-*Pkd1*^{del} mice. **I-III:** PAS staining on formalin fixed, paraffin embedded kidney sections, scale bar = 100 µm. Mild tubular dilation at 5 (**I**), 10 weeks after gene disruption (**II**), and many cysts at kidney failure (**III**). **IV:** BU levels were used to assess renal failure and are presented for individual mice. A slow progression of the disease was observed, with median duration until kidney failure of 19 weeks. **B:** genes selected randomly from the PKD Signature, were subjected to qPCR on the iKsp-*Pkd1*^{del} mice model described in **A** and age-matched Wts at 1, 2, 5, 10 weeks after gene knockout, and at kidney failure. Normalized Ct values (cycle threshold values) are plotted (log2 scale) for each gene separately across five measurement time points for three types of samples: wild-type mice treated with saline (WTPBS, red), iKsp-*Pkd1*^{del} mice treated with saline (Pkd1cko, green) and wild-type mice treated with DCVC (WTDCVC, blue). For each time point, the significance of dysregulation in RNA-levels with respect to WTPBS mice was tested using Student's *t*-test. Grey bars below the x-axis are used in case of no significance ($P \geq 0.01$) and darker shades of colors (green for PKD and blue for injury) are used to denote stronger dysregulation ($P < 0.01$, $P < 0.001$, $P < 0.0001$ for the three different shades of color).

Comparison of the PKD Signature with other kidney diseases

We compared the PKD Signature with other kidney diseases, for which expression profiling studies have been published in the literature[1,7,63,72] (Table 4). The *Fh1* knockout hereditary leiomyomatosis and renal cell cancer (HLRCC) model that develops renal cysts[49], had the highest enrichment with the PKD Signature with RF of 3.3. In addition, the overlap of other kidney diseases such as glomerulonephritis[63] and diabetic nephropathy[72], with the PKD Signature increases as the severity of these diseases increases, evident by data acquired from 4- and 8-weeks-old glomerulonephritis mice (RF of 1.7 and 2.9 respectively) and 8- and 32-weeks-old diabetic nephropathy mice (RF of 1.8 and 2.8 respectively). Functional annotation tests of the genes of the more advanced disease stages revealed their involvement in functions related to the immune system and epithelial-to-mesenchymal transition, suggesting, that most of the overlap of the PKD Signature with other kidney diseases is related to injury repair and inflammation. To test this, we compared the enrichment of each disease with both the injury repair genes and the non-injury repair genes of the PKD Signature (Figure 4C). The results confirmed that the overlap with the injury repair component of PKD was twice as large as the overlap with the non-injury repair component. Utilizing the large variety of datasets that we have compiled and compared with the PKD Signature, we are able to classify the PKD Signature genes into different categories. These categories are based on the level of commonality of the PKD Signature genes to other kidney diseases and injury repair processes (Figure 4D). Interestingly, the unique PKD Signature genes, are the genes with the least known functional annotations (<12% of genes mapped to annotation terms) (Figure 4D).

Table 4. Published Expression Profiling Studies used in the comparison of the PKD Signature to other diseases

Authors	Organism	Accession	Disease	Mouse Model
Adam, J. *et al.*[1]	Mouse	GSE10989	HLRCC	*Fh1* knock-out
Braun, F *et al.*[7]	Mouse	GSE3219	Aging kidney	Aged wild-type mice
Tamura K *et al.*[63]	Mouse	GSE45005	Glomerulonephritis	ICGN mice
Yang *et al.*[72]	Mouse	GSE20844	Diabetic nephropathy	OVE26 mice

HLRCC, hereditary leiomyomatosis and renal cell cancer; ICGN mice, ICR-derived glomerulonephritis.

DISCUSSION

In this work, we have created a robust PKD Signature that would help in the ongoing translational research efforts to find novel treatments for PKD patients. We followed a meta-analysis approach that combined available PKD expression profiling studies with a new dataset that we contributed. Given that the datasets that we could include are limited and variable, we focused on creating a PKD Signature that zooms-in on the commonalities of the disease and included genes that are consistently dysregulated across the different studies. Although in this approach we do not guarantee to include all genes involved or dysregulated in PKD, we managed to include highly relevant PKD genes. To corroborate this, we tested the PKD Signature on an independent PKD dataset that was not used in the making of the PKD Signature. This analysis revealed that the PKD Signature genes are three times more enriched in an independent PKD study compared with the PKD genes that were excluded from our PKD Signature. In addition, significant enrichments were observed in mild, moderate and advanced stages of the disease, in both males and females. These results reveal the robustness of the PKD Signature and support the likelihood of preserved key disease mechanisms between genders. We also experimentally confirmed the dysregulation of a selection of genes from the PKD Signature in an independent PKD model using qPCR. Our functional annotation of the PKD Signature revealed the dysregulation of many PKD-linked pathways, such as epithelial-to-mesenchymal transition[8], TGF-β signaling pathway[8,17], cell cycle, JAK/STAT signaling pathway[17,39,52] and mammalian target of rapamycin (mTOR) signaling[42,55], in addition to downregulated genes in molecular transport[64] and a large set of genes involved in metabolic pathways[5,53].

Being motivated by the rich literature suggesting a strong relationship between PKD and injury repair processes, we went on to characterize the injury repair involved genes in the PKD Signature. We used a novel approach to combine experimental and literature-based renal injury repair profiles. We also contributed a new dataset of injury induced mouse model that covers the late-injury repair response phase. Our results are in line with these suggestions, where we were able to link 35% (581 genes) of the PKD Signature genes to injury repair response. This overlap is two times more enriched than randomly expected (RF=2). Interestingly, these injury repair genes are involved in more than 65% of the functional annotations attributed to PKD. The most enriched functions of the PKD signature injury repair genes include epithelial-to-mesenchymal transition, proliferation, apoptosis, hypoxia, inflammatory response, TNF-α/NF-κB signaling and glycolysis. Furthermore, we showed that the injury repair genes are enriched in all stages of the PKD disease and their enrichment becomes stronger as the disease progresses towards a more severe state. This is in accordance with our understanding of the disease. As PKD progresses, cysts grow in size, putting pressure on nearby cells and giving rise to new cysts. Oxidative stress increases with

disease progression and injury repair processes become significantly evident with visible macrophage infiltration and fibrosis taking place at the cyst site. The functional annotation profiles of the PKD Signature injury repair genes reflect this. In mild and moderate phases of the disease, injury repair genes are associated with cell cycle-related events (i.e. *BIRC5, MCM2, MCM5, PLK1* and *CDKN1A*), genes involved in extracellular matrix development and morphogenesis (i.e. *OPN, TPM4, TGFBI* and *TNFRSF12A*), genes involved in transport of cations/anions and amino acids/oligopeptides (i.e. *SLC25A10, SLC38A2, SLC6A12*) and metabolism (i.e. *CHPF* and *LGALS3*). On the other hand, injury repair genes at the late phases of PKD are involved in the negative regulation of apoptosis, hypoxia, inflammatory response and TNF-α/NF-κB signaling. Additionally, the upregulation of renal injury markers Osteopontin (*OPN*) in the moderate phase and Kidney Injury Molecule 1 (*KIM-1* or *HAVCR1*) in the advanced phase of PKD, confirms the involvement of renal injury repair processes in disease progression[66].

Utilizing the data of Clements *et al.*[11] we looked for PKD genes that are involved in macrophage-related wound healing and fibrosis events after injury induction. Our results revealed that macrophage-related genes activated upon injury induction are more enriched in the PKD Signature injury repair genes than the non-injury repair genes. This is especially evident in the macrophage populations "CD11b+/Ly6C^{intermediate}" and "CD11b+/Ly6C^{low}", suggesting a role for PKD injury repair genes in macrophage-related wound healing and fibrosis events. Syndecan-1 (*SDC1*)[36], secreted protein acidic and cysteine rich (*SPARC*)[48] and collagen type I alpha-2 chain (*COL1A2*)[14] are three known fibrosis genes found in the injury repair PKD Signature genes. However, it remains unclear whether these genes are reflecting only the expression in macrophages or also expression in the epithelium. As macrophages are known to contribute to PKD's pathology, further research is needed to determine their clinical significance in PKD treatment.

We validated the PKD Signature genes in a second PKD model with more sampling time points, using a Fluidigm qPCR chip. We also included Wt and Wt + DCVC samples at matching time points. This analysis showed that our classification into "injury repair" and "non-injury repair" groups was predictive. For instance, *Glis2,* an important gene in kidney function[22,26] is part of the PKD Signature and was consistently upregulated in all qPCR measured time-points of the iKsp-*Pkd1*^{del}. Our computational analysis did not include it as part of the injury repair genes in the PKD Signature, and this was further confirmed in the qPCR results as it did not respond to DCVC injury induction in Wt mice. *Plk2,* on the other hand, is upregulated in the early PKD time point and in the injury induced mice, confirming our classification of *Plk2* as an injury repair related gene.

In conclusion, our computational methodology combined by our experimental validation in

an independent mouse model identified a robust expression signature of PKD. We provide an extensive meta-analysis of PKD transcriptional profile and characterization of the injury repair genes involved. We believe that this study can be used to improve our understanding of the disease and how altered injury repair processes augment it over time. Comparing the PKD Signature to other kidney diseases, revealed that the injury repair genes in the PKD Signature account, in large part, to the evident overlap between PKD and other kidney diseases, revealing the significance of injury repair genes and pathways in the development and progression of kidney diseases. Novel drug targets can be identified from the profiles affecting the common subset of injury repair processes or affecting the PKD-unique targets. This may allow for drug repurposing between renal diseases and/or the identification of PKD unique agents that modulate the regenerative process in PKD patients and may lead to the much sought after treatment for PKD patients.

Acknowledgments

We thank Kristina M. Hettne, Leo Price, and Freek van Eeden for critical reading and editing the manuscript.

Grants

The research leading to these results has received funding from the People Program (Marie Curie Actions) of the European Union's Seventh Framework Program FP7/2077-2013 under Research Executive Agency Grant Agreement 317246 and the Dutch Technology Foundation Stichting Technische Wetenschappen Project 11823, which is part of The Netherlands Organization for Scientific Research.

Disclosures

No conflicts of interest, financial or otherwise, are declared by the authors.

Author contributions

T.B.M., M.R., D.J.P., and P.A.t.H. conceived and designed research; T.B.M., C.F., W.N.L., P.R., and Z.G. performed experiments; T.B.M., C.F., W.N.L., P.R., Z.G., and M.R. analyzed data; T.B.M., C.F., W.N.L., and D.J.P. interpreted results of experiments; T.B.M. and C.F. prepared figures; T.B.M. drafted manuscript; T.B.M., C.F., W.N.L., Z.G., M.R., D.J.P., and P.A.t.H. edited and revised manuscript; T.B.M., C.F., W.N.L., P.R., Z.G., M.R., D.J.P., and P.A.t.H. approved final version of manuscript.

References

1. Adam, J. et al. Renal cyst formation in Fh1-deficient mice is independent of the Hif/Phd pathway: roles for fumarate in KEAP1 succination and Nrf2 signaling. Cancer Cell 20: 524-537, doi:10.1038/ki.2011.217 (2011).

2. Anders, H.J. & Ryu, M. Renal microenvironments and macrophage phenotypes determine progression or resolution of renal inflammation and fibrosis. Kidney Int 80: 915-925, doi:10.1038/ki.2011.217 (2011).

3. Anders, S. et al. HTSeq--a Python framework to work with high-throughput sequencing data. Bioinformatics 31: 166-169, doi:10.1093/bioinformatics/btu638 (2015).

4. The International Polycystic Kidney Disease Consortium. Polycystic kidney disease: the complete structure of the PKD1 gene and its protein. Cell 81: 289-298, doi:10.1016/0092-8674(95)90339-9 (1995).

5. Aukema, H.M. et al. Abnormal lipid and fatty acid compositions of kidneys from mice with polycystic kidney disease. Lipids 27: 429-435, doi:10.1007/BF02536384 (1992).

6. Bell, P.D. et al. Loss of primary cilia upregulates renal hypertrophic signaling and promotes cystogenesis. J Am Soc Nephrol 22: 839-848, doi:10.1681/ASN.2010050526 (2011).

7. Braun, F. et al. Altered lipid metabolism in the aging kidney identified by three layered omic analysis. Aging (Albany NY) 8: 441-457, doi:10.18632/aging.100900 (2016.)

8. Chea, S.W. & Lee, K.B. TGF-beta mediated epithelial-mesenchymal transition in autosomal dominant polycystic kidney disease. Yonsei medical journal 50: 105-111, doi:10.3349/ymj.2009.50.1.105 (2009).

9. Chen, M.J. et al. A global transcriptomic view of the multifaceted role of glutathione peroxidase-1 in cerebral ischemic-reperfusion injury. Free Radic Biol Med 50: 736-748, doi:10.1016/j.freeradbiomed.2010.12.025 (2011).

10. Chen, W.C. et al. Gene expression in early and progression phases of autosomal dominant polycystic kidney disease. BMC Res Notes 1: 131, doi:10.1186/1756-0500-1-131 (2008).

11. Clements, M. et al. Differential Ly6C Expression after Renal Ischemia-Reperfusion Identifies Unique Macrophage Populations. J Am Soc Nephrol 27: 159-170, doi:10.1681/ASN.2014111138 (2016).

12. Correa-Costa, M. et al. Transcriptome analysis of renal ischemia/reperfusion injury and its modulation by ischemic pre-conditioning or hemin treatment. PLoS One 7: e49569, doi:10.1371/journal.pone.0049569 2012.

13. Ferreira, F.M. et al. Polycystins and Molecular Basis of Autosomal Dominant Polycystic Kidney Disease. In: Polycystic Kidney Disease, edited by Li X. Brisbane (AU) (2015).

14. Fragiadaki, M. et al. Interstitial fibrosis is associated with increased COL1A2 transcription in AA-injured renal tubular epithelial cells in vivo. Matrix biology : journal of the International Society for Matrix Biology 30: 396-403, doi:10.1016/j.matbio.2011.07.004 (2011).

15. Gentleman, R.C. et al. Bioconductor: open software development for computational biology and bioinformatics. Genome Biol 5: R80, doi:10.1186/gb-2004-5-10-r80 (2004).

16. Happe H. et al. Toxic tubular injury in kidneys from Pkd1-deletion mice accelerates cystogenesis accompanied by dysregulated planar cell polarity and canonical Wnt signaling pathways. Hum Mol Genet 18: 2532-2542, doi:10.1093/hmg/ddp190 (2009).

17. Hassane, S. et al. Elevated TGFbeta-Smad signalling in experimental Pkd1 models and human patients with polycystic kidney disease. J Pathol 222: 21-31, doi:10.1002/path.2734 (2010).

17a. Hettne, K.M. et al. Explain your data by Concept Profile Analysis Web Services [version1; referees: 2 approved with reservations]. F1000 Res 3: 173, doi:10.12688/f1000research.4830.1 (2014).

18. Huang, W. et al. Bioinformatics enrichment tools: paths toward the comprehensive functional analysis of large gene lists. Nucleic Acids Res 37: 1-13, doi:10.1093/nar/gkn923 (2009).

19. Huang, W. et al. Systematic and integrative analysis of large gene lists using DAVID bioinformatics resources. Nat Protoc 4: 44-57, doi:10.1038/nprot.2008.211 (2009).

20. Husson, H. et al. New insights into ADPKD molecular pathways using combination of SAGE and microarray technologies. Genomics 84: 497-510, doi:10.1016/j.ygeno.2004.03.009 (2004).

21. Jelier, R. et al. Anni 2.0: a multipurpose text-mining tool for the life sciences. Genome Biol 9: R96, doi:10.1186/gb-2008-9-6-r96 (2008).

22. Kang, HS. et al. Gli-similar (Glis) Kruppel-like zinc finger proteins: insights into their physiological functions and critical roles in neonatal diabetes and cystic renal disease. Histol Histopathol 25: 1481-1496, doi:10.14670/HH-25.1481 (2010).

23. Kauffmann, A. et al. Importing ArrayExpress datasets into R/Bioconductor. Bioinformatics 25: 2092-2094, doi:10.1093/bioinformatics/btp354 (2009).

24. Kennefick, T.M. et al. Hypertension and renal injury in experimental polycystic kidney disease. Kidney Int 56: 2181-2190, doi:10.1046/j.1523-1755.1999.00783.x (1999).

25. Kim, D. et al. TopHat2: accurate alignment of transcriptomes in the presence of insertions, deletions and gene fusions. Genome Biol 14: R36, doi:10.1186/gb-2013-14-4-r36 (2013).

26. Kim, Y.S. et al. Kruppel-like zinc finger protein Glis2 is essential for the maintenance of normal renal functions. Mol Cell Biol 28: 2358-2367, doi:10.1128/MCB.01722-07 (2008).

27. Kolesnikov, N. et al. ArrayExpress update--simplifying data submissions. Nucleic Acids Res 43: D1113-1116, doi:10.1093/nar/gku1057 (2015).

28. Krishnamoorthy, A. et al. Fibrinogen beta-derived Bbeta(15-42) peptide protects against kidney ischemia/reperfusion injury. Blood 118: 1934-1942, doi:10.1182/blood-2011-02-338061 (2011).

30. Kugita, M. et al. Global gene expression profiling in early-stage polycystic kidney disease in the Han:SPRD Cy rat identifies a role for RXR signaling. Am J Physiol Renal Physiol 300: F177-188, doi:10.1152/ajprenal.00470.2010 (2011).

31. Langmead, B. & Salzberg, S.L. Fast gapped-read alignment with Bowtie 2. Nat Methods 9: 357-359, doi:10.1038/nmeth.1923 (2012)

32. Lantinga-van Leeuwen, I.S. et al. Kidney-specific inactivation of the Pkd1 gene induces rapid cyst formation in developing kidneys and a slow onset of disease in adult mice. Hum Mol Genet 16: 3188-3196, doi:10.1093/hmg/ddm299 (2007).

33. Leonhard, W.N. et al. Scattered Deletion of PKD1 in Kidneys Causes a Cystic Snowball Effect and Recapitulates Polycystic Kidney Disease. J Am Soc Nephrol 26: 1322-1333, doi:10.1681/ASN.2013080864 (2015).

34. Liberzon, A. et al. The Molecular Signatures Database (MSigDB) hallmark gene set collection. Cell Syst 1: 417-425, doi:10.1016/j.cels.2015.12.004 (2015).

35. Liu, J. et al. Cell-specific translational profiling in acute kidney injury. J Clin Invest 124: 1242-1254, doi:10.1172/JCI72126 (2014).

36. Masola, V. et al. Heparanase and syndecan-1 interplay orchestrates fibroblast growth factor-2-induced epithelial-mesenchymal transition in renal tubular cells. J Biol Chem 287: 1478-1488, doi:10.1074/jbc.M111.279836 (2012).

37. Menezes, L.F. & Germino, G.G. Systems biology of polycystic kidney disease: a critical review. Wiley Interdiscip Rev Syst Biol Med 7: 39-52, doi:10.1002/wsbm.1289 (2015).

38. Menezes, L.F. et al. Fatty Acid Oxidation is Impaired in An Orthologous Mouse Model of Autosomal Dominant Polycystic Kidney Disease. EBioMedicine 5: 183-192, doi:10.1016/j.ebiom.2016.01.027 (2016).

39. Menezes, L.F. et al. Network analysis of a Pkd1-mouse model of autosomal dominant polycystic kidney disease identifies HNF4alpha as a disease modifier. PLoS Genet 8: e1003053, doi:10.1371/journal.pgen.1003053 (2012).

40. Mochizuki, T. et al. PKD2, a gene for polycystic kidney disease that encodes an integral membrane protein. Science 272: 1339-1342, doi:10.1126/science.272.5266.1339 (1996).

41. Mudunuri, U. et al. bioDBnet: the biological database network. Bioinformatics 25: 555-556, doi:10.1093/bioinformatics/btn654 (2009).

42. Novalic, Z. et al. Dose-dependent effects of sirolimus on mTOR signaling and polycystic kidney disease. J Am Soc Nephrol 23: 842-853, doi:10.1681/ASN.2011040340 (2012).

43. O'Meara, C.C. et al. Role of genetic modifiers in an orthologous rat model of ARPKD. Physiol Genomics 44: 741-753, doi:10.1152/physiolgenomics.00187.2011 (2012).

44. Pandey, P. et al. Systems biology approach to identify transcriptome reprogramming and candidate microRNA targets during the progression of polycystic kidney disease. BMC Syst Biol 5: 56, doi:10.1186/1752-0509-5-56 (2011).

45. Park, E.Y. et al. Effects of specific genes activating RAGE on polycystic kidney disease. Am J Nephrol 32: 169-178, doi:10.1159/000315859 (2010).

46. Park, J.Y. et al. p21 is decreased in polycystic kidney disease and leads to increased epithelial cell cycle progression: roscovitine augments p21 levels. BMC Nephrol 8: 12, doi:10.1186/1471-2369-8-12 (2007).

47. Patel, V. et al. Acute kidney injury and aberrant planar cell polarity induce cyst formation in mice lacking renal cilia. Hum Mol Genet 17: 1578-1590, doi:10.1093/hmg/ddn045 (2008).

48. Pichler, R.H. et al. SPARC is expressed in renal interstitial fibrosis and in renal vascular injury. Kidney Int 50: 1978-1989, doi:10.1038/ki.1996.520 (1996).

49. Pollard, P.J. et al. Targeted inactivation of fh1 causes proliferative renal cyst development and activation of the hypoxia pathway. Cancer Cell 11: 311-319, doi:10.1016/j.ccr.2007.02.005 (2007).

50. Ricardo, S.D. et al. Macrophage diversity in renal injury and repair. J Clin Invest 118: 3522-3530, doi:10.1172/JCI36150 (2008).

51. Riera, M. et al. Transcriptome analysis of a rat PKD model: Importance of genes involved in extracellular matrix metabolism. Kidney Int 69: 1558-1563, doi:10.1038/sj.ki.5000309 (2006).

52. Ritchie, M.E. et al. limma powers differential expression analyses for RNA-sequencing and microarray studies. Nucleic Acids Res 43: e47, doi:10.1093/nar/gkv007 (2015).

53. Rowe, I. et al. Defective glucose metabolism in polycystic kidney disease identifies a new therapeutic strategy. Nat Med 19: 488-493, doi:10.1038/nm.3092 (2013).

54. Schieren, G. et al. Gene profiling of polycystic kidneys. Nephrol Dial Transplant 21: 1816-1824, doi:10.1093/ndt/gfl071 (2006).

55. Shillingford, J.M. et al. The mTOR pathway is regulated by polycystin-1, and its inhibition reverses renal cystogenesis in polycystic kidney disease. Proc Natl Acad Sci USA 103: 5466-5471, doi:10.1073/pnas.0509694103 (2006).

56. Song, X. et al. Systems biology of autosomal dominant polycystic kidney disease (ADPKD): computational identification of gene expression pathways and integrated regulatory networks. Hum Mol Genet 18: 2328-2343, doi:10.1093/hmg/ddp165 (2009).

57. Speir, R.W. et al. Effects of valproic acid and dexamethasone administration on early bio-markers and gene expression profile in acute kidney ischemia-reperfusion injury in the rat. PLoS One 10: e0126622, doi:10.1371/journal.pone.0126622 (2015).

58. Subramanian, A. et al. GSEA-P: a desktop application for Gene Set Enrichment Analysis. Bioinformatics 23: 3251-3253, doi:10.1093/bioinformatics/btm369 (2007).

59. Subramanian, A. et al. Gene set enrichment analysis: a knowledge-based approach for interpreting genome-wide expression profiles. Proc Natl Acad Sci USA 102: 15545-15550, doi:10.1073/pnas.0506580102 (2005).

60. Swenson-Fields, K.I. et al. Macrophages promote polycystic kidney disease progression. Kidney Int 83: 855-864, doi:10.1038/ki.2012.446 (2013).

61. Ta, M.H. et al. Role of interstitial inflammation in the pathogenesis of polycystic kidney disease. Nephrology (Carlton) 18: 317-330, doi:10.1111/nep.12045 (2013).

62. Takakura, A. et al. Renal injury is a third hit promoting rapid development of adult polycystic kidney disease. Hum Mol Genet 18: 2523-2531, doi:10.1093/hmg/ddp147 (2009).

63. Tamura, K. et al. Gene expression analysis detected a low expression level of C1s gene in ICR-derived glomerulonephritis (ICGN) mice. Nephron Exp Nephrol 123: 34-45, doi:10.1159/000354057 (2013).

64. Terryn, S. et al. Fluid transport and cystogenesis in autosomal dominant polycystic kidney disease. Biochim Biophys Acta 1812: 1314-1321, doi:10.1016/j.bbadis.2011.01.011 (2011).

65. Torres, V.E. et al. Tolvaptan in patients with autosomal dominant polycystic kidney disease. N Engl J Med 367: 2407-2418, doi:10.1056/NEJMoa1205511 (2012).

66. Vaidya, V.S. et al. Biomarkers of acute kidney injury. Annual review of pharmacology and toxicology 48: 463-493, doi:10.1146/annurev.pharmtox.48.113006.094615 (2008).

67. Ward, C.J. et al. The gene mutated in autosomal recessive polycystic kidney disease encodes a large, receptor-like protein. Nat Genet 30: 259-269, doi:10.1038/ng833 (2002).

68. Waterston, R.H. et al. Initial sequencing and comparative analysis of the mouse genome. Nature 420: 520-562, doi:10.1038/nature01262 (2002).

70. Weimbs, T. Polycystic kidney disease and renal injury repair: common pathways, fluid flow, and the function of polycystin-1. Am J Physiol Renal Physiol 293: F1423-1432, doi:10.1152/ajprenal.00275.2007 (2007).

71. Wilson, P.D. et al. Aberrant epithelial cell growth in autosomal dominant polycystic kidney disease. Am

J Kidney Dis 17: 634-637, doi:10.1016/S0272-6386(12)80338-6 (1991).

72. Yang, L. et al. Inflammatory gene expression in OVE26 diabetic kidney during the development of nephropathy. Nephron Exp Nephrol 119: e8-20, doi:10.1159/000324407 (2011).

73. Yuen, P.S. et al. Ischemic and nephrotoxic acute renal failure are distinguished by their broad transcriptomic responses. Physiol Genomics 25: 375-386, doi:10.1152/physiolgenomics.00223.2005 (2006).

Supplementary Materials can be downloaded from

https://journals.physiology.org/doi/suppl/10.1152/ajprenal.00653.2016

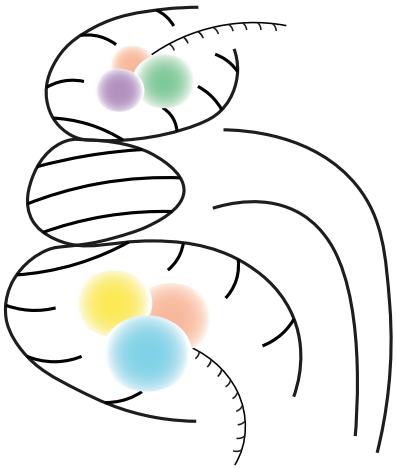

CHAPTER 5

Characterisation of Transcription Factor profiles in Polycystic Kidney Disease (PKD): identification and validation of STAT3 and RUNX1 in the injury/repair response and PKD progression

Chiara Formica[1]*, Tareq Malas[1]*, Judit Balog[1], Lotte Verburg[2], Peter A.C. 't Hoen[1,3], Dorien J.M. Peters[1]

[1]Department of Human Genetics, Leiden University Medical Center, The Netherlands

[2]Department of Pathology, Leiden University Medical Center, The Netherlands

[3]Current address: Centre for Molecular and Biomolecular Informatics, Radboud University Medical Center Nijmegen, The Netherlands

* Authors contributed equally

J Mol Med 2019 Dec;97(12):1643-1656

Abstract

Autosomal Dominant Polycystic Kidney Disease (ADPKD) is the most common genetic renal disease, caused in the majority of the cases by a mutation in either the *PKD1* or the *PKD2* gene. ADPKD is characterised by a progressive increase in the number and size of cysts, together with fibrosis and distortion of the renal architecture, over the years. This is accompanied by alterations in a complex network of signalling pathways. However, the underlying molecular mechanisms are not well characterised. Previously, we defined the PKD Signature, a set of genes typically dysregulated in PKD across different disease models from a meta-analysis of expression profiles. Given the importance of transcription factors (TFs) in modulating disease, we focused in this paper on characterising TFs from the PKD Signature. Our results revealed that out of the 1515 genes in the PKD Signature, 92 were TFs with altered expression in PKD and 32 of those were also implicated in tissue injury/repair mechanisms. Validating the dysregulation of these TFs by qPCR in independent PKD and injury models largely confirmed these findings. STAT3 and RUNX1 displayed the strongest activation in cystic kidneys, as demonstrated by chromatin immunoprecipitation (ChIP) followed by qPCR. Using immunohistochemistry, we showed a dramatic increase of expression after renal injury in mice and cystic renal tissue of mice and humans. Our results suggest a role for STAT3 and RUNX1 and their downstream targets in the aetiology of ADPKD and indicate that the meta-analysis approach is a viable strategy for new target discovery in PKD.

Key messages

- We identified a list of transcription factors (TFs) commonly dysregulated in ADPKD
- Out of the 92 TFs identified in the PKD Signature, 35% are also involved in injury/repair processes
- STAT3 and RUNX1 are the most significantly dysregulated TFs after injury and during PKD progression
- STAT3 and RUNX1 activity is increased in cystic compared to non-cystic mouse kidneys
- Increased expression of STAT3 and RUNX1 is observed in the nuclei of renal epithelial cells, also in human ADPKD samples

Introduction

Autosomal Dominant Polycystic Kidney Disease (ADPKD) is a genetic disease characterised by the formation of fluid-filled renal cysts. Cyst formation and cyst growth are accompanied by inflammation and fibrosis, leading to kidney failure. In the majority of cases, ADPKD is caused by a mutation in the *PKD1* gene or, less frequently, in the *PKD2* gene. Nevertheless, ADPKD is a complex disease which involves the dysregulation of many different signalling pathways[1], and the molecular mechanisms involved in disease progression are not entirely understood. Currently, the vasopressin V2 receptor antagonist, tolvaptan, is the only approved treatment in Europe but only for selected patients. More generic and definitive treatment is still missing.

Both environmental and genetic factors can be considered disease modifiers in ADPKD[1,2]. An important one is renal injury, shown to accelerate cyst formation and expansion in different mouse models[3,4]. Recently, we showed that renal injury shares molecular processes with ADPKD progression. Using a meta-analysis approach, we identified a set of genes dysregulated in a variety of PKD models during disease progression, which we called the "PKD Signature". About 35% of these genes were found to be also implicated in injury/repair mechanisms, confirming the strong relation between ADPKD and injury[5].

Transcription factor proteins (TFs) are master regulators of transcription, which control the expression of genes involved in the establishment and maintenance of cell states, in physiological and pathological situations. Dysregulation of TFs levels and/or activity can lead to the development of a broad range of diseases. Thus, identification of a TFs profile in ADPKD could help to better understand the molecular mechanisms contributing to cyst formation. For this reason, in this study we focus on the signature of TFs. We identified new PKD-related TFs, and we validated altered expression during ADPKD progression and injury/repair in different mouse models. For two of the identified TFs, STAT3 and RUNX1, we also showed increased activity in mouse cystic kidneys, as well as altered expression in human ADPKD kidneys.

Materials and Methods

Identification of Transcription Factors in PKD

Identification of the PKD Signature was described previously[5]. Briefly, in the previous work we performed a meta-analysis of PKD expression profiles across different disease models and identified 1515 genes that showed consistent dysregulation across the different PKD studies. We further identified genes involved in injury/repair processes from the PKD Signature by firstly producing Injury Repair gene profile based on several injury-induced animal models and secondly intersecting the identified PKD Signature and Injury Repair Profiles for the identification of overlapping genes.

In this publication, we used MSigDB's collection of TFs based on Messina *et al.*[6] and Moreland *et al*[7] for the identification of TFs involved in PKD. Furthermore, we identified the transcription factors that are involved in the injury/repair processes of PKD based on the previously identified Injury Repair Profile[5].

The enrichment of TF targets in the PKD Signature was based on the target collections in the ChEA 2016 database[8] that includes TF targets based on experimental evidence. We calculated the enrichment using the representation factor method described below. TFs are considered enriched if they had a representation factor above 1. The representation factor is the number of overlapping genes divided by the expected number of overlapping genes drawn from two independent groups. A representation factor > 1 indicates more overlap than expected of two independent groups, and a representation factor < 1 indicates less overlap than expected. The formula used to calculate the representation factor is: x / (n * D) / N, where x = # of genes in common between two groups; n = # of genes in group 1 (the total number of targets calculated per transcription factor based on ChEA 2016 database); D = # of genes in group 2 (the total number of genes in the PKD Signature up (775) or down (740) regulated lists independently); N = total genes, in this case, the 10271 genes with Entrez IDs.

In silico functional annotation of gene lists

GeneTrail2 v1.6[9] was used to identify the enriched/significant pathways/functions of the identified gene lists. For all analyses, we used Wikipathways as the primary source of annotation. GeneTrail2 v1.6 was run with the following parameters: Over-representation analysis (enrichment algorithm); FDR adjustment (adjustment method); significance level at 0.05; minimum and maximum size of the category equal to 2 and 700 respectively.

Gene expression and statistical analysis of the significance of results

Snap-frozen mouse kidneys were homogenised using Magnalyser technology (Roche). Total RNA was isolated using Tri-Reagent (Sigma-Aldrich). cDNA synthesis was performed using Transcriptor First Strand cDNA Synthesis Kit (Roche), and qPCR was done using 2× FastStart

SYBR-Green Master (Roche) according to the manufacturer's protocol. Alternatively, it was performed at GenomeScan (GenomeScan B.V.) using the 96.96 BioMark™ Dynamic Array for Real-Time PCR (Fluidigm Corporation), as previously described[5]. Gene expression was normalised to the geometric mean of three housekeeping genes (*Rplp0, Hnrnpa2b1, Ywhaz*) for Fluidigm data and *Hprt* for SYBR-Green data. The output of the Fluidigm assay was normalised and converted into Ct values (cycle threshold). For each transcription factor, a two-way ANOVA was conducted to compare the genotype (PKD vs WT) and the treatment (PBS vs DCVC) effects for each age-matched time points. The computation was made using the *Limma package*[10] in R. A list of primer sequences and TaqMan assays can be found in Supplementary Table 3.

Identification of Transcription Factors Binding Sites and primer design

For the TFs that were selected for our ChIP analysis, we identified the binding sites of each TF and its targets by screening the Cistrome database[11] and accessing all studies that performed ChIP-Seq experiments on our selected TFs. We looked for peaks that appeared with an intensity of 10 or higher in more than one ChIP-Seq study. We mapped the *Mus musculus* mm10 genome to the peaks identified using *Peak2Gene* tool that is part of the Cistrome Galaxy tools to identify genes that are within 10000 base pairs of both ends of the peak. The peaks that did not map to a gene target that is part of the PKD Signature were eliminated. Finally, sorting on the intensity level of the peak, we visualised the top peaks on the UCSC Genome Browser[12] and selected the peaks that had sufficient height over noise levels for qPCR enrichment. We designed primers spanning the TFs binding sites on their putative target genes. The binding sites were generally overlapping with the promoter region of the target genes. As a negative control, we designed primers binding at about 5kb from the promoter regions where we did not expect to find any TF binding activity. A list of primers can be found in Supplementary Table 3. Two-way ANOVA with Tukey's multiple comparisons test was performed comparing the input-normalised binding-enrichment of the TFs or the control IgG at the binding site and at the non-binding sites.

Animal Model

All the animal experiments were evaluated and approved by the local animal experimental committee of the Leiden University Medical Center (LUMC) and the Commission Biotechnology in Animals of the Dutch Ministry of Agriculture. Kidney-specific tamoxifen-inducible *Pkd1*-deletion mouse model (iKsp*Pkd1*^{del}) have been described previously[13]. We only used male mice, to reduce variability in disease progression as female mice tend to have a slower and milder progression of the disease compared to male mice[14]. Wt mice have only the LoxP sites around exons 2-11 of the *Pkd1* gene but not the Cre recombinase (*Pkd1*^{loxlox}). For three consecutive days, 5 mg/kg of tamoxifen was administered via oral gavage when mice were 13-14 weeks old. Inactivation of the *Pkd1* gene at this age leads to cyst formation

in all the renal tubule segments. A week later mice were injected intraperitoneally with 15 mg/kg of the nephrotoxic compound S-(1,2-dichlorovinyl)-L-cysteine (DCVC) or vehicle (PBS) as a control. Kidney function was evaluated using blood urea nitrogen level (BUN) as previously described[4]. Renal failure is defined by BUN equal or higher than 25mmol/l. Mice were sacrificed at 1, 2, 5 and 10 weeks after DCVC and kidney failure. The experimental pipeline has been presented in Formica *et al.*[15]. The Wt + PBS, Wt + DCVC and *Pkd1* KO + PBS groups have also been used in Malas *et al.*[5]. At the sacrifice, kidneys were collected and weighed. For RNA and chromatin extraction, kidneys were snap-frozen in liquid nitrogen. For immunohistochemistry (IHC) staining, kidneys were preserved in phosphate-buffered 4% formaldehyde solution. A *t*-test was conducted to compare median survival in PBS treated versus DCVC treated mice and BUN in Wt versus iKsp*Pkd1*^{del} mice.

ChIP

Chromatin was isolated from mouse inner medulla collecting duct (mIMCD3; ATCC, Rockville, USA) cells (about 5 X 10^6/ml). Briefly, cells were crosslinked with 1% formaldehyde for 10 minutes at RT, then lysed with buffer with protease and phosphatase inhibitors (Roche) as described on Nature Protocols (ChIP buffer)[16].

For kidneys chromatin extraction, snap-frozen kidneys, harvested at end-stage renal disease (ESRD) from Wt mice and iKsp*Pkd1*^{del} mice treated with DCVC or PBS, were cut with a blade in a petri dish then fixed with 1% formalin (50 mg/ml) rocking for 12 minutes at RT. Glycine (0.125M) was added to stop the reaction, and the tissue was washed with PBS with serine protease inhibitor phenylmethylsulfonyl fluoride (PMSF). The tissue was resuspended in cytoplasmic lysis buffer and moved in a glass tissue grinder (Kimble Chase) for homogenisation and then filtered using a 50 µm filter (CellTrics® Sysmex). The homogenate was washed and then lysed with ChIP buffer with protease and phosphatase inhibitors. Chromatin was sonicated in ChIP buffer using a Diagenode Bioruptor® Pico (Diagenode) 30 sec on/30 sec off for 15 cycles. Fragment size was checked by gel electrophoresis.

For immunoprecipitation 60 µg of chromatin were used per reaction. Sepharose protein A alone or mixed 4:1 with protein G (GE Healthcare) were used to preclear the chromatin before incubation with primary antibodies for 4h at 4°C. Primary antibodies used: 5 µg rabbit anti-pSTAT3 (Cell Signaling #9145); 8 µg mouse anti-RUNX1 (Santa Cruz Biotechnology, Inc. #sc-365644); rabbit anti-IgG (Abcam #ab37415); mouse anti-IgG (Cell Signaling #5415S).

20 µl of Sepharose protein A (for pSTAT3) or A/G 4:1 (for RUNX1) were added to each sample and incubated overnight at 4°C. Samples were collected by centrifugation and washed with low salt wash buffer (150mM NaCl, 20mM Tris-HCl pH 8.1, 2mM EDTA, 0.1% SDS, 1% Triton X-100), high salt wash buffer (500mM NaCl, 20mM Tris-HCl pH 8.1, 2mM EDTA, 0.1% SDS, 1% Triton X-100), LiCl wash buffer (10mM Tris-HCl pH 8.1, 1mM EDTA, 0.25M LiCl, 1% NP-40, 1% sodium deoxycholate) and twice with TE wash buffer (10mM Tris-HCl pH 8.1, 1mM EDTA). Cross-links were reversed incubating with Chelex®100 resin beads (Bio-Rad #142-1253) at

99°C for 15 minutes on a shaking block, and then the samples were diluted 1:1 with MQ water.

IHC

Kidneys fixed in formalin and embedded in paraffin were cut at 4 µm thickness. Sections were stained with the primary antibodies used for ChIP: rabbit anti-pSTAT3 (1:75; Cell Signaling #9145); mouse anti-RUNX1 (1:250; Santa Cruz Biotechnology, Inc. #sc-365644). Anti-rabbit or anti-mouse Envision HRP (Dako) was used as the secondary antibody.

Renal tissue from ADPKD patients at end-stage renal failure was fixed in formalin as previously described[15]. Control tissues were obtained from donor kidneys non-suitable for transplant. All human tissue samples were collected following procedures approved by the LUMC medical ethical committee (institutional review board).

Results

Transcription Factors in the PKD Signature

Using a meta-analysis approach of published PKD expression profiles and in-house generated RNA-sequencing data on our *Pkd1* mutant mouse model (iKsp*Pkd1*^{del}) we recently identified 1515 genes that are commonly dysregulated across several PKD disease models, hereafter referred to as the PKD Signature[5].

We used MSigDB to identify the TFs that are part of the PKD Signature (Figure 1a). Out of the 1515 genes of the PKD Signature, we identified 92 TFs that were differentially expressed and could be involved in cyst formation and PKD development. Among the 92 TFs identified, 32 were also implicated in tissue injury/repair mechanisms based on our previously defined Injury Repair Profile (Supplementary Table 1)[5]. Several of the herein identified TFs, such as STAT3 and MYC are known players in ADPKD progression[17,18]. Nevertheless, many others have never been described in ADPKD before.

Furthermore, we predicted TFs that are relevant to PKD based on the enrichment of their targets in the PKD Signature. Using the ChEA 2016 database of TF targets, we identified TFs with more experimentally-verified targets (ChIP-chip or ChIP-Seq) overlapping with the PKD Signature than would be expected by chance (Figure 1a). The TFs E2F7, TRIM28, TP63 (two different experiments in different cell lines), EGR1 and STAT3 were most significant in this analysis (Supplementary Table 2a) since targets of these TFs were mostly upregulated in PKD. Five TFs were both in the list of TFs identified based on their targets and among the 92 TFs present in the PKD Signature: EGR1, ESR1, STAT3, FOXM1 and KLF5. Thus, these TFs, as well as their identified direct targets, were dysregulated in PKD (Supplementary Table 2b). Further pathway analysis of these five TFs targets uncovered involvement in the modulation of TGF-β signalling, estrogen signalling, apoptosis, oxidative stress, interleukins signalling, adipogenesis and cellular metabolism (Supplementary Table 2c).

Validation of meta-analysis in independent samples

Our next step was to validate TFs identified in the meta-analysis in independent experimental groups of mice during PKD progression and/or the nephrotoxic injury/repair response[15]. Briefly, we induced *Pkd1* deletion in adult mice via tamoxifen administration, which leads to a slow progression of the disease. Wild-type (Wt) mice received tamoxifen as well. A week after tamoxifen administration, we injected both genotypes with 15 mg/kg of DCVC, a nephrotoxic compound, or PBS as a control. At this dosage, DCVC causes a repairable renal injury that is mostly recovered 1 to 2 weeks after injection but accelerates cyst formation resulting in tubular dilations at 10 weeks and renal failure around 14 weeks of age (Supplementary Figure 1). Mice were sacrificed at 1, 2, 5 and 10 weeks after DCVC and at kidney failure. Kidneys harvested at these time points were used to evaluate gene expression of selected TF using the Fluidigm qPCR chip (Figure 1b).

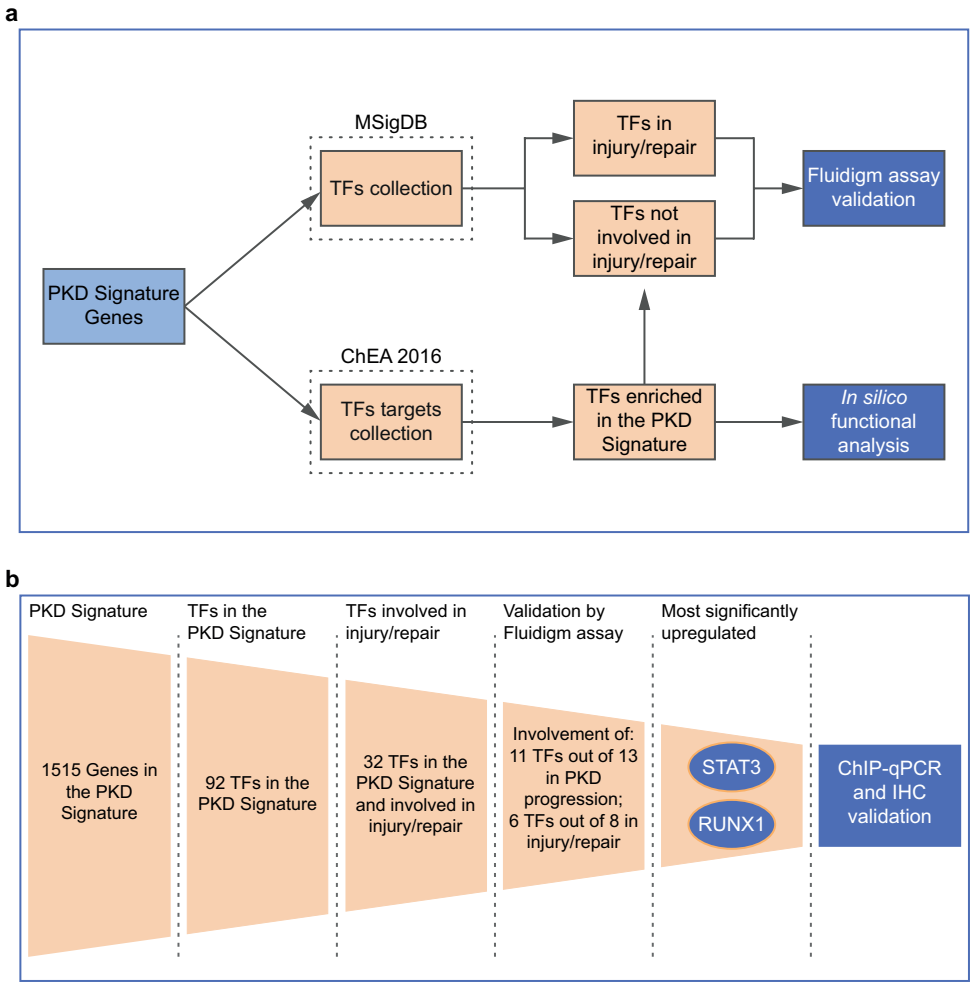

Figure 1. Schematic representation of the workflow used for the identification and validation of TFs involved in PKD and injury/repair

(a) MSigDB was used to select the TFs in the PKD Signature. ChEA 2016 was used to select the TFs with most dysregulated, experimentally-verified targets in the PKD Signature (Note: the ChIP-chip and ChIP-Seq experiments in ChEA 2016 were typically from cell lines not necessarily related to the kidney). The TFs identified with MSigDB in the PKD Signature were intersected with the Injury Signature generated in our previous work[5] to obtain TFs involved in injury/repair mechanisms, and TFs involved only in PKD progression. Fluidigm assay was used to validate the expression of selected TFs identified by this analysis. The TFs identified based on their target genes using the ChEA 2016 database were intersected with the TFs identified in the PKD signature to identify the overlapping TFs. *In silico* pathway analysis was performed on the overlapping TFs and their target genes to identify significant pathways modulated by the TFs. **(b)** Schematic representation of the workflow used to identify and validate selected TFs. The two most significant TFs identified were STAT3 and RUNX1 which were further investigated in cystic kidneys using chromatin immunoprecipitation-qPCR (ChIP-qPCR) and immunohistochemistry (IHC)

Out of the 92 TFs, 13 were selected for further analysis, based on transcript levels, altered expression in the injury/repair response and involvement in multiple molecular pathways

(Supplementary Table 1). In our Fluidigm setup, we had four groups: PBS treated Wt, DCVC treated Wt, PBS treated iKsp*Pkd1*^{del}, and DCVC treated iKsp*Pkd1*^{del} at five time points (1 wk, 2 wks, 5 wks and 10 wks after DCVC treatment and at kidney failure). Out of the 13 tested TFs, 11 were significantly different ($P < 0.05$) in PKD samples compared to Wt, while the involvement of *Irf6* and *JunB* could not be confirmed (Supplementary Table 1, Figure 2). We also evaluated whether expression of the 13 TFs was affected by injury, by comparing DCVC versus PBS treated animals at injury-related timepoints (1 wk, 2 wks and 5 wks after DCVC treatment). Of the 13 selected TFs, 8 were part of the previously reported Injury Repair profile, while 5 were not[5]. We confirmed significant injury-induced dysregulation ($P < 0.05$) of 6 out of 8 TFs predicted to be involved in the injury/repair mechanism by the meta-analysis, while we did not see any significant dysregulation of the expression of 3 out of 5 TFs that were not found in the meta-analysis (Supplementary Table 1, Figure 2)[5]. Notably, the expression of *Runx1* and *Stat3* was most significantly affected by DCVC-induced injury and PKD progression.

Expression of two selected TFs in mouse kidneys during ADPKD progression and after injury

To further support the utility of meta-analysis approaches to new target discovery in ADPKD, we chose STAT3 and RUNX1 for additional experimental validation.

We performed immunohistochemical analysis for the active form of STAT3 (pSTAT3) and RUNX1, and studied activation and subcellular localisation. In non-injured Wt and iKsp*Pkd1*^{del} mice, pSTAT3 and RUNX1 are not detectable, except for some interstitial cells that show nuclear staining. Interestingly, after injury (at 1 wk after DCVC) there was an intense nuclear expression of pSTAT3 and RUNX1 in both Wt and iKsp*Pkd1*^{del} mice (Figure 3a and Supplementary Figure 2a).

At 10 weeks post-DCVC, Wt mice have fully healed the renal damage and have largely pSTAT3 and RUNX1 negative kidneys, comparable to the Wt treated with PBS. Conversely, iKsp*Pkd1*^{del} mice, which already developed some mild cysts at this time-point, showed expression of pSTAT3 and RUNX1 in the cyst-lining epithelial cells and some of the surrounding dilated tubules (Figure 3b, middle panel and Supplementary Figure 2b, middle panel). iKsp*Pkd1*^{del} mice treated with PBS, instead, have not undergone injury/repair phase nor displayed overt cyst formation at this time-point, and showed almost no expression of pSTAT3 and RUNX1, as expected.

At kidney failure, iKsp*Pkd1*^{del} mice present severe renal degeneration and cyst formation. At this time-point, the expression of pSTAT3 and RUNX1 is markedly increased (Figure 3b, right panel and Supplementary Figure 2b, right panel). Interestingly, not only epithelial cells, but also infiltrating cells stained positive for these TFs, suggesting that pSTAT3 and RUNX1 might be important in the regulation of signalling pathways in other cell types in addition to tubular epithelial cells (Figure 3b, arrowheads).

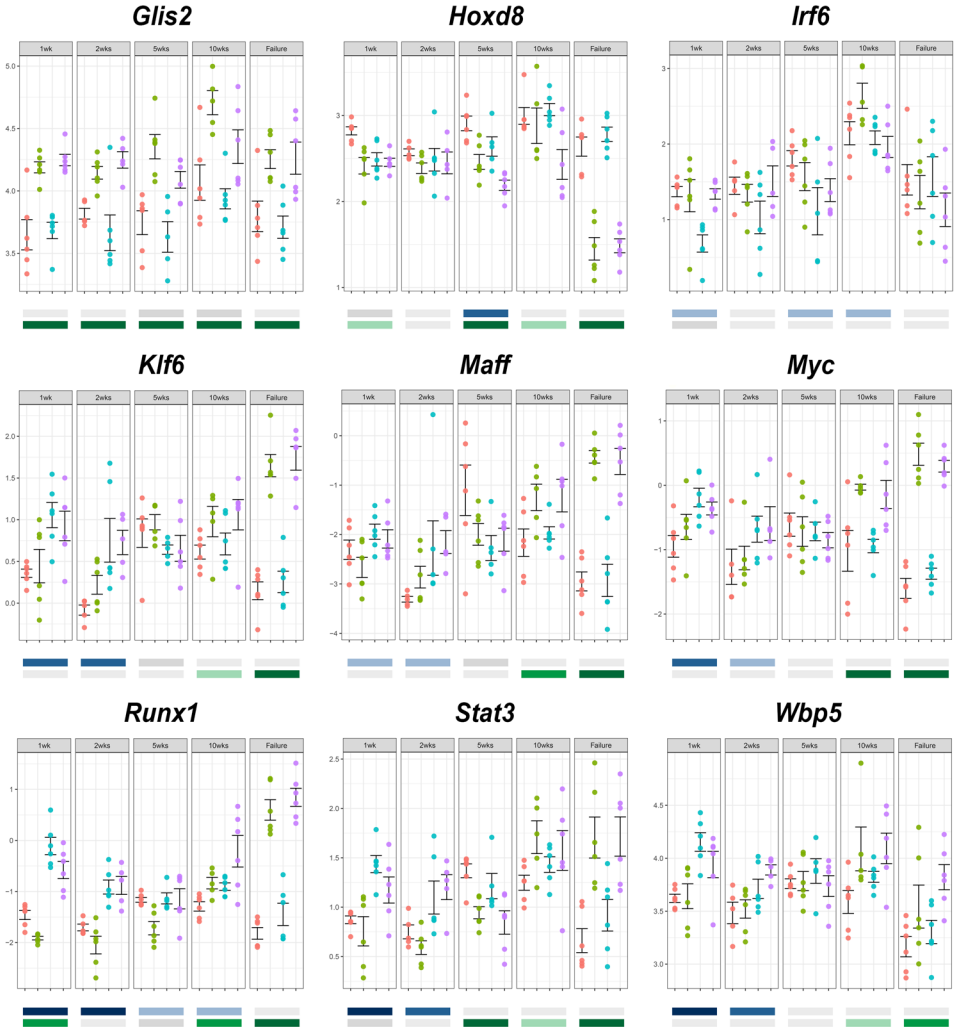

Figure 2. Expression of selected TFs using Fluidigm assay

TFs selected from the PKD Signature for experimental validation were subjected to qRT-PCR on RNA isolated from the kidneys of iKsp*Pkd1*^{del} mice, and age-matched Wt mice at 1, 2, 5, 10 weeks after DCVC and at kidney failure. On the Y-axis normalized Ct values (cycle threshold values) are plotted for each gene separately across the five measurement time points for four types of samples: Wt mice treated with saline (Wt PBS, salmon), iKsp*Pkd1*^{del} mice treated with saline (iKsp*Pkd1*^{del} PBS, light green), Wt mice treated with DCVC (Wt DCVC, light blue), and iKsp*Pkd1*^{del} mice treated with DCVC (iKsp*Pkd1*^{del} DCVC, light purple). The analysis was based on comparing Treatment (DCVC vs PBS) and Genotype (iKsp*Pkd1*^{del} vs Wt) using a two-way ANOVA test. The resulting P values are shown with colour codes: darkest colour shade, P value < 0.0005; medium colour shade, P value < 0.005 and low colour shade at P value < 0.05. P value ≥ 0.05 were not considered significant (grey bars). Each dot is a mouse and whiskers reflect the mean ± SD. Expression of *Glis2* and *Stat3* in Wt PBS, iKsp*Pkd1*^{del} PBS and Wt DCVC have been published in Malas *et al.* (2017)[5].

In summary, we confirmed that pSTAT3 and RUNX1 protein expression were increased in the nuclei of tubular epithelial cells after injury and during PKD progression.

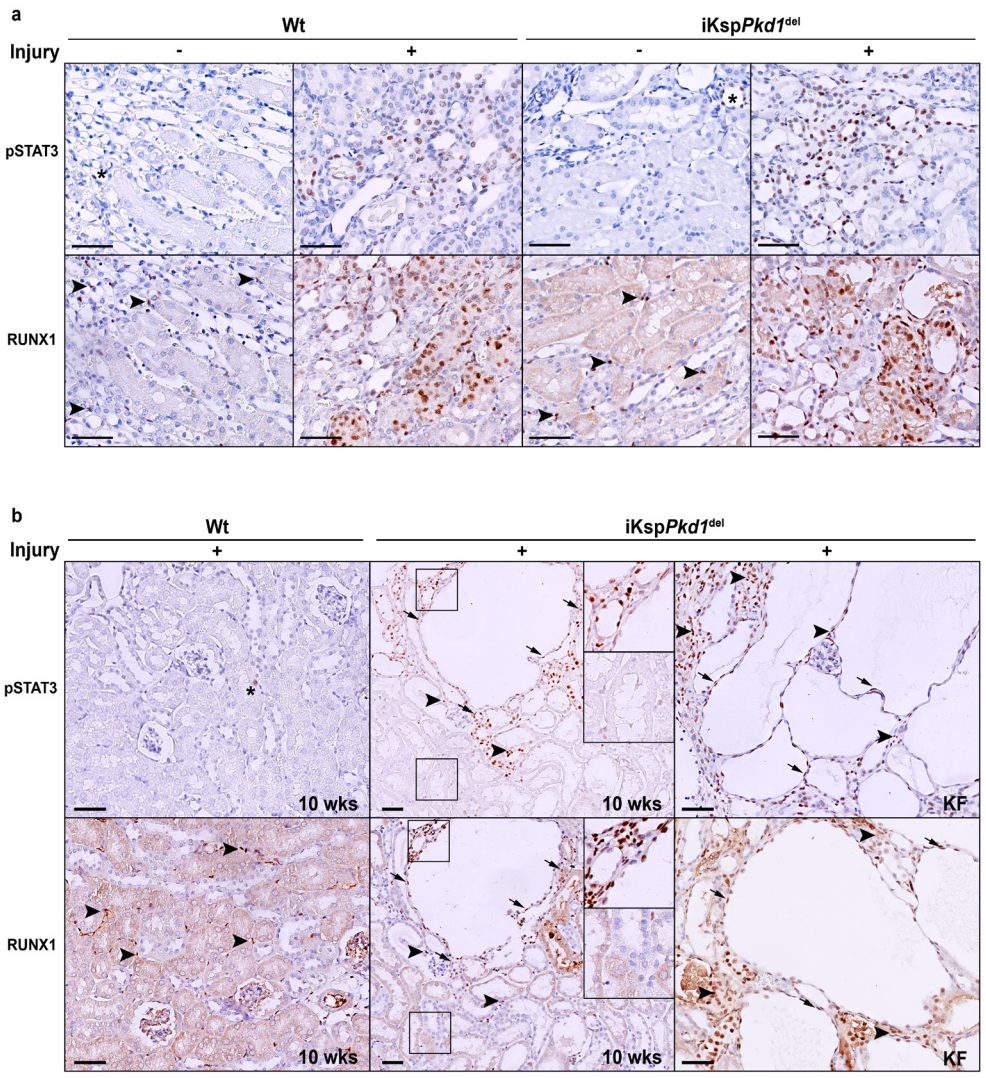

Figure 3. Expression of pSTAT3 and RUNX1 in Wt and iKsp*Pkd1*^{del} mice after injury and during cyst progression

(a) Representative immunohistochemistry of Wt and iKsp*Pkd1*^{del} kidneys at 1 week after DCVC (+ injury) or PBS (- injury). Mice without injury showed only sporadic expression of pSTAT3 in the nuclei of tubular epithelial cells (asterisks); after injury, the expression was markedly increased both in Wt mice and in iKsp*Pkd1*^{del} mice. RUNX1 expression in non-injured kidney was present only in some interstitial cells (arrowheads); after injury, RUNX1 was visible in the nuclei of the epithelial cells. **(b)** Representative immunohistochemistry of Wt and iKsp*Pkd1*^{del} kidneys at 10 weeks after DCVC ("10 wks"; left and middle panel) showed expression of pSTAT3 and RUNX1 in nuclei in cyst-lining epithelia, in the epithelial cells of surrounding dilated tubules (arrows) and in infiltrating cells (arrowheads) only in cystic tissue. Expression of pSTAT3 and RUNX1 was even more increased at kidney failure ("KF"; right panel) when the kidneys are severely cystic. Scale bars 50 µm

STAT3 and RUNX1 target genes were dysregulated during ADPKD progression and after injury

Although we demonstrated that pSTAT3 and RUNX1 expression were increased during ADPKD progression and after injury, both at gene and protein level, we do not know if this would translate into differences in their activity as transcriptional regulators. Thus, we quantified the expression of their target genes during PKD progression and injury/repair. To find TFs' target genes, we used the publicly available Cistrome database. For both TFs we identified ChIP-Seq experiments and searched for peaks (targets) identified in at least two ChIP-Seq experiments. Peaks were prioritised based on 1) the number of studies they were found in, 2) their intensity levels (>10) and 3) whether they mapped to target genes within 10 kb distance. For both TFs the top putative target genes were crossed with the PKD Signature genes to identify targets that show differential expression in PKD. Only target genes that were also present in the PKD Signature were selected for further analysis (Figure 4a).

The final targets we selected are *Scp2*, *Kif22*, *Stat3* (autoregulation) and *Socs3* for STAT3, and *Runx1* (autoregulation), *Tnfrsf12a* and *Bcl3* as targets for RUNX1. We checked the expression of these targets after injury and during PKD progression in iKsp*Pkd1*^{del} and Wt mice. We found that, in iKsp*Pkd1*^{del} mice, all targets were significantly upregulated except for *Scp2*, which was downregulated, suggesting an inhibitory effect of STAT3 on *Scp2* transcription. (Figure 2b - *Stat3* and *Runx1;* Figure 4b - *Scp2*, *Kif22*, *Socs3, Tnfrsf12a* and *Bcl3*).

These data indicate that not only the level of expression of the selected TFs is dysregulated during injury/repair and PKD progression, but likely also their activity, as denoted by the dysregulated expression of their target genes.

STAT3 and RUNX1 ChIP-qPCR in murine renal epithelial cells

To confirm that STAT3 and RUNX1 are directly regulating the expression of the indicated target genes in the renal epithelium, we performed chromatin immunoprecipitation (ChIP) analysis followed by quantitative PCR (ChIP-qPCR). We first confirmed that STAT3 and RUNX1 were expressed in mIMCD3 cells (Supplementary Fig 3). We then isolated chromatin and performed ChIP-qPCR. STAT3 enrichment at the promoter region of the *Scp2*, *Kif22*, *Stat3* and *Socs3* genes was significantly higher than at non-binding regions (Figure 5a). Also, RUNX1 showed significant enrichment at the promoter regions of its targets *Runx1*, *Tnfrsf12a* and *Bcl3* (Figure 5b) compared to non-binding regions.

Thus, we can conclude that STAT3 and RUNX1 are actively binding the selected target genes in renal epithelial cells.

STAT3 and RUNX1 ChIP-qPCR in murine kidney tissue

We then investigated whether binding of STAT3 and RUNX1 at the promoter region of their target genes is increased in cystic kidneys compared to non-cystic kidneys. To do so, we

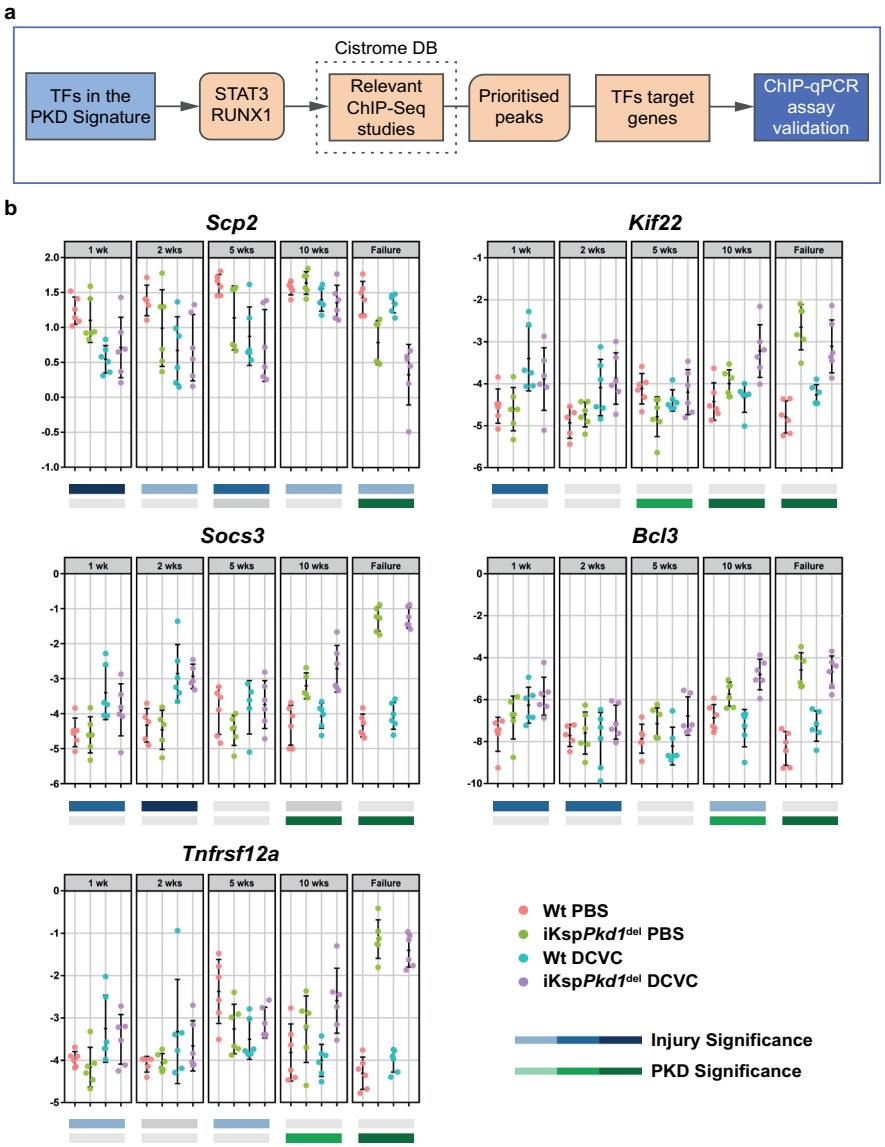

Figure 4. Identification of STAT3 and RUNX1 target genes

(**a**) STAT3 and RUNX1 emerged as two leading candidates for wet-lab validation. Using Cistrome database, we identified ChIP-peaks that were used in the wet-lab validation process and led to the identification of confirmed STAT3 and RUNX1 targets. **(b)** Expression of STAT3 and RUNX1 targets during PKD progression. Total RNA was isolated from kidneys of Wt and iKsp*Pkd1*^{del} mice treated with PBS or DCVC at 1, 2, 5, 10 weeks and at kidney failure. Expression of selected STAT3 (*Scp2*, *Kif22* and *Socs3*) and RUNX1 (*Bcl3*, *Tnfrsf12a*) targets was evaluated using a SYBR-Green based qPCR. On the Y-axis normalised Ct values (cycle threshold values) are plotted. Data were analysed using a two-way ANOVA test based on comparing Treatment (DCVC vs PBS) and Genotype (iKsp*Pkd1*^{del} vs Wt). P values are reported and classified into: high significance (darkest colour shade) at P value < 0.0005, moderate significance (medium colour shade) at P value < 0.005, and acceptable significance at (low colour shade) at P value < 0.05. P value ≥ 0.05 was not considered significant (grey bars). Each dot is a mouse and whiskers represent mean ± SD.

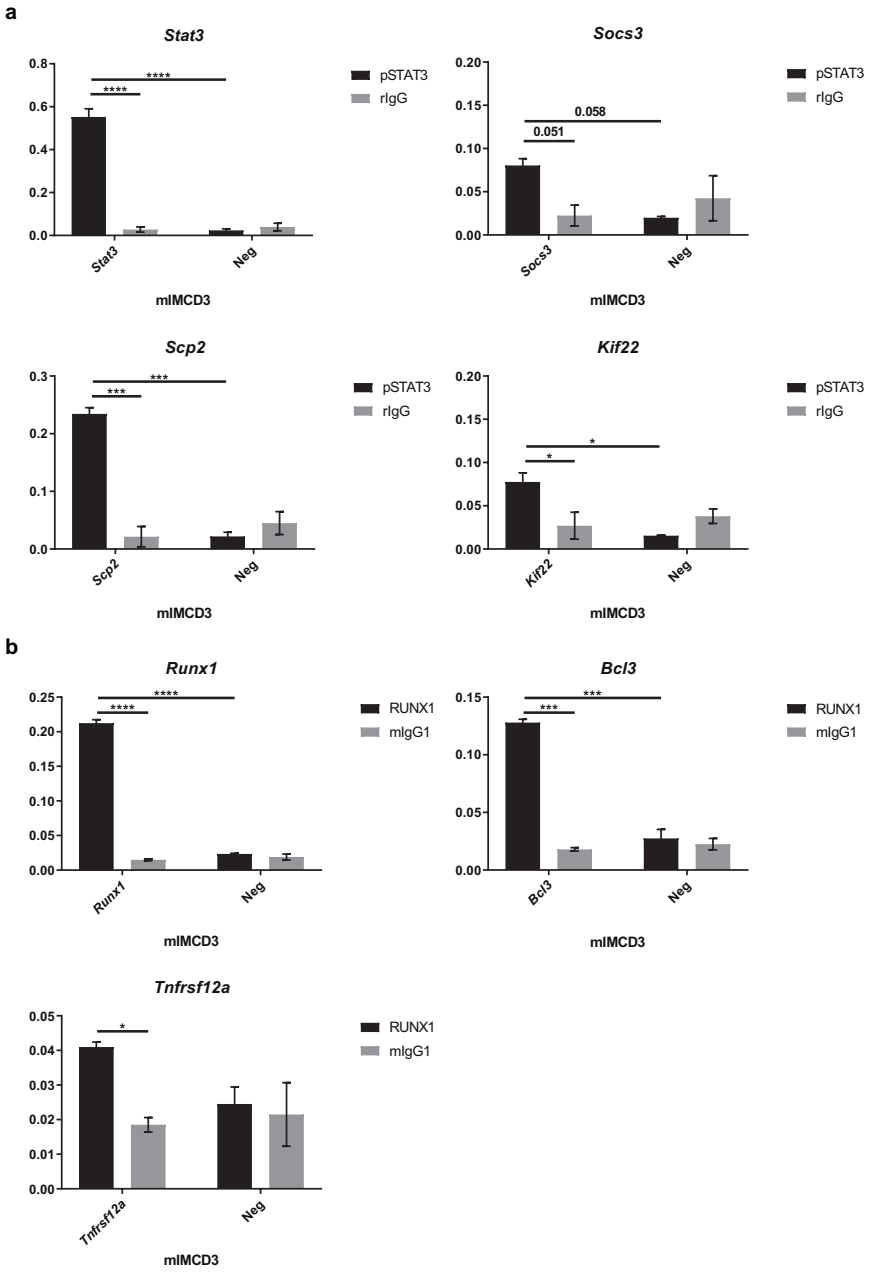

Figure 5. ChIP validation of pSTAT3 and RUNX1 targets in mIMCD3 cells

(a) ChIP with anti-pSTAT3 antibody showed significant enrichment at the promoter region of *Scp2*, *Kif22*, *Stat3* and *Socs3* compared to a negative control antibody (rIgG) and a non-binding region (Neg). **(b)** ChIP with anti-RUNX1 antibody showed a significant enrichment at the promoter region of *Runx1*, *Tnfrsf12a* and *Bcl3* compared to a negative control antibody (mIgG) and a non-binding region (Neg). The Y-axis shows the input-normalised binding-enrichment of the TFs to the indicated genomic region. Data represent the mean of two independent ChIPs ± SD; Two-way ANOVA with Tukey's multiple comparisons test. * P value < 0.05; ** P value < 0.01; *** P value < 0.001

performed ChIP-qPCR using kidneys from iKsp*Pkd1*^{del} mice, harvested at kidney failure, as well as age- and treatment-matched Wt kidneys.
As expected, we observed a significantly increased abundance of STAT3 at *Stat3*, *Socs3*, *Scp2* and *Kif22* promoter regions in iKsp*Pkd1*^{del} mice compared to Wt (Figure 6a - more severe iKsp*Pkd1*^{del} + DCVC and Supplementary Figure 4a - milder iKsp*Pkd1*^{del} + PBS).
RUNX1 enrichment in iKsp*Pkd1*^{del} mice was not significantly higher than in Wt mice. However, RUNX1 enrichment was significantly higher compared to IgG at the promoter region of *Runx1* and *Bcl3* in iKsp*Pkd1*^{del} mice but not in Wt. A similar trend is observed for *Tnfrsf12a*. This means that in iKsp*Pkd1*^{del} mice, RUNX1 binding is specific while in Wt it is not different from the background signal. Thus, RUNX1 is actively binding its targets in cystic kidneys only. (Figure 6b - more severe iKsp*Pkd1*^{del} + DCVC and Supplementary Figure 4b - milder iKsp*Pkd1*^{del} + PBS).
Overall, these data, in addition to the altered expression levels, show that the activity of STAT3 and RUNX1 is increased in advanced stages of PKD in mice.

Expression of TFs in kidneys of ADPKD patients
Lastly, we checked the expression of STAT3 and RUNX1 in human kidney sections obtained from ADPKD patients and healthy controls. Comparably with what was observed in mice, in healthy controls, we found only sporadic expression of pSTAT3 in the nuclei of tubular epithelial cells (Figure 7, asterisks) and expression of RUNX1 in some infiltrating cells (Figure 7, arrowheads). Conversely, in ADPKD patients renal tissue the expression of pSTAT3 and RUNX1 was increased in the nuclei of the epithelial cells and infiltrating cells (Figure 7, right panel and Supplementary Figure 5, right panel).
These data suggest that the TFs identified by our meta-analysis using rodent models are relevant for human ADPKD.

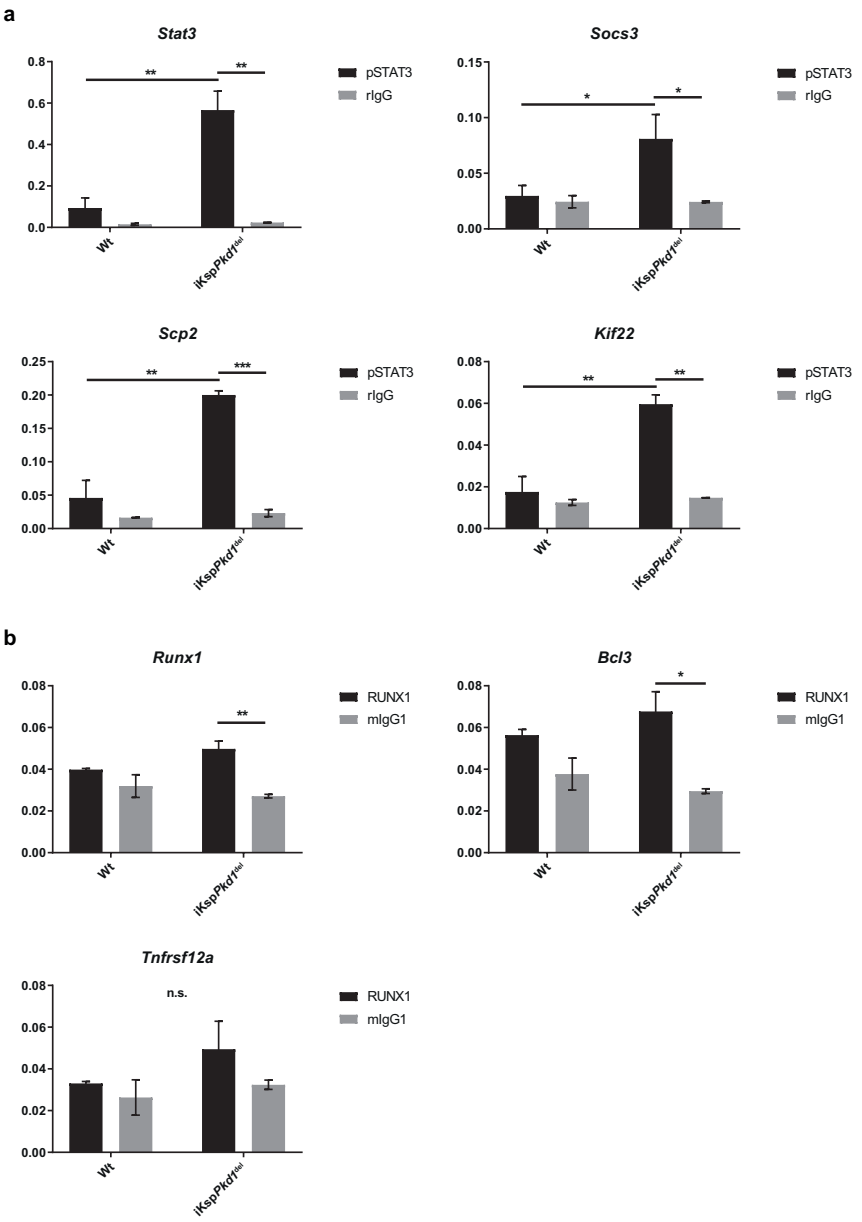

Figure 6. Increased binding of STAT3 and RUNX1 to the promoter of target genes in cystic kidneys, shown by ChIP-qPCR

ChIP-qPCR analysis of end-stage renal disease iKsp*Pkd1*^{del} kidneys or Wt kidneys at 24 weeks after DCVC. **(a)** We confirmed an increased enrichment for STAT3 binding at target genes in iKsp*Pkd1*^{del} kidneys compared to Wt kidneys. **(b)** RUNX1 enrichment at its targets is not detected in Wt samples (no difference between RUNX1 ChIP and IgG ChIP) but detected in iKsp*Pkd1*^{del} samples. Black bars pSTAT3 or RUNX1 antibody, grey bars isotype IgG control (rIgG: rabbit IgG; mIgG: mouse IgG). The Y-axis shows the input-normalised binding-enrichment of the TFs to the indicated genomic region. Data represent the mean of two independent ChIPs ± SD; Two-way ANOVA with Tukey's multiple comparisons test. * P value < 0.05; ** P value < 0.01; *** P value < 0.001

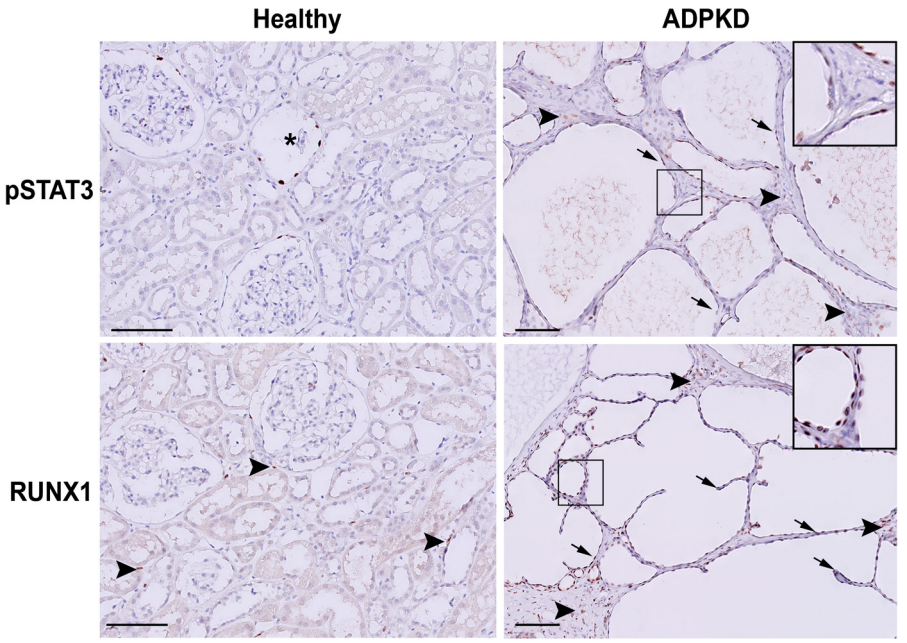

Figure 7. pSTAT3 and RUNX1 expression in human kidneys with ADPKD

Representative immunohistochemistry of human kidneys. In healthy patients, the expression of pSTAT3 and RUNX1 was rarely detected (asterisks). In end-stage cystic kidneys from ADPKD patients, pSTAT3 and RUNX1 localised in the nuclei of the tubular epithelial cells (arrows) and infiltrating cells (arrowheads). Scale bars 100 µm.

Discussion

Previously, we identified a list of 1515 genes dysregulated during PKD progression, which we defined as the PKD Signature. We also showed a consistent overlap (about 35%) of the PKD Signature with genes normally involved in injury/repair mechanisms[5]. Now, we have put this analysis a step further by identifying and characterising TFs involved in ADPKD progression.

Using MSigDB, we identified 92 TFs in the PKD Signature and again showed that about 35% of these genes (32 out of 92) have a strong injury-related component. This is in line with a substantial body of literature indicating that injury is a significant modifier in PKD and a potential trigger of cyst formation. Indeed, renal injury causes faster cystic disease progression suggesting that events activated during the injury/repair phase are also crucial for cyst initiation and expansion[3,4]. Moreover, cyst formation per se is a source of injury for the surrounding tissue making the two pathological processes challenging to dissect[19].

Among these 92 identified TFs we observed known players in PKD, such as STAT3[17,20], c-MYC[18], SMAD2[21], GLIS2[22], c-JUN[23] and E2F1[24], confirming our approach. On the other hand, we did not find TFs such as PPARα, which has been described to play a role in PKD[25]. This is likely due to the high stringency used for the definition of the PKD Signature, which allows us to get specific targets while possibly losing others[5].

Interestingly, we also identified many other TFs, never described before in PKD. Some of these TFs, such as EGR1, KLF5 and FOXM1, have been reported in literature for their involvement in injury/repair mechanisms or pathways dysregulated during PKD progression and might be interesting candidates for future studies. Indeed, *Egr1* is an early growth response gene and is downstream of the mitogen-activated protein kinase (MAPK) pathway, a pathway dysregulated in PKD[23]. EGR1 is a key regulator of proliferation, apoptosis and inflammation and was shown to be involved in renal injury and fibrosis. *Egr1* disruption protected mice from renal failure in a model of tubulointerstitial nephritis and resulted in lower activation of the TGF-β pathway[26]. Moreover, *Egr1* can be downregulated by curcumin, a compound able to reduce cyst formation *in vivo*[17]. Also, KLF5 was shown to play a role in renal inflammation and fibrosis since unilateral ureteral obstruction in mice haploinsufficient for *Klf5* resulted in reduced renal injury, fibrosis and infiltrating cells[27]. Thus, modulation of KLF5 activity might improve the pro-fibrotic and pro-inflammatory phenotype observed especially during the more advanced phases of PKD progression. *Foxm1* is expressed during cell proliferation and is critical for cell-cycle progression. In adult tissues, *Foxm1* expression is low, but after injury its levels are dramatically increased. In particular, FOXM1 can control the expression of genes involved in the G2/M transition phase. Cell-cycle arrest in G2/M phase is associated with pro-fibrotic cytokines production by proximal tubular cells[28]. Not surprisingly, these three

TFs are involved in PKD since aberrant extracellular matrix (ECM) deposition is commonly found in PKD patients and animal models of PKD, not only in ESRD but also in early-stage[29]. This suggests that increased ECM deposition may be contributing to cyst formation and not barely be a consequence of it, as shown for laminin-alpha5[30] and integrins-beta1[31], which mutation could affect the cystic phenotype. Thus, modulation of pro-fibrotic processes could be a valuable strategy to modulate PKD progression.

EGR1, KLF5 and FOXM1, together with ESR1 and STAT3, were also among the significantly enriched PKD Signature TFs identified based on their target genes annotated in the ChEA 2016 database. Pathway analysis of the targets of these TFs, using Genetrail2 and Wikipathways, revealed enrichment for pathways known to play a role in PKD progression, such as the TGF-β pathway, oxidative stress, cellular metabolism, interleukins signalling, adipogenesis, estrogen signalling and apoptosis[21,32-35]. Using this approach, we also identified TFs not directly present in the PKD Signature. Interestingly, the top five TFs identified based on their targets were all described in literature to be involved in the progression of PKD (STAT3)[17,20,36], or in processes relevant for PKD like angiogenesis (E2F7)[37], DNA damage response (E2F7, TRIM28)[38,39], renal injury and fibrosis (EGR1)[26], epithelial cell proliferation, apoptosis and adhesion (TP63)[40]. Nevertheless, apart from STAT3, the TFs themselves had never been associated with PKD before and therefore could be interesting subjects for future studies. Surprisingly, we did not find back RUNX1 in this list as the level of enrichment was just below the significance threshold (data not shown). Nevertheless, we confirmed increased expression and activity of RUNX1 during PKD progression in mice and human ADPKD kidneys. Thus, we speculate that the absence of RUNX1, as well as other TFs potentially involved in PKD, is due to limitations related with the ChEA database, such as the source of ChIP-data, the way the different studies have been analysed and the actual TFs included in the database.

To further test and validate our approach, we selected for additional wet-lab validation STAT3 and RUNX1 as they showed the most significant change in expression both in PKD progression and injury. By performing ChIP-qPCR for STAT3 and RUNX1 in ADPKD-affected kidneys, we confirmed increased transcriptional activity in cystic kidneys for these TFs. Persistent activation of STAT3 has been described in several mouse models for ADPKD as well as in human cystic tissues[17,20,36]. STAT3 usually is not active in adult kidneys but is abundantly present, suggesting that it can be readily activated at needs, such as after injury[36]. Indeed, STAT3 activation has been shown in several different mouse models with renal injury[41,42]. Thus, the fact that we found back STAT3 and several of its putative targets in our signature proved the reliability of our meta-analysis.

RUNX1 involvement in ADPKD has never been described before. RUNX1 is one of the Runt

domain TFs, together with RUNX2 and RUNX3. RUNX2 expression has been shown to be regulated by PC1 in osteoblasts, proving the existence of an interaction between the two proteins[43]. Nevertheless, expression of RUNX2 or RUNX3 is not increased after injury nor during disease progression in murine (cystic) kidneys (RNA-Seq data identifier E-MTAB-5319 published in Malas *et al., 2017*[5]). In contrast, RUNX1 is expressed in the epithelium of several organs during development, among which the kidneys[44]. It participates in the regulation of cell cycle, cell proliferation and apoptosis[45], and has been described in several models for lung, muscle and brain injury[46-48]. Recently, a study was published suggesting that RUNX1 is an important regulator of TGF-β-induced renal tubular epithelial-to-mesenchymal transition (EMT) and fibrosis[49]. As mentioned above, TGF-β signalling is involved in ECM deposition and cyst progression and is partly responsible for the EMT observed in cystic kidneys. Modulation of TGF-β-related signalling is associated with amelioration of the cystic phenotype[21]. Thus, it is plausible that RUNX1 might play a role in ADPKD progression. In fact, inhibition of STAT3 signalling with more or less specific inhibitors, such as curcumin, pyrimethamine and S3I-201, has been proven to improve the cystic phenotype in different mouse models[17,20,36]. Similarly, we propose that targeting RUNX1, for example using microRNAs as described for prostate cancer[50], or other molecular or pharmacological approaches, might also result in amelioration of the cystic phenotype.

We observed increased expression of STAT3 and RUNX1 also after injury in Wt mice, suggesting that these TFs orchestrate injury/repair mechanisms and that increased expression is not necessarily related to *Pkd1* deletion. Notably, dissecting PKD progression and injury is not easy, since injury can speed up cyst initiation/growth, which in turn causes injury to the surrounding tissue. Therefore, it is plausible that both STAT3 and RUNX1 are facilitating PKD progression by activating injury/repair pathways normally inactive in fully developed and healthy kidneys.

To conclude, our comprehensive analyses identified a signature of TFs differentially expressed in PKD and to a certain extent also in injury/repair. Several of these TFs are involved in processes able to support cyst formation and progression, nevertheless were never described before in PKD, suggesting that they might be interesting targets for therapy. Further analyses are needed to identify the molecular pathways that these TFs modulate to contribute to PKD progression and cyst formation. Additionally, the TFs we identified are a subset of the TFs involved in PKD and not a comprehensive list. This is due to limitations in the annotation databases we used and RNA-Seq technology. To establish a comprehensive list of TFs involved in PKD and/or injury, further studies must be conducted on protein levels and protein phosphorylation status. That said, our approach was capable of robustly identifying 92 TFs, and additional wet-lab validations confirmed the involvement of RUNX1 and STAT3 making this paper a starting point to understand the role of TFs in PKD progression.

Author contributions

C.F., T.B.M., P.A.t.H., and D.J.M.P. conceived and designed research; C.F. performed experiments; L.V. performed immunohistochemistry; C.F., T.B.M., and J.B., analysed data; C.F., T.B.M., P.A.t.H. and D.J.M.P. interpreted results of experiments; C.F. and T.B.M. prepared figures; C.F. drafted manuscript; C.F., T.B.M., J.B., P.A.t.H., and D.J.M.P. edited and revised manuscript.

Funding

This work was supported by grants from the People Program (Marie Curie Actions) of the European Union's Seventh Framework Program FP7/2077-2013 under Research Executive Agency Grant Agreement 317246.

Compliance with ethical standards

Conflict of interest

The authors declare no competing financial interests.

References

1 Harris, P. C. & Torres, V. E. Genetic mechanisms and signaling pathways in autosomal dominant polycystic kidney disease. *J Clin Invest* **124**, 2315-2324, doi:10.1172/JCI72272 (2014).

2 Leonhard, W. N., Happe, H. & Peters, D. J. Variable Cyst Development in Autosomal Dominant Polycystic Kidney Disease: The Biologic Context. *J Am Soc Nephrol* **27**, 3530-3538, doi:10.1681/ASN.2016040425 (2016).

3 Patel, V. *et al.* Acute kidney injury and aberrant planar cell polarity induce cyst formation in mice lacking renal cilia. *Hum Mol Genet* **17**, 1578-1590, doi:10.1093/hmg/ddn045 (2008).

4 Happe, H. *et al.* Toxic tubular injury in kidneys from Pkd1-deletion mice accelerates cystogenesis accompanied by dysregulated planar cell polarity and canonical Wnt signaling pathways. *Hum Mol Genet* **18**, 2532-2542, doi:10.1093/hmg/ddp190 (2009).

5 Malas, T. B. *et al.* Meta-analysis of polycystic kidney disease expression profiles defines strong involvement of injury repair processes. *Am J Physiol Renal Physiol* **312**, F806-F817, doi:10.1152/ajprenal.00653.2016 (2017).

6 Messina, D. N., Glasscock, J., Gish, W. & Lovett, M. An ORFeome-based analysis of human transcription factor genes and the construction of a microarray to interrogate their expression. *Genome Res* **14**, 2041-2047, doi:DOI 10.1101/gr.2584104 (2004).

7 Moreland, R. T., Ryan, J. F., Pan, C. & Baxevanis, A. D. The Homeodomain Resource: a comprehensive collection of sequence, structure, interaction, genomic and functional information on the homeodomain protein family. *Database (Oxford)* **2009**, bap004, doi:10.1093/database/bap004 (2009).

8 Lachmann, A. *et al.* ChEA: transcription factor regulation inferred from integrating genome-wide ChIP-X experiments. *Bioinformatics* **26**, 2438-2444, doi:10.1093/bioinformatics/btq466 (2010).

9 Stockel, D. *et al.* Multi-omics enrichment analysis using the GeneTrail2 web service. *Bioinformatics* **32**, 1502-1508, doi:10.1093/bioinformatics/btv770 (2016).

10 Ritchie, M. E. *et al.* limma powers differential expression analyses for RNA-sequencing and microarray studies. *Nucleic Acids Res* **43**, e47, doi:10.1093/nar/gkv007 (2015).

11 Mei, S. *et al.* Cistrome Data Browser: a data portal for ChIP-Seq and chromatin accessibility data in human and mouse. *Nucleic Acids Res* **45**, D658-D662, doi:10.1093/nar/gkw983 (2017).

12 Karolchik, D., Hinrichs, A. S. & Kent, W. J. The UCSC Genome Browser. *Curr Protoc Bioinformatics* **Chapter 1**, Unit1 4, doi:10.1002/0471250953.bi0104s28 (2009).

13 Lantinga-van Leeuwen, I. S. *et al.* Lowering of Pkd1 expression is sufficient to cause polycystic kidney disease. *Human Molecular Genetics* **13**, 3069-3077, doi:10.1093/hmg/ddh336 (2004).

14 Lantinga-van Leeuwen, I. S. *et al.* Kidney-specific inactivation of the Pkd1 gene induces rapid cyst formation in developing kidneys and a slow onset of disease in adult mice. *Hum Mol Genet* **16**, 3188-3196, doi:10.1093/hmg/ddm299 (2007).

15 Formica, C. *et al.* Four-jointed knock-out delays renal failure in an ADPKD model with kidney injury. *J Pathol*, doi:10.1002/path.5286 (2019).

16 Nelson, J. D., Denisenko, O. & Bomsztyk, K. Protocol for the fast chromatin immunoprecipitation (ChIP) method. *Nature protocols* **1**, 179-185, doi:10.1038/nprot.2006.27 (2006).

17 Leonhard, W. N. *et al.* Curcumin inhibits cystogenesis by simultaneous interference of multiple signaling pathways: in vivo evidence from a Pkd1-deletion model. *Am J Physiol Renal Physiol* **300**, F1193-1202, doi:10.1152/ajprenal.00419.2010 (2011).

18 Trudel, M., Dagati, V. & Costantini, F. C-Myc as an Inducer of Polycystic Kidney-Disease in Transgenic Mice. *Kidney Int* **39**, 665-671, doi:DOI 10.1038/ki.1991.80 (1991).

19 Leonhard, W. N. *et al.* Scattered Deletion of PKD1 in Kidneys Causes a Cystic Snowball Effect and Recapitulates Polycystic Kidney Disease. *Journal of the American Society of Nephrology* **26**, 1322-1333, doi:10.1681/Asn.2013080864 (2015).

20 Takakura, A. *et al.* Pyrimethamine inhibits adult polycystic kidney disease by modulating STAT signaling pathways. *Hum Mol Genet* **20**, 4143-4154, doi:10.1093/hmg/ddr338 (2011).

21 Hassane, S. *et al.* Elevated TGFbeta-Smad signalling in experimental Pkd1 models and human patients with polycystic kidney disease. *J Pathol* **222**, 21-31, doi:10.1002/path.2734 (2010).

22 Lu, D. *et al.* Loss of Glis2/NPHP7 causes kidney epithelial cell senescence and suppresses cyst growth in the Kif3a mouse model of cystic kidney disease. *Kidney Int* **89**, 1307-1323, doi:10.1016/j.kint.2016.03.006 (2016).

23 Le, N. H. *et al.* Increased activity of activator protein-1 transcription factor components ATF2, c-Jun, and c-Fos in human and mouse autosomal dominant polycystic kidney disease. *J Am Soc Nephrol* **16**, 2724-2731, doi:10.1681/ASN.2004110913 (2005).

24 Zhou, X. *et al.* Sirtuin 1 inhibition delays cyst formation in autosomal-dominant polycystic kidney disease. *J Clin Invest* **123**, 3084-3098, doi:10.1172/JCI64401 (2013).

25 Lakhia, R. *et al.* PPARalpha agonist fenofibrate enhances fatty acid beta-oxidation and attenuates polycystic kidney and liver disease in mice. *Am J Physiol Renal Physiol* **314**, F122-F131, doi:10.1152/ajprenal.00352.2017 (2018).

26 Ho, L. C. *et al.* Egr-1 deficiency protects from renal inflammation and fibrosis. *J Mol Med (Berl)* **94**, 933-942, doi:10.1007/s00109-016-1403-6 (2016).

27 Fujiu, K., Manabe, I. & Nagai, R. Renal collecting duct epithelial cells regulate inflammation in tubulointerstitial damage in mice. *J Clin Invest* **121**, 3425-3441, doi:10.1172/JCI57582 (2011).

28 Yang, L., Besschetnova, T. Y., Brooks, C. R., Shah, J. V. & Bonventre, J. V. Epithelial cell cycle arrest in G2/M mediates kidney fibrosis after injury. *Nat Med* **16**, 535-543, 531p following 143, doi:10.1038/nm.2144 (2010).

29 Song, C. J., Zimmerman, K. A., Henke, S. J. & Yoder, B. K. Inflammation and Fibrosis in Polycystic Kidney Disease. *Results Probl Cell Differ* **60**, 323-344, doi:10.1007/978-3-319-51436-9_12 (2017).

30 Shannon, M. B., Patton, B. L., Harvey, S. J. & Miner, J. H. A hypomorphic mutation in the mouse laminin alpha5 gene causes polycystic kidney disease. *J Am Soc Nephrol* **17**, 1913-1922, doi:10.1681/asn.2005121298 (2006).

31 Lee, K., Boctor, S., Barisoni, L. M. & Gusella, G. L. Inactivation of integrin-beta1 prevents the development of polycystic kidney disease after the loss of polycystin-1. *J Am Soc Nephrol* **26**, 888-895, doi:10.1681/ASN.2013111179 (2015).

32 Tao, Y. X., Zafar, I., Kim, J., Schrier, R. W. & Edelstein, C. L. Caspase-3 gene deletion prolongs survival in polycystic kidney disease. *Journal of the American Society of Nephrology* **19**, 749-755, doi:10.1681/Asn.2006121378 (2008).

33 Padovano, V., Podrini, C., Boletta, A. & Caplan, M. J. Metabolism and mitochondria in polycystic kidney disease research and therapy. *Nat Rev Nephrol* **14**, 678-687, doi:10.1038/s41581-018-0051-1 (2018).

34 Merta, M. *et al.* Cytokine profile in autosomal dominant polycystic kidney disease. *Biochemistry and molecular biology international* **41**, 619-624 (1997).

35 Stringer, K. D. *et al.* Gender hormones and the progression of experimental polycystic kidney disease. *Kidney Int* **68**, 1729-1739, doi:DOI 10.1111/j.1523-1755.2005.00589.x (2005).

36 Talbot, J. J. *et al.* Polycystin-1 regulates STAT activity by a dual mechanism. *Proc Natl Acad Sci U S A* **108**, 7985-7990, doi:10.1073/pnas.1103816108 (2011).

37 Weijts, B. G. *et al.* E2F7 and E2F8 promote angiogenesis through transcriptional activation of VEGFA in cooperation with HIF1. *The EMBO journal* **31**, 3871-3884, doi:10.1038/emboj.2012.231 (2012).

38 Carvajal, L. A., Hamard, P.-J., Tonnessen, C. & Manfredi, J. J. E2F7, a novel target, is up-regulated by p53 and mediates DNA damage-dependent transcriptional repression. *Genes & Development* **26**, 1533-1545, doi:10.1101/gad.184911.111 (2012).

39 Iyengar, S. & Farnham, P. J. KAP1 protein: an enigmatic master regulator of the genome. *J Biol Chem* **286**, 26267-26276, doi:10.1074/jbc.R111.252569 (2011).

40 Carroll, D. K., Brugge, J. S. & Attardi, L. D. p63, cell adhesion and survival. *Cell cycle (Georgetown, Tex.)* **6**, 255-261, doi:10.4161/cc.6.3.3799 (2007).

41 Liu, J. *et al.* Role of Stat3 Signaling in Control of EMT of Tubular Epithelial Cells During Renal Fibrosis. *Cell Physiol Biochem* **42**, 2552-2558, doi:10.1159/000480216 (2017).

42 Nechemia-Arbely, Y. *et al.* IL-6/IL-6R axis plays a critical role in acute kidney injury. *J Am Soc Nephrol* **19**, 1106-1115, doi:10.1681/ASN.2007070744 (2008).

43 Xiao, Z. *et al.* Cilia-like structures and polycystin-1 in osteoblasts/osteocytes and associated abnormalities in skeletogenesis and Runx2 expression. *J Biol Chem* **281**, 30884-30895, doi:10.1074/jbc.M604772200 (2006).

44 Pozner, A. *et al.* Developmentally regulated promoter-switch transcriptionally controls Runx1 function during embryonic hematopoiesis. *BMC Dev Biol* **7**, 84, doi:10.1186/1471-213X-7-84 (2007).

45 Zhang, L., Fried, F. B., Guo, H. & Friedman, A. D. Cyclin-dependent kinase phosphorylation of RUNX1/AML1 on 3 sites increases transactivation potency and stimulates cell proliferation. *Blood* **111**, 1193-1200, doi:10.1182/blood-2007-08-109702 (2008).

46 Tang, X. *et al.* Runt-Related Transcription Factor 1 Regulates LPS-Induced Acute Lung Injury via NF-kappaB Signaling. *Am J Respir Cell Mol Biol* **57**, 174-183, doi:10.1165/rcmb.2016-0319OC (2017).

47 Umansky, K. B. *et al.* Runx1 Transcription Factor Is Required for Myoblasts Proliferation during Muscle Regeneration. *Plos Genet* **11**, e1005457, doi:10.1371/journal.pgen.1005457 (2015).

48 Logan, T. T., Villapol, S. & Symes, A. J. TGF-beta superfamily gene expression and induction of the Runx1 transcription factor in adult neurogenic regions after brain injury. *PLoS One* **8**, e59250, doi:10.1371/journal.pone.0059250 (2013).

49 Zhou, T. *et al.* Runt-Related Transcription Factor 1 (RUNX1) Promotes TGF-beta-Induced Renal Tubular Epithelial-to-Mesenchymal Transition (EMT) and Renal Fibrosis through the PI3K Subunit p110delta. *EBioMedicine* **31**, 217-225, doi:10.1016/j.ebiom.2018.04.023 (2018).

50 Zhang, G. *et al.* Long non-coding RNA FENDRR reduces prostate cancer malignancy by competitively

binding miR-18a-5p with RUNX1. *Biomarkers* **23**, 435-445, doi:10.1080/1354750X.2018.1443509 (2018).

Supplementary Figure 1. ADPKD mouse model with kidney injury and PKD progression

Experimental pipeline and data partly presented in Formica *et al.*[15] **(a)** Experimental pipeline. Adult mice (around 14 weeks old) were treated with tamoxifen to induce *Pkd1* deletion. One week after gene inactivation mice were injected with the nephrotoxic compound DCVC and sacrificed at 1, 2, 5, 10 weeks after DCVC and when the mice reached end-stage renal disease, indicated by blood urea nitrogen level (BUN) over 25mmol/l. **(b)** BUN of Wt and iKsp*Pkd1*^{del} mice showing increased BUN at 40h after DCVC injection (*t*-test, P value < 0.0001). BUN levels are back to baseline at 1 week after DCVC and remain at a physiological level up to 5 weeks after DCVC injection (t-test, not significant). Each point is the mean of 6 mice ± SD. **(c)** Representative histology of Wt and iKsp*Pkd1*^{del} mice before and after injury. At 1 week it is possible to observe mild tubule dilation in both Wt and iKsp*Pkd1*^{del} mice which are largely resolved at 2 weeks. Scale bar 50 µm. **(d)** In Wt mice BUN is in a physiological range up to 24 weeks after DCVC injection when the mice were sacrificed. The iKsp*Pkd1*^{del} mice injected with DCVC (red solid line) reach end-stage renal disease earlier compared to PBS treated mice (light-blue dashed line). Median DCVC group: 14 weeks; median PBS group: 19 weeks; n=6, Mann-Whitney test, P value < 0.05. **(e)** Representative histology of Wt and iKsp*Pkd1*^{del} kidneys. At 10 weeks after DCVC, iKsp*Pkd1*^{del} mice show tubule dilation and small cyst spread over the kidneys, which are absent in the PBS treated group or in the Wt mice. At kidney failure, iKsp*Pkd1*^{del} kidneys show evident cyst formation while the Wt kidneys show no aberration in both groups with or without injury. Scale bar 1 mm.

Supplementary Figures

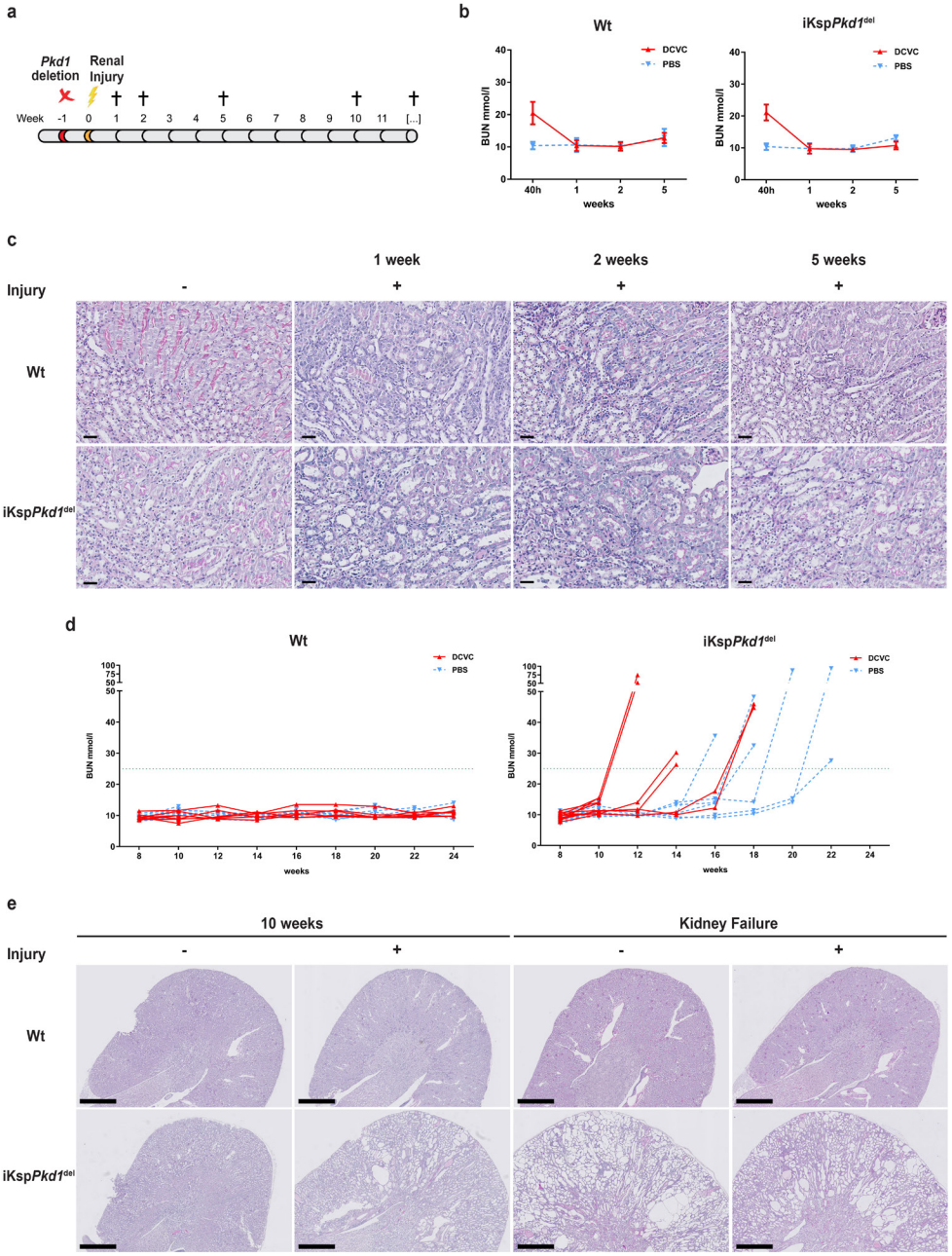

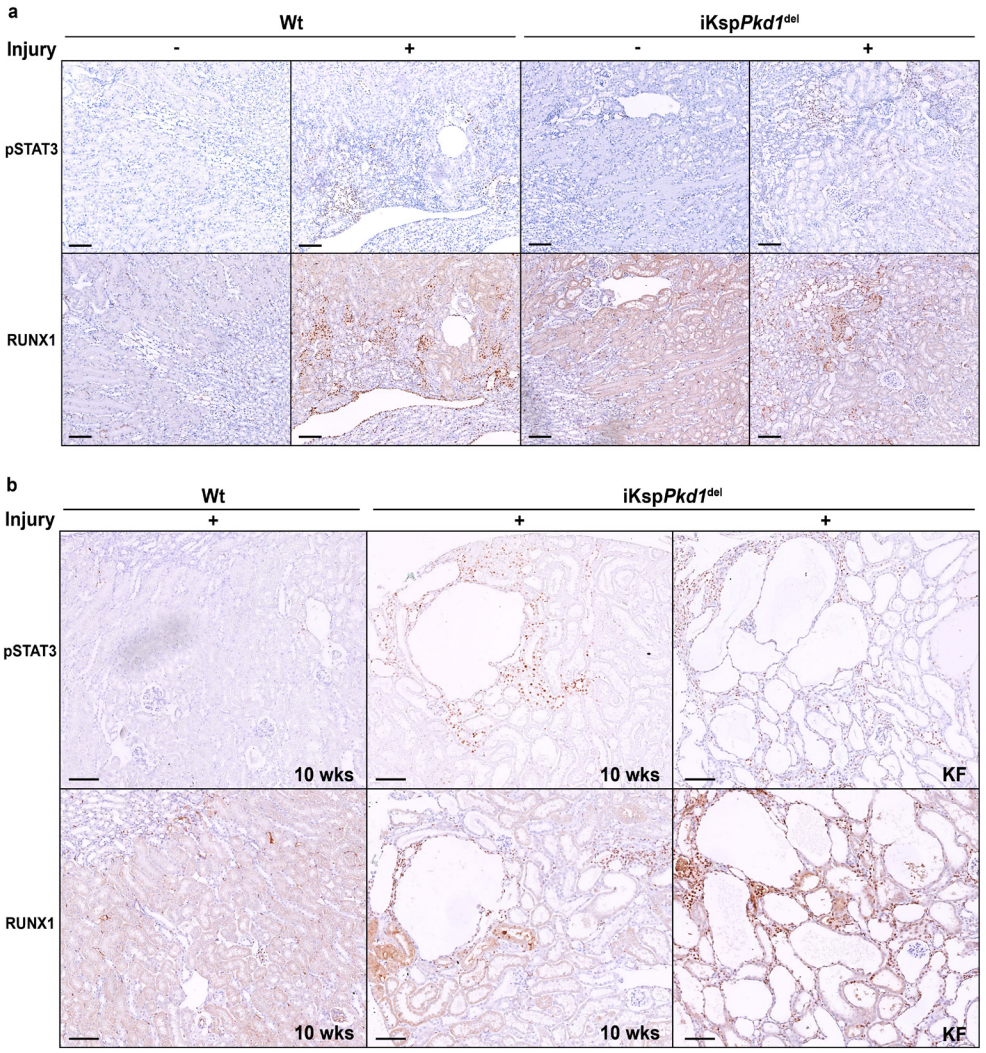

Supplementary Figure 2. Overview of pSTAT3 and RUNX1 expression in Wt and iKsp*Pkd1*^{del} mice after injury and during cyst progression

(a) Low magnification of Wt and iKsp*Pkd1*^{del} kidneys at 1 week after DCVC (+ injury) or PBS (- injury). With this magnification, it is possible to appreciate that the expression of pSTAT3 and RUNX1 in non-injured kidneys was present mainly in some interstitial cells while after injury the expression was clearly visible in the nuclei of the epithelial cells (brown nuclei). In particular, tubules in the cortico-medullary region, which are more sensitive to the toxic insult, showed the most staining. **(b)** Low magnification of Wt and iKsp*Pkd1*^{del} kidneys at 10 weeks after DCVC ("10 wks"; left and middle panel) and at kidney failure ("KF"; right panel) when the kidneys are severely cystic. With this magnification, it is visible that Wt and normal-looking tissue in mutant mice (mildly cystic kidneys at "10 wks") showed expression of pSTAT3 and RUNX1 mainly in some interstitial cells while cyst-lining epithelial cells, epithelial cells of surrounding tubules and infiltrating cells showed clear nuclear pSTAT3 and RUNX1 staining. Scale bars 100 µm.

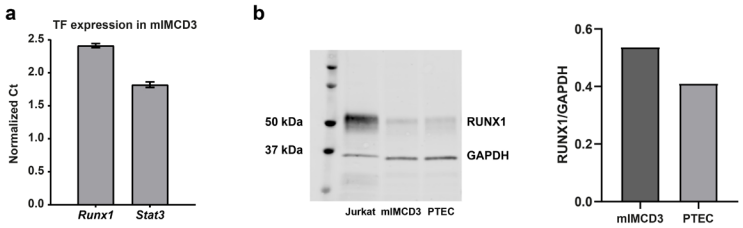

Supplementary Figure 3. Gene and protein expression of the TFs in cells

(a) Gene expression of *Stat3* and *Runx1* in mIMCD3 cells (n=3). On the Y-axis, we show the TFs expression normalised on the geometric mean of two housekeeping genes, *Ywhaz* and *Rplp0*. **(b)** In the middle panel, western blot showing the protein expression of RUNX1 (about 50 kDa) and GAPDH (about 37 kDa) in Jurkat cells (used as a positive control) and two renal epithelial cell lines, mIMCD3 and PTEC. In the right panel, quantification of the Western blot normalised on GAPDH expression is shown. Low but visible RUNX1 expression is observed in both renal epithelial cell lines.

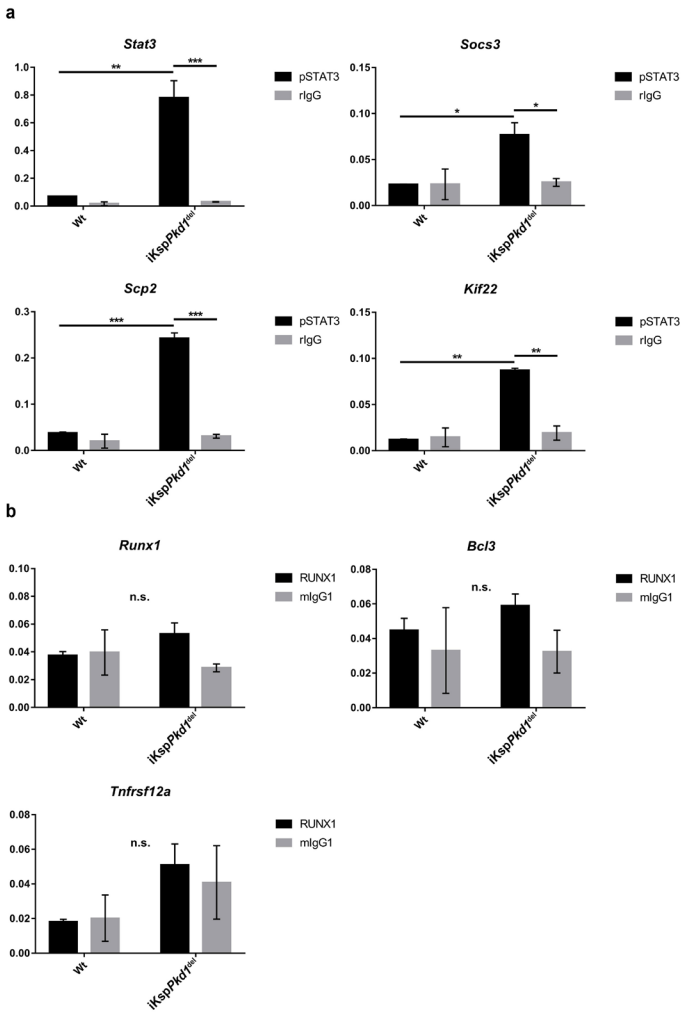

Supplementary Figure 4. Enrichment of STAT3 and RUNX1 at their targets in Wt and iKsp*Pkd1*^{del} mice treated with PBS

ChIP-qPCR analysis of end-stage renal disease iKsp*Pkd1*^{del} kidneys (median 21 weeks after PBS, equals age 8 months) or Wt kidneys (24 weeks after PBS, equals age 9 months). **(a)** We confirmed an increased enrichment for STAT3 at the promoter region of their target genes. **(b)** RUNX1 enrichment at its targets is not detected in Wt samples but show a trend in iKsp*Pkd1*^{del} samples. The Y-axis shows the input-normalised binding-enrichment of the TFs to the indicated genomic region. Data represent the mean of two independent ChIPs ± SD; Two-way ANOVA with Tukey's multiple comparisons test. * P value < 0.05; ** P value < 0.01; *** P value < 0.001

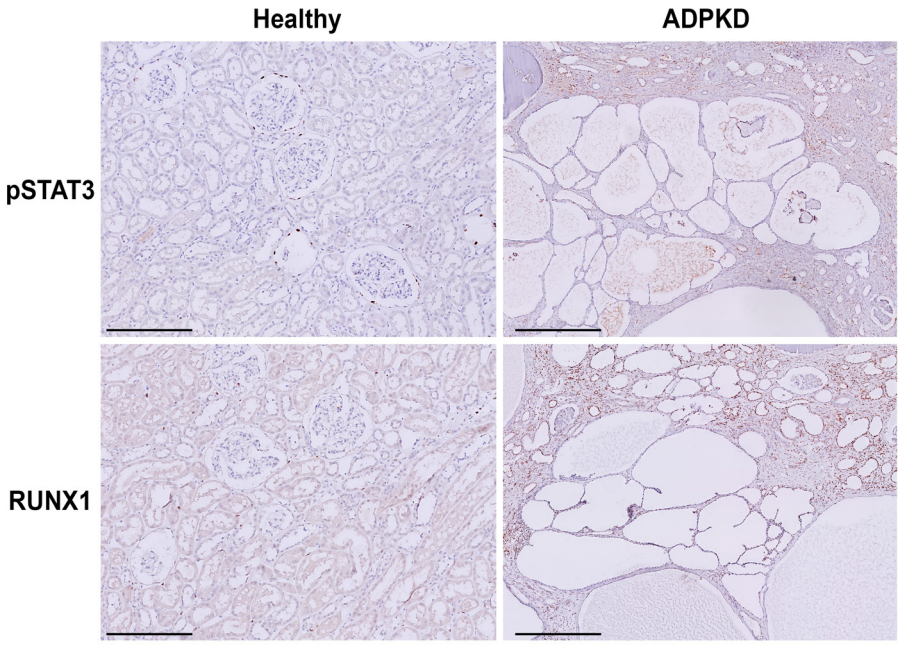

Supplementary Figure 5. Overview of pSTAT3 and RUNX1 expression in human kidneys with ADPKD

Low magnification of healthy and ADPKD affected human kidneys showing that the expression of pSTAT3 and RUNX1 was present mainly in some interstitial cells while cyst-lining epithelial cells, epithelial cells of surrounding tubules and infiltrating cells showed clear nuclear pSTAT3 and RUNX1 staining (brown nuclei). Scale bars 100 µm.

Supplementary Tables can be downloaded from

https://link.springer.com/article/10.1007/s00109-019-01852-3#Sec19

CHAPTER 6

Summarizing discussion

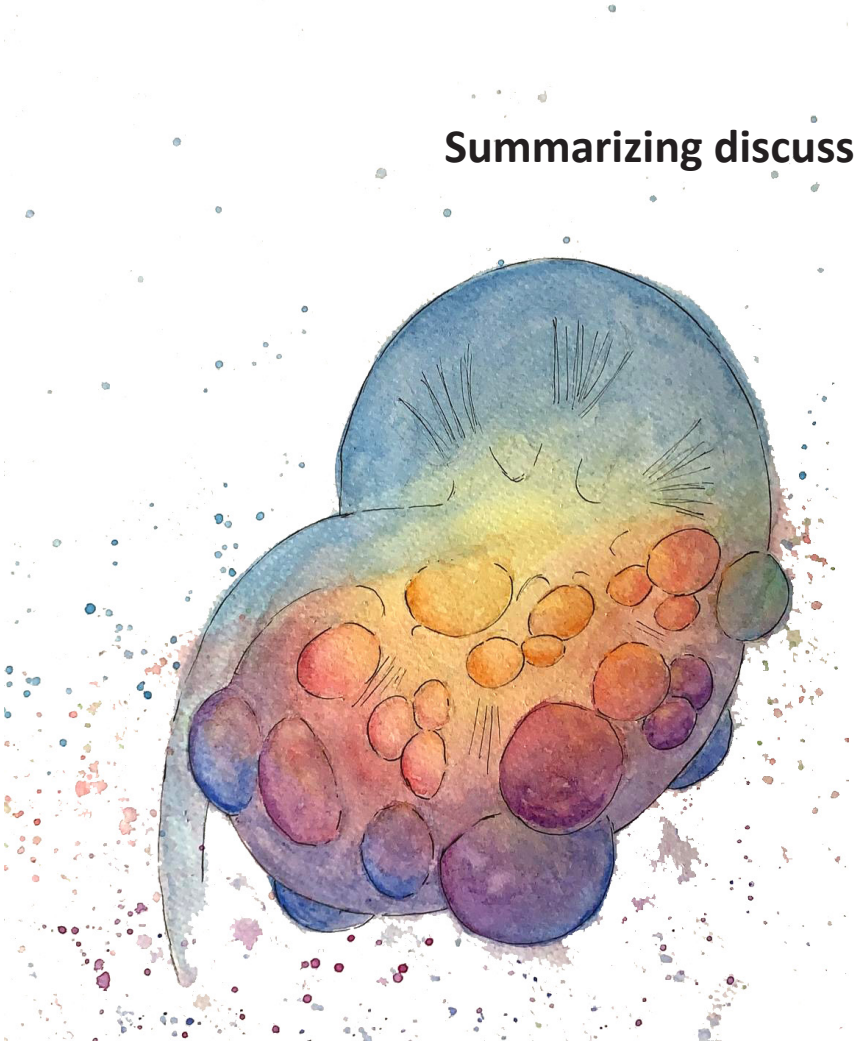

Autosomal Dominant Polycystic Kidney Disease (ADPKD) progression involves a complex interaction of different molecular pathways, ultimately leading to cyst growth and loss of kidney function. The exact mechanism behind cyst formation is still not clearly understood. Moreover, we know some of the molecular pathways involved in cyst initiation and progression, but we do not know at which stage of the disease they play a role.

In this thesis, we investigated the molecular pathways involved in renal injury-repair mechanisms and ADPKD. According to the currently available literature, injury-repair and ADPKD are two extremely intertwined mechanisms, which not only are characterised by activation of similar molecular pathways but are also able to influence each other. In fact, injury is able to accelerate cyst formation and progression, and cyst growth can cause injury to the surrounding tissue. Thus, the introduction of injury in the context of ADPKD can help to characterize the steps of disease progression, particularly in the early phases of cyst initiation, and direct future research to new possible therapeutic targets.

In **chapter 2,** we investigated the role of FJX1 in PKD and injury. We showed that the lack of *Fjx1* in *Pkd1/Fjx1* double KO mice was able to limit the effect of injury on disease progression. Indeed, double KO mice with toxic renal injury lived significantly longer compared to single *Pkd1* KO mice with renal injury. Analysis of the renal tissues revealed that differences in cyst initiation and progression could not explain this. In fact, 2 KW/BW ratios and cystic index at mild stages of disease were comparable in double KO and *Pkd1* KO mice, suggesting that Fjx1 does not play a role in cyst initiation and progression. Consistently, the examination of the two Fjx1 downstream pathways, the planar cell polarity and Hippo pathways, which are believed to be involved in cyst progression, did not show significant changes in the two genotypes[1-7].

Interestingly, even though cyst growth was comparable, we observed reduced injury marker expression and fibrosis in double KO mice compared with *Pkd1* KO. Based on the current knowledge, cyst growth and expansion cause compression of the surrounding tubules and vessels leading to local injury, ECM deposition and activation of pathways involved in ADPKD pathogenesis. Consequently, there is an increased likelihood of additional cyst formation and accumulation of fibrosis, which ultimately result in the organ function decline[8-12]. However, it was always difficult to establish whether inflammation and fibrosis are responsible for, or just a consequence of cyst formation. In chapter 2, we showed a separation between cyst progression and fibrosis in the absence of *Fjx1* expression. Indeed, we confirmed that injury could accelerate cyst formation in *Pkd1* mutant mice, regardless of the presence or absence of *Fjx1*, suggesting that some of the pathways involved in response to injury are crucial in cyst formation and progression. At the same time, we observed that the inflammatory and fibrotic responses, which follow the initial injury event and the chronic local injury

induced by cyst growth and compression, are in part dependent on *Fjx1* expression and do not influence cyst formation significantly. However, they did impact the functionality of the cystic kidneys and the survival of the animal. Altogether, our results suggest that *Fjx1* regulates pathways related to the fibrotic response and that these are critical in the advanced stages of the disease, more than in cyst initiation and expansion. Such results are particularly interesting, as they demonstrate how modulation of the injury response can help mitigate disease progression and might be considered as a part of a therapeutic approach in PKD.

Among the possible pathways that might be responsible for the reduced inflammatory and fibrotic response in double KO mice, TGFβ and WNT pathways are particularly interesting. TGFβ and WNT pathways have been extensively described for their role in renal fibrosis[13-16]. We found reduced expression of *Tgfb1* and three targets genes (*Pdgfb*, *Fn1* and *Col1a1*[17-19]) in double KO mice compared to *Pkd1* KO. Similarly, WNT targets *Axin2*, *Cd44*, *Ccnd1* and *Myc* were lower in double KO mice[20-24]. Future investigation is needed to define the mechanistic link between FJX1 and the TGFβ/WNT pathway. A clarification of the underlying molecular mechanism might open the path for future therapies not only in the context of ADPKD but also of other chronic kidney diseases.

In **chapter 3,** we explored the option of modulating one of the FJX1 downstream pathways, the Hippo pathway, to halt PKD progression. In particular, we decided to target the pathway effector YAP, as we observed increased nuclear localization of YAP in cyst lining epithelial cells[2]. The advantage of our approach lies in the use of a mouse model that develops cyst in all the kidney segments recapitulating the situation in humans closely. In addition, we used Antisense Oligonucleotides (ASO) as a therapeutic strategy, which could be reasonably easily translated into the clinic. Although we were able to achieve a reduction of about 70% of *Yap* expression in the kidneys, we did not see any improvement of the cystic phenotype. Thus, our results suggest that YAP does not play a critical role in cystic proliferation. However, we could not exclude that TAZ might be compensating for YAP reduction, leaving open the option that targeting both YAP and TAZ might be a better approach to cyst growth inhibition. *In vitro* experiments revealed that *Taz* KO cells did not show altered cyst formation and cyst growth compared to wild-type cells. In line with our *in vitro* findings, *Taz* deletion mice developed a mild cystic phenotype, even in the absence of *Pkd1* KO[6,25]. Moreover, TAZ and Polycystin 1 (PC1) can directly interact and participate in common signalling routes[26]. Hence, reduction or depletion of TAZ levels might worsen disease progression. This advises against the possibility of targeting TAZ in PKD.

Another consideration is that YAP and TAZ have mostly overlapping yet also unique functions[27]. This is supported by the partly distinct expression pattern of YAP and TAZ in

the different segments of the kidneys and by the impossibility to generate a *Taz* KO line in mIMCD3 cells, suggesting that YAP and TAZ dynamics may differ in different segments of the nephron. Nevertheless, the modulation of YAP levels might affect TAZ functions and *vice versa.* Indeed, it has been reported that YAP inversely regulates TAZ protein levels, meaning that reducing YAP levels might result in overactivation of TAZ[28]. However, such dynamics are not completely clear and should be addressed in future research.

To complicate the picture further, YAP and TAZ are at the crossroad of several signalling pathways, such as TGFβ and WNT pathways. When phosphorylated, YAP and TAZ are restrained in the cytoplasm of the cell, where they can interact with SMADs and β-catenin and regulate their localization and transcriptional activity[29]. In our study, we observed increased expression of some of the downstream targets of TGFβ and WNT pathways in *Yap* ASO treated mice. In detail, we observed a significant increase in the expression of *Myc* in *Yap* ASO treated mice, and a similar trend for *Axin2*, both WNT pathway targets. Among the TGFβ pathway targets, we found increased expression of alpha-smooth muscle actin (*Acta2*) and vimentin (*Vim*); we also observed a consistent trend for collagen 1 alpha-1 (*Col1a1*), fibronectin (*Fn1*), plasminogen activator inhibitor-1 (*Pai1*) and matrix metallopeptidase 2 (*Mmp2*). Therefore, our results show that reduction of YAP results in increased activation of the WNT pathway target MYC, known to be a critical player in PKD[30,31], and of some of the TGFβ targets involved in fibrosis, a well-known biological process involved in PKD progression[32]. Since activation of TGFβ and WNT pathways has been described in PKD[33,34], the effect of YAP/TAZ modulation on these signalling routes, and how it affects PKD progression, must be addressed before pursuing this line of therapy.

An additional critical take-home message is the importance to use the right set-up in the study of new possible targets and therapeutic approaches. For example, we observed that *Yap* KO in cells was able to impair cyst formation in 3D cyst assays. This may suggest YAP as a perfect candidate for PKD treatment. However, characterization of the mutant cell lines revealed that *Yap* KO resulted in impaired expression of integrins, which are important for the interaction of the cells with the ECM and the correct establishment of the cystic structures. As a consequence, *Yap* KO cells were able to form cysts only sporadically. However, the sporadic cysts could grow normally, suggesting that proliferation was not affected. Consistently, *in vivo*, we did not observe any effect on proliferation after *Yap* ASO treatment.

Although our findings cannot exclude that the Hippo pathway is involved in cyst growth (possibly via YAP independent routes), we believe that a therapeutic intervention for PKD based on the modulation of YAP levels might not be feasible.

In **chapter 4,** we generated a robust PKD gene expression signature using a combination of a meta-analysis of PKD expression profiles mined from the literature and our newly generated expression data. This approach allowed us to overcome single study biases related to experimental or technological variations and to come up with a list of genes likely involved in PKD. Moreover, based on the assumption that PKD progression and renal injury-repair mechanisms are strongly linked together[1,35-37], we characterized the overlap between injury-repair related genes and the PKD signature and found 35% overlap. Even more, injury-repair genes were involved in 65% of the molecular functions connected to PKD progression, confirming the strong link between PKD and injury-repair mechanisms.

From the comparison of our signature with an independent PKD dataset obtained from *Pkd1* mutant mice at different stages of the disease[38], we could see significant enrichment of the PKD Signature genes throughout disease progression. Interestingly, we observed a major contribution of the genes involved in injury-repair mechanisms in the more severe stages of the PKD. In contrast, the genes only involved in PKD and not in injury-repair were more enriched in the early stages. Therefore, we can zoom in on genes consistently dysregulated in PKD, and, at the same time, obtain insights into the temporal and mechanistic importance of the different genes identified.

Additionally, we compared our PKD Signature with a study focused on macrophage populations in renal injury, as macrophages have a critical role in response to injury but also in PKD progression[39-42]. We were able to observe enrichment for genes related to the different macrophages populations in the PKD Signature, with a larger contribution of injury-repair genes than of the non-injury ones. Nevertheless, we could not discriminate the origin of the expression between the macrophages and the epithelial cells as our study used total kidney lysates to generate the expression profile. In the future, generation and integration of datasets from single-cell sequencing in cystic kidneys might help to clarify this point and gain more information about the role of macrophages and other cell populations in PKD.

With this study, we provide an extensive analysis of expression profiles in PKD with a particular focus on the effect of renal injury in the progression of the disease. We believe that this work can provide a proof of principle on how to use this knowledge to expand our understanding of the PKD progression and discover attractive drug targets and molecular processes for therapy.

In **chapter 5,** we further explore the PKD Signature outlined in chapter 4. Mainly, we decided to focus on the Transcription Factors (TFs) in the signature. TFs control the expression of genes involved in a variety of biological functions, which intervene in the establishment and maintenance of cell states, both in physiological and pathological situations. Dysregulation

of TFs activity can be at the base of the development of a broad range of diseases. Using computational approaches, we interrogated the signature in different ways. First of all, we defined the list of TFs dysregulated in PKD using MsigDB, and identified those with an involvement in injury-repair. Several of the TFs identified were already known in PKD, proving the validity of our approach. At the same time, we identified many other TFs never described in PKD before, which might be interesting candidates for future studies. Subsequently, employing the ChEA 2016 database of TFs targets, we predicted TFs that are relevant to PKD based on the enrichment of their targets in the PKD Signature. This method allowed us to identify TFs that were missing in the signature, maybe because their expression level is not changed in PKD. Nevertheless, their activity is likely changed, as the expression of their targets is altered in PKD progression. At the same time, knowing which TFs and their targets were deregulated in the different stages of the disease, gave us insight into which molecular mechanisms might be affected. Finally, pathway analysis of the identified TFs using Genetrail2 and Wikipathways revealed enrichment for pathways like the TGF-β pathway, oxidative stress, cellular metabolism, interleukins signalling, adipogenesis and estrogen signalling and apoptosis, which have been shown to be involved in PKD[43-46].

To validate our approach, we focused on two TFs for further wet-lab experiments. We selected STAT3 and RUNX1 as they showed the most significant change in expression, both in PKD progression and injury. We confirmed that the expression of the TFs and their putative targets were altered in kidneys from *Pkd1* KO mice compared to Wt. Moreover, we set-up and performed a ChIP assay and confirmed an increase in the binding activity of STAT3 and RUNX1 to the promoter region of their target genes in cystic kidneys compared to Wt kidneys. Immunohistochemical analysis revealed that STAT3 and RUNX1 are virtually not expressed in healthy kidneys, both in human and mice. However, their expression is visibly increased in cystic kidneys and after renal injury, confirming our computational analysis. Increased expression of STAT3 has been described before in several ADPKD mouse model, in human cystic tissues and also after renal injury[47-49]. Indeed, we were not surprised to find it back in our analysis, and we consider it a proof of our approach reliability. Additionally, previous *in vitro* evidence suggested that STAT3 might be directly activated by cleaved PC1, although the exact mechanism linking *Pkd1* deletion and STAT3 activation in cystic tubules was still elusive[49,50]. A recent study in *Pkd1* KO mice demonstrated that STAT3 activation occurs after macrophage recruitment by secretion of CCL2 early after gene deletion. However, they observed that tubular STAT3 was only partially responsible for cyst growth, but was central in the establishment of a feedback loop that limits immune cells infiltration in cystic kidneys[51]. The results provided in this work denote that a clear mechanistic evaluation of interesting targets is paramount in the development of targeted therapies in ADPKD. RUNX1 involvement in ADPKD has never been described before. Recently, RUNX1 was proposed as a regulator of TGF-β-induced renal tubular EMT and fibrosis[52]. TGF-β signalling is involved

in ECM deposition and cyst progression[43], making it plausible for RUNX1 to play a role in ADPKD. Still, we need to obtain more insight into the molecular mechanisms behind the involvement of RUNX1 in PKD before being able to select it as a therapeutic target.

With this work, we further dug into the PKD Signature and showed how this could be used to better understand the role of TFs in different steps of disease. Further analyses are needed to clarify the molecular mechanisms behind the contribution of these TFs to PKD progression and cyst formation.

Concluding remarks

To this day, the scientific literature reports a variety of dysregulated molecular mechanisms in ADPKD progression. However, a clear hierarchical overview of these events is still missing, thus making it difficult to separate the early effects of PKD gene disruption on cyst initiation, from the secondary effects of disease progression and cyst expansion. Moreover, we need to keep in mind that different regions of the kidney might be experiencing different steps of progression at any time. Inevitably, we need to deepen our knowledge of the steps of disease progression and the molecular mechanisms behind them. Our functional annotation of the genes in the PKD signature allowed us to identify biological targets that are most relevant in the different phases of the disease, from the initial moderate phase to the more advanced and severe one. The knowledge we generated is just a starting point for future studies that need to evaluate in detail the actual significance of the identified mechanisms in PKD.

We know that by inducing injury and the subsequent repair phase, we can accelerate cyst initiation and growth. However, I believe that injury-repair must be considered more as a means to understand the initial phases of cystogenesis more than a possible target for therapy. Indeed, even though injury-repair mechanisms are involved in PKD progression, some of the biological functions they control are actually employed to cope with the alterations taking place during disease progression.

In my opinion, particular attention should be given to the elucidation of the early stages of cyst formation. However, this is not an easy task. At this stage, the renal tissue is still mostly unaffected. As a consequence, the major input to all kind of -omics data analysis is coming from the healthy tissue, while the signal coming from the diseased tissue is lost in the noise. Thus, to gather information about these early stages, we need to employ different models and more sensitive methodologies. For example, organoids (3D cyst assay and renal organoid) might offer a simplified framework to study the early events that occur after *Pkd1/2* inactivation. However, a significant limitation of these systems is that they cannot take

into account the contribution of infiltrating cells, nor that of the fluid flow, both extremely important in PKD. The implementation of spatial transcriptomics methods gives another possibility. Single-cell RNA sequencing is a powerful technique that can be employed to get insight into the contribution of the different cell types in the kidneys. However, since cells need to be dissociated to perform this technique, the information relative to the positions and interactions of the different cells is lost. A possible way to overcome this is the use of a newly developed technique called Slide-seq[53]. With Slide-seq, the RNA can be transferred from a tissue section to a support covered in barcoded beads allowing to generate a spatially resolved gene expression profile. This kind of approach might be extremely useful in the quest to understand the molecular mechanism of ADPKD progression.

References

1 Happe, H. *et al.* Toxic tubular injury in kidneys from Pkd1-deletion mice accelerates cystogenesis accompanied by dysregulated planar cell polarity and canonical Wnt signaling pathways. *Hum Mol Genet* **18**, 2532-2542, doi:10.1093/hmg/ddp190 (2009).

2 Happe, H. *et al.* Altered Hippo signalling in polycystic kidney disease. *J Pathol* **224**, 133-142, doi:10.1002/path.2856 (2011).

3 Patel, V. *et al.* Acute kidney injury and aberrant planar cell polarity induce cyst formation in mice lacking renal cilia. *Hum Mol Genet* **17**, 1578-1590, doi:10.1093/hmg/ddn045 (2008).

4 Fischer, E. *et al.* Defective planar cell polarity in polycystic kidney disease. *Nat Genet* **38**, 21-23, doi:10.1038/ng1701 (2006).

5 Castelli, M. *et al.* Polycystin-1 binds Par3/aPKC and controls convergent extension during renal tubular morphogenesis. *Nat Commun* **4**, 2658, doi:10.1038/ncomms3658 (2013).

6 Hossain, Z. *et al.* Glomerulocystic kidney disease in mice with a targeted inactivation of Wwtr1. *Proc Natl Acad Sci U S A* **104**, 1631-1636, doi:10.1073/pnas.0605266104 (2007).

7 Reginensi, A. *et al.* Yap- and Cdc42-dependent nephrogenesis and morphogenesis during mouse kidney development. *PLoS Genet* **9**, e1003380, doi:10.1371/journal.pgen.1003380 (2013).

8 Leonhard, W. N. *et al.* Scattered Deletion of PKD1 in Kidneys Causes a Cystic Snowball Effect and Recapitulates Polycystic Kidney Disease. *Journal of the American Society of Nephrology* **26**, 1322-1333, doi:10.1681/Asn.2013080864 (2015).

9 Weimbs, T. & Talbot, J. J. STAT3 Signaling in Polycystic Kidney Disease. *Drug Discov Today Dis Mech* **10**, e113-e118, doi:10.1016/j.ddmec.2013.03.001 (2013).

10 Yamaguchi, T. *et al.* Cyclic AMP activates B-Raf and ERK in cyst epithelial cells from autosomal-dominant polycystic kidneys. *Kidney Int* **63**, 1983-1994, doi:10.1046/j.1523-1755.2003.00023.x (2003).

11 Aguiari, G. *et al.* Polycystin-1 regulates amphiregulin expression through CREB and AP1 signalling: implications in ADPKD cell proliferation. *J Mol Med* **90**, 1267-1282, doi:10.1007/s00109-012-0902-3 (2012).

12 Norman, J. Fibrosis and progression of autosomal dominant polycystic kidney disease (ADPKD). *Biochim Biophys Acta* **1812**, 1327-1336, doi:10.1016/j.bbadis.2011.06.012 (2011).

13 Piersma, B., Bank, R. A. & Boersema, M. Signaling in Fibrosis: TGF-beta, WNT, and YAP/TAZ Converge. *Front Med (Lausanne)* **2**, 59, doi:10.3389/fmed.2015.00059 (2015).

14 Tan, R. J., Zhou, D., Zhou, L. & Liu, Y. Wnt/beta-catenin signaling and kidney fibrosis. *Kidney Int Suppl (2011)* **4**, 84-90, doi:10.1038/kisup.2014.16 (2014).

15 Akhmetshina, A. *et al.* Activation of canonical Wnt signalling is required for TGF-beta-mediated fibrosis. *Nat Commun* **3**, 735, doi:10.1038/ncomms1734 (2012).

16 Meng, X. M., Tang, P. M., Li, J. & Lan, H. Y. TGF-beta/Smad signaling in renal fibrosis. *Front Physiol* **6**, 82, doi:10.3389/fphys.2015.00082 (2015).

17 Geng, H. *et al.* Lysophosphatidic acid increases proximal tubule cell secretion of profibrotic cytokines PDGF-B and CTGF through LPA2- and Galphaq-mediated Rho and alphavbeta6 integrin-dependent activation of TGF-beta. *Am J Pathol* **181**, 1236-1249, doi:10.1016/j.ajpath.2012.06.035 (2012).

18 Ono, K., Ohtomo, T., Ninomiya-Tsuji, J. & Tsuchiya, M. A dominant negative TAK1 inhibits cellular fibrotic responses induced by TGF-beta. *Biochem Biophys Res Commun* **307**, 332-337 (2003).

19 Kim, S. I. *et al.* TGF-beta-activated kinase 1 and TAK1-binding protein 1 cooperate to mediate TGF-beta1-induced MKK3-p38 MAPK activation and stimulation of type I collagen. *Am J Physiol Renal Physiol* **292**, F1471-1478, doi:10.1152/ajprenal.00485.2006 (2007).

20 Jho, E.-h. *et al.* Wnt/beta-catenin/Tcf signaling induces the transcription of Axin2, a negative regulator of the signaling pathway. *Molecular and cellular biology* **22**, 1172-1183, doi:10.1128/MCB.22.4.1172-1183.2002 (2002).

21 Wielenga, V. J. *et al.* Expression of CD44 in Apc and Tcf mutant mice implies regulation by the WNT pathway. *Am J Pathol* **154**, 515-523, doi:10.1016/s0002-9440(10)65297-2 (1999).

22 Tetsu, O. & McCormick, F. Beta-catenin regulates expression of cyclin D1 in colon carcinoma cells. *Nature* **398**, 422-426, doi:10.1038/18884 (1999).

23 Shtutman, M. *et al.* The cyclin D1 gene is a target of the beta-catenin/LEF-1 pathway. *Proc Natl Acad Sci U S A* **96**, 5522-5527 (1999).

24 He, T. C. *et al.* Identification of c-MYC as a target of the APC pathway. *Science* **281**, 1509-1512 (1998).

25 Tian, Y. *et al.* TAZ promotes PC2 degradation through a SCFbeta-Trcp E3 ligase complex. *Mol Cell Biol* **27**, 6383-6395, doi:10.1128/MCB.00254-07 (2007).

26 Merrick, D. *et al.* Polycystin-1 regulates bone development through an interaction with the transcriptional coactivator TAZ. *Human Molecular Genetics* **28**, 16-30, doi:10.1093/hmg/ddy322 (2019).

27 Varelas, X. The Hippo pathway effectors TAZ and YAP in development, homeostasis and disease. *Development* **141**, 1614-1626, doi:10.1242/dev.102376 (2014).

28 Finch-Edmondson, M. L. *et al.* TAZ Protein Accumulation Is Negatively Regulated by YAP Abundance in Mammalian Cells. *Journal of Biological Chemistry* **290**, 27928-27938, doi:10.1074/jbc.M115.692285 (2015).

29 Attisano, L. & Wrana, J. L. Signal integration in TGF-beta, WNT, and Hippo pathways. *F1000Prime Rep* **5**, 17, doi:10.12703/P5-17 (2013).

30 Parrot, C. *et al.* C-MYC is a regulator ofthe PKD1 gene and PC1-induced pathogenesis. *Human Molecular Genetics*, doi:10.1093/hmg/ddy379 (2018).

31 Trudel, M., Dagati, V. & Costantini, F. C-Myc as an Inducer of Polycystic Kidney-Disease in Transgenic Mice. *Kidney Int* **39**, 665-671, doi:DOI 10.1038/ki.1991.80 (1991).

32 Song, C. J., Zimmerman, K. A., Henke, S. J. & Yoder, B. K. Inflammation and Fibrosis in Polycystic Kidney Disease. *Results Probl Cell Differ* **60**, 323-344, doi:10.1007/978-3-319-51436-9_12 (2017).

33 Leonhard, W. N. *et al.* Inhibition of Activin Signaling Slows Progression of Polycystic Kidney Disease. *J Am Soc Nephrol* **27**, 3589-3599, doi:10.1681/ASN.2015030287 (2016).

34 Lancaster, M. A. & Gleeson, J. G. Cystic kidney disease: the role of Wnt signaling. *Trends Mol Med* **16**, 349-360, doi:10.1016/j.molmed.2010.05.004 (2010).

35 Weimbs, T. Polycystic kidney disease and renal injury repair: common pathways, fluid flow, and the function of polycystin-1. *Am J Physiol Renal Physiol* **293**, F1423-1432, doi:10.1152/ajprenal.00275.2007 (2007).

36 Bell, P. D. *et al.* Loss of primary cilia upregulates renal hypertrophic signaling and promotes cystogenesis. *J Am Soc Nephrol* **22**, 839-848, doi:10.1681/ASN.2010050526 (2011).

37 Leonhard, W. N., Happe, H. & Peters, D. J. Variable Cyst Development in Autosomal Dominant Polycystic Kidney Disease: The Biologic Context. *J Am Soc Nephrol* **27**, 3530-3538, doi:10.1681/ASN.2016040425 (2016).

38 Menezes, L. F., Lin, C. C., Zhou, F. & Germino, G. G. Fatty Acid Oxidation is Impaired in An Orthologous Mouse Model of Autosomal Dominant Polycystic Kidney Disease. *Ebiomedicine* **5**, 183-192, doi:10.1016/j.ebiom.2016.01.027 (2016).

39 Clements, M. *et al.* Differential Ly6C Expression after Renal Ischemia-Reperfusion Identifies Unique Macrophage Populations. *J Am Soc Nephrol* **27**, 159-170, doi:10.1681/ASN.2014111138 (2016).

40 Anders, H. J. & Ryu, M. Renal microenvironments and macrophage phenotypes determine progression or resolution of renal inflammation and fibrosis. *Kidney Int* **80**, 915-925, doi:10.1038/ki.2011.217 (2011).

41 Swenson-Fields, K. I. *et al.* Macrophages promote polycystic kidney disease progression. *Kidney Int* **83**, 855-864, doi:10.1038/ki.2012.446 (2013).

42 Cassini, M. F. *et al.* Mcp1 Promotes Macrophage-Dependent Cyst Expansion in Autosomal Dominant Polycystic Kidney Disease. *J Am Soc Nephrol* **29**, 2471-2481, doi:10.1681/ASN.2018050518 (2018).

43 Hassane, S. *et al.* Elevated TGFbeta-Smad signalling in experimental Pkd1 models and human patients with polycystic kidney disease. *J Pathol* **222**, 21-31, doi:10.1002/path.2734 (2010).

44 Tao, Y. X., Zafar, I., Kim, J., Schrier, R. W. & Edelstein, C. L. Caspase-3 gene deletion prolongs survival in polycystic kidney disease. *Journal of the American Society of Nephrology* **19**, 749-755, doi:10.1681/Asn.2006121378 (2008).

45 Padovano, V., Podrini, C., Boletta, A. & Caplan, M. J. Metabolism and mitochondria in polycystic kidney disease research and therapy. *Nat Rev Nephrol* **14**, 678-687, doi:10.1038/s41581-018-0051-1 (2018).

46 Merta, M. *et al.* Cytokine profile in autosomal dominant polycystic kidney disease. *Biochemistry and molecular biology international* **41**, 619-624 (1997).

47 Leonhard, W. N. *et al.* Curcumin inhibits cystogenesis by simultaneous interference of multiple signaling pathways: in vivo evidence from a Pkd1-deletion model. *Am J Physiol Renal Physiol* **300**, F1193-1202, doi:10.1152/ajprenal.00419.2010 (2011).

48 Takakura, A. *et al.* Pyrimethamine inhibits adult polycystic kidney disease by modulating STAT signaling pathways. *Hum Mol Genet* **20**, 4143-4154, doi:10.1093/hmg/ddr338 (2011).

49 Talbot, J. J. *et al.* Polycystin-1 regulates STAT activity by a dual mechanism. *Proc Natl Acad Sci U S A* **108**, 7985-7990, doi:10.1073/pnas.1103816108 (2011).

50 Talbot, J. J. *et al.* The cleaved cytoplasmic tail of polycystin-1 regulates Src-dependent STAT3 activation. *J Am Soc Nephrol* **25**, 1737-1748, doi:10.1681/ASN.2013091026 (2014).

51 Viau, A. *et al.* Tubular STAT3 Limits Renal Inflammation in Autosomal Dominant Polycystic Kidney Disease. *J Am Soc Nephrol*, doi:10.1681/ASN.2019090959 (2020).

52 Zhou, T. *et al.* Runt-Related Transcription Factor 1 (RUNX1) Promotes TGF-beta-Induced Renal Tubular Epithelial-to-Mesenchymal Transition (EMT) and Renal Fibrosis through the PI3K Subunit p110delta. *EBioMedicine* **31**, 217-225, doi:10.1016/j.ebiom.2018.04.023 (2018).

53 Rodriques, S. G. *et al.* Slide-seq: A scalable technology for measuring genome-wide expression at high spatial resolution. *Science* **363**, 1463-1467, doi:10.1126/science.aaw1219 (2019).

6

Appendix

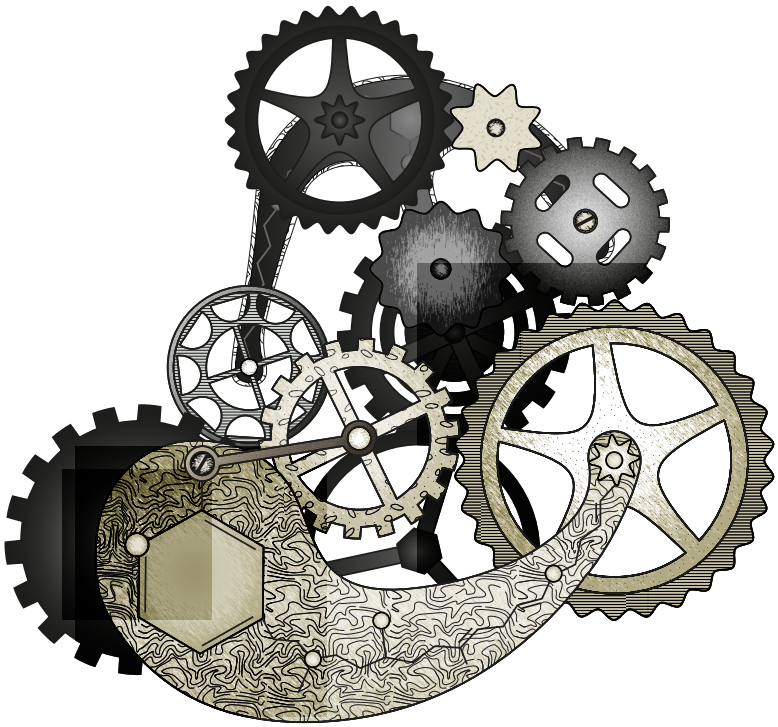

Nederlandse samenvatting

Autosomaal dominant overervende cystenieren, in het Engels Autosomal Dominant Polycystic Kidney Disease (ADPKD), is een systemische ziekte die meestal wordt veroorzaakt door een mutatie in het *PKD1* of *PKD2* gen. Deze genen coderen respectievelijk voor de eiwitten Polycystine 1 (PC1) en Polycystine 2 (PC2). Het belangrijkste kenmerk van ADPKD is het ontstaan van met vocht gevulde cysten in de nieren, welke de normale nierstructuur en nierfunctie aantasten, wat uiteindelijk leidt tot nierfalen. ADPKD heeft ook enkele extra-renale ziektemanifestaties, zoals cystevorming in de lever en alvleesklier, en vasculaire afwijkingen. Momenteel is er geen medicijn dat ADPKD kan genezen, en daarom is het van groot belang om beter inzicht te krijgen in de mechanismen die betrokken zijn bij cystevorming, cystegroei en ziekteprogressie.

In patiënten met ADPKD nemen de cysten gedurende het leven toe, zowel in aantal als in grootte. De cellen die de cystewand bekleden delen actief, en scheiden vloeistof uit in het lumen van de cyste, wat bijdraagt aan de groei. Cystegroei en expansie veroorzaken mechanische stress in het omliggende weefsel. Dit gaat gepaard met de secretie van cytokines en groeifactoren, welke infiltrerende cellen aantrekken. Deze zorgen weer voor lokale schade en fibrose. Constante proliferatie, ontsteking en fibrose verstoren de nierarchitectuur, wat uiteindelijk leidt tot nierfalen. Opvallend is dat proliferatie, ontsteking en fibrose ook vaak worden waargenomen na acute nierschade. In een gezonde nier zorgt de activatie van deze mechanismen voor herstel van het weefsel, maar in patiënten met ADPKD zorgt de activatie van deze mechanismen juist voor het verergeren van de ziekte.

In de literatuur wordt het sterke verband tussen de schade-herstel mechanismen en ADPKD progressie beschreven. Op basis van deze aanname is het doel van dit proefschrift om de moleculaire mechanismen betrokken bij zowel schade-herstel van de nier als ADPKD progressie te bestuderen, om zo de ontwikkeling van de ziekte beter te begrijpen en nieuwe inzichten voor toekomstige studies en therapeutische behandelingen te krijgen.

In **hoofdstuk 1** geven we een uitgebreide beschrijving van de huidige kennis over de moleculaire mechanismen betrokken bij nierschade-herstel en ADPKD progressie.

In **hoofdstuk 2** onderzoeken we de rol van Four-jointed box protein 1 (FJX1) in nierschade en ADPKD progressie. FJX1 is een eiwit dat betrokken is bij de regulatie van twee belangrijke pathways die ontregeld zijn in ADPKD: planar cell polarity (PCP), die de oriëntatie van de epitheelcellen controleert en Hippo signalering, die orgaangrootte controleert. In een eerdere studie, gedaan door onze groep, kwam FJX1 afwijkend tot expressie gedurende zowel de nierschade-herstelfase en PKD progressie in muizen, wat een mogelijke rol voor

FJX1 in cystevorming/groei en ziekteprogressie suggereert. Voor deze studie hebben we *Pkd1* knock-out (KO) muizen (een muismodel voor ADPKD) gebruikt om te onderzoeken of het uitschakelen van *Fjx1* de activiteit van de PCP of de Hippo pathway kon beïnvloeden. Ook hebben we onderzocht of dit een effect had op ziekteprogressie, mét en zonder extra nierschade. We konden geen bewijs vinden voor een veranderde regulatie van de PCP of de Hippo pathway. Echter, we zagen wel een beschermend effect van *Fjx1* uitschakeling op fibrose en de infiltratie van immuuncellen. Dit zorgde ervoor dat de muizen langer in leven bleven, wat suggereert dat de modulatie van de fibrotische respons kan helpen in het controleren van de ziekteprogressie.

In **hoofdstuk 3** doen we verder onderzoek naar de rol van de Hippo pathway in PKD progressie. De Hippo pathway is een sterk geconserveerde signaaloverdrachtsroute die orgaangrootte reguleert. Meerdere moleculaire mechanismen die door de Hippo pathway worden gecontroleerd, zijn ook belangrijk in cystegroei. In een eerdere studie zagen we inderdaad een verhoogde expressie van één van de downstream effectormoleculen van de Hippo pathway, het eiwit YAP, in de kern van het cyste-epitheel. Daarom veronderstellen we in hoofdstuk 3 dat het verlagen van de hoeveelheid YAP in *Pkd1* KO muizen, mogelijk het cysteuze fenotype kan verbeteren. We besloten een strategie te volgen gebaseerd op antisense oligonucleotiden (ASO), waarmee we specifiek de hoeveelheid YAP significant konden verlagen in de nieren. We zagen geen effect op de ziekteprogressie, maar zagen wel dat het vergelijkbare eiwit TAZ sterk ophoopt in de celkernen van nierepitheelcellen. Dit suggereert dat TAZ het verlies van YAP kan compenseren. We hebben ook het effect van het uitschakelen van *Yap* of *Taz* op cystevorming/groei onderzocht in 3-dimensionale celkweken. We zagen dat het uitschakelen van *Yap* leidt tot een verstoorde organisatie van de cellen, waardoor de cellen geen cysten met een lumen vormden, maar groeiden als een soort tumor. De cellen waarin *Taz* was uitgeschakeld lieten daarentegen geen verstoringen zien. Alles bij elkaar genomen concluderen we op basis van onze data dat het moduleren van YAP geen geschikte benadering is om ADPKD te behandelen.

In **hoofdstuk 4** hebben we de analyse van genexpressie (RNAseq analyse) in ons diermodel voor ADPKD, gecombineerd met genexpressieprofielen die openbaar beschikbaar zijn in de literatuur, om zo een lijst van genen te identificeren die ontregeld zijn in PKD (de 'PKD Signature'). Bovendien hebben we de link tussen PKD progressie en nierschade-herstel mechanismen onderzocht door de 'PKD Signature' te vergelijken met nierschade-herstel genexpressieprofielen. Tenslotte hebben we verschillende ADPKD muismodellen, met en zonder toxische nierschade, gebruikt om onze bevindingen te valideren.

In **hoofdstuk 5** bouwen we voort op het werk in hoofdstuk 4. We concentreren ons op de transcriptiefactoren (TFs) die veranderd zijn in zowel PKD progressie als nierschade-herstel.

TFs zijn eiwitten die de transcriptie van genen controleren, en dus hun expressie reguleren. Na het selecteren van een aantal veelbelovende TFs door middel van computeranalyses, hebben we onze selectie gevalideerd met laboratoriumexperimenten. Met verschillende technieken hebben we aangetoond dat twee TFs (STAT3 en RUNX1) actiever zijn tijdens nierschade én in cystenieren, vergeleken met normale nieren, in zowel muizen als patiënten. Ook hebben we laten zien dat de expressie van een aantal voorspelde targetgenen van deze TFs verhoogd is na nierschade én in cystenieren, wat nogmaals laat zien dat de twee gevonden TFs actiever zijn tijdens nierschade en in cystenieren.

Tenslotte worden in **hoofdstuk 6** een algemeen overzicht van de resultaten, zoals beschreven in de vorige hoofdstukken, en suggesties voor verder onderzoek besproken.

Curriculum Vitae

Chiara Formica was born on the 5th of March 1987 in Cisternino, Italy. After completing her secondary education at the Scientific Lyceum in Mesagne in 2006, she enrolled in the Bachelor program "Medical Biotechnology" at the University of Milan, Italy. She obtained her Bachelor degree in 2009 after a final internship at the Leukocyte Laboratory at Istituto Clinico Humanitas where she studied the regulation of tetraspanin-like molecules by glucocorticoids in human macrophages, under the supervision of Prof. Massimo Locati. Afterwards, she enrolled in the Master program "Medical Biotechnology and Molecular Medicine – Curriculum: Transplantology, Medical Immunobiotechnologies and Tissue Engineering" at the University of Milan and graduated *cum laude* in 2011. As part of her Master thesis, she did a 12-months internship characterizing the immunophenotype and the functions of adipose-derived stromal cells, with a focus on possible applications in regenerative medicine, under the supervision of Prof. Paolo Corradini and Dr. Cristiana Carniti in the Department of Hematology, Fondazione IRCCS Istituto Nazionale dei Tumori, Milan. Chiara was awarded a 1-year fellowship to work as a research assistant at the Department of Hematology, Fondazione IRCCS Istituto Nazionale dei Tumori, Milan. In 2013 she started her PhD training in the laboratory of Prof. dr. Dorien J.M. Peters at the Department of Human Genetics, Leiden University Medical Center, to study the effect of renal injury on different pathways and the implications in ADPKD progression. The findings obtained during her PhD studies are described in this thesis.

List of publications

Reducing YAP expression in *Pkd1* mutant mice does not improve the cystic phenotype
Formica C, Kunnen S, Dauwerse JG, Mullick AE, Dijkstra KL, Scharpfenecker M, Peters DJM.
J Cel Mol Med 2020; 10.1111/jcmm.15512

Molecular pathways involved in injury-repair and ADPKD progression.
Formica C, Peters DJM.
Cell Signal. 2020 Aug;72:109648.

Characterisation of transcription factor profiles in polycystic kidney disease (PKD): identification and validation of STAT3 and RUNX1 in the injury/repair response and PKD progression.
Formica C*, Malas* T, Balog J, Verburg L, 't Hoen PAC, Peters DJM.
J Mol Med. 2019 Dec;97(12):1643-1656.

Four-jointed knock-out delays renal failure in an ADPKD model with kidney injury.
Formica C, Happé H, Veraar KA, Vortkamp A, Scharpfenecker M, McNeill H, Peters DJM.
J Pathol. 2019 Sep;249(1):114-125.

Comparative transcriptomics of shear stress treated *Pkd1*$^{-/-}$ cells and pre-cystic kidneys reveals pathways involved in early polycystic kidney disease.
Kunnen SJ, Malas TB, Formica C, Leonhard WN, 't Hoen PAC, Peters DJM.
Biomed Pharmacother. 2018 Dec;108:1123-1134.

Meta-analysis of polycystic kidney disease expression profiles defines strong involvement of injury repair processes.
Malas TB*, Formica C*, Leonhard WN, Rao P, Granchi Z, Roos M, Peters DJM, 't Hoen PA.
Am J Physiol Renal Physiol. 2017 Apr 1;312(4):F806-F817

Allogeneic stem cell transplantation in therapy-related acute myeloid leukemia and myelodysplastic syndromes: impact of patient characteristics and timing of transplant.
Spina F, Alessandrino PE, Milani R, Bonifazi F, Bernardi M, Luksch R, Fagioli F, Formica C, Farina L.
Leuk Lymphoma. 2012 Jan;53(1):96-102

* Authors contributed equally

A

Acknowledgements

This thesis would have never be possible without the help and support of my supervisors, colleagues, family and friends.

Foremost I would like to express my gratitude to my supervisor Prof. Dorien J.M. Peters: you always believed in and supported me but also pushed me outside my comfort zone, thank you. I want to thank also my co-supervisor, Prof. Peter-Bram 't Hoen for the invaluable input in several projects of my thesis.

My sincere thanks also goes to Dr. Emile de Heer, Dr. Hans Baelde, Dr. Marion Scharpfenecker, Kimberley, Lotte, Malu and Kyra from the department of Pathology, to Dr. Marco Roos and Dr. Judit Balog from the Human Genetics department, to Prof. Bart Janssen and Dr. Zoraide Granchi from Genomescan, and to Prof. Andrea Vortkamp, Dr. Adam E. Mullick and Prof. Helen McNeill. To you all goes my gratitude as without your contributions this thesis would not have been possible.

A special mention to all my colleagues in the PKD group: Hester, Wouter, Hans, Steven, Sandra and Julie: thank you for the scientific discussions, the help, but most of all for making me feel welcomed when everything was new and scary. Thanks Sandra and Steven for adopting me in the Kunnen family. Janne, Lin: you were both very professional but also humble and fun, thank you for your help and friendship. Anish, my work spouse, our rocky start is now a funny story we tell to explain how we became such good friends. One BuzzFeed quiz at the time, you helped me smile in the difficult times. Your support and your insane proof reading abilities were crucial in the completion of my PhD, grazie mille. Elena, thanks for explaining so clearly your obscure metabolomics data and for driving in the parking buildings when Anish and I did not dare to. Laura, Sevtap, we did not have a lot of time together but I am sure you will carry the PKD name high, good luck with everything. Also, thanks to my students Tanya, Maaike and Vivian. I want to thank also Dr. Leo Price, Tijmen and Hester from OcellO: you always had the best pictures in your presentations.

I was very lucky to be part of such a vibrant and collaborative department as the Human Genetics. Particularly, I want to thank Mara and Remko: you really made me feel at home here in The Netherlands and took care of me when I needed it. Jenny, Yvonne, Saeed: together with Remko we started as the lab day out committee and we ended up being travel buddies. I also want to thank Kelly, Darina, Maja and Dani: because of you, the long days in the lab, and life in general, have been more fun. I wish I could mention each and every one from the Human Genetics departent because you all contributed to my personal and professional growth, so for this I thank you all.

A giant thanks that overcomes distances to my fellow TranCYST researchers, Tareq, Arianna, Martin, Kanishka, Alkaly, Laura and Aylin. We shared this beautiful experience that is the Marie Curie network and I could not have asked for better companions.

Thanks to the Little Italy of the Netherlands: Luca, Enrico, Marida, Jasmine, Felice, Sofia, Anna and Marta. Moving to a new country is always scary and it is nice to have someone who understands the struggle and misses the Italian food as much as you do.

Nicola, Martina, Giulia and Giulia, from where should I start? Nicola, you have been particularly crucial in these years as we shared the same tough experience of doing a PhD in The Netherlands. You are an incredible man, professionally and personally, probably the best person I have ever known. Thank you for the unbelievably long discussions about experiments, and for always being there as a friend. Martina, Giulia and Giulia, there are no words to explain how important you and Nicola are to me. We share our beginning as biotech but we ended up being so much more. Of course, a big thank you to Gabriele and Alice, and to Claire, Giovanni, Alberto and Roberto for putting up with our crazy relationship.

I cannot forget to mention Davide, Fabiana and Raffaella. With you I took my first steps in the lab back in Milan. Leaving you for my PhD was the hardest part. It is unbelievable how much we could laugh even during a boring flow cytometry run. Davide, you are my best friend and even though there is no proof, I know we share one brain. Thanks also to Federico.

Huge thanks to Vittoria and Antonella, best roommates ever and to Marco, Stefano, Dario, Giorgia, Davide, Claudia, Stefania, Carlo and Chiara: you guys are my home and I can never wait to come back to you. Domenico, we shared the last eleven years. For better or for worse, you are definitely an important part of this journey, thank you for your help.

Last but not least, I want to thank my family. Thanks to my uncle, aunt and cousins. Alessandra and Marco, thank you for your support, I adore you both. Mum and Dad, I owe you everything; I am sorry I moved so far but thanks for never interfering with my decisions.

A